FACIAL FRACTURE TREATMENT

using three-dimensional modelling and finite element analysis principle

Omid Daqiq

FACIAL FRACTURE TREATMENT

using three-dimensional modelling and finite element analysis principle

Omid Daqiq

ISBN: 978-94-6522-816-7

Provided by thesis specialist Ridderprint, ridderprint.nl
Printing: Ridderprint
Layout and design: Hans Schaapherder, persoonlijkproefschrift.nl

university of groningen

Facial fracture treatment using three-dimensional modelling and finite element analysis principle

PhD thesis

to obtain the degree of PhD at the
University of Groningen
on the authority of the
Rector Magnificus Prof. J.M.A. Scherpen
and in accordance with
the decision by the College of Deans.

This thesis will be defended in public on

Wednesday 7 January 2026 at 11.00 hours

by

Omid Daqiq

Promotor
Prof. F.K.L. Spijkervet

Copromotores
Dr. B. van Minnen
Dr. C.C. Roossien

Assessment Committee
Prof. M.J.H. Witjes
Prof. L. Dubois
Prof. P.R. Onck

Paranymphs

Dr. B. Gareb

Mr. J.M. van Dodewaard

In honour of my dad,
who gave his life so I could live,
giving his breath so I could breathe.

TABLE OF CONTENTS

	Section I: General introduction	
Chapter 1	General introduction	13
	Section II: Mandibular FEA input parameters	
Chapter 2	Finite element analysis of the human mandible: A systematic review with meta-analysis of the essential input parameters	29
	Section III: Creating a validated mandibular FEA model	
Chapter 3	Optimisation of osteosynthesis positioning in mandibular body fracture management using finite element analysis	85
Chapter 4	Biomechanical assessment of mandibular fracture fixation using finite element analysis validated by polymeric mandible mechanical testing	109
Chapter 5	Finite element analysis of mandibular fracture fixation authenticated by 3D printed mandible mechanical testing	145
	Section IV: Application of validated FEA in complex fracture	
Chapter 6	In silico analysis of severely atrophic edentulous mandibular body and angle fracture fixation using a validated finite element analysis model	189
	Section V: Application of 3D model	
Chapter 7	Patient satisfaction after conservative treatment of anterior wall frontal sinus fractures	221
	Section VI: Discussion	
Chapter 8	General discussion and future perspective	243
	Section VIII: Summary / Samenvatting	
Chapter 9	Summary	265
Chapter 10	Samenvatting	273
Appendix	About the author	285
	List op publications	287
	Dankwoord	289
	Sponsors	297

SECTION I

General introduction

CHAPTER 1

General introduction

MAXILLOFACIAL FRACTURES

Maxillofacial trauma is considered to be a leading cause of morbidity and mortality worldwide[1,2]. The incidence of maxillofacial fractures varies widely between different countries[3,4]. In the Netherlands, the incidence is 137 (120 to 150) per 100.000 people per year[4,5]. The incidence is higher in individuals aged between 14-29 and › 40 years old[5,6]. The mandible is the most common site of a facial fracture (36.5%), followed by zygomatic bone (31.1), orbital region (11.8%), maxilla (9.8%), frontal bone (4.6%), and nasal bone (2.3%)[1,7] (Figure 1A).

The incidence of mandibular fractures is four times higher in males compared to females until the age of 65 years[1,8–10]. The ratio reverses from the age of 65 to at least 85 years old most likely due to the onset of osteopenia coupled with higher fall incidence in women[8–11]. The trauma mechanism in mandibular fractures is mainly caused by assault 42%, motor vehicle accident 31%, fall 15%, and motorcycle 5%[8]. The fracture sites of the mandible, in order or frequency, are the symphysis (19.2%), body (18,1), angle (16.2), condyle (14.8%), subcondylar area (12.6), ramus (11.3), alveolus (4.5), and coronoid process (3.3%)[8] (Figure 1B).

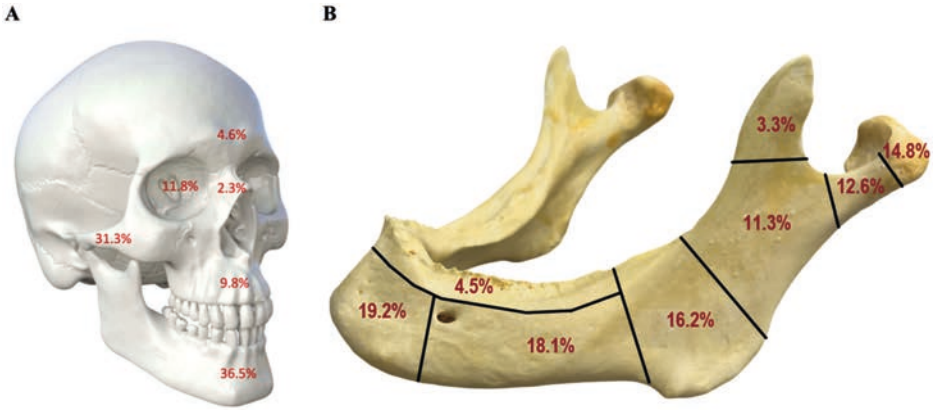

Figure 1. Anatomical incidence of (**A**) facial fractures, and (**B**) mandibular fractures.

In general, fracture management involves restoring normal anatomy including the occlusion, achieving stable fixation, and ensuring the union of fracture fragments[12]. In the case of the mandible, it also involves restoring or establishing the functional movement of the mandible. The aim of optimal fracture management is mainly to: (1) achieve the best anatomical reduction with re-establishing previous occlusion, (2) create stable fixation that allows painless movement of the injured areas, and (3) maintain a sufficient blood supply to the fracture fragments and the tissues surrounding the fracture[12].

BIOMECHANICS

Basics of the biomechanics

Before establishing a treatment plan and starting the treatment of the facial fractures, it is important to have a basic knowledge of the biomechanics, as it allows one to understand what is happening to the bone or osteosynthesis under loading. In general, bone undergoes deformation under the application of a load[13,14]. The amount of deformation in the bone can be quantified by the amount of strain. Strain is defined by the change in length per unit of length, and therefore strain is dimensionless (e.g., 0.01 strain is equal to 1% deformation). Deformation also causes the occurrence of tension in the bone tissue. This is quantified by the amount of stress. Stress is force per unit area (e.g., 1 newton per square meter which is equal to 1 megapascal: 1 N/m^2 = 1 MPa). Stress can be further classified as compressive, tensile, or shear based on how the load is applied[13,14]. Tensile stress occurs when the bone becomes longer or stretched, compressive stress develops when the bone becomes shorter or compressed, and shear stress occurs if one region of the bone moves parallel relative to an adjacent region[13] (Figure 2A).

The relationship between stress and strain can be best described by a stress-strain curve[13,14] (Figure 2B). Observation of the curves shows two deformation regions, namely elastic and plastic regions[13,14]. In the elastic zone, the bone will return to its initial shape when the load is released. However, in the plastic region, the bone has undergone permanent damage and will not return to its original shape when the load is released[13,14]. The elastic or Young's modulus (E), which is the bone's resistance to deformation in the direction of the applied force, is the slope of the elastic region[13–16]. The E-modulus is defined by $E = \sigma \div \epsilon$; where s represents the stress, and ϵ represents the strain. In general, the compact bone has a higher elastic E-modulus than the cancellous bone[13,17–19]. The ability of bone to withstand shear stress in a specific plan is measured by the shear modulus (G)[13]. The shear modulus is defined by $G = \tau \div \gamma$; where τ represents the shear stress, and γ the shear strain[13]. The Poisson ratio measures the bone's ability to resist deformation in a direction perpendicular to that of the applied load[13,15]. In general, the Poisson ratio is defined as $v = \epsilon_y \div \epsilon_x$; where ϵ_y represents the secondary strain, and ϵ_x the primary strain[13,20].

The strength of the bone is also an essential factor. The yield strength is the stress value at the yield point beyond which the load results in tissue damage of the bone, expressed by the point that separates the elastic strain from the plastic strain region in the stress-strain curve[13,14]. The ultimate strength is the maximum stress that bone tissue can withstand[13,14]. A load that exceeds the ultimate strength causes the bone to break[13,21,22].

Finally, the material properties of an object or a structure define how it will interact or react under the application of a load. The elastic constants (E-modulus, shear modulus, and Poisson ratio) describe the relationship between the load and the resulting deformation in the elastic range[13]. In the case of fracture management, it is important to comprehend

how the materials (both the fractured bone and the osteosynthesis material) will behave under the application of load and what are their limitations.

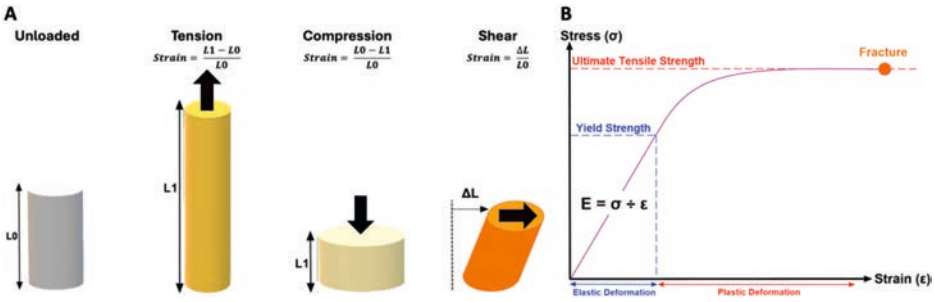

Figure 2. (**A**) Different types of strain for three forms of stress (tension, compression, and shear). (**B**) The stress-strain curve relationship: The elastic and plastic deformation regions are divided by the yield point, beyond which deformation causes damage; the ultimate strength is the stress that bone tissue can maximally sustain.

Osteosynthesis principles and biomechanics of facial fractures

The goal of the use of osteosyntheses in traumatology is to create optimal (1) anatomical fracture reduction (restoring the correct anatomical alignment), and (2) fracture stability (maintaining the interfragmentary alignment during physiological loading) to improve bone healing[12]. In this process, the surgeon will make sure that the blood supply in the bone fragments and surrounding tissue remains sufficient and will try to avoid damage to other structures, like nerves[12]. The osteosynthesis must have certain requirements to achieve optimal fracture fixation: (1) it should have sufficient mechanical properties to withstand various forces (tensile, compression, side bending, and torsional stresses) during healing, (2) it should be malleable enough for adaptation to the bone surface without losing its mechanical strength or properties, (3) it should have minimal dimensions, to reduce incision size and to facilitate stress-free closure of the incision with minimum fracture exposure, and (4) it should have multipurpose applicability for fixating various types of fractures in every patient with his/her individual anatomy[12,23–25].

Biomechanics of facial fractures is best explained by focusing on mandibular fractures. In general, the forces applied on the mandible cause varying compression and tensional zones. These zones depend on the mastication force's location. The inferior portion of the mandible is defined as the compression zone and the superior part the tensional zone[23] (Figure 3A). This knowledge was used by Maxim Champy to define the ideal line of osteosynthesis for mandibular fracture management using miniplate osteosynthesis[23–25] (Figure 3B).

In mandibular fracture management using osteosynthesis, it is important to understand the basics of the osteosynthesis principles. There are two essential principles, namely: load sharing (Champy technique) versus load bearing (Figure 4). (1) The load sharing principle suggests the use of semi-rigid fixation with miniplates, where the tensile forces at the upper border are neutralised by placing the plates at the ideal line of osteosynthesis[12,23,25] (Figure

4A). The accompanying compression forces at the lower border are compensated by the interfragmentary stability of the fracture. However, fracture stability becomes an issue when the lower border is not intact (in case of a bone defect or multiple fractures), and the load sharing principle is no more applicable. Therefore, in those cases fixation using the load bearing principle can be used. (2) In the load bearing principle, the osteosynthesis plate on its own must provide enough rigidity to avoid fragment displacement during functional movement. This is achieved through rigid fixation by placing solid plates at the lower border (Figure 4B). The implant bears the functional load entirely, as the affected bone area is assumed not to be able to share any load with the implant. In case of non-intact lower border, the rigid fixation will take care of compression force and ensures fracture stability[12,23,25].

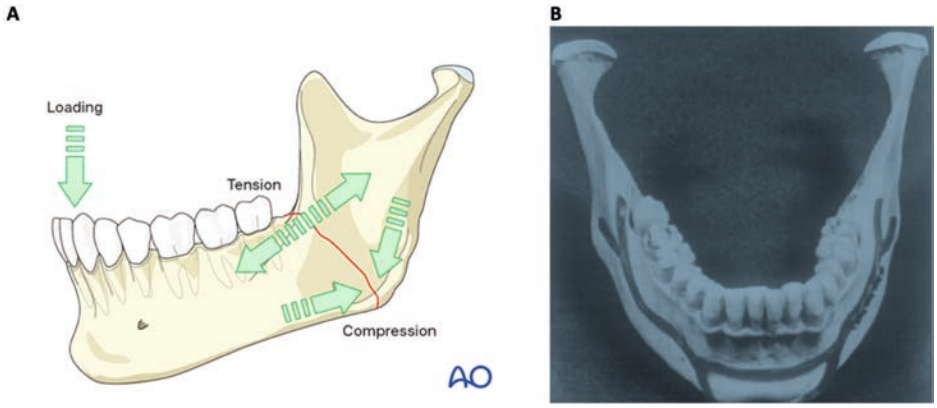

Figure 3. The acting forces on the mandibular fracture based on the location of mastication force. (**A**) incisal force resulting in compression forces inferiorly and tensional forces superiorly. *Source: [© AO Foundation, AO Surgery Reference, surgeryreference.aofoundation.org]. Printed with permission.* (**B**) Champy's ideal line of osteosynthesis. Source: *[Champy M, Lodde JP, Jaeger JH, Wilk A. Ostéosynthèses mandibulaires selon la technique de Michelet. I. Bases biomécaniques [Mandibular osteosynthesis according to the Michelet technic. I. Biomechanical bases]. Rev Stomatol Chir Maxillofac. 1976 Apr-May;77(3):569-76]. Permission to reprint not needed.*

For mandibular body and angle fractures, the dimension and location of the osteosynthesis plate classically differ between the load sharing and load bearing technique. Champy proposed a single miniplate with monocortical screws (diameter 2.0 mm) to be used in the mandible's tensile zone. Whereas, according to Association for Osteosynthesis/Association for Study of Internal Fixation (AO/ASIF) a combination of arch bars and a larger compression plate with bicortical screws (e.g., 2.4 mm). However, an international survey of OMF surgeons, in North America and Europe illustrated that Champys' principle is nowadays the preferred method[12,23,25].

In case of symphysis and parasymphysis fracture management, both Champy and AO/ASIF agree on using two 2.0 mm plates based to withstand the torsional forces acting on the mandible between the canines[12,23,25].

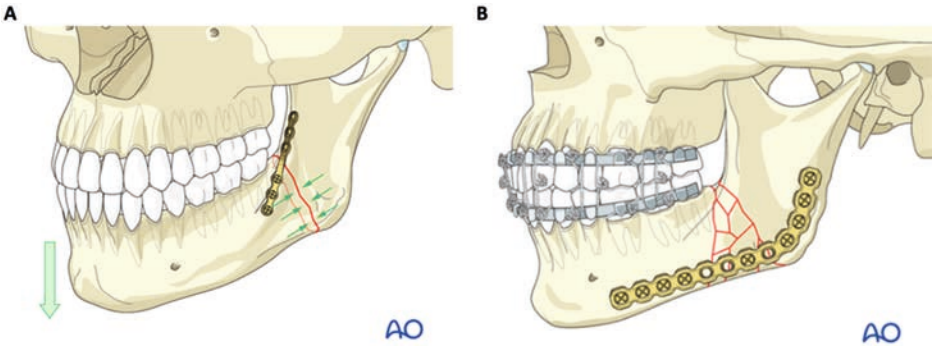

Figure 4. (**A**) Load sharing: the lower border of the angle region is intact and able to withstand the compression forces (arrows). (**B**) Load bearing osteosynthesis principles. *Source: [© AO Foundation, AO Surgery Reference, surgeryreference.aofoundation.org]. Printed with permission.*

COMPUTER AIDED SURGERY USING 3D AND FEA

3D visualisation and processing

Three-dimensional (3D) data visualisation and models are widely used in surgery, particularly in the field of OMF surgery[26–31]. One of the most common sources for 3D fracture visualisation is the use of computed tomography (CT) or cone beam CT (CBCT) scans[27–33]. They can be stored and viewed within the Digital Imaging and Communications in Medicine (DICOM) software for fracture analysis in a 3D plane (e.g., measuring fracture dimensions), or exported for image processing in external 3D software's (e.g., Mimics, or 3-Matic)[15,28–31,33–35]. For example, CT images in DICOM can be used to assess fracture fragmentation, dislocations, and fracture dimensions (e.g., depth, or area), helping to guide the decision-making process of the desired treatment plan between a conservative approach versus surgical treatment (e.g., in case of frontal sinus fracture)[28–30,36,37].

Finite element analysis

Finite element analysis (FEA) originated from the need to unravel issues regarding elasticity and structural design in the field of engineering (e.g., civil, and aeronautical)[38]. Strang and Fix published their seminal work on this topic in 1973, and since then FEA has been developed into a branch of applied mathematics for numeric computational modelling of physical systems that have been used in many engineering disciplines[39]. In the FEA, mathematical simulation is applied to foresee the behaviour of geometry or structure in various scenarios (e.g., under conditions of tension or compression loading)[38–42]. Nowadays, this *in-silico* non-invasive flexible 3D tool is used to study the (bio-)mechanical behaviour of geometries or structures under the application of load; thereby evaluating the amount of force, stress, strain, and displacement distributions[34,43–47]. A typical FEA model comprises a defined geometry to which external loads, boundary conditions, and meshes are applied[15,46,48]. Boundary conditions are constraints applied to a geometry that are necessary for solving boundary value problems, which are systems of differential equations defined in a domain

with specified conditions on its boundary[49]. Meshing is the discretisation process of FEA in which the simulated geometry is divided into finite number of smaller elements or blocks (network of cells and nodes)[15,38,43,50–53]. The size of the elements can significantly affect the approximation of the input geometry and the quality of the FEA results[38,50–53]. The smaller the size, the more accurate the results will be. However, the computation time also increases rapidly when element sizes are decreased. Hence, one should aim for as large as possible element sizes such that the results are accurate enough for practice.

Computer aided surgery in OMF region

In OMF surgery, following Champy's theory, many studies started using cadaveric or polymeric bone models for testing various scenarios of fracture treatment[40,41,54,55]. Not every issue regarding the best possible osteosynthesis has been resolved, e.g., for complex comminuted fractures or extremely atrophic mandibles[34,54,56]. It is important to note that the fixation of routine simple fractures has been extensively studied in the literature, leading to well-established fixation methodologies and standardised guidelines (e.g., Champy or AO techniques)[12,23–25]. However, in case of complex fractures, many questions and uncertainties remain regarding the most effective treatment methods and the best approach to achieving optimal fracture stability[12,23,57–59]. As these cases are less common than non-complex fractures, any subsequent clinical studies are very time-consuming or impossible without the required inclusions[34,52–54,60–62]. Therefore, to address the questions and uncertainties in complex fracture management, it would be beneficial if FEA could replace physical model testing, which is generally more expensive and time-consuming than in silico testing[15,34,35,45,46,52,53,63–65]. For reliable use of FEA, there is a need for a validated 3D computer modelling and FEA simulation method to analyse these fractures, and to search for the best osteosynthesis system for each scenario, possibly by introducing new implants (e.g., degradable, or patient-specific 3D printed plates)[15,35,62,66–69].

Additionally, 3D models (e.g., using CBCT or CT images) can be used for fracture analysis, such as fracture dimensional measurements (e.g., assessing depth or area) or quantifying fracture displacement[70–74]. This approach to 3D fracture analysis can assist surgeons in determining whether a fracture can be treated conservatively (e.g., frontal sinus or zygomatic fractures up to a certain degree of displacement) or surgical reposition is required[70–74]. Therefore, it is worthwhile to further investigate the impact of 3D image model analysis, such as assessing fracture dimensions or the degree of dislocation, on the decision-making process in fracture management.

Principle template

In the general terms, the FEA principle contains a standard template that can be applied for bone fracture analysis (Figure 5). The basic setup starts with the 3D modelling of the bone (e.g., mandibular fracture) and the fixation method (e.g., osteosynthesis miniplate system). The 3D bone model is usually obtained by segmentation of the CBCT or CT images in a medical imaging software (e.g., Mimics or 3-Matic)[15,75,76]. The 3D model then can be

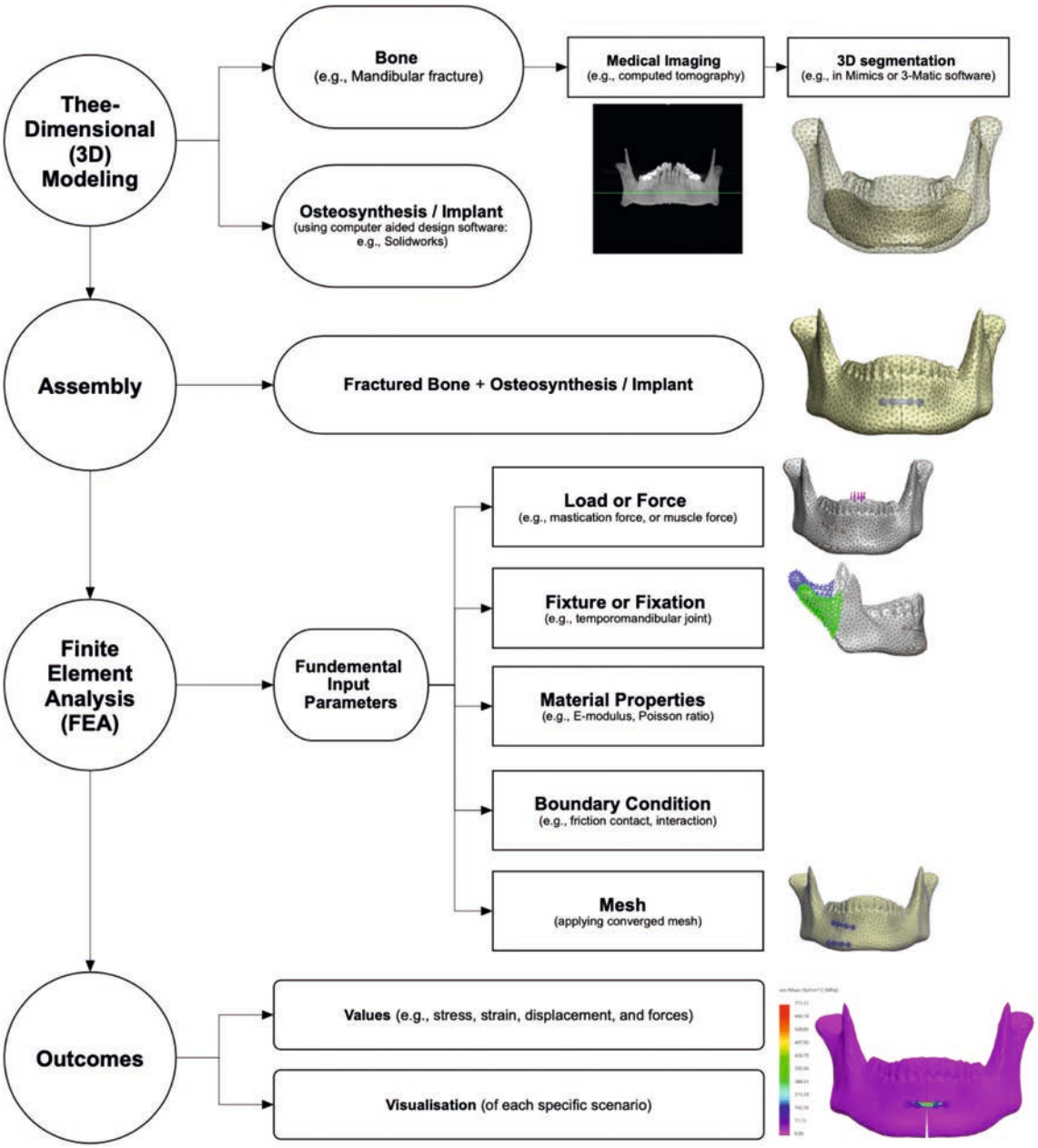

Figure 5. Flow chart of essential steps of finite element analysis of a fixated bone fracture, in this case of the mandible.

exported into any 3D software package with FEA capability to perform extensive analysis (e.g., Solidworks or Comsol Multiphysics)[15,76,77]. The 3D model of the osteosynthesis can be created by computer-aided design (CAD) software. The next step is forming an assembly,

containing the bone fracture and the osteosynthesis positioned at a predetermined position for fracture management. After assembly, the actual FEA setup can start. The essential input parameters of FEA are the load (e.g., bite force, or muscle force), the fixation or fixture site (e.g., temporomandibular joint), the material properties (e.g., Elastic modulus, Poisson ratio), the boundary conditions between the components (e.g., contact, friction, interaction), and the proper converged mesh (where the outcomes become independent of the mesh size)[15,46,48,65]. Literature reveals variations and discrepancies regarding the values of these FEA input parameters (e.g., bite force, muscle force, or mandibular bone properties). Additionally, some FEA parameter values remaining unclear or unknown (e.g., friction)[34,35,61,62,66,67,69,78,79].

AIM OF THIS THESIS

This thesis focuses on the integration of 3D modelling and application of FEA principle in management of facial fractures, with the aim of advancing precision in treatment strategies and improving clinical outcomes. The main purpose of this thesis is to develop a validated 3D modelling and FEA principle for treatment of mandibular fractures using osteosynthesis or implants. This is achieved by a systematic approach to develop a valid, precise, and reproducible FEA model. The FEA model could potentially be routinely applied for fixation of complex mandibular fractures (e.g., in case of atrophic, comminuted, segmental, or defect fractures), thereby enhancing surgical planning and outcomes. Furthermore, the validated FEA principle is potentially applicable and translatable to other bone fractures within the OMF region. The impact of this FEA model principle can be best described as follows:

1. In general terms: the FEA model will provide objective quantitative data and characterise the biomechanical behaviour of fracture(s) fixated with osteosynthesis under various conditions (e.g., under incisal versus molar load). It will offer detailed insights into the distribution of forces, stress, strain, or displacement across the fracture and fixation system under different conditions. This information intended to support surgeons in the clinical decision-making process by facilitating the selection of the most appropriate treatment strategy. Thereby, it can serve as a valuable tool in enhancing the clinical management of complex fractures.
2. In context of fracture treatment: the FEA model will illustrate the effect on fracture fixation stability when a surgeon experiments with different types of osteosynthesis or fixation configurations (e.g., load sharing versus load bearing approach).
3. In terms of fixation method: the FEA model enables the comparison of different implants or fixation methods (e.g., differences in plate geometry and material properties). Furthermore, it can contribute to the improvement of current osteosynthesis systems (e.g., standard commercially available titanium miniplates) or lead to the development of new type of implants (e.g., 3D printed patient specific implants), thereby advancing personalised fracture management.

Additionally, this thesis further explores the application of 3D in the assessment of other craniomaxillofacial bone fractures by evaluating frontal sinus fractures.

The specific aims are:

1. To determine the essential known and unknown input parameter values necessary for developing an accurate mandibular FEA model, through an evidence-based systematic review with meta-analysis of literature on physical in vivo human mandibular tests or experiments (**Chapter 2**).
2. To assess the relevance and applicability of FEA for 3D modelling of the mandible and mandibular fracture fixation analysis as a proof of concept; thereby, taking the initial steps toward the development of a validated and clinically applicable FEA model (**Chapter 3**).
3. To create a validated FEA model principle for mandibular fracture treatment, a precise FEA methodology will be developed and authenticated through a series of mechanical tests conducted on polymeric mandibular replicas in a mechanical test bench (**Chapter 4**). The experimental conditions will be precisely matched to the FEA simulations setup and boundary conditions.
4. To accurately optimise the validated mandibular FEA model by systematically fine-tuning both the FEA model and the corresponding mechanical testing validation setup, ensuring precisely matched conditions between both the FEA simulations and physical experiments using 3D printed mandible replicas (**Chapter 5**).
5. To apply the validated FEA model to investigate non-routine complex mandibular fractures by analysing the fracture fixation of severely atrophic edentulous mandible under a range of clinically relevant fixation scenarios, thereby generating critical insight into the biomechanical behaviour of these non-standard fractures, which are often associated with significant clinical challenges and controversy regarding their optimal treatment (**Chapter 6**).
6. To further explore the applicability of 3D in the OMF region, by assessment of patient satisfaction in conservatively treated subjects with non-dislocated and dislocated anterior wall frontal sinus fractures compared to matched control group (**Chapter 7**).

REFERENCES

1. Lee, K. Global Trends in Maxillofacial Fractures. *Craniomaxillofac Trauma Reconstr* **5**, 213–222 (2012).
2. Shumynskyi, I., Gurianov, V., Kaniura, O. & Kopchak, A. Prediction of mortality in severely injured patients with facial bone fractures. *Oral Maxillofac Surg* **26**, 161–170 (2022).
3. Ahmed, H. E. Al, Jaber, M. A., Abu Fanas, S. H. & Karas, M. The pattern of maxillofacial fractures in Sharjah, United Arab Emirates: A review of 230 cases. *Oral Surgery, Oral Medicine, Oral Pathology, Oral Radiology, and Endodontology* **98**, 166–170 (2004).
4. van den Bergh, B., Karagozoglu, K. H., Heymans, M. W. & Forouzanfar, T. Aetiology and incidence of maxillofacial trauma in Amsterdam: A retrospective analysis of 579 patients. *Journal of Cranio-Maxillofacial Surgery* **40**, e165–e169 (2012).
5. Lalloo, R. *et al.* Epidemiology of facial fractures: incidence, prevalence and years lived with disability estimates from the Global Burden of Disease 2017 study. *Injury Prevention* **26**, 1–9 (2020).
6. Stewart, R. M. *et al. Committee on Trauma American College of Surgeons. National Trauma Data Bank Annual Report*. https://www.facs.org/media/ez1hpdcu/ntdb-annual-report-2016.pdf (2016).
7. Wu, J., Min, A., Wang, W. & Su, T. Trends in the incidence, prevalence and years lived with disability of facial fracture at global, regional and national levels from 1990 to 2017. *PeerJ* **9**, e10693 (2021).
8. Afrooz, P. N., Bykowski, M. R., James, I. B., Daniali, L. N. & Clavijo-Alvarez, J. A. The Epidemiology of Mandibular Fractures in the United States, Part 1: A Review of 13,142 Cases from the US National Trauma Data Bank. *J Oral Maxillofac Surg* **73**, 2361–6 (2015).
9. Bollen, A.-M., Taguchi, A., Hujoel, P. P. & Hollender, L. G. Case-control study on self-reported osteoporotic fractures and mandibular cortical bone. *Oral Surgery, Oral Medicine, Oral Pathology, Oral Radiology, and Endodontology* **90**, 518–524 (2000).
10. Hohlweg-Majert, B., Schmelzeisen, R., Pfeiffer, B. M. & Schneider, E. Significance of osteoporosis in craniomaxillofacial surgery: a review of the literature. *Osteoporos Int* **17**, 167–79 (2006).
11. Lee, K. H. Epidemiology of mandibular fractures in a tertiary trauma centre. *Emergency Medicine Journal* **25**, 565–568 (2008).
12. Haerle, F., Champy M. & Terry B.C. *Atlas of Craniomaxillofacial Osteosynthesis*. (Thieme, Stuttgart, 2009). doi:10.1055/b-002-72255.
13. van Eijden, T. M. Biomechanics of the Mandible. *Critical Reviews in Oral Biology & Medicine* **11**, 123–136 (2000).
14. Cullinane, D. M. & Einhorn, T. A. Biomechanics of Bone. in *Principles of Bone Biology* (eds. Bilezikian, J. P., Raisz, L. G. & Rodan, G. A.) 17–32 (Elsevier, 2002). doi:10.1016/B978-012098652-1.50104-9.
15. Merema, B. B. J., Kraeima, J., Glas, H. H., Spijkervet, F. K. L. & Witjes, M. J. H. Patient-specific finite element models of the human mandible: Lack of consensus on current set-ups. *Oral Dis* **27**, 42–51 (2021).
16. Scott, N. H. An Area Modulus of Elasticity: Definition and Properties. *J Elast* **58**, 269–275 (2000).
17. Turner, C. H., Cowin, S. C., Rho, J. Y., Ashman, R. B. & Rice, J. C. The fabric dependence of the orthotropic elastic constants of cancellous bone. *J Biomech* **23**, 549–561 (1990).
18. Rho, J. Y., Ashman, R. B. & Turner, C. H. Young's modulus of trabecular and cortical bone material: Ultrasonic and microtensile measurements. *J Biomech* **26**, 111–119 (1993).
19. Dechow, P. C. & Hylander, W. L. Elastic properties and masticatory bone stress in the Macaque mandible. *Am J Phys Anthropol* **112**, 553–574 (2000).
20. Tschoegl, N. W., Knauss, W. G. & Emri, I. Poisson's Ratio in Linear Viscoelasticity-A Critical Review. *Mech Time Depend Mater* **6**, 3–51 (2002).
21. Reilly, D. T. & Burstein, A. H. The elastic and ultimate properties of compact bone tissue. *J Biomech* **8**, 393–405 (1975).
22. Turner, C. H. Yield Behavior of Bovine Cancellous Bone. *J Biomech Eng* **111**, 256–260 (1989).
23. Ehrnfeld, M., Manson, PN. & Perin, J. *Principles of Internal Fixation of the Craniomaxillofacial Skeleton: Trauma and Orthogenetic Surgery.* (Georg Thieme Verlag, 2012).
24. Lodde, J. P. & Champy, M. Justification biomécanique d'un nouveau matériel d'ostéosynthèse en chirurgie faciale [Biomechanical justification of a new osteosynthesis device in facial surgery].
25. Champy, M., Lodde, J. P., Jaeger, J. H. & Wilk, A. Bases biomécaniques de l'ostéosynthèse mandibulaire selon la méthode de F.X. Michelet [Biomechanical basis of mandibular osteosynthesis according to the F.X. Michelet method]. *Rev Stomatol Chir Maxillofac* **77**, 248–51 (1976).
26. Bartella, A. K. *et al.* Virtual reality in preoperative imaging in maxillofacial surgery: implementation of "the next level"? *British Journal of Oral and Maxillofacial Surgery* **57**, 644–648 (2019).
27. Haßfeld, S., Mühling, J. & Zöller, J. Intraoperative navigation in oral and maxillofacial surgery. *Int J Oral Maxillofac Surg* **24**, 111–119 (1995).

28. Orentlicher, G., Goldsmith, D. & Horowitz, A. Applications of 3-Dimensional Virtual Computerized Tomography Technology in Oral and Maxillofacial Surgery: Current Therapy. *Journal of Oral and Maxillofacial Surgery* **68**, 1933–1959 (2010).
29. Quereshy, F. A., Savell, T. A. & Palomo, J. M. Applications of Cone Beam Computed Tomography in the Practice of Oral and Maxillofacial Surgery. *Journal of Oral and Maxillofacial Surgery* **66**, 791–796 (2008).
30. Wang, S. & Ford, B. Imaging in Oral and Maxillofacial Surgery. *Dent Clin North Am* **65**, 487–507 (2021).
31. Mathew, N., Gandhi, S., Singh, I., Solanki, M. & Bedi, N. S. 3D Models Revolutionizing Surgical Outcomes in Oral and Maxillofacial Surgery: Experience at Our Center. *J Maxillofac Oral Surg* **19**, 208–216 (2020).
32. Frame, J. W. & Wake, M. J. C. The value of computerized tomography in oral surgery. *Oral Surgery, Oral Medicine, Oral Pathology* **52**, 357–363 (1981).
33. Ahmad, M., Jenny, J. & Downie, M. Application of cone beam computed tomography in oral and maxillofacial surgery. *Aust Dent J* **57**, 82–94 (2012).
34. Aftabi, H. *et al.* Computational models and their applications in biomechanical analysis of mandibular reconstruction surgery. *Comput Biol Med* **169**, 107887 (2024).
35. Xue, R. *et al.* Finite element analysis and clinical application of 3D-printed Ti alloy implant for the reconstruction of mandibular defects. *BMC Oral Health* **24**, (2024).
36. Calis, M. *et al.* Algorithms for the management of frontal sinus fractures: A retrospective study. *Journal of Cranio-Maxillofacial Surgery* **50**, 749–755 (2022).
37. Buller, J. *et al.* Frontal Sinus Morphology: A Reliable Factor for Classification of Frontal Bone Fractures? *Journal of Oral and Maxillofacial Surgery* **76**, 2168.e1-2168.e7 (2018).
38. Szucs, A., Bujtár, P., Sándor, G. K. B. & Barabás, J. Finite element analysis of the human mandible to assess the effect of removing an impacted third molar. *J Can Dent Assoc* **76**, a72 (2010).
39. Strang, Gilbert. & Fix, G. Joseph. *An Analysis of the Finite Element Method.* (Prentice-Hall, Englewood Cliffs (N.J.), 1973).
40. Sittitavornwong, S. *et al.* Integrity of a Single Superior Border Plate Repair in Mandibular Angle Fracture: A Novel Cadaveric Human Mandible Model. *Journal of Oral and Maxillofacial Surgery* **76**, 2611.e1-2611.e8 (2018).
41. Huang, C.-M., Chan, M.-Y., Hsu, J.-T. & Su, K.-C. Biomechanical analysis of subcondylar fracture fixation using miniplates at different positions and of different lengths. *BMC Oral Health* **21**, 543 (2021).
42. Hart, R. T., Hennebel, V. V., Thongpreda, N., Van Buskirk, W. C. & Anderson, R. C. Modeling the biomechanics of the mandible: A three-dimensional finite element study. *J Biomech* **25**, 261–286 (1992).
43. Aquilina, P., Chamoli, U., Parr, W. C. H., Clausen, P. D. & Wroe, S. Finite element analysis of three patterns of internal fixation of fractures of the mandibular condyle. *British Journal of Oral and Maxillofacial Surgery* **51**, 326–331 (2013).
44. Anthrayose, P., Nawal, R. R., Yadav, S., Talwar, S. & Yadav, S. Effect of revascularisation and apexification procedures on biomechanical behaviour of immature maxillary central incisor teeth: a three-dimensional finite element analysis study. *Clin Oral Investig* **25**, 6671–6679 (2021).
45. Patussi, C. *et al.* Evaluation of different stable internal fixation in unfavorable mandible fractures under finite element analysis. *Oral Maxillofac Surg* **23**, 317–324 (2019).
46. Lisiak-Myszke, M. *et al.* Application of Finite Element Analysis in Oral and Maxillofacial Surgery—A Literature Review. *Materials* **13**, 3063 (2020).
47. Park, B. *et al.* The Stability of Hydroxyapatite/Poly-L-Lactide Fixation for Unilateral Angle Fracture of the Mandible Assessed Using a Finite Element Analysis Model. *Materials* **13**, 228 (2020).
48. Gröning, F., Fagan, M. & O'higgins, P. Modeling the Human Mandible Under Masticatory Loads: Which Input Variables are Important? *Anat Rec* **295**, 853–863 (2012).
49. Okereke, M. & Keates, S. Boundary Conditions. in *Springer Tracts in Mechanical Engineering* 243–297 (Springer International Publishing, 2018). doi:10.1007/978-3-319-67125-3_8.
50. Nemade, A. & Shikalgar, A. The Mesh Quality significance in Finite Element Analysis. *IOSR Journal of Mechanical and Civil Engineering (IOSR-JMCE* **17**, 44–48.
51. Ramos, A. & Simões, J. A. Tetrahedral versus hexahedral finite elements in numerical modelling of the proximal femur. *Med Eng Phys* **28**, 916–924 (2006).
52. Sancar, B., Çetiner, Y. & Dayı, E. Evaluation of the pattern of fracture formation from trauma to the human mandible with finite element analysis. Part 1: Symphysis region. *Dental Traumatology* **39**, 352–360 (2023).
53. Sancar, B., Çetiner, Y. & Dayı, E. Evaluation of the pattern of fracture formation from trauma to the human mandible with finite element analysis. Part 2: The corpus and the angle regions. *Dental Traumatology* **39**, 437–447 (2023).

54. Sukegawa, S. *et al.* A retrospective comparative study of mandibular fracture treatment with internal fixation using reconstruction plate versus miniplates. *Journal of Cranio-Maxillofacial Surgery* **47**, 1175–1180 (2019).
55. Trainotti, S. *et al.* Locking versus nonlocking plates in mandibular reconstruction with fibular graft-a biomechanical ex vivo study. *Clin Oral Investig* **18**, 1291–1298 (2014).
56. Emam, H. A., Ferguson, H. W. & Jatana, C. A. Management of atrophic mandible fractures: an updated comprehensive review. *Oral Surg* **11**, 79–87 (2018).
57. Panesar, K. & Susarla, S. M. Mandibular Fractures: Diagnosis and Management. *Semin Plast Surg* **35**, 238–249 (2021).
58. Shokri, T., Misch, E., Ducic, Y. & Sokoya, M. Management of Complex Mandible Fractures. *Facial Plastic Surgery* **35**, 602–606 (2019).
59. Singleton, C., Manchella, S., Nastri, A. & Bordbar, P. Mandibular fractures – what a difference 30 years has made. *British Journal of Oral and Maxillofacial Surgery* **60**, 1202–1208 (2022).
60. Novelli, G., Sconza, C., Ardito, E. & Bozzetti, A. Surgical Treatment of the Atrophic Mandibular Fractures by Locked Plates Systems: Our Experience and a Literature Review. *Craniomaxillofac Trauma Reconstr* **5**, 65–74 (2012).
61. Dario, V., Michelangelo-Santo, G., Roberto, B. & Fabio, F. Is All-on-four effective in case of partial mandibular resection? A 3D finite element study. *J Stomatol Oral Maxillofac Surg* **124**, 101463 (2023).
62. Altuncu, F., Kazan, D. & Özden, B. Comperative evaluation of the current and new design miniplate fixation techniques of the advanced sagittal split ramus osteotomy using three-dimensional finite element analysis. *Med Oral Patol Oral Cir Bucal* **28**, 0–0 (2020).
63. Limjeerajarus, N. *et al.* Comparison of ultimate force revealed by compression tests on extracted first premolars and FEA with a true scale 3D multi-component tooth model based on a CBCT dataset. *Clin Oral Investig* **24**, 211–220 (2020).
64. Daas, M., Dubois, G., Bonnet, A. S., Lipinski, P. & Rignon-Bret, C. A complete finite element model of a mandibular implant-retained overdenture with two implants: Comparison between rigid and resilient attachment configurations. *Med Eng Phys* **30**, 218–225 (2008).
65. Ammar, H. H., Ngan, P., Crout, R. J., Mucino, V. H. & Mukdadi, O. M. Three-dimensional modeling and finite element analysis in treatment planning for orthodontic tooth movement. *American Journal of Orthodontics and Dentofacial Orthopedics* **139**, e59–e71 (2011).
66. Maintz, M. *et al.* Parameter optimization in a finite element mandibular fracture fixation model using the design of experiments approach. *J Mech Behav Biomed Mater* **144**, 105948 (2023).
67. Falcinelli, C., Valente, F., Vasta, M. & Traini, T. Finite element analysis in implant dentistry: State of the art and future directions. *Dental Materials* **39**, 539–556 (2023).
68. Schönegg, D., Koch, A., Müller, G. T., Blumer, M. & Wagner, M. E. H. Two-screw osteosynthesis of the mandibular condylar head with different screw materials: a finite element analysis. *Comput Methods Biomech Biomed Engin* **27**, 878–882 (2024).
69. Gupta, A., Dutta, A., Dutta, K. & Mukherjee, K. Biomechanical influence of plate configurations on mandible subcondylar fracture fixation: a finite element study. *Med Biol Eng Comput* **61**, 2581–2591 (2023).
70. MAYER, J. S. *et al.* The Role of Three-dimensional Computed Tomography in the Management of Maxillofacial Trauma. *The Journal of Trauma: Injury, Infection, and Critical Care* **28**, 1043–1053 (1988).
71. Koltai, P. J. & Wood, G. W. Three Dimensional CT Reconstruction for the Evaluation and Surgical Planning of Facial Fractures. *Otolaryngology–Head and Neck Surgery* **95**, 10–15 (1986).
72. Lee, M., Yoo, J. & Lee, H. Objective analysis of orbital rim fracture CT images using curve and area measurement. *Sci Rep* **14**, 27925 (2024).
73. Kim, J. *et al.* Objective analysis of facial bone fracture CT images using curvature measurement in a surface mesh model. *Sci Rep* **13**, 1932 (2023).
74. Johnson, N. R. & Roberts, M. J. Frontal sinus fracture management: a systematic review and meta-analysis. *Int J Oral Maxillofac Surg* **50**, 75–82 (2021).
75. Shadid, W. G. & Willis, A. Bone fragment segmentation from 3D CT imagery. *Computerized Medical Imaging and Graphics* **66**, 14–27 (2018).
76. Belvedere, C. *et al.* Comparison of Bone Segmentation Software over Different Anatomical Parts. *Applied Sciences* **12**, 6097 (2022).
77. Dotremont, K. From medical images to 3D model: processing and segmentation. in *Handbook of Surgical Planning and 3D Printing* (ed. Gargiulo, P.) 65–91 (Academic Press, 2023). doi:10.1016/B978-0-323-90850-4.00009-0.
78. Garutti, F. C. M. B., Lehmann, R. B., Gialain, I. O. & Lima, F. F. B. de. Analysis of the atrophic mandible rehabilitated with fixed total prosthesis on mono or bicortical implants. *Braz Dent J* **35**, e245621 (2024).
79. Guerra, R. C. *et al.* Finite element analysis of low-profile reconstruction plates for atrophic mandibles: a comparison of novel 3D grid and conventional plate designs. *Oral Maxillofac Surg* **28**, 595–603 (2024).

SECTION II

Mandibular FEA input parameters

CHAPTER 2

Finite element analysis of the human mandible: A systematic review with meta-analysis of the essential input parameters

Omid Daqiq[1]*, Barzi Gareb[1], Frederik Karst Lucien Spijkervet[1], Friederik Wilhelm Wubs[2], Charlotte Christina Roossien[3] & Baucke van Minnen[1]

[1] *Department of Oral and Maxillofacial Surgery, University Medical Center Groningen, University of Groningen, Hanzeplein 1, 9713 GZ, Groningen, The Netherlands.*
[2] *Bernoulli Institute for Mathematics, Computer Science and Artificial Intelligence, University of Groningen, Nijenborgh 9, 9747 AG, Groningen, The Netherlands.*
[3] *Engineering and Technology Institute Groningen, Department of Bio-Inspired MEMS and Biomedical Devices, University of Groningen, Nijenborgh 4, 9747 AG, Groningen, The Netherlands.*

Accepted: 23 May 2025 & Published: 4 June 2025
Nature Scientific Reports
Cite: Daqiq O, Gareb B, Spijkervet FKL, Wubs FW, Roossien CC, van Minnen B. Finite element analysis of the human mandible: a systematic review with meta-analysis of the essential input parameters. Sci Rep. 2025 Jun 4;15(1):19582. doi: 10.1038/s41598-025-03959-9. PMID: 40467626.

Link: https://www.nature.com/articles/s41598-025-03959-9

ABSTRACT

Human mandibular finite element analysis (FEA) requires essential parameters for proper simulation, namely: the forces, fixtures, material properties, and the boundary conditions. The purpose of this systematic review is to determine the evidence-based values of these input parameters.

A systematic search strategy was formulated with the search conducted in PUBMED and EMBASE (PROSPERO: CRD42022315303). Only the values from in vivo physical testing were included. Risk of bias was assessed using validated checklists.

After screening 13023 records, 66 records were included; where only the maximum bite force (MBF) (n=60), muscle force (n=5), and mandible material properties (n=5) were found and assessed. Meta-analysis could be only applied for the MBF studies. MBF in the healthy dentulous populations varies, with male and adults (20-60 years) illustrating higher force. A fracture results in MBF reduction, with force increase in postoperative follow-ups. Further, MBF remains higher in partial versus complete denture wearers.

In conclusion, the systematic review gives a comprehensive overview of MBF, muscle force, and mandible material properties that can be applied as guideline for defining mandibular FEA input parameters. Further, future in vivo studies are required to uncover the unknown parameters (e.g., friction) and to better specify the known parameters (e.g., muscle force).

INTRODUCTION

Finite element analysis (FEA) has been widely applied in oral and maxillofacial (OMF) surgery, particularly in a traumatological, reconstructive, or oncological setting[1–9]. FEA is an *in silico* non-invasive computational tool with high precision for investigating the force, stress, strain, or displacement[1–6,10–13]. It assists the surgeon in understanding various clinical issues, e.g., through three-dimensional (3D) visualisation of the different mandibular fracture fixation methods in complex cases or development of new types of implants (e.g., personalised 3D printed or biodegradable osteosynthesis)[1–4,7,10,11,14–20]. The FEA simulation of the mandible requires the input of several fundamental parameter variables, namely: the applied load (bite force, and muscle force), the fixture or fixation configuration (temporomandibular joint), the biomechanical material properties (cortical bone, trabecular bone, and the applied implant for fracture fixation), and the boundary conditions (type of interactions between the components or parts, e.g., the interaction between the fracture surfaces or fragments, and between the osteosynthesis or implant components with the mandible)[1–4,21]. These parameters are the defining traits of the FEA setup and are required before the execution of the numerical simulation or creating a state of the art FEA model[2–4,21,22].

However, literature displays variations and discrepancies regarding these parameters (e.g., amount of bite force), along with uncertainties about what the exact true values are[7–9,23–28]. The true values refer to those investigated based on physical tests, rather than derived from computational simulations or mathematical derivations. Furthermore, there is no standard guideline that illustrates a personalised systematic overview of true mandibular FEA parameters values (e.g., according to different age or sex). Observation of the literature illustrates that the input values for the mandibular FEA studies are largely derived from other earlier studies, with some studies even using assumptions or unclear definitions[7–9,23–28]. It is essential to have a clear overview of the mandibular FEA parameter values to eliminate the assumptions. This will enable more realistic and precise mandibular FEA simulations, especially in the clinical setting, by taking interindividual differences into the account (e.g., bite force in different sex or age categories).

The main purpose of this systematic review and meta-analysis was to determine the values of the essential input parameters needed for an evidence-based model of human mandibular FEA, based on physical tests. The review aims to present both values of mandibles with and without fractures from clinical, biomechanical, laboratory, or experimental setting. These values can be used for realistic in silico models for treatment of mandibular fractures and development of new osteosynthesis concepts. First, the study aimed to assess the essential input parameter based on physical experiments. Second, the effect of sex and age on these essential parameters were evaluated. Third, the effect of bite location or region (e.g., molar, premolar, or incisal) on maximum bite force and muscle force were assessed. Finally, a systematic overview of the known input parameter values was created as a guideline for the mandibular FEA simulations.

METHODS

Protocol and registration

This systematic review and meta-analysis were conducted according to the recommendations of the *Cochrane Handbook for Systematic Review of Interventions*[29], and is reported according to the *Preferred Reporting Items for Systematic Review and Meta-Analysis* (PRISMA)[30]. A protocol for this systematic review was specified in advance and registered in PROSPERO (CRD42022315303).

Eligibility criteria and Information Sources

A systematic literature search was conducted in PUBMED (MEDLINE) and EMBASE and was last updated on the 6th of November 2024. A sensitive search strategy, comprising medical subject heading terms and free-text words (Supplementary Table S1), was composed with the help of a medical information specialist. The search strategy was developed using the CSO method due to the nature of the study. The "C" (condition) was the human mandible or lower jaw with or without fracture. The "S" (Setting) was the in vivo studies with physical tests, namely: clinical, mechanical, biomechanical, laboratory, or experimental. The "O" (outcome) was the FEA parameters values, namely: bite or mastication force, muscle force, mandible fixture or fixation (temporomandibular joint), mandible material properties, and boundary conditions or interactions (connections, constraints, friction, and tolerance).

Study selection

Eligibility of articles consisted of studies that met the CSO inclusion criteria. The exclusion criteria were: 1) in silico or computer studies (three-dimensional, finite element analysis, finite element method, and numerical or computational simulation); 2) reviews; 3) animal studies; 4) studies that evaluated only osteosynthesis or implants for the mandibular fractures, and 5) studies not published in the English language. Furthermore, no other restrictions were imposed regarding the study design.

The retrieved articles were de-duplicated following the method of Bramer et al.[31]. Title and abstract screening were independently performed by 2 reviewers (O.D. and B.G.). Any disagreement between the reviewers were resolved through discussion. If the title and abstract did not provide sufficient information or in case of any doubt, they were included for full text assessment. Subsequently, the full text papers were screened for inclusion. Any remaining disagreement was resolved through discussion. If no consensus was found during the screening phase, a third reviewer (B.v.M.) was consulted to provide a final decision. After each selection stage, the inter-observer agreement was expressed as Cohen's kappa and percentage of agreement.

Methodological quality assessment

The methodological quality and the risk of bias assessment of the included studies was assessed by 2 reviewers (O.D. and B.G.). Any disagreement between the two reviewers

was resolved during consensus meetings. If necessary, the final decision was made by a third reviewer (B.v.M.). In the study, three different risk of bias (ROB) assessment tools were used based on the study type. Cross-sectional studies were evaluated according to the *National Institutes of Health* (NIH)[32]. The NIH consists of 15 items, with the first of 14 items could be answered by filling: yes, no, cannot determine (CD), not applicable (NA), or not mentioned (NM). The last item, the quality rating, could be graded as poor (high risk of bias), fair (medium or unclear risk of bias), or good (low or no risk of bias). Cohort studies were evaluated according to *Methodological Index for Non-Randomized Studies* (MINORS)[32,33]. The MINORS includes 12 items, with each item scored as follows: 0 (not reported), 1 (reported but inadequate), and 2 (reported and adequate). Cadaveric studies were evaluated according to *QUality Appraisal for Cadaveric Studies* (QUACS)[34]. The QUACS contains 13 items with each item scored as either 0 (no/not stated) or 1 (yes/present).

Data collection and extraction

A predesigned table was used for extracting data from the included studies. Data extraction was performed by one reviewer (O.D.) and was cross-checked by two others (B.G. and B.v.M.). The following data were extracted from the articles (if applicable or mentioned): 1) basic study information (first author's name, year of publication, study period, study type, and study form); 2) inclusion and exclusion criteria; 3) group allocation and sample type, 4) general characteristics (number of samples or subjects, age, sex); 5) interventions (e.g., surgical fracture treatment, or using dentures); 6) type of measurements (e.g., bite force, muscle force, or mandible material properties) and their SI units (International System of Units); 7) outcomes (e.g., maximum bite force, muscle force, or mandible material properties); 8) follow-up outcomes (e.g., postoperative bite force); 9) conflict of interests; and 10) funding sources.

In the bite force studies, additional information was extracted from the studies depending on the availability of the data, namely: the location or the region of the measured bite force (e.g., molar, premolar, or incisal), the type of instrument model used for the measurements, whether the bite force measurement instrument was calibrated in advance, the unit used to measure the force (e.g., newton, or kilogram), how many times the measurement was repeated, whether the participants were well instructed, which values were shown in the study (e.g., mean, or maximum), and how the outcomes were specified (e.g., total population, sex, or different age category).

Regarding the muscle force studies, the following extra data were extracted from the studies, namely: what method or instrument was used for the muscle force measurement (e.g., electromyography), whether the instrument was calibrated in advance, the muscle name where the force was measured (e.g., masseter), the muscle force unit (e.g., newton, or kilogram), number of times the measurement was conducted, at what condition the muscle force was measured (e.g., at rest, or biting position), and how the outcomes were specified (e.g., total population, sex, or different age category).

For the mandible material properties, additional data were extracted from the studies, namely: what type of bone segment was studied (cortical or trabecular bone), how many cadavers were used in the study, how the cadavers were prepared, the number of specimens used for the testing, the method used for creating the samples, the method and instrument type used for the measurements (e.g., mechanical test bench), whether the machine or instruments were calibrated in advance, what type of property output was measured (e.g., elastic modulus), if applicable the unit of the measured value, and how the outcomes were specified (e.g., general, sex, or different age category).

Statistical analysis

SPSS statistics (version 24, IBM, Chicago, IL, USA) was used for the calculation of the inter-observer agreements for the abstract and full text screening. Descriptive data were reported as means with standard deviations (SD), standard errors (SE) or ranges. Nominal data were reported as number with corresponding percentages.

Meta-analysis was conducted in R (version v4.3.3, r-project.org) using a random-effects model with the DerSimonian-Laird estimator, due to the presence of clinical heterogeneity. The effect measure of the outcomes was the weighted mean with corresponding 95% confidence interval (95% CI). A summary effect estimate was calculated if two or more studies could be pooled. Meta-analysis was performed if the primary studies were comparable (i.e., lack of substantial clinical heterogeneity). A priori defined maximum bite force (MBF) subgroup analyses were performed for the healthy dentulous population, partial or complete edentulous subjects with partial or complete dentures, and for the mandibular fracture population fixated with osteosynthesis. In each analysis, if applicable, MBF was stratified based on the bite force location (molar, premolar, and/or incisal region). In addition, the effects of sex and different age categories (‹20 years, 20 to 60 years, and ›60 years) on MBF were evaluated. Whenever possible, multivariable meta-regression analysis was performed assessing the adjusted effect of sex and age on outcomes. Finally, in the mandibular fracture treated with osteosynthesis subgroup, the postoperative bite force changes were evaluated in three follow-up periods, namely: after 2 to 7 days, after 3 to 4 weeks, and after 6 weeks to 3 months. Statistical heterogeneity was regarded substantial if I^2 › 50%. In all analyses, p ‹ 0.05 (two-tailed) was considered statistically significant.

RESULTS

Study identification and selection

The study identification and selection process are shown in Fig. 1. The search resulted in 19409 potentially eligible papers. After the de-duplication process, 13023 articles were screened by title and abstract. The Cohen's kappa and percentage of the agreement were 0.86 and 99.51%, respectively. The full text of 206 articles was screened for inclusion in the second screening round with 66 articles included (Supplementary Table S2: included

studies characteristics, and Supplementary Table S3: list of excluded studies with the exclusion reason). The percentage of agreement and Cohen's kappa for full title screening were 80.96% and 0.61, respectively. There was no consultation needed with the third reviewer in any phase of the study identification or selection.

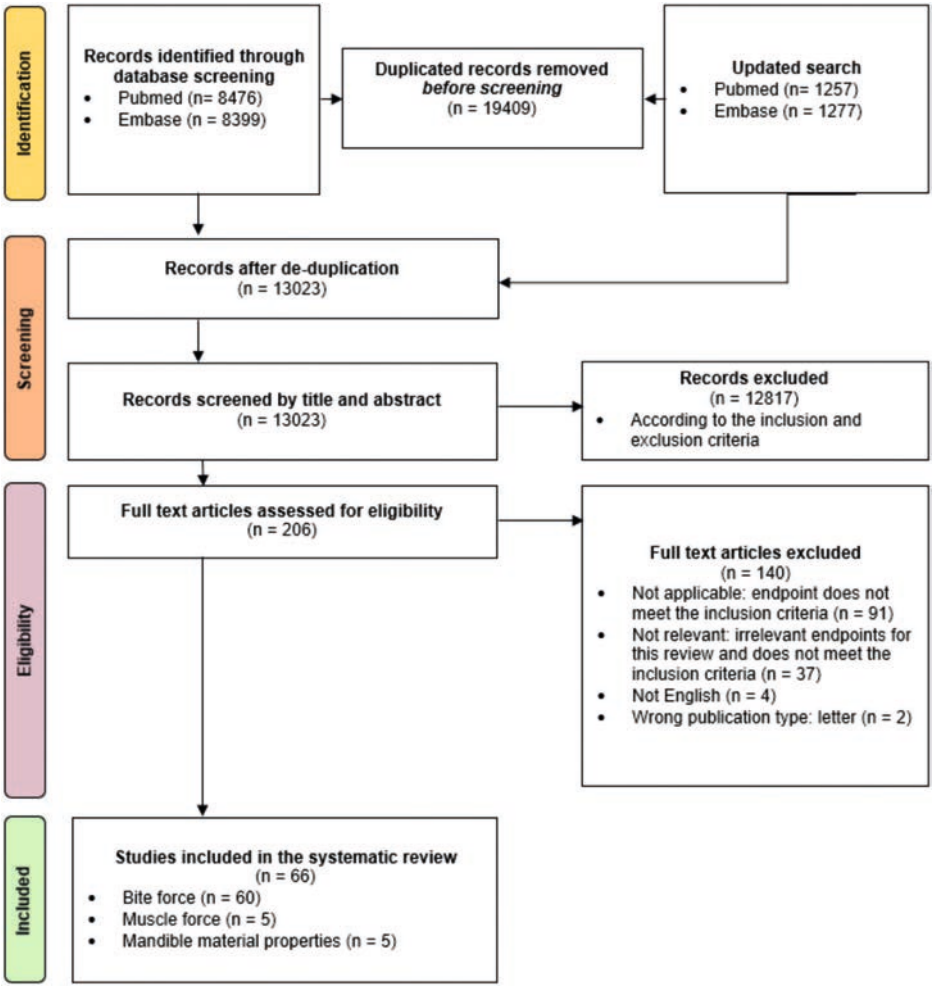

Figure 1. Study identification and selection flow chart.

Study characteristics

From the 66 included studies, 60 studies measured the maximum bite force (MBF)[35–94], 5 studies the muscle force[35,53,69,75,95], and 5 studies the mandible material properties[96–100]. Therefore, only the values for the three main essential parameters were found in the literature. The meta-analysis could only be conducted for the bite force studies. Meta-analysis was not performed for the other outcomes due to the limited data and the incomparable outcomes between the studies.

Assessment of methodological quality

The included studies consisted of 44 cross-sectional studies[35–76,94,95], 15 cohort studies[77–91], 2 randomised control trail (RCT) studies[92,93], and 5 human cadaveric mandible studies[96–100]. In the cross-sectional studies, 43 studies investigated the bite force[35–76,94], 5 studies measured the muscle force[35,53,69,75,95], and 4 studies investigated both bite and muscle force[35,53,69,75]. The cohort studies [77–91] and the RCT studies [92,93] only measured the bite force. The cadaveric studies investigated the mandible material properties [96–100].

Figure 2. The risk of bias assessment checklists.

(a) National Institutes of Health (NIH) for Cross Sectional Studies

Author (Year)	Research question or objective clearly stated	Study population clearly specified and defined	Participation rate of eligible persons at least 50%	Subjects selected from similar populations (with inclusion and exclusion criteria prespecified and unfirmly applied)	Provided sample size justification, power description, or variance and effect estimates	Exposure(s) of interest measured prior to the outcome(s) being measured	Sufficient time frame for reasonably determining exposure and outcome association	Examines different exposure levels as related to outcome (for exposure that can vary in amount/level)	Cleary defined exposure measures (independent variables) with consistent implementation across all participants	Exposure(s) assessed more than once over time	Clearly defined outcome measures (dependent variables) with consistent implementation across all participants	Outcome assessors blinded to the exposure status of participants	Loss to follow-up after baseline 20% or less	Key potential confounding variables measured and adjusted statistically	Quality Rating
Abe et al. (2006)	Yes	Yes	CD	Yes	No	NA	Yes	Yes	CD	Yes	Yes	No	NA	CD	Fair
Abu-Alhaija et al. (2018)	Yes	Yes	Yes	Yes	Yes	Yes	Yes	Yes	Yes	Yes	Yes	No	NA	Yes	Good
Al-Omiri et al. (2014)	Yes	Yes	CD	Yes	No	Yes	CD	NA	Yes	NA	Yes	No	NA	CD	Fair
Al-Qassar et al. (2015)	Yes	Yes	CD	Yes	Yes	Yes	CD	CD	Yes	CD	Yes	No	NA	CD	Fair
Al-Zarea et al. (2015)	Yes	Yes	CD	Yes	No	NA	CD	Yes	Yes	CD	Yes	No	NA	CD	Fair
Braun et al. (1996)	Yes	Yes	CD	Yes	No	CD	CD	NA	NA	CD	CD	No	CD	CD	Poor
Carlsoo (1952)	CD	No	CD	CD	No	NA	CD	NA	NA	NA	CD	NA	NA	CD	Poor
Chong et al. (2016)	Yes	Yes	Yes	No	Yes	No	Yes	NA	NA	No	Yes	CD	NA	NA	Fair
De Abreu et al. (2014)	Yes	Yes	CD	Yes	No	Yes	CD	No	Yes	No	Yes	No	NA	Yes	Fair
Gudipaneni et al. (2020)	Yes	Yes	Yes	Yes	Yes	Yes	Yes	Yes	Yes	No	Yes	No	NA	Yes	Good
Helkimo et al. (1977)	Yes	No	CD	Yes	No	CD	NA	NA	NA	NA	CD	NA	NA	CD	Poor
Helkimo et al. (1978)	Yes	Yes	Yes	Yes	No	CD	NA	NA	NA	NA	CD	NA	NA	CD	Poor
Khan et al. (2020)	Yes	Yes	CD	Yes	No	NA	NA	NA	NA	NA	Yes	NA	NA	No	Fair
Kiliaridis et al. (1993)	Yes	Yes	CD	No	No	NA	NA	NA	NA	NA	Yes	NA	NA	CD	Fair
Koc et al. (2011)	Yes	CD	CD	CD	No	Yes	NA	Yes	Yes	NA	Yes	NA	NA	Yes	Fair
Linderholm et al. (1970)	CD	No	CD	Yes	No	NA	NA	NA	NA	NA	Yes	No	NA	No	Fair
Miura et al (2001)	Yes	Yes	CD	Yes	No	NA	NA	NA	NA	NA	Yes	NA	NA	Yes	Fair
Mountain et al. (2011)	Yes	Yes	Yes	Yes	No	NA	NA	NA	NA	NA	Yes	NA	NA	Yes	Fair
Owais et al. (2012)	Yes	Yes	Yes	Yes	No	Yes	Yes	Yes	Yes	No	Yes	No	NA	Yes	Good
Palinkas et al. (2010)	Yes	Yes	Yes	Yes	No	NA	NA	NA	NA	NA	Yes	CD	NA	CD	Fair
Pruim et al. (1980)	Yes	No	CD	Yes	No	NA	NA	NA	NA	NA	CD	No	NA	CD	Poor
Ringqist (1973)	Yes	Yes	CD	Yes	No	Yes	CD	Yes	CD	No	CD	CD	CD	CD	Poor
Rismanchian et al. (2009)	Yes	Yes	Yes	Yes	No	Yes	CD	Yes	Yes	CD	Yes	CD	NA	CD	Fair
Sasaki et al. (1989)	Yes	No	CD	CD	No	NA	NA	NA	NA	NA	Yes	NA	NA	NA	Poor
Sathyanarayana et al. (2012)	Yes	Yes	Yes	Yes	No	Yes	CD	Yes	Yes	No	CD	No	NA	Yes	Fair
Singh et al. (2012)	Yes	Yes	Yes	CD	No	Yes	Yes	NA	Yes	No	Yes	NA	NA	Yes	Fair
Takaki et al. (2014)	Yes	Yes	Yes	CD	No	NA	NA	NA	NA	NA	Yes	No	NA	Yes	Fair
Tortopidis et al. (1999)	Yes	CD	CD	CD	No	NA	NA	NA	NA	NA	Yes	No	Yes	NA	Poor
Tripathi et al. (2014)	Yes	Yes	Yes	Yes	CD	Yes	Yes	Yes	Yes	CD	Yes	No	Yes	Yes	Good
van der Bilt et al. (2008)	Yes	Yes	CD	Yes	No	NA	NA	NA	NA	NA	Yes	No	NA	Yes	Fair
van Eijden (1991)	CD	No	CD	CD	No	NA	NA	NA	NA	NA	Yes	CD	NA	CD	Poor
Vozza et al. (2021)	Yes	Yes	Yes	Yes	Yes	CD	CD	Yes	Yes	No	Yes	No	NA	CD	Fair
Wennström 1971	Yes	No	CD	CD	No	NA	NA	NA	NA	NA	Yes	No	NA	CD	Poor
Wennström 1971	Yes	Yes	CD	Yes	No	CD	CD	NA	CD	No	Yes	No	NA	CD	Poor
Widmalm et al. (1982)	Yes	Yes	CD	CD	No	NA	NA	NA	NA	NA	Yes	NA	NA	No	Poor
Zivko-Babic (2002)	Yes	No	CD	CD	No	NA	NA	NA	NA	NA	Yes	No	NA	CD	Fair
Bogdanov (2023)	Yes	Yes	CD	Yes	No	NA	NA	NA	NA	NA	Yes	No	NA	NA	Fair
Ustrell-Barral et al. (2024)	Yes	Yes	CD	Yes	No	NA	NA	NA	NA	NA	Yes	No	NA	NA	Fair
de Sonnaville et al. (2023)	Yes	Yes	CD	Yes	CD	NA	NA	NA	NA	NA	Yes	No	NA	NA	Fair
Mutt et al. (2023)	Yes	Yes	Yes	Yes	Yes	NA	NA	NA	NA	NA	Yes	CD	NA	NA	Good
Nimura et al. (2023)	Yes	Yes	CD	Yes	Yes	NA	NA	NA	NA	NA	Yes	No	NA	NA	Fair
Ranjan et al. (2024)	Yes	Yes	CD	CD	No	NA	NA	NA	NA	NA	Yes	No	NA	NA	Poor
Mani et al. (2024)	Yes	Yes	Yes	Yes	Yes	Yes	Yes	CD	CD	Yes	Yes	No	NA	Yes	Fair
Reddy et al. (2022)	Yes	Yes	Yes	Yes	Yes	NA	NA	NA	NA	NA	Yes	No	NA	NA	Good

[continued on next page]

Figure 2. *[continued]*

(b) Methodological Index for Non-Randomized Studies (MINORS) for Cohort Studies

Author (Year)	A clearly stated aim	Inclusion of consecutive patients	Prospective collection of data	Endpoints appropriate to the aim of the study	Unbiased assessment of the study endpoint	Follow-up period appropriate to the aim of the study	Loss to Follow-up less than 5%	Prospective calculation of the study size	An adequate control group	Contemporary groups	Baseline equivalence of groups	Adequate statistical analyses
Ahlberg et al. (2003)	2	2	2	2	1	NA	NA	1	NA	NA	NA	2
Ahmed et al. (2016)	2	2	2	2	2	2	2	1	2	2	1	2
Bakke et al. (1989)	2	1	2	1	2	NA	NA	0	2	2	1	2
Bakke et al. (1990)	2	2	2	2	2	NA	NA	0	NA	2	1	2
Kampe et al. (1987)	2	1	2	1	0	NA	NA	0	1	1	1	1
Kshirsagar et al. (2011)	1	1	2	2	1	2	2	0	2	1	0	0
Kumar et al. (2014)	2	2	2	2	1	2	2	0	1	2	1	1
Rastogi et al. (2016)	2	2	2	2	0	2	2	1	NA	2	1	1
Rentes et al. (2002)	2	2	2	2	0	NA	NA	0	NA	2	1	2
Sener et al. (2015)	2	1	2	2	0	2	2	0	0	NA	NA	1
Singh et al. (2020)	2	2	2	2	0	2	2	2	NA	NA	NA	2
Sybil et al. (2013)	2	1	2	1	0	2	0	0	0	0	0	2
Ali Alkhalaf et al. (2024)	2	2	2	2	0	NA	NA	0	NA	NA	NA	2
Gamit et al. (2024)	2	2	2	2	0	2	2	0	2	2	2	2
Munisekhar et al. (2023)	2	2	2	2	0	NA	2	0	1	2	0	1
Wasinwasukul et al. (2022) *	2	2	2	2	0	2	2	2	2	2	2	2
Kashiwazaki et al. (2023) *	2	2	2	2	0	2	2	0	2	2	2	2

(c) QUality Appraisal for Cadaveric Studies (QUACS) for Cadaveric Studies

Author (Year)	Objective stated	Basic information about sample is included	Applied methods are described comprehensibly	Study reports condition of the examined specimens	Education of dissecting researchers is stated	Findings are observed by more than one researcher	Results presented thoroughly and precise	Statistical methods appropriate	Details about consistency of findings are given	Photographs of the observations are included	Study is discussed within the context of the current evidence	Clinical implications of the results are discussed	Limitations of the study are addressed
Ashman et al. (1987)	1	0	1	1	0	0	1	0	1	0	0	0	0
Nomura et al. (2007)	1	1	1	1	0	0	1	1	1	1	0	1	0
Schwartz-Dabney et al. (2003)	1	1	1	1	1	0	1	1	1	1	0	1	1
Vitins et al. (2003)	1	1	1	1	1	0	1	1	1	0	0	0	0

* Originally randomized control trail study; however, the systematic review only used the bite force values of control group containing healthy dentulous population. In this case, for the systematic review the study design becomes a cohort study.

Abbreviations: CD (cannot decide), and NA (not applicable).

Colour coding: no or low risk of bias (green), some concerns (yellow), high risk of bias (red), not applicable (blue).

The NIH checklist (Fig. 2a) showed that the bite force measurements were generally done systematically, and the measurements were properly described [35–76,94,95]. However, studies, where the muscle force was examined [35,53,69,75,95], lacked a proper muscle force measurement, reported unclear methodology, or the assumptions that were made in the studies to derive the muscle force values were not reported. Furthermore, in 3 studies it was difficult to define whether the research question was properly defined[48,63,95] and only 9 studies illustrated a proper prospective study size justification[36,40,42,64,72,73,75,76,94]. The MINORS checklist (Fig. 2b) illustrates that most of the included studies did not contain an unbiased assessment of the study endpoints[81,83–93], with 5 studies reporting the prospective calculation of the study size[77,78,84,87,92], and 1 study not performing any statistics[82]. The QUACS checklist (Fig. 2c) of human cadaveric mandible studies illustrated a clearly defined aim, material property measurement methodology, and measurement outcomes[96–100]. However, 1 study did not include the basic information of the used cadaveric sample[96], and 3 studies did not mention how the cadavers were dissected[96,97,99].

Finally, in none of the included studies, a blinding system was used in the sampling, measurements, or outcome comparison process. The studies contain no or poor statistical method justification. Furthermore, it was also unclear whether the measurements, observations or data processing was done by one or more than one researcher. The included studies did not declare any conflict of interest. Ten studies declared that their research was funded[41,46,49,51,52,62,70,86,93,97]; however, there is no indication that the funding organisations did play a role in the design and conduct of the study (including collection, management, analysis, and interpretation of data) as well as preparation, review, and approval of the article.

Endpoints

Maximum bite force (MBF)

The overall values of MBF after meta-analysis is shown in Table 1, with the meta-analyses forest plots presented in the Supplementary Fig. S1 and the raw data from the included articles illustrated in Supplementary Table S5.

Firstly, MBF for the healthy dentulous population was 443.6 N [384.2; 502.9] in the molar region, 428.4 N [371.8; 485] in the premolar region, and 209.2 N [132.5; 285.9] in the incisal region (Supplementary Fig. S1.1 and Table S5.1). MBF was higher in the male versus the female population (Supplementary Fig. S1.2 and Table S5.2); namely: 509.9 N [425.9; 594] versus 413.6 N [354.8; 595.6] in the molar region with a difference of 96.3 N (p=0.08), 475.2 N [354.8; 595.6] versus 343.2 N [298.5; 387.9] in the premolar region with difference of 132 N (p=0.04), and 295.9 N [138.4; 453.4] versus 259.1 N [127.1; 391.1] in the incisal region with difference of 36.8 N (p=0.73).

Table 1. Meta-analysis maximum bite fore (MBF) values in Newtons (N).

		Mean MBF at different bite locations [95%CI] (n)		
		Molar	**Premolar**	**Incisal**
Healthy dentulous population	Total	443.6 [384.2; 502.9] (35)	428.4 [371.8; 485.0] (5)	209.2 [132.5; 285.9] (18)
Sex	Male	509.9 [425.9; 594.0] (24)	475.2 [354.8; 595.6] (3)	295.9 [138.4; 453.4] (9)
	Female	413.6 [347.3; 479.9] (23)	343.2 [298.5; 387.9] (1)	259.1 [127.1; 391.1] (9)
Age (years)	‹ 20	287.3 [178.7; 395.5] (7)	-	-
	20 - 60	470.7 [310.7; 630.7] (5)	-	-
	› 60	345.0 [253.2; 436.8] (3)	-	-
Postoperative after fracture treatment	3 - 7 d	63.1 [2.6; 123.6] (4)	-	23.8 [1.5; 46.0] (3)
	3 - 4 wk	126.9 [31.3; 225.5] (5)	-	70.3 [25.5; 115.2] (4)
	6 wk - 3 mo	176.2 [33.5; 318.8] (5)	-	102.1 [33.7; 170.5] (4)
Denture wearer	Total	269.0 [88.3; 449.8] (7)	-	-
Sex	Male	363.5 [58.5; 668.6] (4)	-	-
	Female	297.8 [37.3; 558.2] (4)	-	-
Partial denture wearer	Total	604.5 [557.0; 671.9] (2)	-	-
Sex	Male	632.4 [617.5; 647.4] (2)	-	-
	Female	527.0 [515.6; 538.4] (2)	-	-
Complete denture wearer	Total	131.5 [49.9; 213.1] (5)	-	-
Sex	Male	96.2 [6.7; 185.7] (2)	-	-
	Female	68.9 [5.5; 132.2] (2)	-	-

Abbreviations: MBF (maximum bite force), 95%CI (95% confidence interval), n (number of studies), d (days), wk (weeks), and mo (months).

Second, MBF for the healthy dentulous population in the three different age categories (‹20, 20-60, and › 60 years old) could be only evaluated in the molar region in the meta-analysis (Supplementary Fig. S1.3 and Table S5.3). MBF was 287.3 N [178.7; 395.5] in the ‹ 20 years old (until young adult), 470.7 N [310.7; 630.7] in the 20-60 (adults), and 345.0 N [253.2; 346.8] in the ›60 (elderly) individuals (p=0.18). The meta-regression analysis of bite force in different age categories for the male and the female population is shown in Table 2.

Table 2. Meta-regression analysis of mean maximum bite force in different age categories for the male and female population.

	Model Results	
	Estimate [95%CI]	p-value
Intercept	293.7 [162.1; 425.3]	‹.01
Age 20-60 (ref: ‹20 years)	116.6 [-41.8; 274.9]	0.15
Age ›60 (ref: ‹20 years)	4.0 [-193.5; 201.5]	0.97
Sex (ref: female)	95.1 [-47.5; 237.7]	0.19

Explanation: The estimate for the intercept correspond to the mean maximum bite force of a female under 20 years old. E.g., calculating the MBF for the male population between 20-60 years old: 293.69 + 116.56 + 95.12 = 505.37 N.
Abbreviations: CI (confidence interval at the lower and the upper limit), and p-value (considered significant ‹ .05).

Third, in the case of mandibular fracture treated with osteosynthesis, MBF was evaluated in three follow-up periods (2 to 7 days, 3 to 4 weeks, and between 6 weeks to 3 months postoperatively) (Supplementary Fig. S1.4 and Table S5.5). MBF in the molar region increased (Supplementary Fig. 1.4A), respectively: 63.1 N [2.6; 123.6], 126.9 N [31.3; 225.5], and 176.2 N [33.5; 318.8] in the follow-up. MBF in the incisal region also increased (Supplementary Fig. 1.4B), respectively: 23.8 N [1.5; 46], 70.3 N [25.5; 115.2], and 102.1 N [33.7; 170.5]. The studies did not report MBF measurement in the premolar region. Further, MBF for the male and the female population was not reported. Furthermore, three studies measured MBF preoperatively[78,83,90] (Supplementary Table S5.6). The mean preoperative molar MBF was 56.7 N (range 20.5 to 94.8 N), and the mean preoperative incisal MBF was 51.8 N (range 20.6 to 102.4 N). However, the studies did not report a clear statement regarding how the preoperative bite force measurements were conducted. Therefore, they were not included in the meta-analysis.

Fourth, MBF in the molar region for the denture wearer population (containing partial and complete edentulous subjects) was 269.0 N [88.3; 449.8] (Supplementary Fig. 1.5a), for the partial denture wearer population (containing partially edentulous subjects) was 604.5 N [557; 671.9] (Supplementary Fig. 1.5b and Table S5.7), and for the complete denture wearer population (containing complete edentulous subjects) was 131.5 N [49.9; 213.1] (Supplementary Fig. 1.5c and table S5.10). MBF was higher in the male versus the female population in the molar region, respectively: in the total denture wearer population it was 363.5 N [58.5; 668.6] versus 297.8 N [37.3; 558.2] with a difference of 65.7 N (p=0.75,

Table 3. Muscle force in Newtons (N).

Author (Year)			Abe et al (2006)[a]	Carlsoo (1952)[b]	Pruim et al. (1980)[c]	Mani et al. (2024)[d]	Bogdanov (2023)[d]
Population	number of participants		3	7	7	112	68
Sex	Male: Female		3:0	-	7:0	-	33:35
Age	Mean±SD and/or range (years)		29.6	-	-	-	18.4±6.1
Muscle	Masseter	Total	M: 471.8±50.3 (405.4-527.1) PM: 446.7±44.6 (385.8-491.1)	-	1279±351 (886-1772)	548±150.1 (350-820)	914.5±516.8
		Superficial	M: 166.3 PM: 152.1	R: 18.6 T: 980.7	-	-	-
		Profunda	M: 73.7 PM: 74.1	R: 23.5 T: 49	-	-	-
	Temporalis	Anterior	M: 166.3±17 (142.4-180.1) PM: 152.06±15.94 (131.5-143.5)	R: 22.6 T: 19.6	724±129 (608-930)	-	940.3±368.4
		Posterior	M: 73.7±16.4 (52.8-92.8) PM: 74.1±4.9 (69.2-80.7)	R: 37.3 T: 10.8	395±52 (304-462)	-	-
	Pterygoid	Lateral	-	-	757±211 (438-988)	-	-
		Medial	-	R: 27.5 T: 98.1	1279±351 (886-1772)	-	-

[a] Muscle force is shown for molar (M) and premolar (PM) maximum bite force.
[b] Muscle force is shown for rotational (R) and translational (T) movements.
[c] Combined muscle force of masseter and medial pterygoid is shown and not for each individual muscle separately.
[d] Muscle force is measured for the maximum molar bite force.
Abbreviations: n (number), SD (standard deviation), - (unknown or unclear).

Table 4. Mandible mechanical material properties.

Bone	Author (Year)	Cadaver (n)	Sex M:F	Age[a]	E- modulus Mean±SD (range)	Other Values Mean±SD (range)
Mandible	**Ashman et al. (1987)**	1 (Canine)	-	-	14.5 (10.8-19.4) [GPa]	• Elastic Coefficient: 11.4 (3.8-27.1) [GPa]
	Wright et al. (2016)	12 (TMJ)	6:6	M: 67.5 F: 70.3	M: 11.2±6.8 [MPa] F: 14.3±8.5 [MPa]	• Instantaneous Modulus: o M: 7±3.1 [MPa] o F: 8.4±4.1 [MPa] • Relaxed Modulus: o M: 3.2±1.5 [MPa] o F: 4.1±2.3 [MPa]
	Vitins et al. (2003)	5	5:0	49-56	M: 4.9±1.5 (3.9-5.5) [GPa]	• Flexura failure strain: 0.03±0.01 (3-4.1%) [mm/mm] • Flexural failure stress: 159.8±42.4 (60.8-256) [MPa] • Compressive stress: 19.7 (5-26.6) [MPa]
Cortical	**Schwartz-Dabney et al. (2003)**	10	7:3	48-81	10.0-29.9 [GPa]	• Cortical Thickness: 1.4-3.7 [mm] • Density: 1247-2024 [mg/cm3] • Shear Moduli: 4.3-8.2 [GPa] • Poisson Ratio: 0.1 (0.08-0.13)
Trabecular	**Nomura et al. (2007)**	1	0:1	66	F: 25±5.6 (14.4-33.7) [GPa] • Marginal: 23.7 [GPa] • Centre: 25.3 [GPa]	None

[a] Age: shown in mean or range in years.

Abbreviation: E-modulus (elastic modulus), n (number of cadavers), M (male), F (female), SD (standard deviation), mm (millimetre), mg/cm3 (milligram per cubic centimetre), GPa (gigapascal unit), MPa (megapascal unit), and TMJ (temporomandibular joint).

Supplementary Fig. 1.6a), in the partial denture wearer population it was 632.4 N [617.5; 647.4] versus 527.0 N [515.6; 538.4] with a difference of 105.4 N (p<0.0001, Supplementary Fig. 1.6b), and in the complete denture wearer population it was 96.2 N [6.7; 185.7] versus 68.9 N [5.5; 132.2] in the molar region with a difference of 27.3 N (p=0.63, Supplementary Fig. 1.6c). Finally, MBF in the premolar and the incisal region was not measured in the denture wearer studies.

Muscle force

For the muscle force (n=5), only the total masseter, masseter superficial, masseter profunda, temporalis anterior, temporalis posterior, lateral pterygoid, and medical pterygoid muscle force were found in the included studies (Table 3)[35,53,69,75,95]. Each study investigates the muscle force under different conditions, and the muscle grouping was not fully comparable between the studies.

Mandible material properties

In the cadaveric studies (n=5) where the mechanical material properties of the mandible were tested (Table 4), all studies evaluated the elastic modulus (E-modulus or Young's modulus) of the mandible[96–100]. In general, the mandible elastic modulus can range between 4.9 to 14.5 GPa (gigapascal unit)[96–98], for the mandibular cortical bone from 10 to 29.9 GPa[100], and for the mandibular trabecular bone from 14.4 to 33.7 GPa[99]. Furthermore, one study differentiated the elastic modulus difference at the temporomandibular joint (TMJ) between the male and the female mandibular cadavers, namely: 11.2 versus 14.3 MPa (megapascal unit)[97]. Finally, in each study, other types of mandibular material properties (e.g., Poisson ratio, compressive strength, shear modulus) were analysed with each measuring different properties.

DISCUSSION

This systematic review and meta-analysis aimed to identify the real physical test values of the essential input parameters required for an accurate mandibular finite element analysis (FEA). The study illustrates that not every essential parameter value for mandibular FEA analysis is known (e.g., fixation or boundary definition). Only the values of three main parameters were discovered, namely: (1) maximum bite force, (2) muscle force, and (3) mandible material properties.

Endpoint parameters

Maximum bite force (MBF) and meta-analysis heterogeneity

The systematic review shows that many factors can influence the MBF in an individual (e.g., measured bite force location, age, sex, and the presence of a fracture, or (partial)dentures) (Table 1 and Table 2). MBF variation and heterogeneity in the forest plots of the healthy dentulous population seems to be influenced by two components, namely: the population sampling characteristics, and the measurements-method variation.

Firstly, regarding the population sampling characteristics, the sample size, sex distribution, and participants' age were not similar in the included studies. In the case of sample size, most studies had a small number of participants resulting in a wide confidence interval, with nineteen studies having a size larger than 100[36,46,49–52,64,70–75,77,79,80,89,91,93], and two studies containing more than 1000 subjects[36,51]. In terms of sex, there were only five studies with an equal number of male and female participants in their study population[37,47,59,61,64]. There were four studies that only included male participants[35,44,53,63], two studies that only included female subjects[54,65], and five studies that did not mention the sex of the participants[42,57,75,91,92]. The study shows male subjects exhibiting higher MBF compared to female population. Regarding age, ten studies differentiated MBF in different age categories[39,40,46,51,52,59,71,72,80,92]. Additionally, there were eleven studies that only included children and/or adolescents[36,42,50,51,58,71,72,81,85,87,92], six studies with a mix of children and adult participants[39,43,46,52,59,80], thirty studies that included young adults and/or adults[35,37,38,40,41,43–45,47,48,54,56,57,59,62,63,65,67–70,73–77,79,82,89,94], nine studies that included partly or fully an elderly population[38,40,49,52,62,73,79,80,93], and two studies that did not mention the age at all[53,91]. In the study, higher MBF was measured in adults aged 20-60 years, followed by those under 20 and over 60. Additionally, six studies demonstrated an increase in MBF for in adolescents compared to young children[39,46,51,52,72,80]. Therefore, in future MBF studies, it is advisable to have a large sample size, with an equal number of male and female participants distributed within a standardised age category system. Regarding the type of occlusion, three studies investigated the MBF for different types of occlusions[36,57,58], with all studies illustrating a higher MBF in normal occlusion subjects versus malocclusion groups. Concerning facial morphology, three studies evaluated the facial dimension using cephalometric measurements and concluded that facial morphology may correlate with the amount of MBF[47,54,57]. Regarding dental restoration history (e.g., caries or cavities), four studies investigated this topic and concluded a higher MBF in non-caries or after caries treatment[42,81,87,91]. Concerning the dental stage (primary versus permanent teeth), two studies mentioned the effect and concluded an increase in MBF during different dentition stages from early primary to permanent dentition[51,72]. Dominant versus non-dominant biting side effects were examined in one study[45], with a significantly higher force generated in the dominant side in both male and female subjects. Furthermore, body mass index (BMI) seems to have no significant effect on MBF[37,47,59,77]. Finally, other factors such as the effect of tooth wear (ranging from slight to advanced wear), ethnicity, or the exact location of MBF measurement (e.g., first or second molar) should be taken into consideration in future studies.

Secondly, the measurement method may vary in the studies. There were only eight studies reporting whether their device was calibrated in advance[40,41,47,53,54,60,68,72]. Further, variations in the number of measurements, biting duration, and inter-measurement resting time may influence the outcomes. Most studies measured the bite force three times[35–42,45,47,48,51,54,57,59,70,72,74–76,81,85,87,91,94]. There were four studies that measured the bite force only twice[43,46,63,77], five studies measured it more than three times[65–67,80,92], and seventeen studies did not mention it or contain unclear description[44,49,50,52,53,56,61,62,69,71,73,76,79,81,89,90,93]. In general, the biting duration was only a few seconds in all the included studies but the

rest time between each repeated measurement varied with a range of 2 to 120 seconds[35–94]. Therefore, it is advisable to consider these aspects in future MBF studies.

Finally, MBF is influenced by the presence of dentures or fractures. In the case of partial versus complete edentulous subjects, the study shows a higher force in partial denture wearers[37,38,64] compared to complete denture wearers[55,60,61,66,86]. However, it would be interesting to further investigate MBF for the partial and complete edentulous subjects (e.g., teeth number and names as well as denture type and location). Additionally, the mean MBF value obtained from the meta-analysis was unexpectedly higher in partial denture wearers (n=2) compared to individuals with healthy dentition (n=35). This discrepancy may be attributed to the limited number of studies on partial denture wearers with a relatively small sample size and including only adult participants with a mean age of 43 years. This may have affected the robustness of the outcomes and contributed to notably high bite force values reported in those specific studies. As such, further research is recommended to draw more reliable conclusions.

In the case of mandibular fracture, only six studies investigated MBF in patients with non-comminuted mandibular fracture treated with osteosynthesis[78,82–84,88,90]. All studies illustrated MBF increase in the follow-up periods. However, the postoperative bite force increase is much less compared to the MBF in the normal healthy non-fractured mandible, showing a factor of 2.5 in the molar region and a factor of 2 in the incisal region for the mean MBF difference between the healthy dentulous population versus the 3 months postoperative fractured mandible subjects. Furthermore, it would be advisable to further investigate the effect of fracture type (e.g., simple versus comminuted) and osteosynthesis system (e.g., single versus double 2.0 mm titanium miniplate) on MBF development.

Muscle force

Only five studies were found where the muscle force was examined (Table 3)[35,53,69,75,95]. It was not possible to make subgroups or conduct a meta-analysis due to the limited and incomparable data. The studies give an impression of muscle forces; however, it would be challenging to apply the values in the mandibular FEA simulation. Firstly, the studies only show the muscle forces for the total masseter, masseter superficial, masseter profunda, temporalis anterior, temporalis posterior, lateral pterygoid, and medical pterygoid muscles. Nevertheless, each study uses different muscle groups and applies different methodologies. Therefore, they are not comparable. Secondly, the studies used EMG (electromyography for measuring muscle force) but did not clarify the full condition where the bite force was measured (e.g., resting or biting; in case of biting at what bite force). Thirdly, two studies used only male subjects[35,53], one study a mix of male and female subjects[69], and two studies did not mention the sex in their studies[75,95]. Therefore, none of the studies could be applied to the female subjects. Finally, regarding participants age, only two studies mention the mean age[35,69], one study only provided the age range[75], and two studies not mentioning it[53,95]. Therefore, it is recommendable to have more extensive future studies where the

muscle force is physically measured (e.g., using electromyography). Preferably, using a large sample size, with a better differentiation of force in the male versus the female subjects at different age categories or age ranges.

Mandible material properties

There were five studies found where the mechanical material properties of the mandible were investigated based on the physical testing of human cadaveric mandibles (Table 4)[96–100]. It was not possible to conduct a meta-analysis due to the limited and incomparable data. All the studies measured the elastic modulus (E-modulus or Young's modulus) of the mandible. However, the testing in the studies was done under different conditions and test setups. From the five included studies, three studies measured the mandibular E-modulus as a whole (no differentiation between the cortical and the trabecular bone) with wide interstudy variations[96–98], one study measured the E-modulus in the mandibular cortical bone (10-29.90 GPa)[100], and one study measured it for the trabecular bone in the temporomandibular joint (14.4-33.70 GPa)[99]. Further, in one study the E-modulus was investigated in the male and the female cadavers, respectively 11.20 versus 14.3 MPa, illustrating a lower E-modulus compared to the rest of the included studies[97]. Furthermore, the included studies also investigated other material properties (e.g., shear modulus, or Poisson ratio), but each study investigated different properties. Therefore, the literature gives a good overview of the mandibular E-modulus; however, it is wise to see more future investigations on this topic. Preferably, investigating the material properties for different bone sections simultaneously (cortical versus trabecular bone), with a larger sample size to differentiate the properties between the sexes and if possible, for different age categories.

Other parameters

There were no studies found in the literature regarding the fixture or fixation definition (temporomandibular joint), and the boundary conditions (interactions between the components). This can be explained by the fact that these components are difficult to define by means of physical in vivo testing. However, if possible, it would be of great interest to have future studies focusing on these topics.

Quality of evidence

The risk of bias assessment of the included studies illustrates that all the studies contain two or more domains with a high risk of bias (Fig. 2). For the NIH and Minors checklist, there were also components that were not applicable due to the nature of the study (e.g., no follow-up or control group). In all the studies, it seems that the participants (in the bite and muscle force studies) and the assessors (in all the studies) were not blinded to the applied measurement method and the outcomes of the study, while this should be possible by preventing any visual availability of the data during the measurements. In few studies, the methodology was not sufficiently described, or it lacked detailed information (e.g., regarding the sample size justification in the force measurement studies, or how the cadavers were obtained in the mandible material properties studies). Furthermore,

the general application of the statistics was limited or not present in most of the studies. However, the nature of the study justifies the choices made in the literature studies. Finally, the included studies did not declare any conflict of interest. Ten studies declared that their research was funded or used a grant[41,46,49,51,52,62,70,86,93,97]; no indication has been found that the funding organisations did have a role in the design and conduct of the study.

Strength

This study is, to our knowledge, the first of its kind. The systematic review and meta-analysis were performed following a prespecified and transparent protocol, and was conducted in accordance to the PRIMSA statement[30] and the Cochrane Handbook[29], following the current guidelines of systematic reviews with meta-analysis. The search strategy was composed by a medical information specialist, incorporating board search terms to ensure that no relevant articles were missed during the search. However, this led to a large volume of retrieved articles during tile and abstract screening phase, which resulted in an extended time for the reviewers to thoroughly screen all the articles. The literature screening was performed by two independent reviewers with a good inter-observer agreement. Furthermore, the data eligibility, data extraction, and risk of bias assessment were also done independently by two reviewers. In the end, the data- and meta-analysis were conducted in detail and clearly defined in the study. Finally, this systematic review shows the exact values of the known essential parameters needed for the mandibular FEA, illustrates the literature discrepancies, and reveals the unknown or unclear parameters.

Comparison to other systematic reviews

There is no previous systematic review comparable to our study. We found one review regarding the patient specific FEA models of the human mandible where the author discussed the lack of consensus on the current set-ups[2]. Furthermore, another review was found where the FEA application in OMF surgery was evaluated[1]. Both reviews illustrate that there are many uncertainties regarding the application of the FEA to OMF surgery. It illustrates that there is a need for consensus in the current FEA setups. However, they are only general reviews that also included in silico studies and did not contain any meta-analysis. Therefore, the current systematic review is an essential study that can be used as tool for future mandibular FEA studies.

Limitations

The study only shows the true physical in vivo test values of three essential parameters (bite force, muscle force, and mandible material properties), with no values found for the other essential parameters (fixture or fixation, and boundary conditions) due to lack of found studies in the literature (in accordance with our study protocol) (Table 1-4). Only including in vivo studies may explain the absence of fixation and boundary condition values, where these parameters might be evaluated by other type of studies (e.g., in silico). Further, no subgroup or meta-analysis could be conducted for muscle force and material property studies, due to incomparable data or lack of sufficient data. The subgroup and meta-analysis could be

only done for the bite force studies. For the bite force studies, the inter-study observation showed a wider range of MBF with heterogeneity that is probably caused by differences in the population sampling characteristics and the measurement method variations. All the included studies contained a certain risk of bias which may have an influence on the data (Supplementary Table S4).

Implication for future research

This study gives a straightforward and transparent overview of the maximum bite force, muscle force, and mandible material properties which can be used in the mandibular FEA studies. Therefore, the review can be used as guideline for illustrating the mandibular FEA input parameters. The study further illustrates that there are still uncertainties regarding some of the parameter values for the mandibular FEA. Therefore, it would be of a great interest to see more extensive in vivo studies regarding the muscle force and mandible material properties to get more diverse values (e.g., according to different age categories and sex). Furthermore, if possible, it would be attractive to conduct in vivo studies to measure the fixture or fixation and boundary condition values (e.g., measuring friction).

Conclusions

This systematic review presents the exact known mandibular FEA parameters based on real physical in vivo experiments, namely: the maximum bite force, muscle force, and mandible material properties. The study illustrates that MBF has been extensively measured in the literature where the values can certainly be used in the mandibular FEA simulations. Regarding the muscle force, the values can be implemented in a general mandibular FEA model; however, it was not possible to determine the exact muscle force values for specific cases (e.g., based on sex, age, or biting condition). Therefore, future analysis is required to obtain more diverse and accurate values when it comes to different scenarios (e.g., different age categories, or sex), and a clear definition of how muscle force is measured (e.g., at rest or biting; in case of biting the location of applied force: e.g., molar, incisal, unilateral, or bilateral). Concerning the mandible material properties, the mechanical properties of the mandibular bone can be incorporated into an FEA model; however, it was not possible to define a single exact value for each mandibular bone property (e.g., elastic modulus, Poisson's ratio). Consequently, it is sensible to conduct more studies on this topic based on different age categories, sex, and bone segments (e.g., cortical, trabecular). Furthermore, the study did not find any values for how to properly define the fixture or fixation (e.g., temporomandibular joint, or mandibular ligament attachments), and the boundary conditions (interaction between the components, friction, or tolerance). Therefore, it is necessary to devise a method to measure these currently unknown parameters. In conclusion, this systematic review and meta-analysis provide a comprehensive overview of the known and unknown in vivo tested input parameter values for the mandibular FEA.

REFERENCES

1. Lisiak-Myszke, M. *et al.* Application of Finite Element Analysis in Oral and Maxillofacial Surgery—A Literature Review. *Materials* **13**, 3063 (2020).
2. Merema, B. B. J., Kraeima, J., Glas, H. H., Spijkervet, F. K. L. & Witjes, M. J. H. Patient-specific finite element models of the human mandible: Lack of consensus on current set-ups. *Oral Dis* **27**, 42–51 (2021).
3. Daqiq, O., Roossien, C. C., Wubs, F. W. & van Minnen, B. Biomechanical assessment of mandibular fracture fixation using finite element analysis validated by polymeric mandible mechanical testing. *Sci Rep* **14**, 11795 (2024).
4. Daqiq, O., Roossien, C. C., Wubs, F. W., Bos, R. R. M. & van Minnen, B. Optimisation of osteosynthesis positioning in mandibular body fracture management using finite element analysis. *Eur J Transl Clin Med* **6**, 10–25 (2023).
5. Aquilina, P., Chamoli, U., Parr, W. C. H., Clausen, P. D. & Wroe, S. Finite element analysis of three patterns of internal fixation of fractures of the mandibular condyle. *British Journal of Oral and Maxillofacial Surgery* **51**, 326–331 (2013).
6. Szucs, A., Bujtár, P., Sándor, G. K. B. & Barabás, J. Finite element analysis of the human mandible to assess the effect of removing an impacted third molar. *J Can Dent Assoc* **76**, a72 (2010).
7. Xue, R. *et al.* Finite element analysis and clinical application of 3D-printed Ti alloy implant for the reconstruction of mandibular defects. *BMC Oral Health* **24**, 95 (2024).
8. Gupta, A., Dutta, A., Dutta, K. & Mukherjee, K. Biomechanical influence of plate configurations on mandible subcondylar fracture fixation: a finite element study. *Med Biol Eng Comput* **61**, 2581–2591 (2023).
9. Dario, V., Michelangelo-Santo, G., Roberto, B. & Fabio, F. Is All-on-four effective in case of partial mandibular resection? A 3D finite element study. *J Stomatol Oral Maxillofac Surg* **124**, 101463 (2023).
10. Anthrayose, P., Nawal, R. R., Yadav, S., Talwar, S. & Yadav, S. Effect of revascularisation and apexification procedures on biomechanical behaviour of immature maxillary central incisor teeth: a three-dimensional finite element analysis study. *Clin Oral Investig* **25**, 6671–6679 (2021).
11. Limjeerajarus, N. *et al.* Comparison of ultimate force revealed by compression tests on extracted first premolars and FEA with a true scale 3D multi-component tooth model based on a CBCT dataset. *Clin Oral Investig* **24**, 211–220 (2020).
12. Kilinç, Y., Erkmen, E. & Kurt, A. Biomechanical Evaluation of Different Fixation Methods for Mandibular Anterior Segmental Osteotomy Using Finite Element Analysis, Part One. *Journal of Craniofacial Surgery* **27**, 32–35 (2016).
13. Strang, Gilbert. & Fix, G. Joseph. *An Analysis of the Finite Element Method.* (Prentice-Hall, Englewood Cliffs (N.J.), 1973).
14. Hart, R. T., Hennebel, V. V., Thongpreda, N., Van Buskirk, W. C. & Anderson, R. C. Modeling the biomechanics of the mandible: A three-dimensional finite element study. *J Biomech* **25**, 261–286 (1992).
15. Adamović, P., Matoc, L., Knežević, P., Sabalić, S. & Kodvanj, J. Biomechanical analysis of a novel screw system with a variable locking angle in mandible angle fractures. *Med Biol Eng Comput* **61**, 2951–2961 (2023).
16. Ruf, P. *et al.* Biomechanical evaluation of CAD/CAM magnesium miniplates as a fixation strategy for the treatment of segmental mandibular reconstruction with a fibula free flap. *Comput Biol Med* **168**, 107817 (2024).
17. Sancar, B., Çetiner, Y. & Dayı, E. Evaluation of the pattern of fracture formation from trauma to the human mandible with finite element analysis. Part 1: Symphysis region. *Dental Traumatology* **39**, 352–360 (2023).
18. Sancar, B., Çetiner, Y. & Dayı, E. Evaluation of the pattern of fracture formation from trauma to the human mandible with finite element analysis. Part 2: The corpus and the angle regions. *Dental Traumatology* **39**, 437–447 (2023).
19. Schönegg, D., Koch, A., Müller, G. T., Blumer, M. & Wagner, M. E. H. Two-screw osteosynthesis of the mandibular condylar head with different screw materials: a finite element analysis. *Comput Methods Biomech Biomed Engin* 1–5 (2023) doi:10.1080/10255842.2023.2209247.
20. Patil, P. G., Seow, L. L., Uddanwadikar, R., Pau, A. & Ukey, P. D. Different implant diameters and their effect on stress distribution pattern in 2-implant mandibular overdentures: A 3D finite element analysis study. *J Prosthet Dent* **131**, 675–682 (2024).
21. Ammar, H. H., Ngan, P., Crout, R. J., Mucino, V. H. & Mukdadi, O. M. Three-dimensional modeling and finite element analysis in treatment planning for orthodontic tooth movement. *American Journal of Orthodontics and Dentofacial Orthopedics* **139**, e59–e71 (2011).

22. Patussi, C. *et al.* Evaluation of different stable internal fixation in unfavorable mandible fractures under finite element analysis. *Oral Maxillofac Surg* **23**, 317–324 (2019).
23. Aftabi, H. *et al.* Computational models and their applications in biomechanical analysis of mandibular reconstruction surgery. *Comput Biol Med* **169**, 107887 (2024).
24. Altuncu, F., Kazan, D. & Özden, B. Comperative evaluation of the current and new design miniplate fixation techniques of the advanced sagittal split ramus osteotomy using three-dimensional finite element analysis. *Med Oral Patol Oral Cir Bucal* **28**, 0–0 (2020).
25. Falcinelli, C., Valente, F., Vasta, M. & Traini, T. Finite element analysis in implant dentistry: State of the art and future directions. *Dental Materials* **39**, 539–556 (2023).
26. Maintz, M. *et al.* Parameter optimization in a finite element mandibular fracture fixation model using the design of experiments approach. *J Mech Behav Biomed Mater* **144**, 105948 (2023).
27. Guerra, R. C. *et al.* Finite element analysis of low-profile reconstruction plates for atrophic mandibles: a comparison of novel 3D grid and conventional plate designs. *Oral Maxillofac Surg* **28**, 595–603 (2024).
28. Garutti, F. C. M. B., Lehmann, R. B., Gialain, I. O. & Lima, F. F. B. de. Analysis of the atrophic mandible rehabilitated with fixed total prosthesis on mono or bicortical implants. *Braz Dent J* **35**, e245621 (2024).
29. Higgins, JPT. *et al. Cochrane Handbook for Systematic Reviews of Interventions Version 6.4 (Updated August 2023).* (Cochrane, 2023).
30. Liberati, A. *et al.* The PRISMA statement for reporting systematic reviews and meta-analyses of studies that evaluate health care interventions: explanation and elaboration. *J Clin Epidemiol* **62**, e1-34 (2009).
31. Bramer, W. M., Giustini, D., de Jonge, G. B., Holland, L. & Bekhuis, T. De-duplication of database search results for systematic reviews in EndNote. *J Med Libr Assoc* **104**, 240–3 (2016).
32. Ma, L.-L. *et al.* Methodological quality (risk of bias) assessment tools for primary and secondary medical studies: what are they and which is better? *Mil Med Res* **7**, 7 (2020).
33. Slim, K. *et al.* Methodological index for non-randomized studies (minors): development and validation of a new instrument. *ANZ J Surg* **73**, 712–6 (2003).
34. Wilke, J. *et al.* Appraising the methodological quality of cadaveric studies: validation of the QUACS scale. *J Anat* **226**, 440–6 (2015).
35. Abe, M., Medina-Martinez, R. U., Itoh, K. & Kohno, S. Temporomandibular joint loading generated during bilateral static bites at molars and premolars. *Med Biol Eng Comput* **44**, 1017–1030 (2006).
36. Abu-Alhaija, E., Owais, A. & Obaid, H. Maximum occlusal bite force in pre-school children with different occlusal patterns. *J Clin Exp Dent* **10**, 0–0 (2018).
37. AL-Omiri, M. K. *et al.* Maximum bite force following unilateral implant-supported prosthetic treatment: within-subject comparison to opposite dentate side. *J Oral Rehabil* **41**, 624–629 (2014).
38. Al-Zarea, B. K. Maximum Bite Force following Unilateral Fixed Prosthetic Treatment: A Within-Subject Comparison to the Dentate Side. *Medical Principles and Practice* **24**, 142–146 (2015).
39. Braun, S. *et al.* A study of maximum bite force during growth and development. *Angle Orthod* **66**, 261–4 (1996).
40. Chong, M. X., Khoo, C. D., Goh, K. H., Rahman, F. & Shoji, Y. Effect of age on bite force. *J Oral Sci* **58**, 361–363 (2016).
41. de Abreu, R. A. M. *et al.* Masticatory efficiency and bite force in individuals with normal occlusion. *Arch Oral Biol* **59**, 1065–1074 (2014).
42. Gudipaneni, R. K., Alam, M. K., Patil, S. R. & Karobari, M. I. Measurement of the Maximum Occlusal Bite Force and its Relation to the Caries Spectrum of First Permanent Molars in Early Permanent Dentition. *Journal of Clinical Pediatric Dentistry* **44**, 423–428 (2020).
43. Helkimo, E., Carlsson, G. E. & Helkimo, M. Bite force and state of dentition. *Acta Odontol Scand* **35**, 297–303 (1977).
44. Helkimo, E. & Ingervall, B. Bite force and functional state of the masticatory system in young men. *Swed Dent J* **2**, 167–75 (1978).
45. Khan, S. I. R., Rao, D., Ramachandran, A. & Ashok, B. V. Comparison of bite force on the dominant and nondominant sides of patients with habitual unilateral chewing: a pilot study. *Gen Dent* **68**, 60–63 (2020).
46. Kiliaridis, S., Kjellberg, H., Wenneberg, B. & Engström, C. The relationship between maximal bite force, bite force endurance, and facial morphology during growth: A cross-sectional study. *Acta Odontol Scand* **51**, 323–331 (1993).
47. Koç, D., Doğan, A. & Bek, B. Effect of gender, facial dimensions, body mass index and type of functional occlusion on bite force. *J Appl Oral Sci* **19**, 274–9 (2011).
48. Linderholm, H. & Wennström, A. Isometric bite force and its relation to general muscle forge and body build. *Acta Odontol Scand* **28**, 679–89 (1970).

49. Miura, H., Watanabe, S., Isogai, E. & Miura, K. Comparison of maximum bite force and dentate status between healthy and frail elderly persons. *J Oral Rehabil* **28**, 592–5 (2001).
50. Mountain, G., Wood, D. & Toumba, J. Bite force measurement in children with primary dentition. *Int J Paediatr Dent* **21**, 112–8 (2011).
51. Owais, A. I., Shaweesh, M. & Abu Alhaija, E. S. J. Maximum occusal bite force for children in different dentition stages. *Eur J Orthod* **35**, 427–33 (2013).
52. Palinkas, M. *et al.* Age and gender influence on maximal bite force and masticatory muscles thickness. *Arch Oral Biol* **55**, 797–802 (2010).
53. Pruim, G. J., de Jongh, H. J. & ten Bosch, J. J. Forces acting on the mandible during bilateral static bite at different bite force levels. *J Biomech* **13**, 755–63 (1980).
54. Ringqvist, M. Isometric bite force and its relation to dimensions of the facial skeleton. *Acta Odontol Scand* **31**, 35–42 (1973).
55. Rismanchian, M., Bajoghli, F., Mostajeran, Z., Fazel, A. & Eshkevari, P. sadr. Effect of implants on maximum bite force in edentulous patients. *J Oral Implantol* **35**, 196–200 (2009).
56. Sasaki, K., Hannam, A. G. & Wood, W. W. Relationships between the size, position, and angulation of human jaw muscles and unilateral first molar bite force. *J Dent Res* **68**, 499–503 (1989).
57. Sathyanarayana, H. P., Premkumar, S. & Manjula, W. S. Assessment of maximum voluntary bite force in adults with normal occlusion and different types of malocclusions. *J Contemp Dent Pract* **13**, 534–8 (2012).
58. Singh, S., Sandhu, N. & Kashyap, R. A Study of Bite Force and Various Variables in Children Segregated by Angle's Classification. *Int J Clin Pediatr Dent* **5**, 118–23 (2012).
59. Takaki, P., Vieira, M. & Bommarito, S. Maximum bite force analysis in different age groups. *Int Arch Otorhinolaryngol* **18**, 272–6 (2014).
60. Tortopidis, D., Lyons, M. F. & Baxendale, R. H. Bite force, endurance and masseter muscle fatigue in healthy edentulous subjects and those with TMD. *J Oral Rehabil* **26**, 321–8 (1999).
61. Tripathi, G. *et al.* Comparative evaluation of maximum bite force in dentulous and edentulous individuals with different facial forms. *J Clin Diagn Res* **8**, ZC37-40 (2014).
62. van der Bilt, A., Tekamp, A., van der Glas, H. & Abbink, J. Bite force and electromyograpy during maximum unilateral and bilateral clenching. *Eur J Oral Sci* **116**, 217–22 (2008).
63. van Eijden, T. M. Three-dimensional analyses of human bite-force magnitude and moment. *Arch Oral Biol* **36**, 535–9 (1991).
64. Vozza, I. *et al.* The Effects of Wearing a Removable-Partial-Denture on the Bite Forces: A Cross-Sectional Study. *Int J Environ Res Public Health* **18**, (2021).
65. Wennström, A. Psychophysical investigation of bite force. 1. Bite force in healthy adult women. *Sven Tandlak Tidskr* **64**, 807–19 (1971).
66. Wennström, A. Psychophysical investigation of bite force. 2. Studies in individuals with full dentures. *Sven Tandlak Tidskr* **64**, 821–8 (1971).
67. Widmalm, S. E. & Ericsson, S. G. Maximal bite force with centric and eccentric load. *J Oral Rehabil* **9**, 445–50 (1982).
68. Zivko-Babić, J. *et al.* Bite force in subjects with complete dentition. *Coll Antropol* **26**, 293–302 (2002).
69. Bogdanov, V. Type of correlation between bite force and EMG activity of the temporalis and masseter muscles during maximal and submaximal clenching. *Folia Med (Plovdiv)* **65**, 975–985 (2023).
70. Ustrell-Barral, M., Zamora-Olave, C., Khoury-Ribas, L., Rovira-Lastra, B. & Martinez-Gomis, J. Reliability, reference values and factors related to maximum bite force measured by the Innobyte system in healthy adults with natural dentitions. *Clin Oral Investig* **28**, 620 (2024).
71. de Sonnaville, W. F. C. *et al.* Reliability and measurement error of anterior maximum voluntary bite force in children with juvenile idiopathic arthritis and healthy children. *PLoS One* **18**, e0280763 (2023).
72. Mutt, N. H. *et al.* Estimation of Maximum Occlusal Bite Force of School-going Children in Different Dentition: A Cross-sectional Study. *Int J Clin Pediatr Dent* **16**, 804–809 (2023).
73. Nimura, K., Shiga, H. & Yokoyama, M. Relationships of physical constitution with occlusal force and masticatory performance in adults with natural dentition. *Odontology* **111**, 1018–1024 (2023).
74. Ranjan, M. *et al.* A Preliminary Report of Maximum Voluntary Bite Force of Young Indian Population. *J Pharm Bioallied Sci* **16**, S803–S805 (2024).
75. Mani, U., Arun, A. & Mohamed, K. Validation and Analysis of an Integrated Device for Recording Bite Force and Masseter Muscle Activity in Dentate Participants: An Observational Study. *JOURNAL OF CLINICAL AND DIAGNOSTIC RESEARCH* (2024) doi:10.7860/JCDR/2024/71177.20147.

76. Reddy, N. A. *et al.* COMPARISON OF PERIODONTAL PARAMETERS, BITE FORCE, STRESS IN PERIODONTITIS AND HEALTHY INDIVIDUALS: CASE CONTROL STUDY. *J Pharm Negat Results* **13**, 8014–8032 (2022).
77. Ahlberg, J. P. *et al.* Maximal Bite Force and Its Association with Signs and Symptoms of TMD, Occlusion, and Body Mass Index in a Cohort of Young Adults. *CRANIO®* **21**, 248–252 (2003).
78. Ahmed, S. *et al.* A comparative study on evaluation of role of 1.5 mm microplates and 2.0 mm standard miniplates in management of mandibular fractures using bite force as indicator of recommendation. *Natl J Maxillofac Surg* **7**, 39 (2016).
79. Bakke, M., Michler, L., Han, K. & Möller, E. Clinical significance of isometric bite force versus electrical activity in temporal and masseter muscles. *Scand J Dent Res* **97**, 539–51 (1989).
80. Bakke, M., Holm, B., Jensen, B. L., Michler, L. & Möller, E. Unilateral, isometric bite force in 8-68-year-old women and men related to occlusal factors. *Scand J Dent Res* **98**, 149–58 (1990).
81. Kampe, T., Haraldson, T., Hannerz, H. & Carlsson, G. E. Occlusal perception and bite force in young subjects with and without dental fillings. *Acta Odontol Scand* **45**, 101–107 (1987).
82. Kshirsagar, R., Jaggi, N. & Halli, R. Bite Force Measurement in Mandibular Parasymphyseal Fractures: A Preliminary Clinical Study. *Craniomaxillofac Trauma Reconstr* **4**, 241–244 (2011).
83. Kumar, S. *et al.* Comparative evaluation of bite forces in patients after treatment of mandibular fractures with miniplate osteosynthesis and internal locking miniplate osteosynthesis. *J Int Soc Prev Community Dent* **4**, 26 (2014).
84. Rastogi, S., Reddy, M. P., Swarup, A. G., Swarup, D. & Choudhury, R. Assessment of Bite Force in Patients Treated with 2.0-mm Traditional Miniplates versus 2.0-mm Locking Plates for Mandibular Fracture. *Craniomaxillofac Trauma Reconstr* **9**, 62–8 (2016).
85. Rentes, A. M., Gavião, M. B. D. & Amaral, J. R. Bite force determination in children with primary dentition. *J Oral Rehabil* **29**, 1174–1180 (2002).
86. Sener, I. *et al.* The effect of implant therapy on maximum bite force in edentulous elderly patients: An in vivo study. *Turkish Journal of Geriatrics* **18**, 75–80 (2015).
87. Singh, R. *et al.* Comparative evaluation of bite force in paediatric patients. *J Family Med Prim Care* **9**, 2002–2005 (2020).
88. Sybil, D. & Gopalkrishnan, K. Assessment of masticatory function using bite force measurements in patients treated for mandibular fractures. *Craniomaxillofac Trauma Reconstr* **6**, 247–50 (2013).
89. Ali Alkhalaf, Z. *et al.* Unveiling the Influence of the Curve of Spee on Bite Force and Chewing Ability: A Comparative Study. *Int J Clin Pract* **2024**, 1–9 (2024).
90. Gamit, M. *et al.* Comparison of bite force evaluation for mandibular angle fracture fixation by conventional miniplates versus new design miniplates: a clinical study. *Oral Maxillofac Surg* **28**, 645–652 (2023).
91. Munisekhar, M. S. *et al.* Assessment of Bite Forces in Restored Teeth with Different Commonly Used Restorative Materials: A Comparative Study. *Pesqui Bras Odontopediatria Clin Integr* **23**, (2023).
92. Wasinwasukul, P., Nalamliang, N., Pairatchawan, N. & Thongudomporn, U. Effects of anterior bite planes fabricated from acrylic resin and thermoplastic material on masticatory muscle responses and maximum bite force in children with a deep bite: A 6-month randomised controlled trial. *J Oral Rehabil* **49**, 980–992 (2022).
93. Kashiwazaki, K. *et al.* Improvements in Maximum Bite Force with Gum-Chewing Training in Older Adults: A Randomized Controlled Trial. *J Clin Med* **12**, 6534 (2023).
94. Al Qassar, S. S. S., Mavragani, M., Psarras, V. & Halazonetis, D. J. The anterior component of occlusal force revisited: direct measurement and theoretical considerations. *The European Journal of Orthodontics* **38**, 190–196 (2016).
95. Carlsoo, S. Nervous coordination and mechanical function of the mandibular elevators; and electromyographic study of the activity, and an anatomic analysis of the mechanics of the muscles. *Acta Odontol Scand Suppl* **10**, 1–132 (1952).
96. Ashman, R. B. & Van Buskirk, W. C. The Elastic Properties of a Human Mandible. *Adv Dent Res* **1**, 64–67 (1987).
97. Wright, G. J. *et al.* Tensile biomechanical properties of human temporomandibular joint disc: Effects of direction, region and sex. *J Biomech* **49**, 3762–3769 (2016).
98. Vitins, V., Dobelis, M., Middleton, J., Limbert, G. & Knets, I. Flexural and creep properties of human jaw compact bone for FEA studies. *Comput Methods Biomech Biomed Engin* **6**, 299–303 (2003).
99. Nomura, T., Katz, J. L., Powers, M. P. & Saito, C. A micromechanical elastic property study of trabecular bone in the human mandible. *J Mater Sci Mater Med* **18**, 629–633 (2007).
100. Schwartz-Dabney, C. L. & Dechow, P. C. Variations in cortical material properties throughout the human dentate mandible. *Am J Phys Anthropol* **120**, 252–77 (2003).

OTHER INFORMATION

Registration and protocol

A protocol for this systematic review was specified in advance and published on 7 April 2022 in the PROSPERO (registration number CRD42022315303) (www.crd.york.ac.uk/PROSPERO).

Data availability

Data is provided within the supplementary information files. Further, the manuscript is written in accordance to PRISMA checklist. Furthermore, all data are available from corresponding author upon reasonable request.

Acknowledgments

We would like to thank Ms. S. van der Werf (Medical Information Specialist at the University of Groningen) for her assistance in composing the search strategy.

Competing of interest

The authors state that they have no conflict of interests.

Funding

No funding was received to conduct this study.

Authors contribution

O.D. was responsible for the whole study (including study design, study set-up, article screening, data extraction, data, analysis, risk of bias assessment, and writing the manuscript). O.D. and B.G. did the article screening with B.v.M. as a third reviewer in case if needed. B.G. conducted the meta-analysis. Further, B.G. and B.v.M. assisted throughout the study (e.g., study protocol, composing the search strategy, data collection, and data-analysis), provided continuous guidance, and helped with writing the manuscript. F.K.L. Spijkervet, F.W.W. and C.C.R. provided additional guidance and proofread the manuscript. The authors approve the manuscript.

Informed consent

Not applicable. For this type of study, formal consent is not required.

Supplementary material overview

- **Supplementary Table S1.** Electronic database with corresponding search detail**.**
- **Supplementary Table S2.** Included studies characteristics
- **Supplementary Table S3.** Excluded studies after full-text screening with exclusion reasons.
- **Supplementary Fig. S1.** Meta-analysis forest plots
  - **Supplementary Fig. S1.1:** Maximum bite force in healthy dentulous individuals measure in the (**a**) molar, (**b**) premolar, and (**c**) incisal regions.

- **Supplementary Fig. S1.2.** Maximum bite force in healthy dentulous individuals for the male and the female population measured in the (**a**) molar, (**b**) premolar, and (**c**) incisal regions.
- **Supplementary Fig. S1.3.** Maximum bite force in dentulous individuals at different age categories in the molar region, namely: ‹ 20, 20-60, › 60 years old.
- **Supplementary Fig. S1.4.** Maximum force measurements in 3 postoperative follow-up (2-7 days, 3-4 weeks, and 6 weeks to 3 months) for the mandibular fractures treated with osteosynthesis in the (**a**) molar, and (**b**) incisal regions.
- **Supplementary Fig. S1.5.** Maximum bite force in mandibular denture wearer (partial or complete edentulous) subjects measured in the molar region: (**a**) total population (containing partial and complete denture wearer), and (**b**) partial denture wearer, and (**c**) complete denture wearer.
- **Supplementary Fig. S1.6.** Maximum bite force in mandibular denture wearer (partial or complete edentulous) subjects measured in the molar region for the male and the female population: (**a**) total population (containing partial and complete denture wearer), and (**b**) partial denture wearer, and (**c**) complete denture wearer.

- **Supplementary Table S4.** Maximum bite force (MBF) values.
  - **Supplementary Table S4.1.** Normal healthy dentulous population.
  - **Supplementary Table S4.2.** Normal healthy dentulous population for the male and the female population.
  - **Supplementary Table S4.3.** Normal healthy dentulous population in different age category.
  - **Supplementary Table S4.4.** Normal healthy dentulous population in different age category for the male and the female population.
  - **Supplementary Table S4.5.** Preoperative maximum bite force in non-comminuted simple fracted mandible.
  - **Supplementary Table S4.6.** Postoperative follow-up maximum bite force development in non-comminuted simple fracted mandible fixated with osteosynthesis.
  - **Supplementary Table S4.7.** Partial denture wearer.
  - **Supplementary Table S4.8.** Partial denture wearer for the male and the female population.
  - **Supplementary Table S4.9.** Edentulous individuals with complete dentures.
  - **Supplementary Table S4.10.** Edentulous individuals with complete dentures for the male and the female population.
  - Note: in all the supplementary tables S4:
    - Location: the location of recorded biteforce: molar, premolar, or incisal.
    - Age: the age is shown in Mean ± SD or range in brackets; shown in years.
    - Sample: n is the number of participants.
    - MBF: maximum bite force is shown in N (newtons); depending on the measurements (if applicable) illustrating: the Mean ± SD (standard deviation), range, SE (standard error).

Supplementary Table S1. Electronic database with corresponding search detail.

Database	Search terms	Initial search date	Hits	Updated search date	Additional hits after update
PubMed	("Mandible"[Mesh] OR "Mandibular Fractures"[Mesh] OR "Temporomandibular Joint"[Mesh] OR "Bite Force"[Mesh] OR mandib*[tiab] OR "lower jaw" OR ((condyle[tiab] OR subcond*[tiab] OR condilar[tiab] OR coronoid*[tiab] OR ramus[tiab] OR alveolar[tiab] OR symphys*[tiab] OR parasymphys*[tiab]) *AND* ("skull" OR maxillofac* OR crani* OR "jaw" OR "facial" OR "oral")) OR "bite force"[tiab] OR "masticatory force"[tiab]) AND ("Stress, Mechanical"[Mesh] OR "Biomechanical Phenomena"[Mesh:NoExp] OR mechanical[tiab] OR biomechanic*[tiab] OR bite force*[ti] OR mechanic*[ti] OR propert*[tiab] OR mechanobehav*[tiab] OR elasti*[tiab] OR strength[tiab]) NOT (("Animals"[Mesh] NOT "Humans"[Mesh]) OR "Case Reports"[pt] OR "Review" [pt])	14 September 2022	8476	6 November 2024	1257
Embase	('mandible'/exp OR 'mandible fracture'/exp OR 'temporomandibular joint'/exp OR 'mastication'/exp OR mandib*:ab,ti OR "lower jaw":ab,ti OR ((condyle:ab,ti OR subcond*:ab,ti OR condilar:ab,ti OR coronoid*:ab,ti OR ramus:ab,ti OR alveolar:ab,ti OR symphys*:ab,ti OR parasymphys*:ab,ti) *AND* ("skull" OR maxillofac* OR crani* OR "jaw" OR "facial" OR "oral")) OR "bite force":ab,ti OR "masticatory force":ab,ti) AND ('mechanical stress'/exp OR 'biomechanics'/exp OR (mechanical OR biomechanic* OR propert* OR mechanobehav*):ab,ti OR ('bite force*' OR mechanic*):ti) NOT (('animal'/exp NOT 'human'/exp) OR 'case report'/de OR 'review'/it OR 'conference abstract'/it)	14 September 2022	8399	6 November 2024	1277

Supplementary Table S2. Included studies characteristics

Author (Year)	Study design	Measurements	Groups	Sample (n)	Sex (Male:Female)	Age (mean±SD (range) in years)	Remarks
Abe et al. (2006)[35]	CS	BF (M, PM) MF	-	3	3:0	29.6	MF (Masseter force was measured at M and PM bite).
Abu-Alhaija et al. (2018)[36]	CS	BF (M)	Occlusion type: 1. Flush terminal 2. Mesial step 3. Distal step	1085 1. 335 2. 450 3. 300	515:570 1. 165:170 2. 200:250 3. 150:150	4.9±0.9 (3-6) 1. 4.8±0.9 2. 4.9±0.9 3. 5±0.8	Mean BF values were applied.
Ahlberg et al. (2003)[77]	C	BF (M, I)	Helkimo clinical dysfunction index score (Di0-DiIII).	430	222:208	(21-23)	Only healthy group with no clinical sign of dysfunction (Helkimo index Di0) included: M (n: 114) and I (n:116).
Ahmed et al. (2016)[78]	C	BF (M, I)	Fracture vs. Control: 1. Fracture 1.5 mm plate 2. Fracture 2.0 mm plate 3. Control non-fractured	70 1. 20 2. 20 3. 30	NM 1. 16:4 2. 17:3 3. NM	NM 1. 30.6 (18-55) 2. 30.7 (19-55) 3. 26.3 (18-24)	Unilateral fracture was fixated with single 1.5 or 2.0 mm osteosynthesis plate. Postoperative follow-up:1, 2, 4, and 6 wk.
Al-Omiri et al. (2014)[37]	CS	BF (M)	-	40	20:20	42.7±9.6 (28-57)	Unilateral 1st molar fixed partial denture vs. contralateral natural 1st molar dentate side.
Al-Qassar et al. (2015)[94]	CS	MBF (M)	-	30	16:14	(18-25)	-
Al-Zarea et al. (2015)[38]	CS	BF (M)	-	85	43:42	43±9 (28-66)	Unilateral 1st or 2nd molar fixed partial denture side vs. contralateral natural molar dentate side.
Ali Alkhalaf et al. (2024)[89]	C	BF (M)	-	231	118:113	28±7.2 (18-54)	-
Ashman et al. (1987)[96]	Cad	MMP	-	1 cadaver (10 specimen)	NM	NM	Mandibular properties (young's modulus and elastic coefficient).
Bakke et al. (1989)[79]	C	BF (M)	Healthy vs. CMF disorder: 1. Healthy control 2. CMF disorder	42 1. 19 2. 23	13:29 1. 19:11 2. 5:18	28±1 (14-63) 1. 29±1 (20-60) 2. 27±1 (14-63)	Only using the BF in the healthy control group.

[continued on next page]

Supplementary Table S2. *[continued]*

Author (Year)	Study design	Measurements	Groups	Sample (n)	Sex (Male:Female)	Age (mean±SD (range) in years)	Remarks
Bakke et al. (1990)[80]	C	BF (M) MF	Age categories (yrs): 1. 5-10 2. 11-20 3. 21-30 4. 31-40 5. 41-50 6. 51-60 7. 61-70	122 1. 17 2. 20 3. 20 4. 20 5. 20 6. 17 7. 8	59:63 1. 8:9 2. 10:10 3. 9:11 4. 10:10 5. 9:11 6. 10:7 7. 3:5	32.8±17.6 (8-68) 1. 5-10 2. 11-20 3. 21-30 4. 31-40 5. 41-50 6. 51-60 7. 61-70	-
Bogdanov (2023)[69]	CS	BF (M) MF	-	68	33:35	18.4±6.1	MF (Measures masseter force).
Braun et al. (1996)[39]	CS	BF (M)	-	457	231:226	(6-20)	-
Carlsoo (1952)[95]	CS	MF	-	7	NM	NM	MF (masseter, temporalis, and medial pterygoid)
Chong et al. (2016)[40]	CS	BF (M)	Age groups (yrs): 1. 18-25 2. › 60	64 1. 44 2. 20	31:33 1. 22:22 2. 9:11	(18-66) 1. 22 (18-25) 2. 66	-
De Abreu et al. (2014)[41]	CS	BF (M)	-	55	27:28	28.1±4 (18-40)	-
de Sonnaville et a. (2023)[71]	CS	BF (I)	Healthy vs. JIA (children): 1. Healthy 2. JIA	458 1. 168 2. 290	164:290 1. 83:81 2. 93:197	(1-18) 1. 11.4±3.5 2. 12.8±3.4	Only healthy group included.
Gamit et al. (2024)[90]	C	BF (M, I)	Fracture fixation: 1. 2.0 mm 6-hole 1.5 mm thick new design titanium plate 2. 2.0-mm 4-hole 1.5 mm thick conventional titanium plate	20 1. 10 2. 10	16:4 1. 8:2 2. 8:2	(11-70) 1. 28.1±5.1 2. 34.6±14.9	Unilateral fracture fixated with 2.0 mm 1.5 mm thick: new design 6-hole versus conventional 4-hole osteosynthesis plate. Postoperative follow-up: 12d, 1mo, 3mo, and 6mo.

[continued on next page]

Supplementary Table S2. *[continued]*

Author (Year)	Study design	Measurements	Groups	Sample (n)	Sex (Male:Female)	Age (mean±SD (range) in years)	Remarks
Gudipaneni et al. (2020)[42]	CS	BF (M)	Carries Assessment Spectrum and Treatment (CAST) score: 1. CAST: 0-2 2. CAST: 3 3. CAST: 4-5	120	60:60	M: 8.9±1.6 F: 8.8 ±1.5	Only healthy group (CAST 0-2) was included.
Helkimo et al. (1977)[43]	CS	BF (M, I)	-	125	57:68	32.6 (15-65)	-
Helkimo et al. (1978)[44]	CS	BF (M, I)	-	100	100:0	24.8 (21-36)	-
Kampe et al. (1987)	C	BF (M)	Dentition state: 1. Intact dentition 2. Minor restoration	29 1. 13 2. 16	NM	(16-18)	Only intact dentition group included.
Kashiwazaki et al. (2023)[81]	RCT	BF (M)	2 groups: 1. Intervention: chew gun for 2 months 2. Control: not chewing gum	218 (after 2 months n = 211) 1. 109 2. 109	108:103 1. 54:53 2. 54:50	(65-85) 1. 70±7 2. 69±6	Started with 218 participants: after 2mo where 211 participants (intervention n:104; and control n:107). Only control group included.
Khan et al. (2020)[45]	CS	BF (M)	-	95	52:43	27.4±4.7	-
Kiliaridis et al. (1993)[46]	CS	BF (M, I)	Age categories (yrs): 1. 7-9 2. 10-13 3. 20-24	136	57:79 1. 25:29 2. 17:28 3. 15:22	(7-24)	-
Koc et al. (2011)[47]	CS	BF (M)	-	42	17:17	(19-20)	-
Kshirsagar et al. (2011)[82]	C	BF (M, I)	Fracture vs. Control: 1. Fracture double 2.5 mm plate 2. Control non-fractured	66 1. 6 2. 60	NM	(18-60)	Unilateral fracture was fixated with two 2.5 mm osteosynthesis plate. Postoperative follow-up: 1, 2, 4, 6, 8, 10, and 12 wk.

[continued on next page]

Supplementary Table S2. *[continued]*

Author (Year)	Study design	Measurements	Groups	Sample (n)	Sex (Male:Female)	Age (mean±SD (range) in years)	Remarks
Kumar et al. (2014)[83]	C	BF (M, I)	Fracture vs. Control: 1. Fracture single 4-hole locking 2 mm plate 2. Fracture double conventional 2 mm plate 3. Control non fracture	50 1. 10 2. 10 3. 30	NM	NM	Unilateral fracture was fixated with single 2.0 mm locking or with double conventional 2.0 mm osteosynthesis plate. Postoperative follow-up: 1wk, 2wk, 3wk, 4wk, 3mo.
Linderholm et al. (1970)[48]	CS	BF (M, PM, I)	-	72	58:14	(18-31)	-
Mani et al. (2024)[75]	CS	BF (M, I) MF	-	112	NM	(21-35)	MF (masseter force was measured).
Miura et al (2001)[49]	CS	BF (M)	Healthy vs. Frail elderly: 1. Healthy elderly 2. Frail elderly	373 1. 349 2. 24	156:217 1. 149:200 2. 7:17	(65-74)	Only healthy elderly group included.
Mountain et al. (2011)[50]	CS	BF (M, I)	-	199	120:85	4.8±0.6 (3-6)	Started with 205 participants; however, BF only recorded in 199 participants.
Munisekhar et al. (2023)[91]	C	BF (M)	-	133	NM	NM	Mean restoration side and contralateral side was included.
Mutt et al. (2023)[72]	CS	BF (M, I)	Children dental stage: 1. Primary 2. Mixed 3. Permanent	392 1. 132 2. 128 3. 132	214:178 1. 84:48 2. 53:75 3. 77:55	(3-13) 1. 4.3±0.6 2. 9.3±2.2 3. 13.4±0.5	-
Nimura et al. (2023)[73]	CS	BF (M)	-	251	110:141	49.6±17.8 (21-87)	-
Nomura et al. (2007)[99]	Cad	MMP	-	1 cadaver (12 specimen)	0:1	66	Mandibular trabecular bone properties (elastic modulus).
Owais et al. (2012)[51]	CS	BF (M)	Children dentition stage: 1. Early primary 2. Late primary 3. Early mixed 4. Late mixed 5. Permanent	1011 1. 200 2. 204 3. 200 4. 200 5. 207	511:500 1. 100:100 2. 104:100 3. 100:100 4. 100:100 5. 107:100	(3-18) 1. 3.4±0.2 2. 5.9±1.2 3. 8.2±0.7 4. 10±0.9 5. 14±2.1	-

[continued on next page]

Supplementary Table S2. *[continued]*

Author (Year)	Study design	Measurements	Groups	Sample (n)	Sex (Male:Female)	Age (mean±SD (range) in years)	Remarks
Palinkas et al. (2010)[52]	CS	BF (M)	Life stage: 1. Children 2. Adolescents 3. Young Adults 4. Adult 5. Elderly	177 1. 40 2. 40 3. 40 4. 40 5. 17	88:89 1. 20:20 2. 20:20 3. 20:20 4. 20:20 5. 20:20	(7-80) 1. 7-12 2. 13-20 3. 21-40 4. 41-60 5. 61-80	-
Pruim et al. (1980)[53]	CS	BF (M, PM) MF	-	7	9:0	NM	MF (Measured for masseter together with the medial pterygoid muscle).
Ranjan et al. (2024)[74]	CS	BF (M, I)	-	405	183:222	(18-40)	-
Rastogi et al. (2016)[84]	C	BF (M, I)	Fracture fixation miniplate: 1. Single conventional 2.0 mm 2. Single locking 2.0 mm	20 1. 10 2. 10	17:3	(11-40)	Unilateral fracture was fixated with single 2.0 mm locking or 2.0 mm conventional osteosynthesis plate. Postoperative follow-up: 2d, 1wk, 3wk, and 6wk.
Reddy et al. (2022)[76]	CS	BF (M, I)	Healthy vs. Periodontitis: 1. Healthy 2. Periodontitis	60 1. 30 2. 30	35:25 1. 17:13 2. 18:12	NM 1. 28.6±8.2 2. 37.8±9.8	Only healthy group included.
Rentes et al. (2002)[85]	C	BF (M)	Occlusion type: 1. Normal occlusion 2. Cross bite 3. Open bite	30	NM	(3-5.5)	Only normal occlusion group included.
Ringqvist (1973)[54]	CS	BF (M, I)	-	29	0:29	(18-23)	-
Rismanchian et al. (2009)[55]	CS	BF (M)	Denture type: 1. Conventional for last 6 mo 2. Conventional for last 10 yrs 3. Conventional maxillary denture and mandibular implant supported ball-attachment-retained overdentures on 2 implants placed on canine regions	75 1. 25 2. 25 3. 25	30:45 1. 10:15 2. 10:15 3. 10:15	(45-65)	Edentulous subjects with different type of complete dentures.

[continued on next page]

Supplementary Table S2. *[continued]*

Author (Year)	Study design	Measurements	Groups	Sample (n)	Sex (Male:Female)	Age (mean±SD (range) in years)	Remarks
Sasaki et al. (1989)[56]	CS	BF (M)	-	11	6:5	29 (23-45)	-
Sathyanarayana et al. (2012)[57]	CS	BF (M, PM)	Occlusion type and facial morphology in 5 groups. 1. Class I normal occlusion 2. Angles class I malocclusion 3. Skeletal class II malocclusion 4. Hypodivergent 5. Hyper-divergent	110 1. 30 2. 20 3. 20 4. 20 5. 20	55:55	(17-25)	Occlusion type was based on angle classification and facial morphology based on whether hypo- or hyperdivergent. Only first control group with normal occlusion (n:30) included.
Schwartz-Dabney et al. (2003)[100]	Cad	MMP	-	10 cadavers (600 specimen)	7:3	(48-81) M: 64.3±11.7 F: 62±17.1	Mandibular cortical bone properties (elastic modulus, cortical thickness, density, shear modulus, Poisson ratio)
Sener et al. (2015)[86]	C	BF (M)	-	15	10:5	(55-80)	Edentulous participant wearing conventional complete dentures switch to new implant retained complete overdentures with two ball bearing attachment.
Singh et al. (2012)[58]	CS	BF (M, I)	Angle malocclusion type: 1. Normal occlusion 2. Angle class I 3. Angle class II 4. Angle class III	60 1. 15 2. 15 3. 15 4. 15	29:31 1. M7:F8 2. M6:F9 3. M8:F7 4. M8:F7	(12-16) 1. 14.8±1.5 2. 14.4±1.6 3. 13.8±1.3 4. 14.6±1.3	Only normal occlusion group included.
Singh et al. (2020)[87]	C	BF (M, I)	-	30	14:16	6.5 (3.8-9.8)	-
Sybil et al. (2013)[88]	C	BF (M)	-	60	NM	27 (17 - 44)	Isolated Fracture with ORIF (unclear what type of osteosynthesis). Postoperative follow-up: 1, 4, 6, and 9 wk.

[continued on next page]

Supplementary Table S2. *[continued]*

Author (Year)	Study design	Measurements	Groups	Sample (n)	Sex (Male:Female)	Age (mean±SD (range) in years)	Remarks
Takaki et al. (2014)[59]	CS	BF (M)	Life stage: 1. Prepubescent 2. Pubescent 3. Postpubescent 4. Young Adult 5. Adult	100 1. 20 2. 20 3. 20 4. 20 5. 20	50:50 1. 10:10 2. 10:10 3. 10:10 4. 10:10 5. 10:10	(11-60)	-
Tortopidis et al. (1999)[60]	CS	BF (M)	Healthy vs. TMD (complete denture wearer): 1. Healthy 2. TMD	21 1. 11 2. 10	NM	67 (64-75)	Only healthy group included.
Tripathi et al. (2014)[61]	CS	BF (M)	Dentulous vs. Edentulous: 1. Dentulous 2. Edentulous	160 1. 80 2. 80	80:80 1. 40:40 2. 40:40	(20-70) 1. (20-25) 2. (50-70)	-
Ustrell-Barral et al. (2024)[70]	CS	BF (I)	-	101	13:88	22.8±3.5 (18-45)	-
van der Bilt et al. (2008)[62]	CS	BF (M)	-	81	13:68	(19-69)	-
van Eijden (1991)[63]	CS	BF (M, PM)	-	7	7:0	31.1±4.9	-
Vitins et al. (2003)[98]	Cad	MMP		5 (15 sample creep test)	5:0	(49-56)	Mandibular properties (elastic modulus, flexura failure strain, flexura failure stress, compressive stress).
Vozza et al. (2021)[64]	CS	BF (M)	Partial Removable Dentures (PRD): 1. One PRD mandibular side 2. Two PRD maxillary and mandibular side	240 1. 120 2. 120	120:120 1. 60:60 2. 60:60	NM	-

[continued on next page]

Supplementary Table S2. *[continued]*

Author (Year)	Study design	Measurements	Groups	Sample (n)	Sex (Male:Female)	Age (mean±SD (range) in years)	Remarks
Wasinwasukul et al. (2022)[92]	RCT	BF (M, I)	Control vs. ABP Appliance: 1. Control 2. ABP Acrylic Resin 3. ABP Laminate Thermoplastic	66 1. 22 2. 22 3. 22	NM	(9-13)	Only control group included.
Wennström (1971)[65]	CS	BF (M)	-	10	0:10	(18-27)	-
Wennström (1971)[66]	CS	BF (M)	-	8	7:1	(30-55)	-
Widmalm et al. (1982)[67]	CS	BF (PM)	-	5	NM	(24-27)	-
Wright et al. (2016)[97]	Cad	MMP	12 cadavers (with 6 specimens from right articular disc)	12	6:6	67.5±8.4 to 70.3±8.7	Mandibular properties (elastic, instantaneous, and relaxed modulus).
Zivko-Babic et al. (2002)[68]	CS	BF (M, I)	-	47	23:24	25±5.7 (22-50)	-

Abbreviations: C (cohort study), CS (cross sectional study), RCT (randomised control trail), Cad (Cadaver), n (number), SD (standard deviation), BF (bite force) [bite force is measurement in M (molar), PM (premolar), I (Incisal) region], MF (muscle force), MMP (mandible material properties), NM (not mentioned), CMF (craniomaxillofacial), ORIF (open reduction and internal fixation), JIA (juvenile idiopathic arthritis), ABP (Anterior Bite Plane), d (days), wk (weeks), and mo (months).

Supplementary Fig. S1. Metanalysis forest plots.

Supplementary Fig. S1.1. Maximum bite force in healthy dentulous individuals measure in the (**a**) molar, (**b**) premolar, and (**c**) incisal regions.

a

Study	Mean	SD	95% CI	N	Weight
Linderholm et al. (1970)	469.1	118.1	[441.8; 496.4]	72	2.9%
Wennström (1971)	501.1	94.9	[442.3; 559.9]	10	2.9%
Ringqvist (1973)	467.8	92.2	[434.2; 501.3]	29	2.9%
Helkimo et al. (1977)	412.5	161.4	[364.8; 460.2]	44	2.9%
Helkimo et al. (1978)	471.0	136.0	[444.3; 497.7]	100	2.9%
Pruim et al. (1980)	965.0	276.0	[760.5; 1169.5]	7	2.2%
Kampe et al. (1987)	532.0	189.0	[429.3; 634.7]	13	2.7%
Bakke et al. (1989)	347.0	132.0	[287.6; 406.4]	19	2.9%
Sasaki et al. (1989)	189.0	78.4	[142.7; 235.3]	11	2.9%
Bakke et al. (1990)	482.3	130.6	[459.1; 505.4]	122	2.9%
Kiliaridis et al. (1993)	572.1	158.1	[545.6; 598.7]	136	2.9%
Zivko–Babic et al. (2002)	392.3	151.0	[349.2; 435.5]	47	2.9%
Ahlberg et al. (2003)	825.5	199.2	[788.9; 862.1]	114	2.9%
Abe et al. (2006)	626.5	191.3	[410.0; 842.9]	3	2.1%
van der Bilt et al. (2008)	569.0	170.0	[532.0; 606.0]	81	2.9%
Palinkas et al. (2010)	271.2	64.0	[261.7; 280.6]	177	2.9%
Koc et al. (2011)	312.8	114.9	[274.2; 351.4]	34	2.9%
Mountain et al. (2011)	179.7	72.2	[169.7; 189.8]	199	2.9%
Owais et al. (2012)	323.1	158.5	[313.4; 332.9]	1011	2.9%
Sathyanarayana et al. (2012)	601.8	60.8	[580.1; 623.6]	30	2.9%
Singh et al. (2012)	445.5	52.2	[419.0; 471.9]	15	2.9%
De Abreu et al. (2014)	527.7	187.2	[478.3; 577.2]	55	2.9%
Takaki et al. (2014)	269.5	140.5	[242.0; 297.0]	100	2.9%
Tripathi et al. (2014)	439.1	149.1	[406.4; 471.8]	80	2.9%
Al–Qassar et al. (2015)	666.7	36.1	[653.8; 679.6]	30	2.9%
Chong et al. (2016)	503.6	284.2	[434.0; 573.3]	64	2.8%
Abu–Alhaija et al. (2018)	197.4	67.7	[193.4; 201.5]	1085	2.9%
Khan et al. (2020)	694.7	110.5	[672.5; 716.9]	95	2.9%
Singh et al. (2020)	168.2	63.5	[143.3; 193.0]	25	2.9%
Reddy et al. (2022)	284.6	120.6	[241.4; 327.7]	30	2.9%
Wasinwasukul et al. (2022)	429.2	173.6	[356.7; 501.7]	22	2.8%
Mutt et al. (2023)	109.3	10.1	[107.6; 111.0]	132	2.9%
Munisekhar et al. (2023)	510.7	91.7	[495.1; 526.3]	133	2.9%
Ranjan et al. (2024)	389.9	79.4	[382.2; 397.7]	405	2.9%
Mani et al. (2024)	570.0	152.0	[541.9; 598.1]	112	2.9%
Random effects model	**443.6**		**[384.2; 502.9]**		**100.0%**
Heterogeneity: I^2 = 99.9%					

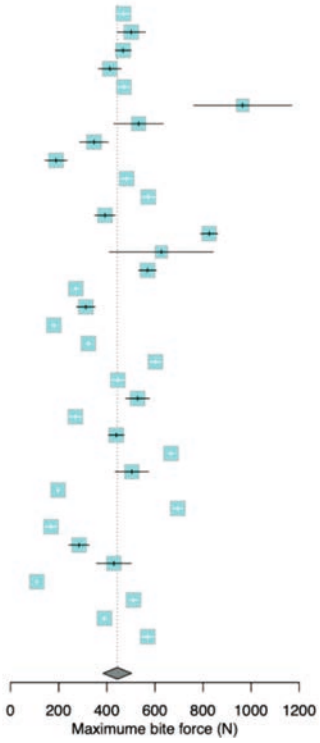

b

Study	Mean	SD	95% CI	N	Weight
Linderholm et al. (1970)	390.6	129.6	[360.7; 420.6]	72	29.3%
Pruim et al. (1980)	633.0	210.0	[477.4; 788.6]	7	9.4%
Widmalm et al. (1982)	422.2	162.2	[280.0; 564.4]	5	10.6%
Abe et al. (2006)	448.5	72.6	[366.4; 530.7]	3	19.1%
Sathyanarayana et al. (2012)	392.7	31.4	[381.5; 403.9]	30	31.6%
Random effects model	**428.4**		**[371.8; 485.0]**		**100.0%**
Heterogeneity: I^2 = 63.6%					

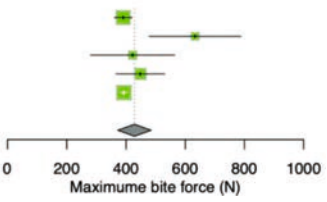

[continued on next page]

Supplementary Fig. S1.1. *[continued]*

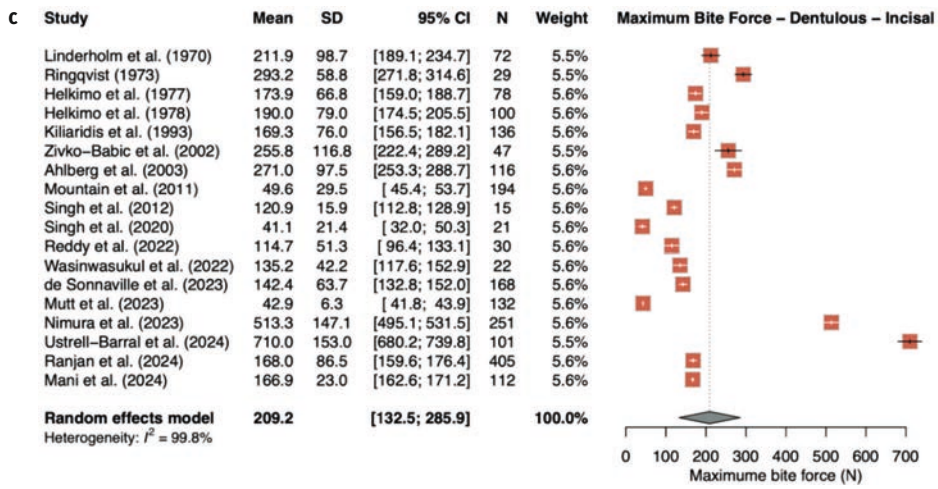

Supplementary Fig. S1.2. Maximum bite force in healthy dentulous individuals for the male and the female population measured in the (**a**) molar, (**b**) premolar, and (**c**) incisal regions.

a

Study	Mean	SD	95% CI	N	Weight
Male					
Linderholm et al. (1970)	480.5	121.6	[449.2; 511.8]	58	2.2%
Helkimo et al. (1977)	444.2	156.9	[386.1; 502.4]	28	2.1%
Helkimo et al. (1978)	471.0	136.0	[444.3; 497.7]	100	2.2%
Pruim et al. (1980)	965.0	276.0	[760.5; 1169.5]	7	1.7%
Kiliaridis et al. (1993)	594.2	173.9	[549.0; 639.3]	57	2.1%
Ahlberg et al. (2003)	908.0	179.0	[865.5; 950.5]	68	2.1%
Abe et al. (2006)	626.5	191.3	[410.0; 842.9]	3	1.6%
van der Bilt et al. (2008)	652.0	151.0	[569.9; 734.1]	13	2.1%
Palinkas et al. (2010)	322.4	86.9	[304.2; 340.5]	88	2.2%
Koc et al. (2011)	349.1	116.7	[293.6; 404.6]	17	2.1%
Mountain et al. (2011)	188.8	66.7	[176.8; 200.7]	120	2.2%
Owais et al. (2012)	347.5	154.0	[334.1; 360.8]	511	2.2%
De Abreu et al. (2014)	632.0	174.1	[566.3; 697.7]	27	2.1%
Takaki et al. (2014)	285.0	149.2	[243.7; 326.4]	50	2.2%
Tripathi et al. (2014)	439.1	149.1	[392.9; 485.3]	40	2.1%
Al–Omiri et al. (2014)	651.5	59.9	[625.2; 677.8]	20	2.2%
Al–Qassar et al. (2015)	688.8	19.4	[679.3; 698.3]	16	2.2%
Al–Zarea et al. (2015)	649.6	50.0	[634.7; 664.5]	43	2.2%
Chong et al. (2016)	602.6	318.2	[490.6; 714.6]	31	2.0%
Abu–Alhaija et al. (2018)	207.8	67.7	[202.0; 213.6]	515	2.2%
Khan et al. (2020)	755.7	102.7	[727.8; 783.7]	52	2.2%
Singh et al. (2020)	175.4	64.7	[141.5; 209.3]	14	2.2%
Ranjan et al.	346.0	82.4	[334.1; 357.9]	183	2.2%
Ali Alkhalaf et al.	585.8	264.6	[538.1; 633.6]	118	2.1%
Random effects model	**509.9**		**[425.9; 594.0]**		**50.5%**
Heterogeneity: I^2 = 99.8%					
Female					
Linderholm et al. (1970)	421.7	91.2	[373.9; 469.5]	14	2.1%
Wennström (1971)	501.1	94.9	[442.3; 559.9]	10	2.1%
Ringqvist (1973)	467.8	92.2	[434.2; 501.3]	29	2.2%
Helkimo et al. (1977)	357.0	158.9	[279.1; 434.8]	16	2.1%
Kiliaridis et al. (1993)	556.0	154.7	[521.8; 590.1]	79	2.2%
Ahlberg et al. (2003)	743.0	188.0	[688.7; 797.3]	46	2.1%
van der Bilt et al. (2008)	553.0	170.0	[512.6; 593.4]	68	2.2%
Palinkas et al. (2010)	221.1	55.8	[209.5; 232.7]	89	2.2%
Koc et al. (2011)	276.5	104.0	[227.1; 325.9]	17	2.1%
Mountain et al. (2011)	169.9	69.8	[155.1; 184.8]	85	2.2%
Owais et al. (2012)	320.1	157.9	[306.3; 334.0]	500	2.2%
De Abreu et al. (2014)	427.2	139.7	[375.5; 478.9]	28	2.1%
Takaki et al. (2014)	254.0	131.0	[217.7; 290.3]	50	2.2%
Tripathi et al. (2014)	314.2	121.2	[276.7; 351.8]	40	2.2%
Al–Omiri et al. (2014)	583.7	35.0	[568.4; 599.0]	20	2.2%
Al–Qassar et al. (2015)	641.4	34.5	[623.3; 659.5]	14	2.2%
Al–Zarea et al. (2015)	539.4	55.3	[522.7; 556.1]	42	2.2%
Chong et al. (2016)	410.6	213.3	[337.9; 483.4]	33	2.1%
Abu–Alhaija et al. (2018)	188.3	62.7	[183.2; 193.5]	570	2.2%
Khan et al. (2020)	621.0	65.7	[601.3; 640.6]	43	2.2%
Singh et al. (2020)	166.3	68.9	[132.5; 200.1]	16	2.2%
Ranjan et al.	389.9	79.3	[379.5; 400.4]	222	2.2%
Ali Alkhalaf et al.	394.4	160.7	[364.8; 424.0]	113	2.2%
Random effects model	**413.6**		**[347.3; 479.9]**		**49.5%**
Heterogeneity: I^2 = 99.7%					
Random effects model	**461.8**		**[407.2; 516.4]**		**100.0%**
Heterogeneity: I^2 = 99.8%					
Test for subgroup differences: χ^2_1 = 3.11, df = 1 (p = 0.0777)					

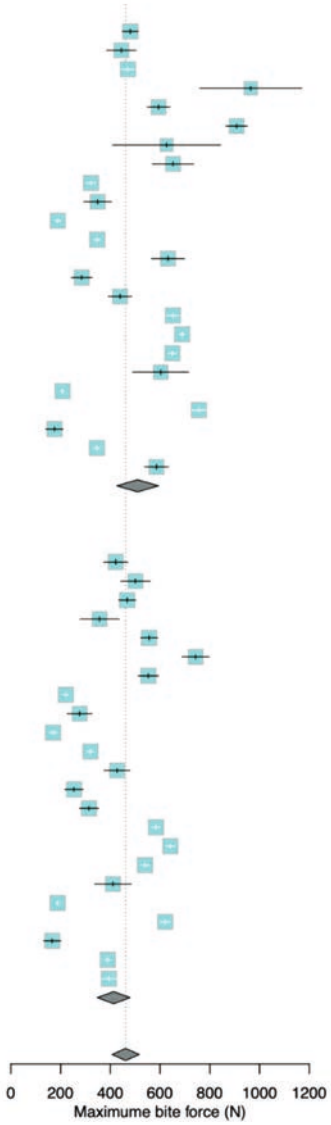

[continued on next page]

Supplementary Fig. S1.2. *[continued]*

b

Study	Mean	SD	95% CI	N	Weight
Male					
Linderholm et al. (1970)	402.1	136.3	[367.0; 437.2]	58	28.9%
Pruim et al. (1980)	633.0	210.0	[477.4; 788.6]	7	17.7%
Abe et al. (2006)	448.5	72.6	[366.4; 530.7]	3	25.1%
Random effects model	**475.2**		**[354.8; 595.6]**		**71.7%**
Heterogeneity: I^2 = 76.9%					
Female					
Linderholm et al. (1970)	343.2	85.3	[298.5; 387.9]	14	28.3%
Random effects model	**437.9**		**[335.6; 540.3]**		**100.0%**
Heterogeneity: I^2 = 81.2%					
Test for subgroup differences: χ^2_1 = 4.05, df = 1 (p = 0.0441)					

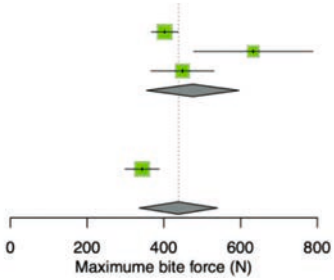

c

Study	Mean	SD	95% CI	N	Weight
Male					
Linderholm et al. (1970)	215.8	105.9	[188.5; 243.0]	58	5.6%
Helkimo et al. (1977)	189.3	71.6	[168.1; 210.4]	44	5.6%
Helkimo et al. (1978)	190.0	79.0	[174.5; 205.5]	100	5.6%
Kiliaridis et al. (1993)	174.4	80.5	[153.5; 195.3]	57	5.6%
Ahlberg et al. (2003)	292.0	95.0	[269.7; 314.3]	70	5.6%
Mountain et al. (2011)	53.4	30.3	[48.0; 58.8]	120	5.6%
Nimura et al. (2023)	573.7	163.9	[543.1; 604.3]	110	5.6%
Ustrell–Barral et al. (2024)	826.0	154.0	[742.3; 909.7]	13	5.4%
Ranjan et al. (2024)	165.0	86.5	[152.4; 177.5]	183	5.6%
Random effects model	**295.9**		**[138.4; 453.4]**		**49.9%**
Heterogeneity: I^2 = 99.6%					
Female					
Linderholm et al. (1970)	196.1	60.8	[164.3; 228.0]	14	5.5%
Ringqvist (1973)	293.2	58.8	[271.8; 314.6]	29	5.6%
Helkimo et al. (1977)	154.0	54.9	[135.5; 172.4]	34	5.6%
Kiliaridis et al. (1993)	165.6	73.0	[149.5; 181.7]	79	5.6%
Ahlberg et al. (2003)	250.0	100.0	[221.1; 278.9]	46	5.6%
Mountain et al. (2011)	44.1	27.5	[38.3; 50.0]	85	5.6%
Nimura et al. (2023)	452.9	130.2	[431.4; 474.4]	141	5.6%
Ustrell–Barral et al. (2024)	693.0	147.0	[662.3; 723.7]	88	5.6%
Ranjan et al. (2024)	85.2	38.1	[80.1; 90.2]	222	5.6%
Random effects model	**259.1**		**[127.1; 391.1]**		**50.1%**
Heterogeneity: I^2 = 99.8%					
Random effects model	**277.3**		**[177.5; 377.1]**		**100.0%**
Heterogeneity: I^2 = 99.7%					
Test for subgroup differences: χ^2_1 = 0.12, df = 1 (p = 0.7254)					

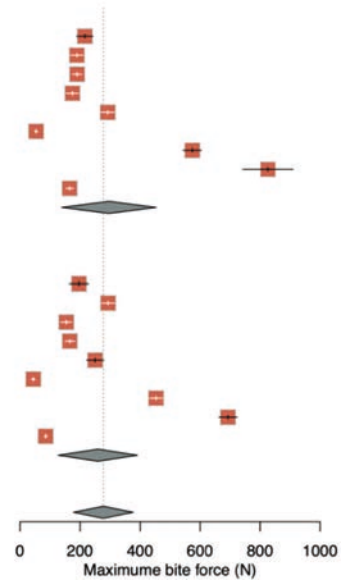

Supplementary Fig. S1.3. Maximum bite force in dentulous individuals at different age categories in the molar region, namely: ‹ 20, 20-60, › 60 years old.

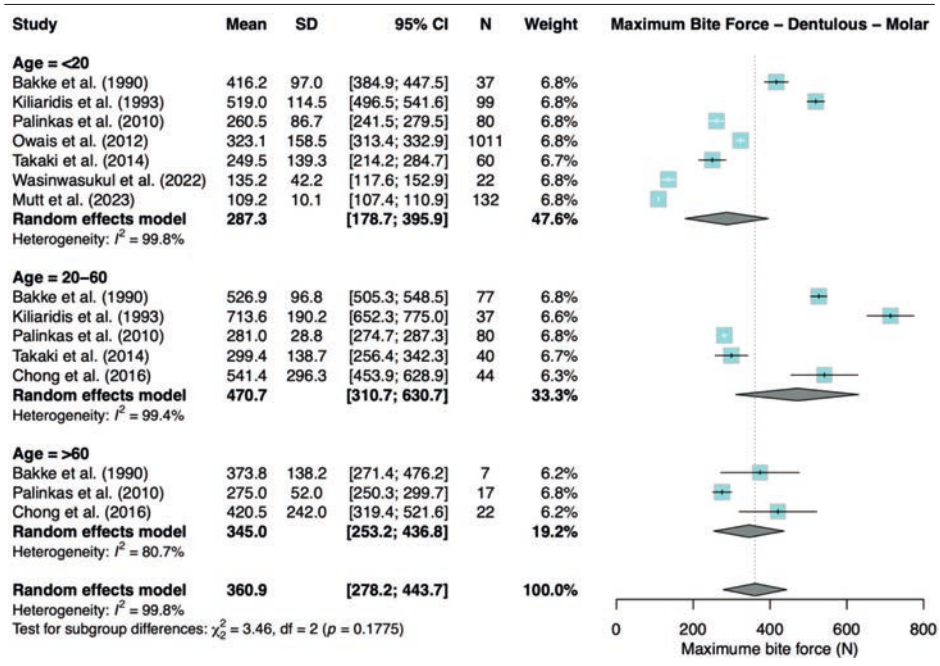

Supplementary Fig. S1.4. Maximum force measurements in 3 postoperative follow-up (2-7 days, 3-4 weeks, and 6 weeks to 3 months) for the mandibular fractures treated with osteosynthesis in the (**a**) molar, and (**b**) incisal regions.

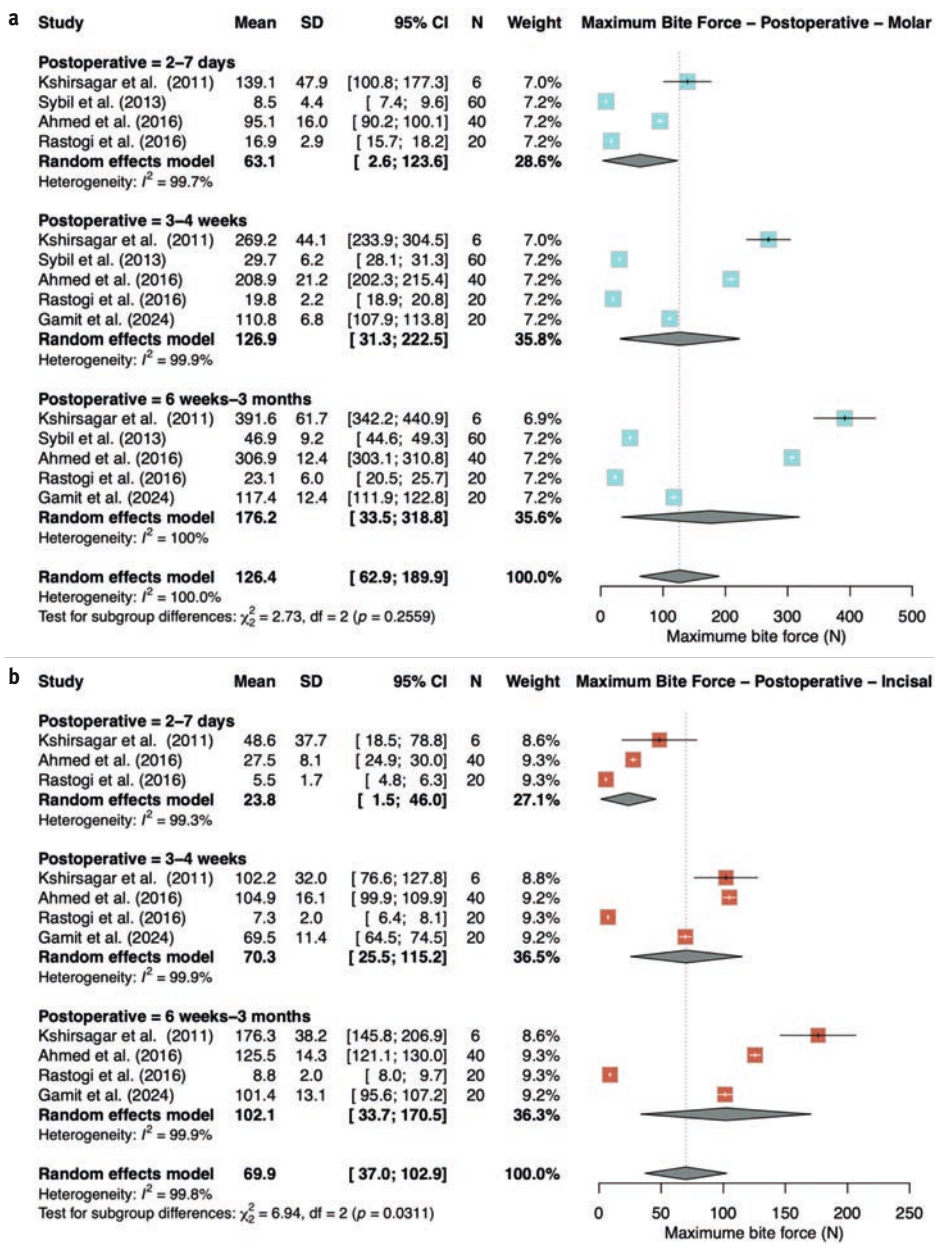

Supplementary Fig. S1.5. Maximum bite force in mandibular denture wearer (partial or complete edentulous) subjects measured in the molar region: (**a**) total population (containing partial and complete denture wearer), and (**b**) partial denture wearers, and (**c**) complete denture wearers.

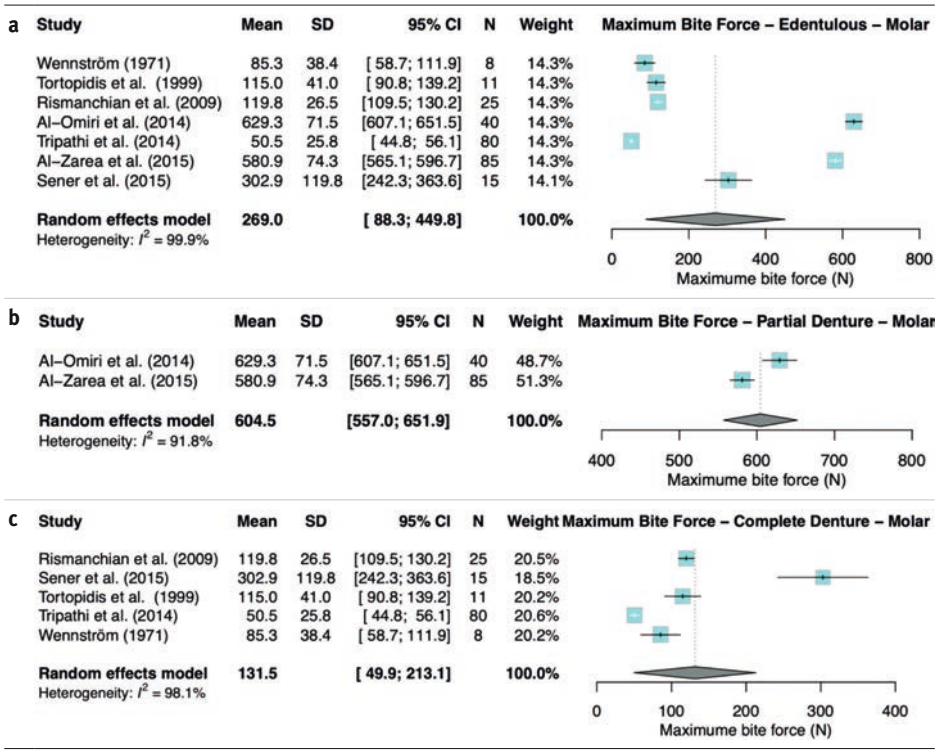

Supplementary Fig. S1.6. Maximum bite force in mandibular denture wearer (partial or complete edentulous) subjects measured in the molar region for the male and the female population: (**a**) total population (containing partial and complete denture wearer), and (**b**) partial denture wearers, and (**c**) complete denture wearers.

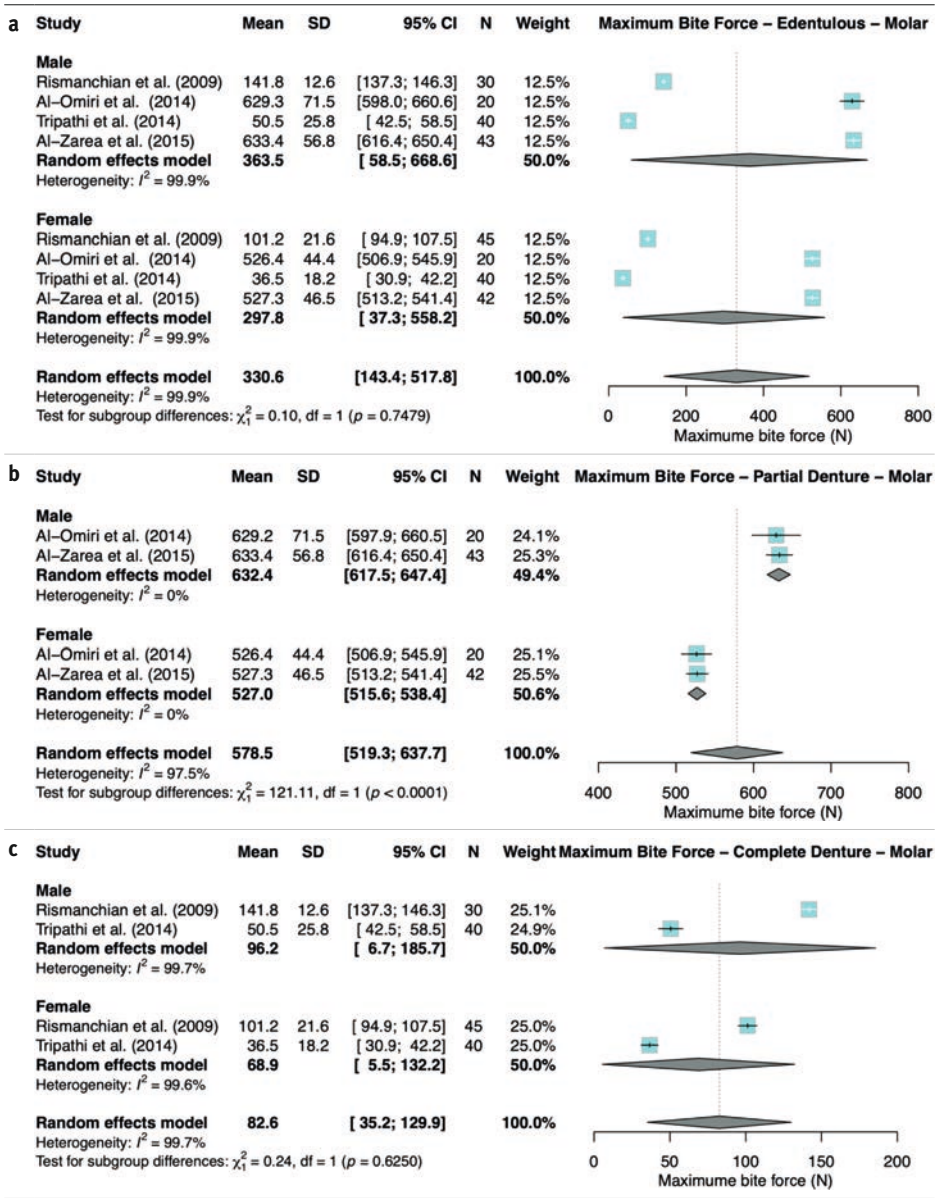

Supplementary Table S4. Maximum bite force (MBF) values.

Supplementary Table S4.1. Maximum bite force in the normal healthy dentulous population.

		Age (years)	Sample	MBF [N]		
Location	**Author (Year)**	**Mean±SD (Range)**	**n**	**Mean±SD**	**Range**	**SE**
Molar	Abe et al. (2006)[35]	29.6	3	626.5±191.3	405.3-747.3	110.4
	Abu-Alhaija et al. (2018)[36]	4.9±0.9 (3-6)	1085	197.4±67.7	179.2-245.1	2.1
	Ahmed et al. (2016)[78]	26.3 (18-24)	30	510.9	-	-
	Ahlberg et al. (2003)[77]	21-23	114	825.50±199.21	-	18.66
	Al-Omiri et al. (2014)[37]	42.7±9.6 (28-57)	40	596.2 ± 76.3	490-800	11.84
	Al-Qassar et al. (2015)[94]	30 (18-25)	30	666.7±36.1	645.2-751.2	6.6
	Al-Zarea et al. (2015)[38]	43±9 (28-66)	85	596.2±76.3	433-825	8.3
	Ali Alkhalaf et al. (2024)[89]	18±7.2	231	491.6±187.6	147.5-925.5	12.4
	Bakke et al. (1989)[79]	29±11 (20-60)	19	347±132	237-609	30.3
	Bakke et al. (1990)[80]	32.8±17.6 (8-68)	122	482.3 ± 130.6	336.9-572.3	11.8
	Bogdanov (2023)[69]	18.4±6.1	68	396.3±128.1	-	15.5
	Braun et al. (1996)[39]	13 (6-20)	457	-	78-176	-
	Chong et al. (2016)[40]	-	64	503.6±284.2	-	35
	De Abreu et al. (2014)[41]	-	55	527.7±187.2	-	25.2
	Gudipaneni et al. (2020)[42]	(7-9)	-	320.9±54.2	-	-
	Helkimo et al. (1977)[43]	-	44	412.5±161.5	-	24.3
	Helkimo et al. (1978)[44]	24.8 (21-36)	100	471±136	191-802	13.6
	Kampe et al. (1987)[81]	(16-18)	13	532±189	-	52.4
	Kashiwazaki et al. (2023)[93]	70±7 (65-85)	109	457±80	-	-
	Khan et al. (2020)[45]	27.4±4.7 (20-35)	95	694.7±110.5	411-913	11.3
	Kiliardis et al. (1993)[46]	(7-24)	136	572.1±158.1	-	13.6
	Koc et al. (2011)[47]	(19-20)	34	312.8±114.9	-	19.7
	Linderholm et al. (1970)[48]	(18-31)	72	469.1±118.1	-	13.9
	Mani et al. (2024)[75]	(21-35)	112	570±152	360-850	14.4
	Miura et al. (2001)[49]	(65-74)	349	321.5	-	-
	Mountain et al. (2011)[50]	4.8±0.6 (3.3-6.3)	199	179.7±72.2	8.1-353.6	5.1
	Munisekhar et al. (2023)[91]	-	133	510.7±91.7	-	8
	Mutt et al. (2023)[72]	(3-13)	132	109.3±10.1	-	0.9

[continued on next page]

Supplementary Table S4.1. *[continued]*

		Age (years)	Sample	MBF [N]		
Location	**Author (Year)**	**Mean±SD (Range)**	**n**	**Mean±SD**	**Range**	**SE**
	Owais et al. (2012)[51]	(3-18)	1011	323.1±158.5	-	5
	Palinkas et al. (2010)[52]	(7-80)	177	271.2±64	-	4.8
	Pruim et al. (1980)[53]	-	7	965±276	785-1308	104
	Ranjan et al. (2024)[74]	(18-40)	405	368±80.9	182-571	3.9
	Reddy et al. (2022)[76]	28.6±8.2	30	528.9±93.2	-	22
	Rentes et al. (2002)[85]	(3-5)	-	213.2±94	161.1-294.4	11
	Ringquist (1973)[54]	(18-23)	29	467.8±92.2	202-679.6	17.1
	Sasaki et al. (1989)[56]	29 (23-45)	11	189±78.4	119-390	23.6
	Sathyanarayana et al. (2012)[57]	(17-25)	30	601.8±60.8	-	11.1
	Singh et al. (2012)[58]	14.8±1.5 (12-16)	15	445.5±52.2	-	13.5
	Singh et al. (2020)[87]	6.5 (3.8-9.8)	25	168.2±63.5	57.4-323.3	12.7
	Takaki et al. (2014)[59]	(11-60)	100	269.5±140.5	-	14.1
	Tripathi et al. (2014)[61]	(20-70)	80	439.1±149.1	-	20
	Van der Bilt et al. (2008)[62]	(19-69)	81	569±170 (18.89)	-	18.9
	Van Eijden (1991)[63]	31.1±4.9	7	615	-	-
	Wasinwasukul et al. (2022)[92]	(9-13)	22	429.2±173.6	-	37
	Wennström (1971)[65]	(18-27)	10	501.1±94.9 (30)	-	30
	Widmalm et al. (1982)[67]	(24-27)	5	-	-	-
	Zivko-Babic et al. (2002)[68]	24.9±5.7 (22-50)	47	392.3±151	51-398	22
Premolar	Abe et al. (2006)[35]	29.60	3	448.5±72.6	384-527.1	41.9
	Linderholm et al. (1970)[48]	(18-31)	72	390.6±129.6	-	15.3
	Pruim et al. (1980)[53]	-	7	633±210	386-908	79
	Sathyanarayana et al. (2012)[57]	(17-25)	30	392.7±31.4	-	5.7
	Van Eijden (1991)[63]	31.1±4.9	7	508.9	-	-
	Widmalm et al. (1982)[67]	(24-27)	5	422.2±162.2	181-508	72.5
Incisal	Ahlberg et al. (2003)[77]	21-23	116	271±97.5	-	9.1
	Ahmed et al. (2016)[78]	26.3 (18-24)	30	159.9	-	-
	De Sonnaville et al. (2023)[71]	11.4±3.5 (1-18)	168	142.4±63.7	-	4.9
	Helkimo et al. (1977)[43]	-	78	173.9±66.8	-	7.6

[continued on next page]

Supplementary Table S4.1. *[continued]*

		Age (years)	Sample	MBF [N]		
Location	**Author (Year)**	**Mean±SD (Range)**	**n**	**Mean±SD**	**Range**	**SE**
	Helkimo et al. (1978)[44]	24.8 (21-36)	100	190±79	34-459	7.9
	Kiliardis et al. (1993)[46]	(7-24)	136	169.3±76	-	6.5
	Linderholm et al. (1970)[48]	(18-31)	72	211.9±98.7	-	11.6
	Mani et al. (2024)[75]	(21-35)	112	570±152	360-850	14.4
	Mountain et al. (2011)[50]	4.8±0.6 (3.3-6.3)	194	49.6±29.5	6.9-140.1	2.1
	Mutt et al. (2023)[72]	(3-13)	132	42.9±6.3	-	0.6
	Nimura et al. (2023)[73]	49.6±17.8 (21-87)	251	513.3±147.1	-	9.3
	Ranjan et al. (2024)[74]	(18-40)	405	168±86.5	20-348	4.3
	Reddy et al. (2022)[76]	28.6±8.2	30	114.7±51.3	-	9.4
	Ringquist (1973)[54]	(18-23)	29	293.2±58.8	201-448.2	10.9
	Singh et al. (2012)[58]	14.8±1.5 (12-16)	15	120.9±15.9	-	4.1
	Singh et al. (2020)[87]	6.5 (3.8-9.8)	21	41.4±21.4	9.3-96.5	4.7
	Ustrell-Barral et al. (2024)[70]	22.8±3.5 (18-45)	101	710±153	-	15.2
	Wasinwasukul et al. (2022)[92]	(9-13)	22	135.2±42.2	-	9
	Zivko-Babic et al. (2002)[68]	24.9±5.7 (22-50)	47	255.8±116.8	28-605	17

Abbreviations: MBF (maximum bite force), N (newtons unit), n (number of participants), SD (standard deviation), SE (standard error), and - (not given, unknown, or cannot define).

Supplementary Table S4.2. Maximum bite force in the normal dentulous population for male versus female.

				MBF [N]			
		Age (years)	Sex (n)	Male		Female	
Location	Author (Year)	Mean±SD (Range)	M:F	Mean±SD	SE	Mean±SD	SE
Molar	Abe et al. (2006)[35]	29.6	3:0	626.5±191.3	110.4	-	-
	Abu-Alhaija et al. (2018)[36]	4.9±0.9	515:570	207.8±67.7	3	188.3±62.7	2.6
	Ahlberg et al. (2003)[77]	(21-23)	68:46	908±179	21.8	743±188	27.72
	Al-Omiri et al. (2014)[37]	(28-57)	20:20	651.5±59.9	13.3	538.7±35	7.83
	Al-Qassar et al. (2015)[94]	30 (18-25)	16:14	668.8±19.4	4.9	641.4±34.5	9.21
	Al-Zarea et al. (2015)[38]	(28-66)	43:42	649.6 ± 50	7.6	539.4 ± 55.3	8.53
	Ali Alkhalaf et al. (2024)[89]	18±7.2 (18-54)	118:113	385.8±264.6	24.4	394.4±160.7	15.12
	Chong et al. (2016)[40]	-	31:33	602.6±318.2	57.15	410.6±213.3	37.13
	De Abreu et al. (2014)[41]	-	27:28	632±174.10	33.50	427.2±139.7	26.40
	Gudipaneni et al. (2020)[42]	(7-9)	-	363.4±35.2	-	311.9±55.7	-
	Helkimo et al. (1977)[43]	-	28:16	444.2±156.9	29.7	357±158.9	39.7
	Helkimo et al. (1978)[44]	24.8 (21-36)	100:0	471±136	13.6	-	-
	Khan et al. (2020)[45]	27.4±4.7 (20-35)	52:43	755.7±102.7	14.3	621±65.7	10
	Kiliardis et al. (1993)[46]	(7-24)	57:79	594.2±174	23	556±154.7	17.4
	Koc et al. (2011)[47]	(19-20)	17:17	349.1±116.7	28.3	276.5±104	25.2
	Linderholm et al. (1970)[48]	(18-31)	58:14	480.5±121.6	16	422±91.2	24.4
	Miura et al. (2001)[49]	(65-74)	149:200	408	-	235	-
	Mountain et al. (2011)[50]	4.8±0.6 (3.3-6.3)	120:85	188.8±66.7	66.7	169.9±69.9	7.58
	Owais et al. (2012)[51]	(3-18)	511:500	347.5±154	6.81	320.2±158	7.06
	Palinkas et al. (2010)[52]	(7-80)	88:89	322.4±87	9.26	221.1±55.8	5.91

[continued on next page]

Supplementary Table S4.2. *[continued]*

				MBF [N]			
		Age (years)	Sex (n)	Male		Female	
Location	**Author (Year)**	**Mean±SD (Range)**	**M:F**	**Mean±SD**	**SE**	**Mean±SD**	**SE**
	Pruim et al. (1980)[53]	-	7:0	965±276	104	-	-
	Ranjan et al. (2024)[74]	(18-40)	183:222	346±82.4	6.1	390±79.3	5.32
	Ringquist (1973)[54]	(18-23)	0:29	-	-	467.8±92.2	17.12
	Sathyanarayana et al. (2012)[57]	(17-25)	-	650.7±34.2	-	553±34.2	-
	Singh et al. (2020)[87]	6.5 (3.8-9.8)	14:16	175.4±64.7	17.3	166.3±68.9	16.24
	Takaki et al. (2014)[59]	(11-60)	50:50	285±149.2	21.1	254±131	18.53
	Tripathi et al. (2014)[61]	(20-70)	40:40	439.1±149.1	23.6	314.3±121.2	19.17
	Van der Bilt et al. (2008)[62]	(19-69)	13:68	652±151	41.9	553±170	20.61
	Van Eijden (1991)[63]	31.1±4.9	7:0	615	-	-	-
	Wennström (1971)[65]	(18-27)	0:10	-	-	501.1±95	30
	Zivko-Babic et al. (2002)[68]	24.9±5.7 (22-50)	23:24	416.83	416.8	383.1	383.13
Premolar	Abe et al. (2006)[35]	29.6	3:0	448.5±72.6	41.9	-	-
	Linderholm et al. (1970)[48]	(18-31)	58:14	402.1±136.3	17.9	343.2±85.3	22.80
	Pruim et al. (1980)[53]	-	7:0	633±210	79	-	-
	Sathyanarayana et al. (2012)[57]	(17-25)	-	422.9±22.2	-	359.5±24.1	-
	Van Eijden (1991)[63]	31.1±4.9	7:0	508.9	-	-	-
Incisal	Ahlberg et al. (2003)[77]	21-23	70:46	292±95	11.4	250±100	14.7
	Helkimo et al. (1977)[43]	-	44:34	189.3±72	10.8	154±54.9	9.4
	Helkimo et al. (1978)[44]	24.8 (21-36)	100:0	190±79	7.9	-	-
	Kiliardis et al. (1993)[46]	(7-24)	57:79	174.4±80.5	10.7	165.6±7	8.2

[continued on next page]

Supplementary Table S4.2. *[continued]*

				MBF [N]			
		Age (years)	Sex (n)	Male		Female	
Location	Author (Year)	Mean±SD (Range)	M:F	Mean±SD	SE	Mean±SD	SE
	Linderholm et al. (1970)[48]	(18-31)	58:14	215.8±105.9	13.9	196.1±60.8	16.3
	Mountain et al. (2011)[50]	4.8±0.6 (3.3-6.3)	120:85	53.4±30.3	2.8	44.1±27.5	3
	Nimura et al. (2023)[73]	49.6±17.8 (21-87)	110:141	573.7±163.9	15.6	452.9±130.2	11
	Ranjan et al. (2024)[74]	(18-40)	183:222	165±86.5	6.4	85.2±38.1	2.6
	Ringquist (1973)[54]	(18-23)	0:29	-	-	293.2±58.8	10.9
	Ustrell-Barral et al. (2024)[70]	22.8±3.5 (18-45)	13:88	826±154	22	693±147	15.7
	Zivko-Babic et al. (2002)[68]	24.9±5.7 (22-50)	23:24	289.70	-	223.29	-

Abbreviations: N (newtons unit), n (number of participants), SD (standard deviation), SE (standard error), and - (not given, unknown, or cannot define).

Supplementary Table S4.3. Maximum bite force in different age category of normal healthy dentulous population.

Location	Age (years)	Author (Year)	MBF [N]		
			n	Mean±SD	SE
Molar	**<20**	Bakke et al. (1990)[80]	37	460.2±97	16
		Braun et al. (1996)[39]	457	78-176	-
		Kiliaridis et al. (1993)[46]	99	519±114.5	11.5
		Mutt et al. (2023)[72]	132	109.3±10.1	0.9
		Owais et al. (2012)[51]	1011	323.1±158.5	5
		Palinkas et al. (2010)[52]	80	260.5±86.7	9.7
		Takaki et al. (2014)[59]	60	249.5±139.3	18
		Wasinwasukul et al. (2022)[92]	22	429.2±173.6	37
	20-60	Bakke et al. (1990)[80]	77	526.9±96.8	11
		Chong et al. (2016)[40]	44	541.4±296.3	44.6
		Kiliaridis et al. (1993)[46]	37	713.7±190.3	31.3
		Palinkas et al. (2010)[52]	80	281±28.8	3.2
		Takaki et al. (2014)[59]	80	299.6±138.7	21.9
	>60	Bakke et al. (1990)[80]	8	373.8±138.2	52.2
		Chong et al. (2016)[40]	22	420.5±242	51.6
		Palinkas et al. (2010)[52]	17	275±52	12.6
Incisal	**<20**	De Sonnaville et al. (2023)[71]	168	142.4±63.7	4.9
		Mutt et al. (2023)[72]	132	42.9±6.3	0.6
		Kiliaridis et al. (1993)[46]	99	146±68.5	6.9
		Wasinwasukul et al. (2022)[92]	22	135.2±42.2	9
	20-60	Kiliaridis et al. (1993)[46]	37	231.5±58.4	9.6

Abbreviations: MBF (maximum bite force), N (newtons), n (number of participants), SD (standard deviation), SE (standard error), and - (not given, unknown, or cannot define).

Table Supplementary Table S4.4. Maximum bite force in different age category of normal healthy dentulous population for male versus female.

			MBF [N]					
			Male			Female		
Location	Age (years)	Author (Year)	n	Mean±SD	SE	n	Mean±SD	SE
Molar	**‹20**	Kiliaridis et al. (1993)[46]	42	518.2±110.1	17	57	519.6±118.6	15.7
		Owais et al. (2012)[51]	511	347.5±154	6.8	500	320.2±158	7.1
		Palinkas et al. (2010)[52]	40	295±115.3	18.2	40	228.5±66.9	10.6
		Takaki et al. (2014)[59]	30	292.4±134.2	24.5	30	206.6±132.9	24.4
	20-60	Chong et al. (2016)[40]	22	633.9±320.9	68.4	22	448.9±242.7	51.74
		Kiliaridis et al. (1993)[46]	15	807±140.3	36.2	22	650±196.1	41.8
		Palinkas et al. (2010)[52]	40	338.5±33.6	5.3	40	225±37.9	6
		Takaki et al. (2014)[59]	20	273.6±172.2	38.5	20	325.1±91.8	20.5
	›60	Chong et al. (2016)[40]	9	526.2±317.5	105.8	11	334.1±111.2	33.5
		Palinkas et al. (2010)[52]	8	391±50	17.7	9	171±47	15.7
Incisal	**‹20**	Kiliaridis et al. (1993)[46]	42	149.6±72.3	11.1	57	143.4±66.3	8.8
	20-60	Kiliaridis et al. (1993)[46]	15	244±59.8	15.4	22	233±57.2	12.2

Abbreviations: N (Newtons), n (number of participants), SD (standard deviation), and SE (standard error).

Supplementary Table S4.5. Preoperative maximum bite force in non-comminuted simple fractured mandible.

Author (Year)	Age (years)	Sample	MBF Molar [N]		MBF Incisal [N]	
	Mean±SD (Range)	n	Mean±SD	SE	Mean±SD	SE
Ahmed et al. (2016)[78]	30.7 (18-55)	40	54.9±6.4	1	20.6±10	1.6
Gamit et al. (2024)[90]	34.6±14.9 (11-40)	20	20.5±3.8	1.2	32.5±2.9	0.9
Kumar et al. (2014)[83]	27.2 (14-46)	40	94.8	-	102.4	-

Abbreviations: MBF (maximum bite force), N (newtons), n (number of participants), SD (standard deviation), SE (standard error), and - (not given, unknown, or cannot define).

Supplementary Table 4.6. Postoperative follow-up maximum bite force development in non-comminuted simple fractured mandible fixated with osteosynthesis.

				MBF postoperative follow-up					
		Age (years)	Sample	2-7 days		3-4wk		6wk-3m	
Location	Author (Year)	Mean±SD (Range)	n	Mean±SD	SE	Mean±SD	SE	Mean±SD	SE
Molar	Ahmed et al. (2016)[78]	30.7 (18-55)	40	95.1±16	3.6	208.9±21.2	4.7	307±12.5	2.8
	Gamit et al. (2024)[90]	34.6±14.9 (11-40)	20	-	-	110.8±2.1	2.1	117.4±12.5	3.9
	Kshirsagar et al. (2011)[82]	(18-60)	6	139±47.9	19.6	269.2±44.1	18	391.6±61.7	25.2
	Kumar et al. (2014)[83]	27.2 (14-46)	20	392.7	-	613.2	-	906.5	-
	Rastogi et al. (2016)[84]	(11-40)	20	16.9±2.9	0.9	19.8±2.2	0.7	23.1±6	1.9
	Sybil et al. (2013)[88]	27 (17-44)	60	8.5±4.5	0.6	29.7±6.3	0.8	46.9±9.2	1.2
Incisal	Ahmed et al. (2016)[78]	30.7 (18-55)	40	27.5±8.1	1.8	104.9±16.1	3.6	125.5±14.3	3.2
	Gamit et al. (2024)[90]	34.6±14.9 (11-40)	20	-	-	69.5±11.4	3.6	101.4±13.1	4.2
	Kshirsagar et al. (2011)[82]	(18-60)	6	48.6±37.7	16.9	102.2±32	14.3	176.3±17.1	17.1
	Rastogi et al. (2016)[84]	(11-40)	20	5.5±1.7	0.5	7.3±2	0.6	8.8±2	0.6

Abbreviations: MBF (maximum bite force), N (newtons unit), n (number of sample), SD (standard deviation), SE (standard error), and - (not given, unknown, or cannot define).

Supplementary Table S4.7. Maximum molar bite force in partial denture wearers.

	Age (years)	Sample	MBF Molar [N]		
Author (Year)	**Mean±SD (Range)**	**n**	**Mean±SD**	**Range**	**SE**
Al-Omiri et al. (2014)[37]	42.7±9.6 (28-57)	40	629.2±71.5	-	11.3
Al-Zarea et al. (2015)[38]	43±9 (28-66)	85	580.9±74.3	401-815	8.1
Vozza et al. (2021)[64]	-	240	387.6	-	-

Abbreviations: MBF (maximum bite force), N (newtons unit), n (number of sample), SD (standard deviation), SE (standard error), and - (not given, unknown, or cannot define).

Supplementary Table 4.8. Maximum molar bite force in partial denture wearers for male versus female.

		Sample	MBF Molar [N]			
	Age (years)	(n)	Male		Female	
Author (Year)	**Mean±SD (Range)**	M:F	**Mean±SD**	**SE**	**Mean±SD**	**SE**
Al-Omiri et al. (2014)[37]	42.7±9.6 (28-57)	20:20	629.2±71.5	11.3	526.4±44.4	9.9
Al-Zarea et al. (2015)[38]	43±90 (28-66)	43:42	633.4±56.8	8.7	527.3±46.5	7.2
Vozza et al. (2021)[64]	-	120:120	387.6	-	259.9	-

Abbreviations: MBF (maximum bite force), N (newtons unit), n (number of sample), SD (standard deviation), SE (standard error), and - (not given, unknown, or cannot define).

Supplementary Table S4.9. Maximum molar bite force in edentulous individuals with complete dentures.

	Age (years)	Sample	MBF Molar [N]		
Author (Year)	**Mean±SD (Range)**	**n**	**Mean±SD**	**Range**	**SE**
Rismanchian et al. (2009)[55]	54.3±5.4 (45-75)	25	119.9±26.5	-	5.3
Sener et al. (2015)[86]	(55-80)	15	302.9±119.8	-	30.9
Tortopidis et al. (2014)[60]	(64-75)	11	115±41	83-190	12.4
Tripathi et al. (2014)[61]	(20-70)	80	50.5±25.8	-	2.9
Wennström (1971)[66]	(30-55)	8	85.3±38.4	-	13.6

Abbreviations: MBF (maximum bite force), N (newtons unit), n (number of sample), SD (standard deviation), SE (standard error), and - (not given, unknown, or cannot define).

Supplementary Table S4.10. Maximum molar bite force in edentulous individuals with complete dentures for male versus female.

			MBF Molar [N]			
	Age (years)	Sample	Male		Female	
Author (Year)	**Mean±SD (Range)**	M:F	**Mean±SD**	**SE**	**Mean±SD**	**SE**
Rismanchian et al. (2009)[55]	54.3±5.4 (45-75)	30:45	141.8±12.7	4.00	101.2±21.6	5.6
Tripathi et al. (2014)[61]	20-70	40:40	50.5±25.8	4.08	36.6±18.2	2.9

Abbreviations: MBF (maximum bite force), N (newtons unit), n (number of sample), SD (standard deviation), SE (standard error), and - (not given, unknown, or cannot define).

SECTION III

Creating a validated mandibular FEA model

CHAPTER 3

Optimisation of osteosynthesis positioning in mandibular body fracture management using finite element analysis

Omid Daqiq[1]*, Charlotte Christina Roossien[2], Friederik Wilhelm Wubs[3], Rudolf Robert Maria Bos[1] & Baucke van Minnen[1]

[1] *Department of Oral and Maxillofacial Surgery, University Medical Center Groningen, University of Groningen, Hanzeplein 1, 9713 GZ, Groningen, The Netherlands.*
[2] *Department of Rehabilitation Medicine, University Medical Center Groningen, University of Groningen, Hanzeplein 1, 9713 GZ, Groningen, The Netherlands.*
[3] *Bernoulli Institute for Mathematics, Computer Science and Artificial Intelligence, University of Groningen, Nijenborgh 9, 9747 AG, Groningen, The Netherlands.*

Accepted: 19 April 2023 & Published: 26 June 2023
Journal: European Journal of Translational and Clinical Medicine
Cite: Daqiq O, Roossien CC, Wubs FW, Bos RR, van Minnen B. Optimisation of osteosynthesis positioning in mandibular body fracture management using finite element analysis. Eur J Transl Clin Med 2023;6(2):10-25. doi:10.31373/ejtcm/163427.

Link: https://ejtcm.gumed.edu.pl/articles/163427

ABSTRACT

Background

This proof of principle study aims to investigate the applicability of finite element analysis (FEA) in Oral and Maxillofacial (OMF) surgery, by studying the effect of mandibular body height and osteosynthesis positioning on unilateral mandibular body fractures based on Champy's technique.

Material and methods

Mandibles made of polyurethane foam (Synbone®), with heights of 18, 14, and 10 mm were used to create a FEA model with a unilateral straight-line fracture, fixated with a standard commercially available 6-hole 2 mm titanium miniplate. Two different FEA programs were used for the comparison, namely: Solidworks and Comsol Multiphysics. The FEA outcomes were compared with a series of mechanical tests with polymeric models fixed in a customised device and loaded onto a mechanical test bench.

Results

First, the study illustrated that the optimal plate position appeared to be the upper border. Second, lower mandibular height increases instability and requires a stronger osteosynthesis system.

Conclusions

FEA's and polymeric model testing outcomes of unilateral non-comminuted fractures were highly comparable with current opinions of mandibular fracture management. The promising outcome of this study makes it worthwhile to do more extensive analysis in order to determine whether FEA alone is sufficient for optimisation of fracture management.

Keywords

mandibular body fracture, finite element analysis (FEA), polymeric model testing, mandibular body height, miniplate positioning

INTRODUCTION

Osteosynthesis plates and screws are routinely used in oral and maxillofacial (OMF) surgery [1-5]. In OMF surgery, mandibular fracture management is based on two completely different principles: (1) the osteosynthesis plate must provide enough rigidity to avoid fragment displacement during functional movement achieved through rigid fixation by placing solid plates at the lower border (load-bearing principle), and (2) the Champy technique suggesting the use of semi-rigid fixation with miniplates in which the tensile forces are neutralized by placing the plates in the so-called ideal line of osteosynthesis, resulting in interfragmentary stability between the bone segments (load-sharing principle) [6-8].

The applied (mastication) forces on the mandible cause different tension and compression zones [9]. The mandibular body's upper border is a tension zone, whereas the lower border is a compression zone [8-9]. According to current clinical understanding and literature, a decrease in mandibular body height in an atrophic mandible results in a narrow range between the tension and compression zones [10-13]. In a severely atrophic mandible, the tension and compression zones more or less overlap each other and the load-sharing principle is not valid anymore [6-8, 14-15].

Following Champy's theory, many studies started using expensive and time-consuming cadaveric or polymeric bone models [16-19]. It could be beneficial to use three-dimensional (3D) modelling and finite element analysis (FEA) instead of model testing. FEA is a non-invasive computational method to evaluate the stress distribution and displacement within a structure on load application [20-21]. It is a reliable and accurate numerical simulation tool for studying force distribution in the OMF area [21-22]. FEA enables the studying of mandibular fracture fixation, possibly leading to solutions regarding plate positioning and predicting the consequences of mandibular height decrease [23-26]. So far, the use of FEA to address clinical issues has been limited. In OMF surgery, not every issue regarding the best possible osteosynthesis has been resolved, e.g. complex comminuted fractures or extremely atrophic mandibles [14-15]. As these cases are less common than non-complex fractures, any subsequent clinical studies are very time-consuming or impossible without the required inclusions [15, 27]. Therefore, there is a need for a validated three-dimensional (3D) computer modelling and FEA simulation method to analyse these fractures and to plan the best osteosynthesis system for each clinical scenario, possibly by introducing new implants (e.g. degradable or patient-specific 3D printed plates) [23].

Hence, the purpose of our study was to compare mandibular model testing with FEA as a first step towards developing a validated 3D computer model for optimising mandibular fracture management. As proof of principle, we studied the effect of plate positioning and the effect of reduced mandibular body height in mandibular body fracture management based on the FEA simulations. In this initial study, the model was simplified by using mandibles with a unilateral straight-line body fracture only. Our first hypothesis was that

the clinical observations of plate positioning and its effect on fracture stability, according to the load-bearing versus load-sharing principles, are reproducible in the 3D computer model. The second hypothesis was that the 3D computer model will confirm the theory that a reduction in atrophic mandible height leads to a decrease in interfragmentary stability making load-bearing fixation necessary. Finally, we hypothesized that FEA is a suitable tool to facilitate the visualisation of fixation stability which may subsequently help the surgeon in selecting an appropriate osteosynthesis system and in positioning the plate correctly.

MATERIAL AND METHODS

Study design

We used FEA to analyse the effect of plate positioning for different mandibular body heights with a unilateral mandibular body fracture. The FEA simulations were conducted primarily in the computer simulation software Solidworks version SP5.0, 2020, 3D Modelling and Simulation, Waltham, Massachusetts, USA). The eligibility, reproducibility and accuracy of the outcomes generated in Solidworks were compared with those from a second simulation software Comsol Multiphysics (version 5.5, 3D Modelling and Simulation, Stockholm, Sweden). Further validation was done by comparing the results with a series of polymeric models fixated in a customized device on a mechanical test bench (DYNA-MESS Prüfsysteme, Stolberg, Germany). All the mandibles were fixated with the same type of osteosynthesis system (2.0 mm titanium miniplates, KLS Martin Group, Tuttlingen, Germany) and identical simulations were conducted for each study.

Assembly modelling

Synbone (Zizers, Switzerland) mandibles with body heights of 18, 14, and 10 mm (representing the slightly, moderately and severely atrophic mandibles, respectively) were used to create the 3D computer models of the mandible. Cone beam computed tomography (CBCT) (Planmeca, Promax 3D Max ProFace, Helsinki, Finland) was conducted on each Synbone mandible and digital imaging and communication in medicine (DICOM) files were generated. The CBCT scans were made at the bone setting with a voxel size of 400 µm, tube current of 2.5 mA, and tube voltage of 120 kV. DICOM files were used for the 3D modelling of the mandibles. The 3D computer modelling dimension measurements were performed using the Mimics software (version 25.0, Materialise, Leuven, Belgium). The 3D mandible models were then created in Solidworks after which they were geometrically simplified to eliminate mesh errors and simplify the simulation computations (Figure 1). In the study, the same type of straight-line unilateral mandibular body fracture was applied to each model. The distance between the fracture surfaces was set at 0.1 mm. The fracture type, size, and placement were identical in all the 3D models. The fracture was placed in the middle of the mandibular body, in between the first molar and second premolar. A standard commercially available 6-hole 2 mm osteosynthesis titanium miniplate (KLS Martin Group, Tuttlingen, Germany) with a length of 36.3 mm and 6 x 2 mm diameter screws with a length of 18.4 mm were modelled in Solidworks. The 6-hole miniplate was used for all the FEA computer simulation analyses (Figure 2).

Figure 1. 3D computer modelling of the mandible: (**A**) Synbone® mandible, (**B**) DICOM file from CBCT, and (**C**) a simplified 3D model of a mandible.

FEA Solidworks

FEA was primarily performed in the Solidworks software. The analysis started with positioning the osteosynthesis miniplate at the mandible's upper border and subsequently lowering it towards the lower border along the fracture line. This was done to determine the effect of plate positioning at different mandibular body heights (Figure 2). Plate positions 1 to 3 represent the miniplate at the upper border, in the middle, and at the lower border of the mandible, respectively.

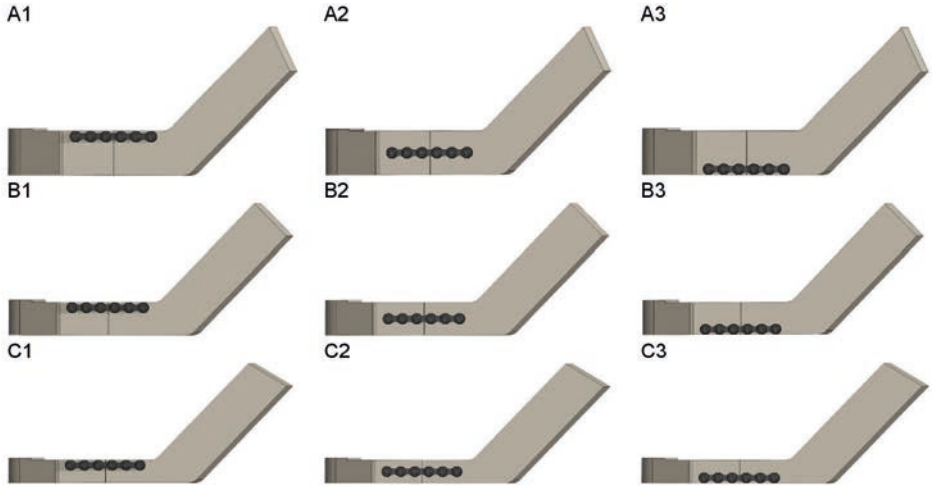

Figure 2. Plate positioning at the (**A**) 18 mm, (**B**) 14 mm, and (**C**) 10 mm mandibular body heights: (**1**) miniplate positioned at the upper border, (**2**) in the middle, and (**3**) at the lower border of the mandible.

The average mastication force (200 N) was applied downward on the symphysis of the mandible (Figure 3A) [28-29]. The mandibles were fixed at the condylar head to replicate the temporomandibular joint by applying the fixed geometry option from the Solidworks fixture property manager tab (Figure 3B). Furthermore, the effect of fixation site was evaluated by conducting a series of sensitivity tests for different fixation locations (Supplementary Figure S1).

The chosen mandible material properties were similar to those of the Synbone® polyurethane foam mandible to allow for a comparison with polymeric model testing. The mandible material

properties were set at an elastic modulus of 2410 MPa, shear modulus of 862.2 MPa, mass density of 1.26 g/cm^3, tensile strength of 40 MPa, and a Poisson's ratio of 0.39 [30-32]. The properties of the titanium miniplates and screws were as follows: an elastic modulus of 104800 MPa, mass density of 4.43 g/cm^3 , tensile strength of 1100 MPa, yield strength of 827.4 MPa, and a Poisson's ratio of 0.31 [1]. Using the Solidworks contact-sets property manager tab we defined the boundary conditions between the mandibles, miniplates, and screws (Figure 3C). The connection between the two fracture surfaces was defined by using the contact-sets with a fixed distance of 0.1 mm between the fracture surfaces (Figure 3D), representing optimal fracture reduction. When the fracture surfaces touch, only the forces normal to the surfaces would be exchanged and there was no friction force present. The mandible screw holes and the screws were set as bounded, meaning that the screws were fixed tightly in the mandible, pressing the plate against the mandibular body. The connection between the miniplate and the screws, as well as the connection between the miniplate and the mandible, were set using the contact option from the contact-sets property manager. Only normal forces and no friction were present here, which is in accordance with the current opinion on stabilising mandibular fractures using non-locking plates. The boundary conditions and parameters were identical in all of the FEA studies.

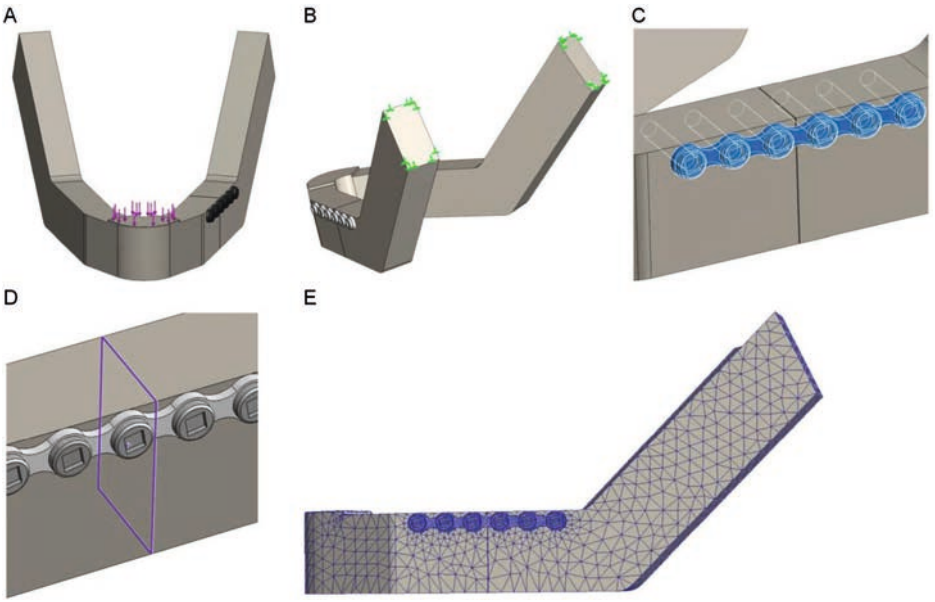

Figure 3. FEA set up in Solidworks: (**A**) Mastication force of 200 N is applied downward on the symphysis, (**B**) Fixation at the condylar head, (**C**) Contact boundary condition between the mandible and osteosynthesis system, (**D**) Contact-set boundaries between the fracture surfaces with a fracture distance of 0.1 mm and no penetration, and (**E**) Impression of the used mesh.

FEA Comsol

Comsol was used to verify the Solidworks results and to evaluate whether the outcomes were reproducible, reliable, and accurate. The 3D computer model assemblies of each mandible and the osteosynthesis miniplate were imported from Solidworks in STEP file format. The imported assemblies were processed and saved in the Comsol 3D environment. All the FEA inputs were performed identically as in Solidworks. A force of 200 N was applied downwards on the symphysis of the mandible and fixation was set at the condylar head. The connections between the miniplate and the screws, as well as between the miniplate and the mandible, were set using the contact constraint option. The connection between the mandible and the screws was set as fixed using the continuity constraint option. The applied mesh was similar to the one in Solidworks.

FEA mesh convergence

The chosen mesh dimensions were checked in the simulation models to determine whether they were correct. The mesh size was reduced until the results were independent of the mesh size and mesh convergence was reached (Supplementary Figure S2). The converged mesh was used for the remaining FEA studies (Figure 3E). The mesh applied in Solidworks was similar to the mesh in Comsol.

Polymeric model testing

A polymeric mandible is made of polyurethane foam and is an adequate substitute for cadaveric human bone for testing purposes [30-32]. It has been shown to be a successful simulator for a similar sized and shaped human bone [30, 3334]. Polymeric model testing was conducted on a mechanical test bench to validate the FEA. Polymeric mandible replicas with body heights of 18, 14, and 10 mm were obtained from Synbone. A straight-line unilateral fracture was applied to each mandibular body and fixated with the osteosynthesis miniplate system. Polymeric model testing of 18 and 14 mm mandibular heights entailed using a 4-hole miniplate with four screws. A 6-hole miniplate with six screws was used for the 10 mm mandibular height. Only the osteosynthesis miniplates positioned at the upper border of the mandible were tested. Each of the three polymeric mandible replicas (the 18, 14 and 10 mm heights) was tested three times. A custom device was built to position the mandibles on the mechanical test bench (Figure 4). A load representing the mastication force was applied to the mandible and gradually increased at a rate of 10 N/s (Figure 4A). The values were set in the computer system of the mechanical test bench. The force on the mandible was increased continuously until the failure point where the mandible breaks down was reached (Figure 4D). Computerised sensors on the mechanical test bench recorded the data. All three mandible heights were tested using the same technique.

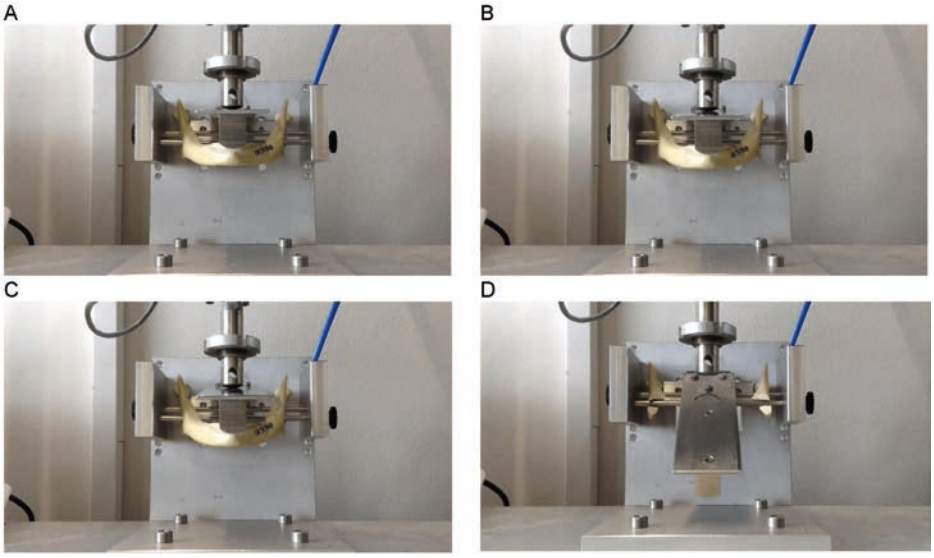

Figure 4. Mandible (with straight-line fracture and miniplate fixation) positioned on the custom-made device and loaded in a mechanical test bench; the starting point is (**A**) until it reaches the breaking point (**D**).

Data analysis

The FEA Solidworks outcomes were compared with the Comsol outcomes. This was done by first measuring the amount and the location of the maximum Von-Mises stress (Figure 7A-B). Then the displacement in the Z-axis was compared (Figure 7C-D). Finally, the Von-Mises stress pattern at a selected stress point was compared between the two FEA studies (Figure 6). The FEA outcomes were also compared with the polymeric model testing by observing the displacement patterns of the miniplates positioned at the upper borders of the mandibles with the different fracture heights (Figure 8). The displacement in the Z-axis of the FEA was used for the comparisons with the displacement in the polymeric model testing. Finally, data were evaluated with help of experts in statistics, however due to the small sample size statistical analysis did not make sense in this study.

RESULTS

FEA Solidworks

The results of the FEA are presented in Table 1, showing the maximum Von-Mises stress [MPa] and displacement [mm] outcomes. The maximum Von-Mises stress was located at the miniplates curvature between the third and the fourth screw holes, specifically at the edge of the plate where it was touching the mandibular body at the unilateral fracture site (Figure 5A-F). The table shows that stress and displacement increased with a decrease in mandibular body height. The same applies to when the miniplate was lowered from the mandibular upper border towards the lower border along the fracture line. The ratio of the

Von-Mises stress and the ratio of the displacement in relation to plate positioning (miniplate at the lower border versus the upper border) and mandibular body height (10 mm versus 18 mm) are presented in Table 2. Observing the fracture surfaces shows that when the miniplate was positioned at the upper border, the fractures remained closed, intact, and stable. This was due to the tension zone at the upper border of the mandible and the compression zone at the lower border. However, when the miniplate was lowered, particularly when positioned at the lower border, the fracture surfaces tended to open from the upper border in a wedge-shaped form. In this situation the fixation was unstable (Figure 5).

Table 1. FEA outcomes in Solidworks and Comsol regarding the maximum Von-Mises stress and displacement.

Mandible Height [mm]	Plate Position	Solidworks		Comsol	
		Von-Mises stress [MPa]	Displacement Z-axis [mm]	Von-Mises stress [MPa]	Displacement Z-axis [mm]
18	1	643	4.30	646	4.31
	2	919	4.69	911	4.73
	3	1198	5.35	1120	5.47
14	1	894	5.12	880	5.16
	2	1273	5.69	1253	5.78
	3	1599	6.46	1560	6.64
10	1	1516	8.76	1521	8.85
	2	2065	9.65	2072	9.76
	3	2536	10.53	2560	10.70

Plate position: (1) upper border, (2) middle, and (3) lower border of the mandible. The Z-axis was in the same direction as the applied 200 [N] force.

Table 2. Ratio of the Von-Mises stress [MPa] and displacement [mm] (Z-axis) for plate positioning and mandibular body height.

Ratio		Solidworks		Comsol	
		Von-Mises stress	Displacement	Von-Mises stress	Displacement
Plate Positioning *	18	1.86	1.24	1.73	1.27
	14	1.79	1.26	1.77	1.29
	10	1.67	1.20	1.68	1.21
Mandibular Body Height **	1	2.36	2.04	2.35	2.05
	2	2.25	2.06	2.27	2.06
	3	2.12	1.97	2.29	1.96

* Ratio of the miniplate positioned at the lower border compared to the upper border for the 18, 14, and 10 mm mandibular body heights.
** Ratio between the 10 mm versus the 18 mm mandibular body heights for the plates positioned at the upper (1), in the middle (2) and the lower borders (3).

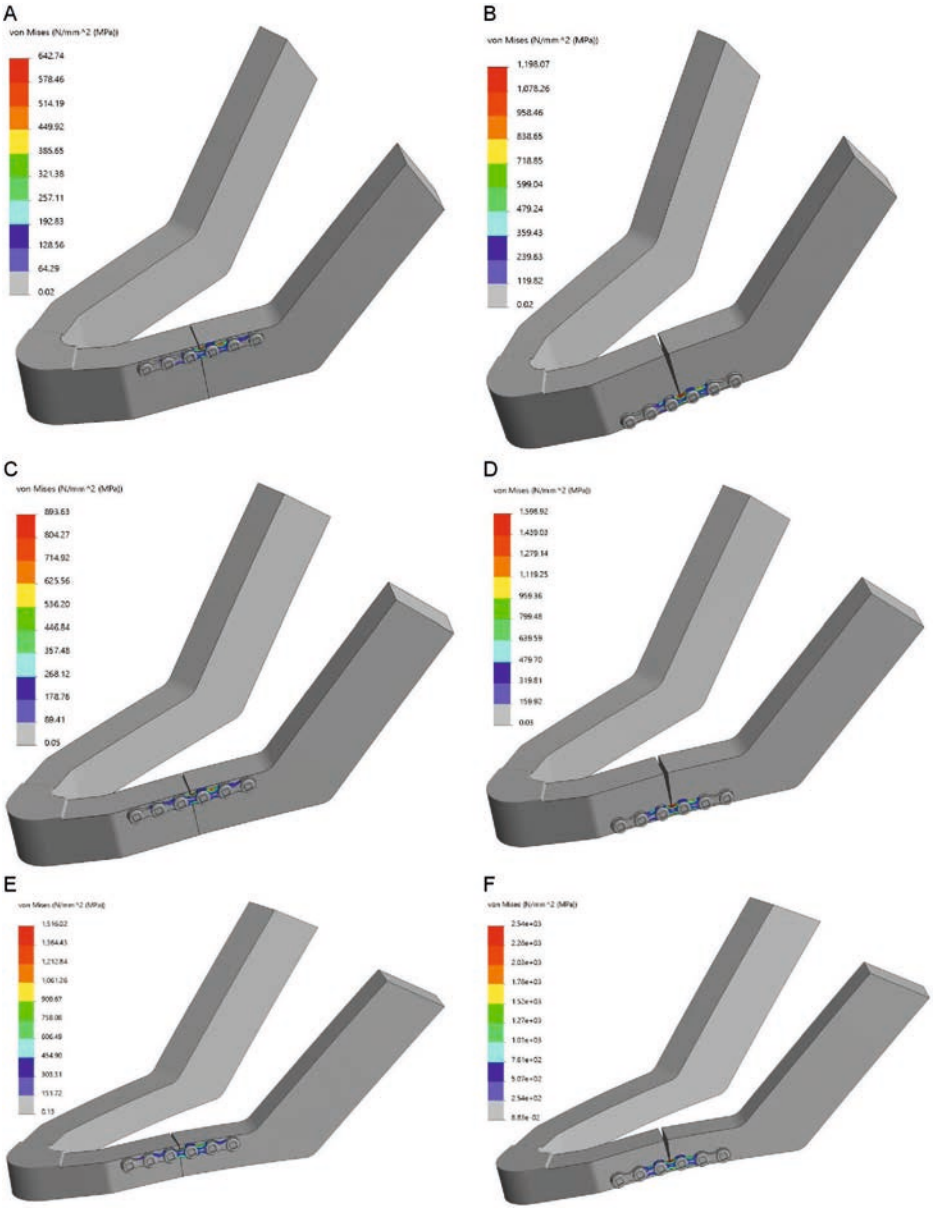

Figure 5. FEA Von-Mises stress [MPa]: (**A-B**) 18 mm height mandible, (**C-D**) 14 mm height mandible, and (**E-F**) 10 mm height mandible; note: plate positioned at the upper border (**right**) and plate positioned at the lower border of the mandible (**left**).

FEA Comsol

Comsol was used to check the reproducibility and accuracy of the Solidworks simulations. The Von-Mises stress [MPa] and displacement [mm] are shown in Table 1. The maximum stress location according to Comsol was identical to all the Solidworks FEA outcomes,

namely at the edge of the plate where it was touching the mandibular body at the unilateral fracture site (Figure 5). The Von-Mises stress pattern comparison illustrates that the stress pattern remained identical in both FEA simulations at any selected stress point (Figure 6). This demonstrates that the Solidworks FEA outcomes are reproducible, accurate and correct. Furthermore, the Von-Mises stress ratio and the displacement ratio for the plate positioning and mandibular body height were similar to those generated in Solidworks (Table 2).

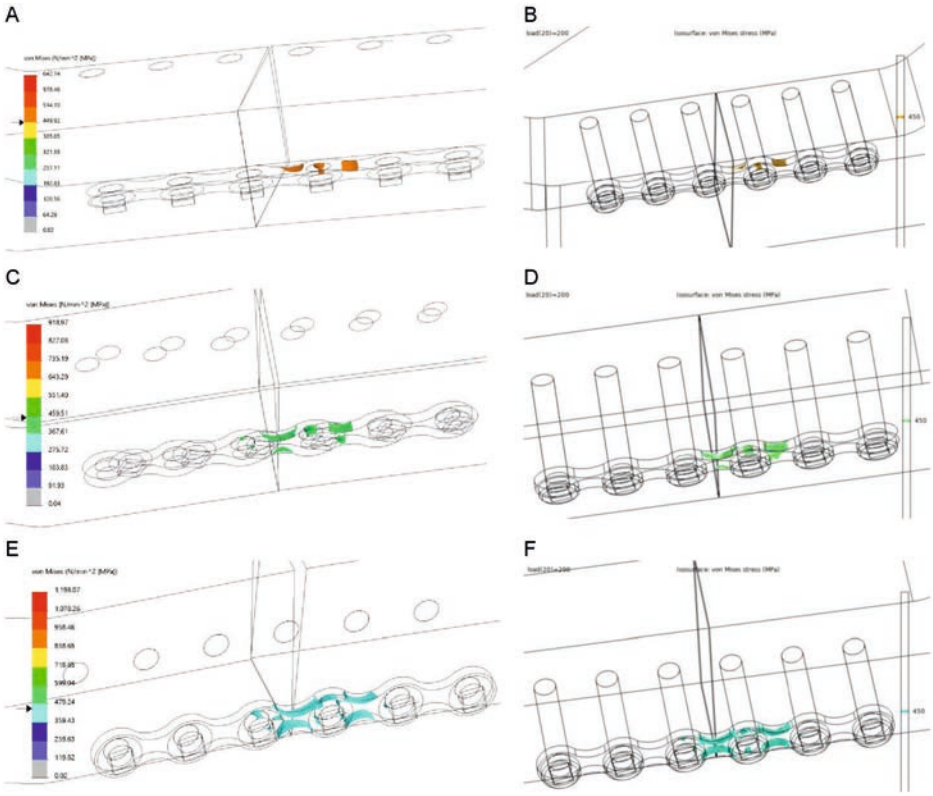

Figure 6. Comparison of Von-Mises stress between Solidworks (**right**) and Comsol (**left**) at 450 MPa for the 18 mm mandible height: (**A-B**) plate positioned at the upper border, (**C-D**) in the middle, and (**E-F**) at the lower border of the mandible.

Fixation location sensitivity test

Sensitivity test evaluations of the different fixation locations illustrated a change of less than 10% for the maximum stress and displacement values. However, no changes were observed in the stress or displacement distribution patterns, as they remained identical. Furthermore, the FEA outcomes for analysing the effect of different mandibular body heights and plate positioning remained identical with no changes observed for the different fixation locations (Supplementary Figure S2).

Polymeric model testing

The displacement outcomes of the polymeric model testing are displayed in Table 3, showing that a decrease in mandibular body height resulted in an increased displacement. This indicates that the probability of failure increases when the mandibular body height decreases. Furthermore, the polymeric testing patterns were similar to the FEA, namely: a decrease in mandibular body height increased the fixation instability leading to implant failure.

Table 3. Polymeric model testing displacement at 200 N compared to FEA displacement.

Mandibular body height [mm]	Test number	Displacement [mm]		
		Polymeric Model Testing	Solidworks (FEA)	Comsol (FEA)
18	I	3.85		
	II	3.46		
	III	3.28		
	Mean	*3.53*	*4.30*	*4.31*
14	I	4.26		
	II	3.74		
	III	5.09		
	Mean	*4.36*	*5.12*	*5.16*
10	I	4.49		
	II	5.68		
	III	5.93		
	Mean	*5.37*	*8.76*	*8.85*

All the test numbers (Test Number I-III) were done under the same conditions as miniplate located on the mandibular upper border.
Italics: the mean polymeric model displacement (average test I-III) compared to the FEA study's displacement values.

Outcomes comparison

The FEA plots show that the Von-Mises stress (Figure 7A-B) and displacement (Figure 7C-D) increased with a decrease in mandibular body height. The same applies when the miniplate was lowered from the mandibular upper border towards the lower border along the fracture line (Figure 7). The maximum Von-Mises stress location at any selected stress point was similar in both simulation software (Figure 6). Furthermore, Figure 8 shows the 200 N displacement comparisons between the FEA and polymeric model testing, where displacement increased with a decrease in mandibular body height. Both the FEA simulations and polymeric model testing illustrated a similar pattern: a decrease in height resulted in an increase in displacement (Figure 8). Finally, the FEA outcomes were similar and highly comparable with those from the polymeric model testing.

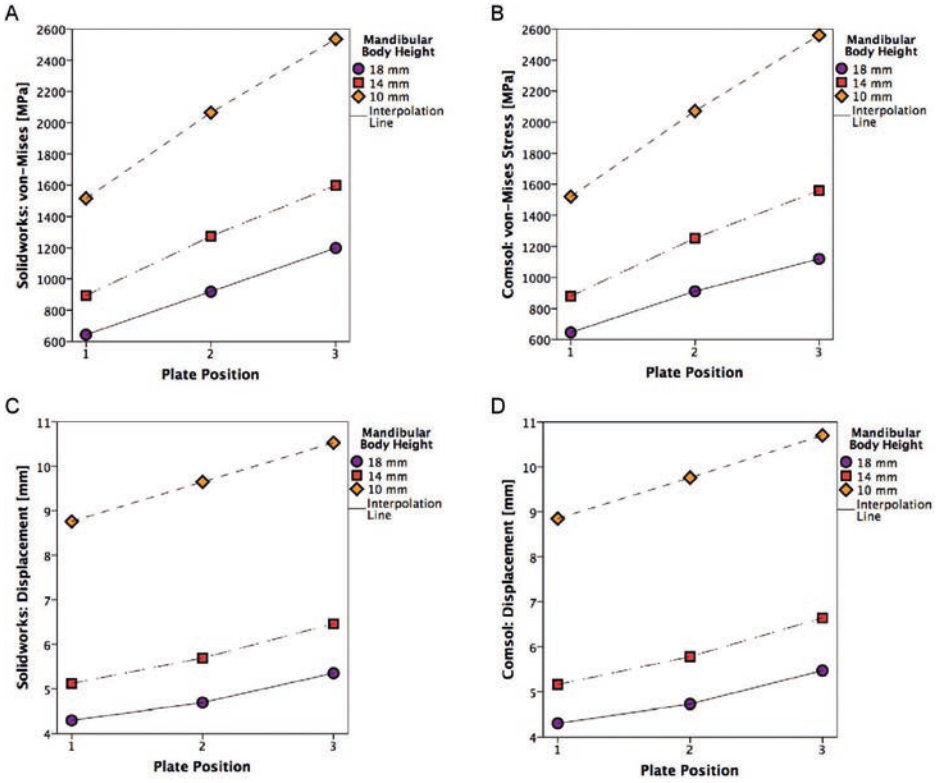

Figure 7. (**A-B**) FEA Von-Mises stress plots: (**A**) Solidworks and (**B**) Comsol; (**C-D**) FEA displacement plots: (**C**) Solidworks and (**D**) Comsol.

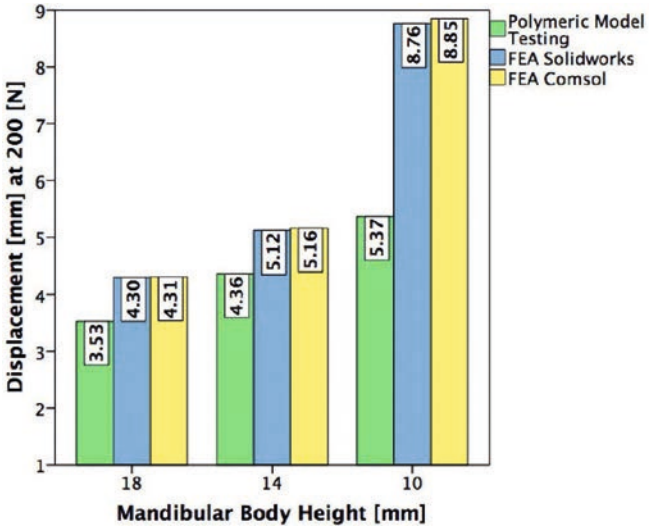

Figure 8. Displacement comparison between polymeric model testing and FEA at 200 N; the displacements are in the z-axis; the same direction as the applied mastication force.

DISCUSSION

According to the literature, FEA has been a promising applicable tool in OMF surgery to analyse different types of fracture management and osteosynthesis implants [20-24, 35].

The outcomes of our study are consistent with some of the data that can be found in the literature. According to Tams et al. plate positioning is a crucial factor for mandibular fracture fixation stability [9]. Lowering the plate along the fracture line from the mandibular upper border toward the lower border decreases the fracture fixation stability. Therefore, locating the plate on the upper border results in better stability, even with small plates. Based on Champy et al., upper border plate placement is based on the fact that mastication creates a tensile force in the upper border and a compression force at the lower border resulting in the closure of the fracture (Figure 5) [8]. This study's FEA simulation results are similar, whereby the Von-Mises stress and displacement increase when the plate is moved along the fracture line from the upper border towards the lower border of the mandibular body (Table 1, Figure 7).

According to Ellis et al. and Gerbino et al., the mandibular body height significantly affects fracture fixation stability [36-37]. A decrease in mandibular height increases fracture fixation instability [38]. It is more difficult to achieve fixation stability with a miniplate in the atrophic mandible than in cases with a normal mandibular height. In terms of stability, it means that a miniplate that does well in slightly or moderately atrophied mandibles (18 or 14 mm height) and performs poorly in severely atrophic mandibles (10 mm) (Table 2). The literature suggests several solutions for instability in the management of mandibular fractures with decreased height: e.g., thicker plates and/or more screws at each side of the fracture [36-38].

We used the polymeric model testing method to verify the FEA simulation outcomes. They both showed that displacement increases when the mandibular body height decreases (Table 3, Figure 8). This is in line with the literature [5, 8, 37] and the current clinical observation. This suggests that both FEA studies are good models for analysing mandibular fractures. Furthermore, the polymeric model testing outcomes indicate that using a 6-hole miniplate is not sufficient for lower mandibular height fracture management. It is plausible that a 4-hole miniplate would have performed even worse in this case. Therefore, 10 mm or lower mandibular height fracture fixation requires a stronger osteosynthesis system. In this case, the load-sharing principle is not valid and the load-bearing principle should be applied [6-7].

There are some limitations regarding the polymeric model testing. Namely, only displacement outcomes in the Z-axis (the same direction as the applied force) could be compared between the polymeric tests and the FEA studies. This is because the mechanical test bench used in this study could only calculate the displacement as the output result. Furthermore, the displacement values between the FEA studies compared to polymeric model testing were not exactly similar (Table 3) due to: (1) the shape of mandibles (the geometrical shapes

of the polymeric models were similar to human mandibles, whereas the FEA mandibles were simplified models to eliminate mesh errors, (2) FEA uses numerical simulation to calculate the amount of displacement. However, on the mechanical test bench, displacement was measured based on the movement of the loading bar from the predetermined zero position to the end position where the mandible fractured or fixation failed. Nevertheless, the displacement results from the FEA studies and polymeric model testing are highly comparable (Table 3, Figure 8).

Finally, our FEA and polymeric model testing outcomes are similar and comparable with earlier studies [1-9, 19]. The similar displacement patterns of the FEA and polymeric model testing, together with the comparability with earlier studies [6-9, 36-38], show that our study was conducted correctly.

The outcomes of the 3D simulation software programs were similar and comparable (Table 1 and 2) including stress and displacement patterns (Figure 6 and 7). This indicates that the FEA setup and outcomes are reproducible and correct. The minor differences in the Solidworks and Comsol outcome values are caused by the inherent differences in the computational calculations in the 3D simulation environments of both software.

Currently we are working on improving our current mandible model by developing a 3D computer model based on the exact geometrical shape of the mandible instead of using a simplified version, as we did in this study. An approachable method for 3D mandible modelling is being designed based on CT images. We believe that the FEA approach could significantly help the surgeon by giving a better understanding of the preferred fracture management regime via creating a 3D visualisation of the fracture, guiding towards an optimal reposition approach and enabling the selection of the most suitable fixation technique. Regarding complex fracture cases (e.g. comminuted or atrophic mandibles), FEA could be applied to design a patient-specific osteosynthesis system. To achieve this, we are analysing other types of mandibular fractures (e.g. angle, symphysis or parasymphysis) based on the FEA simulation and polymeric model testing validation. The model should help the surgeon to optimise mandibular fracture treatment, thereby improving the surgical practice and the clinical outcome. It is possible the same FEA methodology approach can be used for optimisation of other bone fractures. However, extensive model testing is necessary to validate whether FEA can be used to test other kinds of fracture management. Such studies could determine whether FEA alone is sufficient to optimise surgical fracture management.

CONCLUSION

This study illustrates that FEA is a promising applicable tool for simulating various types of fractures and fixation systems in OMF surgery. It can be applied in the clinical setting for fracture management. FEA can provide clinicians with a lot of information regarding the

selection of suitable osteosynthesis and the positioning of the plate concerning fracture fixation stability. This is achieved by evaluating the biomechanical behaviour between the plate and the fracture (e.g., stress, displacement, and forces). Further, FEA provides a clear visualisation of what could be expected in terms of fracture stability.

REFERENCES

1. Gareb B, Roossien CC, van Bakelen NB, Verkerke GJ, Vissink A, Bos RRM, et al. Comparison of the mechanical properties of biodegradable and titanium osteosynthesis systems used in oral and maxillofacial surgery. Sci Rep. 2020;10(1):1–18. Available from: https://doi.org/10.1038/s41598-020-75299-9.
2. Payan Y, Chabanas M, Pelorson X, Vilain C, Levy P, Luboz V, et al. Biomechanical models to simulate consequences of maxillofacial surgery. Comptes Rendus - Biol. 2002;325(4):407–17. Available from: https://doi.org/10.1016/S1631-0691(02)01443-9.
3. Wong RCW, Tideman H, Merkx MAW, Jansen J, Goh SM, Liao K. Review of biomechanical models used in studying the biomechanics of reconstructed mandibles. Int J Oral Maxillofac Surg. 2011;40(4):393–400. Available from: http://dx.doi.org/10.1016/j.ijom.2010.11.023.
4. Buijs GJ, Van Bakelen NB, Jansma J, De Visscher JGAM, Hoppenreijs TJM, Bergsma JE, et al. A randomized clinical trial of biodegradable and titanium fixation systems in maxillofacial surgery. J Dent Res. 2012;91(3):299–304. Available from: https://doi.org/10.1177/0022034511434353.
5. Bohner L, Beiglboeck F, Schwipper S, Lustosa RM, Segura CPM, Kleinheinz J, et al. Treatment of mandible fractures using a miniplate system: A retrospective analysis. J Clin Med. 2020;9(9):1–8. Available from: https://doi.org/10.3390/jcm9092922.
6. Haerle F, Champy M, Terry BC. Atlas of Craniomaxillofacial Osteosynthesis. 2nd ed. Stuttgart: Thieme; 2009. Available from: https://doi:10.1055/b-002-72255.
7. Ehrnfeld M, Manson PN, Perin J. Principles of Internal Fixation of the Craniomaxillofacial Skeleton: Trauma and Orthogenetic Surgery. 1st ed. Thieme; 2012. 137-177 p.
8. Champy M, Lodde JP. Synthèses mandibulaires. Localization des synthèses en fonction des contraintes mandibulaires [Mandibular synthesis. Placement of the synthesis as a function of mandibular stress]. Rev Stomatol Chir Maxillofac. 1976 Dec;77(8):971–6.
9. Tams J, van Loon JP, Otten E, Rozema FR, Bos RR. A three-dimensional study of bending and torsion moments for different fracture sites in the mandible: an in vitro study. Int J Oral Maxillofac Surg. 1997;26(5):383–8. Available from: https://doi.org/10.1016/S0901-5027(97)80803-X.
10. Franciosi E, Mazzaro E, Larranaga J, Rios A, Picco P, Figari M. Treatment of Edentulous Mandibular Fractures with Rigid Internal Fixation: Case Series and Literature Review. Craniomaxillofac Trauma Reconstr. 2014;7(1):35–41. Available from: https://doi.org/10.1055/s-0033-1364195.
11. Batbayar EO, Bos RRM, van Minnen B. A Treatment Protocol for Fractures of the Edentulous Mandible. J Oral Maxillofac Surg. 2018;76(10):2151–60. Available from: https://doi.org/10.1016/j.joms.2018.04.010.
12. Brucoli M, Boffano P, Romeo I, Corio C, Benech A, Ruslin M, et al. Surgical management of unilateral body fractures of the edentulous atrophic mandible. Oral Maxillofac Surg. 2020;24(1):65–71. Available from: https://doi.org/10.1007/s10006-019-00824-8.
13. Goh BT, Lee S, Tideman H, Stoelinga PJW. Mandibular reconstruction in adults: a review. Int J Oral Maxillofac Surg. 2008;37(7):597–605. Available from: https://doi.org/10.1016/j.ijom.2008.03.002.
14. Emam HA, Ferguson HW, Jatana CA. Management of atrophic mandible fractures: an updated comprehensive review. Oral Surg. 2018;11(1):79–87. Available from: https://doi.org/10.1111/ors.12300.
15. Sukegawa S, Kanno T, Masui M, Sukegawa-Takahashi Y, Kishimoto T, Sato A, et al. A retrospective comparative study of mandibular fracture treatment with internal fixation using reconstruction plate versus miniplates. J Cranio-Maxillofacial Surg. 2019;47(8):1175–80. Available from: https://doi.org/10.1016/j.jcms.2018.09.025.
16. Sittitavornwong S, Denson D, Ashley D, Walma DC, Potter S, Freind J. Integrity of a Single Superior Border Plate Repair in Mandibular Angle Fracture: A Novel Cadaveric Human Mandible Model. J Oral Maxillofac Surg. 2018;76(12):2611.e1-2611.e8. Available from: https://doi.org/10.1016/j.joms.2018.07.029.
17. Huang CM, Chan MY, Hsu JT, Su KC. Biomechanical analysis of subcondylar fracture fixation using miniplates at different positions and of different lengths. BMC Oral Health. 2021;21(1):1–12. Available from: https://doi.org/10.1186/s12903-021-01905-5.
18. Trainotti S, Raith S, Kesting M, Eichhorn S, Bauer F, Kolk A, et al. Locking versus nonlocking plates in mandibular reconstruction with fibular graft-a biomechanical ex vivo study. Clin Oral Investig. 2014;18(4):1291–8. Available from: https://doi.org/10.1007/s00784-013-1105-1.
19. Hart RT, Hennebel V V., Thongpreda N, Van Buskirk WC, Anderson RC. Modeling the biomechanics of the mandible: A three-dimensional finite element study. J Biomech. 1992;25(3):261–86. Available from: https://doi.org/10.1016/0021-9290(92)90025-V.

20. Anthrayose P, Nawal RR, Yadav S, Talwar S, Yadav S. Effect of revascularisation and apexification procedures on biomechanical behaviour of immature maxillary central incisor teeth: a three-dimensional finite element analysis study. Clin Oral Investig. 2021;25(12):6671–9. Available from: http://dx.doi.org/10.1007/s00784-021-03953-1.

21. Patussi C, Sassi LM, Cruz R, Klein Parise G, Costa D, Rebellato NLB. Evaluation of different stable internal fixation in unfavorable mandible fractures under finite element analysis. Oral Maxillofac Surg. 2019;23(3):317–24. Available from: http://doi.org/10.1007/s10006-019-00774-1.

22. Limjeerajarus N, Dhammayannarangsi P, Phanijjiva A, Tangsripongkul P, Jearanaiphaisarn T, Pittayapat P, et al. Comparison of ultimate force revealed by compression tests on extracted first premolars and FEA with a true scale 3D multi-component tooth model based on a CBCT dataset. Clin Oral Investig. 2020;24(1):211–20. Available from: https://doi.org/10.1007/s00784-019-02919-8.

23. Merema BBJ, Kraeima J, Glas HH, Spijkervet FKL, Witjes MJH. Patient-specific finite element models of the human mandible: Lack of consensus on current set-ups. Oral Dis. 2021;27(1):42–51. Available from: https://doi.org/10.1111/odi.13381.

24. Lisiak-Myszke M, Marciniak D, Bieliński M, Sobczak H, Garbacewicz Ł, Drogoszewska B. Application of finite element analysis in oral and maxillofacial surgery-A literature review. Materials (Basel). 2020;13(14):1–16. Available from: https://doi.org/10.3390/ma13143063.

25. Daas M, Dubois G, Bonnet AS, Lipinski P, Rignon-Bret C. A complete finite element model of a mandibular implant-retained overdenture with two implants: Comparison between rigid and resilient attachment configurations. Med Eng Phys. 2008;30(2):218–25. Available from: https://doi.org/10.1016/j.medengphy.2007.02.005.

26. Ammar HH, Ngan P, Crout RJ, Mucino VH, Mukdadi OM. Three-dimensional modeling and finite element analysis in treatment planning for orthodontic tooth movement. Am J Orthod Dentofac Orthop. 2011;139(1):e59–71. Available from: http://dx.doi.org/10.1016/j.ajodo.2010.09.020.

27. Novelli G, Sconza C, Ardito E, Bozzetti A. Surgical Treatment of the Atrophic Mandibular Fractures by Locked Plates Systems: Our Experience and a Literature Review. Craniomaxillofac Trauma Reconstr. 2012;5(2):65–74. Available from: https://doi.org/10.1055/s-0031-1300961.

28. Schupp W, Arzdorf M, Linke B, Gutwald R. Biomechanical Testing of Different Osteosynthesis Systems for Segmental Resection of the Mandible. J Oral Maxillofac Surg. 2007;65(5):924–30. Available from: https://doi.org/10.1016/j.joms.2006.06.306.

29. Kumar S, Sankhla B, Garg A, Dagli N, Gattumeedhi S, Ingle E. Comparative evaluation of bite forces in patients after treatment of mandibular fractures with miniplate osteosynthesis and internal locking miniplate osteosynthesis. J Int Soc Prev Community Dent. 2014;4(4):26. Available from: https://doi.org/10.4103/2231-0762.144575.

30. Brown AD, Walters JB, Zhang YX, Saadatfar M, Escobedo-Diaz JP, Hazell PJ. The mechanical response of commercially available bone simulants for quasi-static and dynamic loading. J Mech Behav Biomed Mater. 2019;90:404–16. Available from: https://doi.org/10.1016/j.jmbbm.2018.10.032.

31. Park YC, Chae DS, Kang KY, Ding Y, Park SJ, Yoon J. Comparative pull-out performances of cephalomedullary nail with screw and helical blade according to femur bone densities. Appl Sci. 2021;11(2):1–12.

32. Haug RH, Peterson GP, Goltz M. A biomechanical evaluation of mandibular condyle fracture plating techniques. J Oral Maxillofac Surg. 2002;60(1):73–80. Available from: https://doi.org/10.1053/joms.2002.29078.

33. Bredbenner TL, Haug RH. Substitutes for human cadaveric bone in maxillofacial rigid fixation research. Oral Surg Oral Med Oral Pathol Oral Radiol Endod. 2000;90(5):574–80. Available from: https://doi.org/10.1067/moe.2000.111025.

34. Aymach Z, Nei H, Kawamura H, Bell W. Biomechanical evaluation of a T-shaped miniplate fixation of a modified sagittal split ramus osteotomy with buccal step, a new technique for mandibular orthognathic surgery. Oral Surgery, Oral Med Oral Pathol Oral Radiol Endodontology. 2011;111(1):58–63. Available from: http://dx.doi.org/10.1016/j.tripleo.2010.03.028.

35. Park B, Jung BT, Kim WH, Lee JH, Kim B, Lee JH. The stability of hydroxyapatite/poly-L-lactide fixation for unilateral angle fracture of the mandible assessed using a finite element analysis model. Materials (Basel). 2020;13(1). Available from: https://doi.org/10.3390/ma13010228.

36. Ellis E, Price C. Treatment Protocol for Fractures of the Atrophic Mandible. J Oral Maxillofac Surg. 2008;66(3):421–35. Available from: https://doi.org/10.1016/j.joms.2007.08.042.

37. Gerbino G, Cocis S, Roccia F, Novelli G, Canzi G, Sozzi D. Management of atrophic mandibular fractures: An Italian multicentric retrospective study. J Cranio-Maxillofacial Surg. 2018;46(12):2176–81. Available from: https://doi.org/10.1016/j.jcms.2018.09.020.

38. Sugiura T, Yamamoto K, Murakami K, Kawakami M, Kang YB, Tsutsumi S, et al. Biomechanical Analysis of Miniplate Osteosynthesis for Fractures of the Atrophic Mandible. J Oral Maxillofac Surg. 2009;67(11):2397–403. Available from: http://dx.doi.org/10.1016/j.joms.2008.08.042.

DECLARATIONS

Ethical approval and consent to participate
Not applicable. This study does not contain any procedure with human participants or animals performed by any of the authors. All applicable international, national, and/or institutional guidelines were followed.

Informed consent
Not applicable. For this type of study, formal consent is not required.

Competing interests
The authors declare no competing of interests.

Consent for publication
The authors give consent to publish.

Author contribution
Omid Daqiq conducted the study design (including 3D modelling, FEA simulation studies, and polymeric model testing) and wrote the manuscript. Fred W. Wubs assisted with the Solidworks and Comsol FEA simulations and verification. Charlotte C. Roossien helped with the technical part of the article and Solidworks. Ruud R.M. Bos and Baucke van Minnen were responsible for the supervision and provided continuous guidance. All the authors read and approved the manuscript.

Funding
No funding was obtained for this study.

Availability of data and materials
Data are available upon request from the corresponding author.

SUPPLEMENTARY MATERIAL

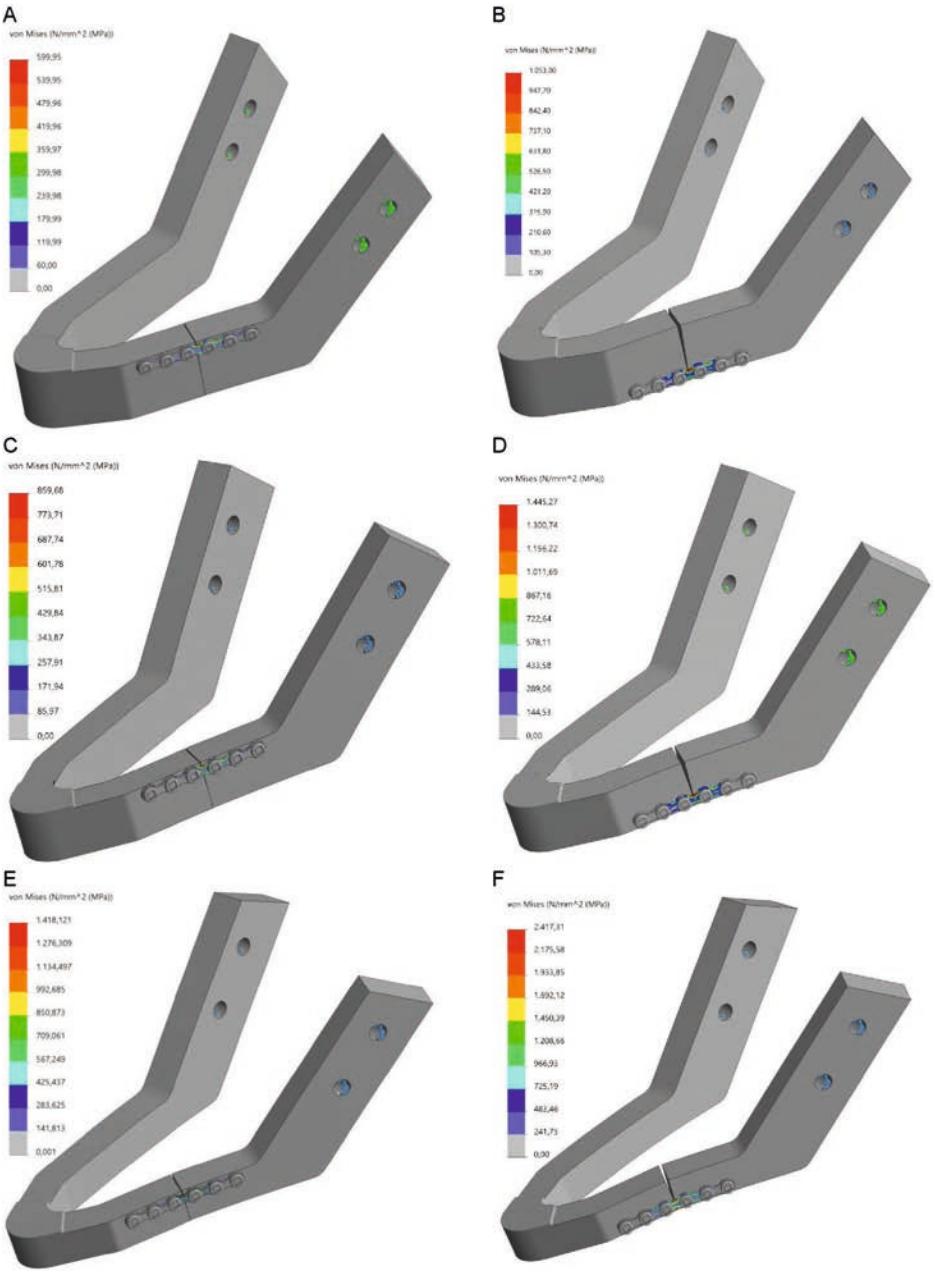

Supplementary Figure S1. FEA Von-Mises stress [MPa] for different fixation location: (**A-B**) 18 mm height mandible, (**C-D**) 14 mm height mandible, and (**E-F**) 10 mm height mandible; note: plate positioned at the upper border (**right**) and plate positioned at the lower border of the mandible (**left**).

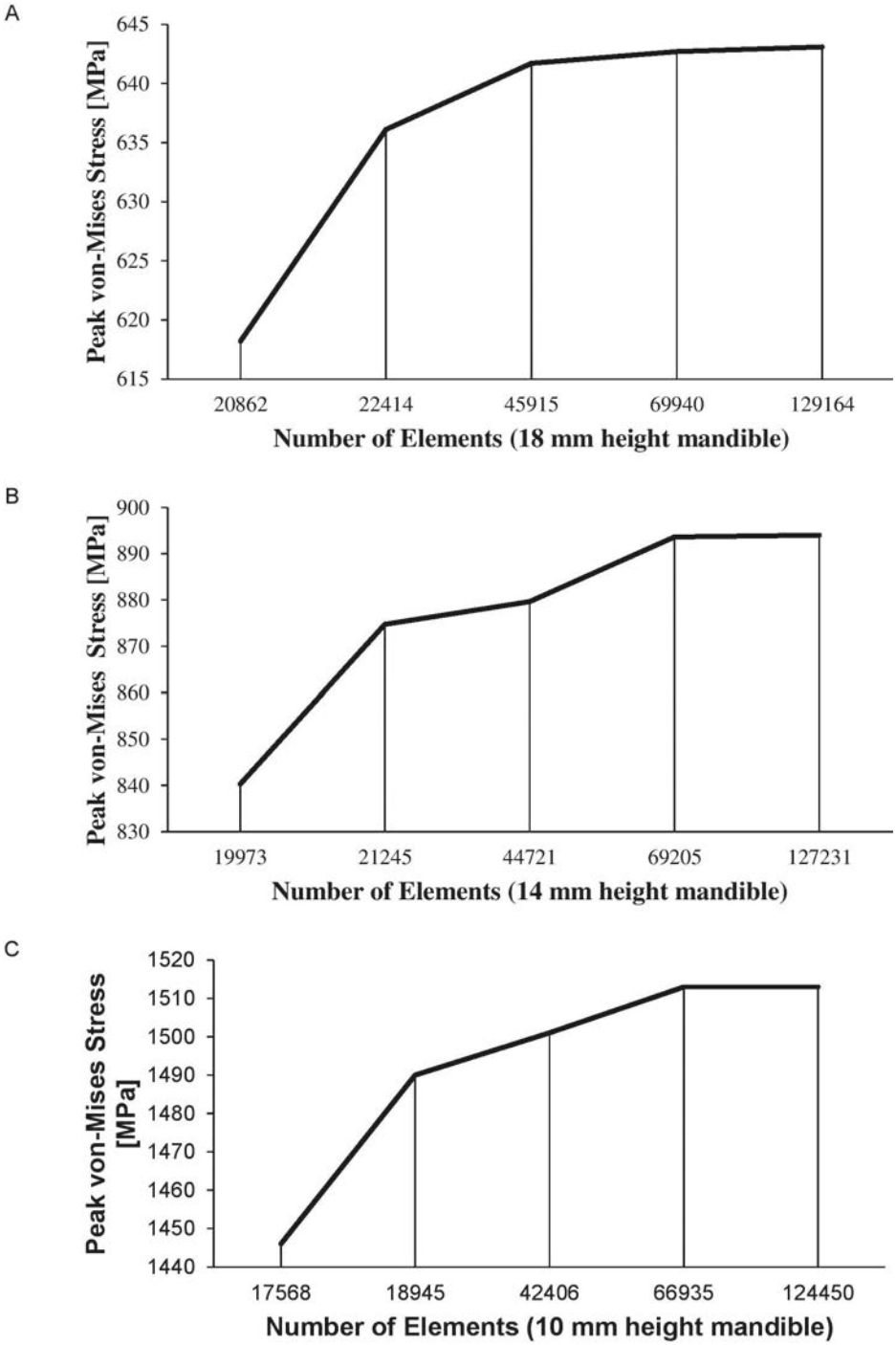

Supplementary Figure S2. Mesh convergence plots: (**A**) 18 mm height mandible, (**B**) 12 mm height mandible, and (**C**) 10 mm height mandible

ADDITIONAL APPENDIX:

Test setup 3D drawings and dimensions

Total assembly

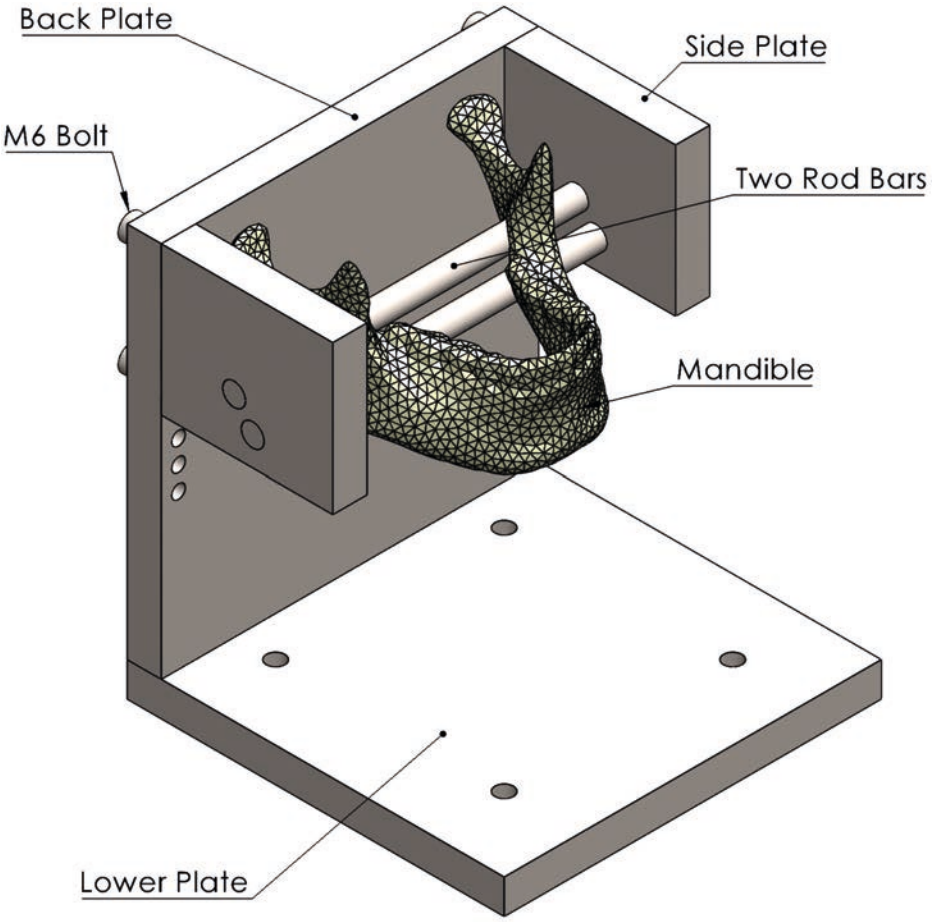

Test setup

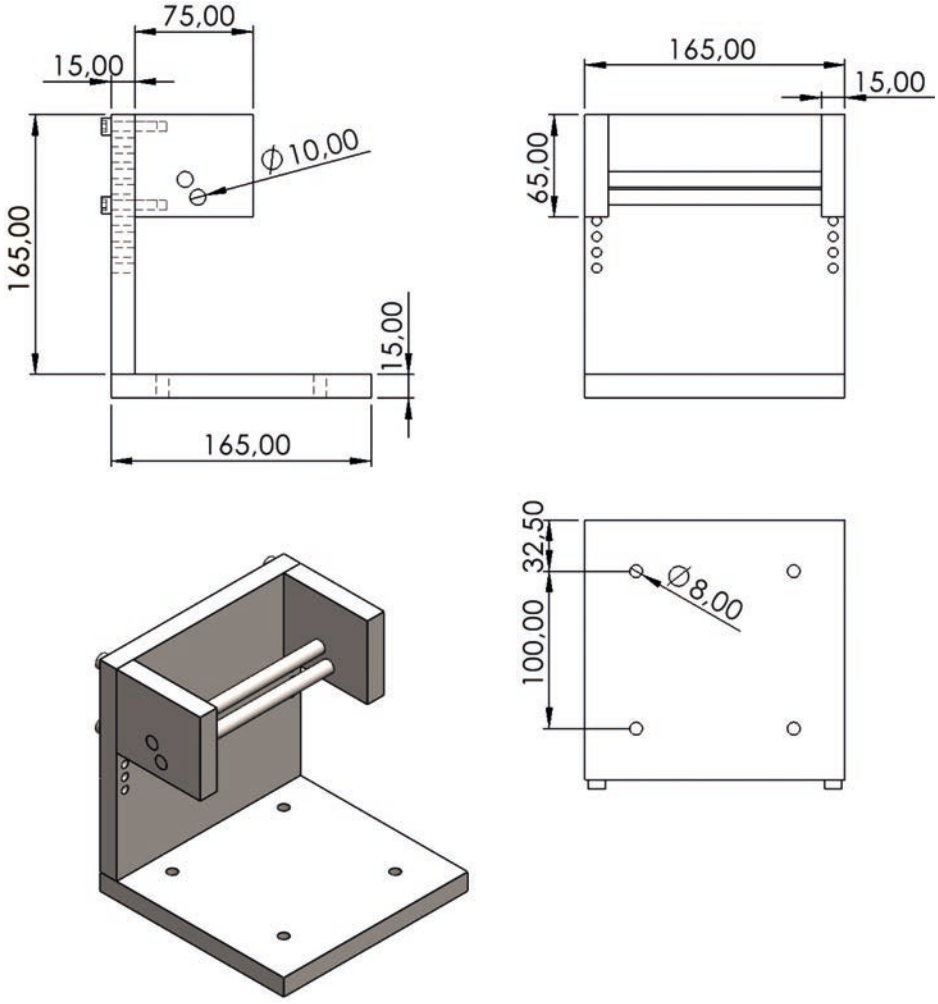
75,00
15,00
Ø10,00
165,00
15,00
165,00
165,00
15,00
65,00
32,50
Ø8,00
100,00

CHAPTER 4

Biomechanical assessment of mandibular fracture fixation using finite element analysis validated by polymeric mandible mechanical testing

Omid Daqiq[1]*, Charlotte Christina Roossien[2], Frederik Wilhelm Wubs[3], & Baucke van Minnen[1]

[1] *Department of Oral and Maxillofacial Surgery, University Medical Center Groningen, University of Groningen, Hanzeplein 1, 9713 GZ, Groningen, The Netherlands.*

[2] *Engineering and Technology Institute Groningen, Department of Bio-inspired MEMS and Biomedical Devices, University of Groningen, Nijenborgh 4, 9747 AG, Groningen, The Netherlands.*

[3] *Bernoulli Institute for Mathematics, Computer Science and Artificial Intelligence, University of Groningen, Nijenborgh 9, 9747 AG, Groningen, The Netherlands.*

Accepted 13 May 2024 & Published: 23 May 2024
Journal: Nature Scientific Reports
Cite: Daqiq O, Roossien CC, Wubs FW, van Minnen B. Biomechanical assessment of mandibular fracture fixation using finite element analysis validated by polymeric mandible mechanical testing. Sci Rep. 2024 May 23;14(1):11795. doi: 10.1038/s41598-024-62011-4. PMID: 38782942.

Link: https://www.nature.com/articles/s41598-024-62011-4

ABSTRACT

The clinical finite element analysis (FEA) application in maxillofacial surgery for mandibular fracture is limited due to the lack of a validated FEA model. Therefore, this study aims to develop a validated FEA model for mandibular fracture treatment, by assessing non-comminuted mandibular fracture fixation. FEA models were created for mandibles with single simple symphysis, parasymphysis, and angle fractures; fixated with 2.0 mm 4-hole titanium miniplates located at three different configurations with clinically known differences in stability, namely: superior border, inferior border, and two plate combinations. The FEA models were validated with series of Synbone polymeric mandible mechanical testing (PMMT) using a mechanical test bench with an identical test set-up. The first outcome was that the current understanding of stable simple mandibular fracture fixation was reproducible in both the FEA and PMMT. Optimal fracture stability was achieved with the two plate combination, followed by superior border, and then inferior border plating. Second, the FEA and the PMMT findings were consistent and comparable (a total displacement difference of 1.13 mm). In conclusion, the FEA and the PMMT outcomes were similar, and hence suitable for simple mandibular fracture treatment analyses. The FEA model can possibly be applied for non-routine complex mandibular fracture management.

INTRODUCTION

In Oral & Maxillofacial surgery (OMF), mandibular fracture management is based on two essential principles: (1) Champy's load sharing principle of placing semi-rigid miniplates corresponding to the ideal line of osteosynthesis to neutralise the tensile forces. The accompanying compression forces are compensated by the interfragmentary stability of the fracture. (2) The load bearing principle involves positioning a rigid solid plate at the lower border to avoid fragment displacement during functional movement of the mandible.[1–4]

In the last few decades after Champy's principle was introduced, many studies have been conducted to evaluate mandibular fracture fixation, e.g., to develop new osteosynthesis materials, using time consuming and expensive polymeric or cadaveric model testing.[5–7] Nowadays, it might be favourable to replace physical mandible model assessments with computer aided three dimensional (3D) modelling and finite element analysis (FEA) tools for new developments.[5–8] FEA is a computational method to evaluate stress, strain, and displacement distribution within an assembly or structure applied in different fields (e.g., engineering or medicine).[9–11] It is a non-invasive, flexible, valid, and precise instrument that can be used in OMF surgery for assessing the distribution of forces in different types of fractures or fixation methods (e.g., mandibular reconstruction and treatment in traumatology or oncological settings).[11–17]

In recent years, there have been more FEA studies in the OMF area[14–23] However, the application of FEA in clinical cases is limited in OMF surgery due to non-availability of a validated FEA model that can be routinely applied to mandibular fracture treatment. In principle, regarding complex fractures (e.g., comminuted or extremely resorbed mandibles), FEA can lead to a better understanding of fracture management (e.g., by determining and the visualisation of stress, strain, or displacements) and perhaps to new types of implants (e.g., patient tailored osteosynthesis). This means that there is a need for a validated FEA computation for mandibular fracture analysis. In a previous study, we investigated the Champy principle for unilateral simple mandibular body fracture management, using a simplified geometrical FEA model, as a proof of principle.[24] Our ultimate goal is to use a validated FEA model for analysis of more complex fractures, thereby avoiding the expensive and time consuming *in vitro* or *in vivo* tests.

The purpose of this study was to develop a validated FEA model for mandibular fracture management. This was achieved by assessing common mandibular fracture fixation with an innovative *in silico* FEA model, verified by a series of polymeric mandible mechanical testing (PMMT). We hypothesised that the mechanical behaviour of different types of simple mandibular fracture fixations correspond to the PMMT verified FEA model.

MATERIAL AND METHODS

Study outline

The study applied the FEA simulation principle to analyse simple mandibular symphysis, parasymphysis, and angle fracture fixation with varying plate positions, using a 2.0 mm 4-hole miniplate system (1.0 mm miniplate thickness) with the maxDrive 2.0 x 6 mm screws (KLS Martin, Gebrüder Martin GmbH & Co., Tuttlingen, Germany). The FEA simulations were conducted in the Solidworks software computer simulation program (version SP5.0, 2021, 3D Modelling and Simulation, Waltham, Massachusetts, USA).

The FEA outcomes were validated by a series of polymeric mandible models fixated onto a custom-built apparatus in a mechanical test bench (Instron 3400, 34TM-5 dual column table model, Norwood, USA). The FEA simulations were conducted in an identical setting as the polymeric mandible mechanical testing (PMMT), namely: identical miniplate positioning, load application, fixation, and boundary conditions.

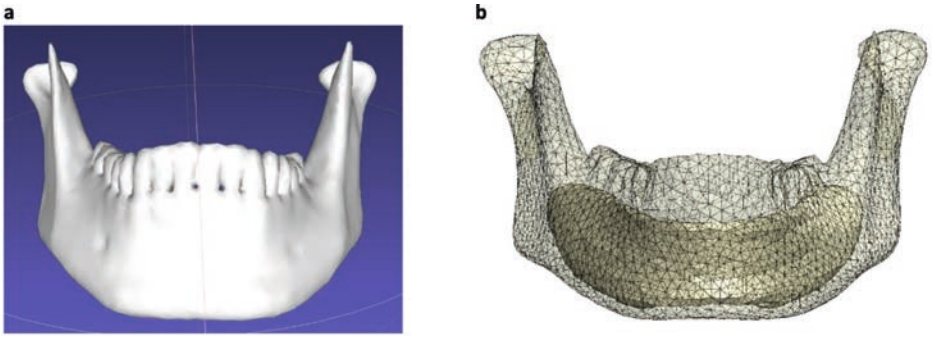

Figure 1. 3D modelling of the mandible: (**a**) Synbone mandible segmentation in Mimics, (**b**) 3D mandible model containing the cortical and trabecular bones.

3D model

Three mandibles with symphysis, parasymphysis, and angle fractures (Synbone, zizers, Switzerland) were selected to create 3D models of the mandible. Digital imaging and communication in medicine (DICOM) files of the mandibles were obtained from cone beam computed tomography (CBCT) scans (Planmeca Promax, 3D-Max ProFace, Helsinki, Finland). The CBCT scans were performed according to bone setting with 400 µm voxel size, 120 kV tube voltage, and 2.5 mA tube current. Mandible segmentation was performed by using the Mimics software (version 20.0, Materialise, Leuven, Belgium) (Fig. 1a). The trabecular bone volume segmentation was assigned by using a new mask, changing the Hounsfield unit (HU) threshold, and using multiple slice editors in Mimics. The segmented mandible was wrapped and smoothened with the 3-Matic software (version 15, Materialise, Leuven, Belgium). The cortical and trabecular bone sections were then combined into a single mandible assembly file using Geomagic (Solidworks 2021 add-in, 3D systems, Rock Hill, South Carolina, USA).

Geomagic was used to solve the segmentation geometrical mesh errors and to create a workable organic mandible assembly file that could be flawlessly imported and used in the Solidworks software. The 3D mandible model (containing the cortical and trabecular bone) was exported to the Solidworks computer simulation software in a stereolithography (STL) file format (Fig. 1b). The study used Solidworks software for 3D modelling and FEA simulation analysis. The 3D mandibles contained a single simple fracture at the symphysis, parasymphysis, and angle region, identical to the Synbone polyurethane models, with a fracture surface distance of 0.1 mm (Fig. 2). The 0.1 mm distance was based on the measured fracture surface distances from the fixated mandible replicas used in the PMMT.

A 2.0 mm 4-hole osteosynthesis titanium miniplate (KLS Martin: nr. 25-551-04-09; Dimensions: 26 mm length, 4.3 mm width, and 1 mm thickness) and a maxDrive 2.0 x 6 mm screw (KLS Martin, nr. 25-872-05-09; Screw dimensions: 2 mm diameter and 6 mm length) were modelled in Solidworks. The miniplate was used for all the fracture fixations (Fig. 2).

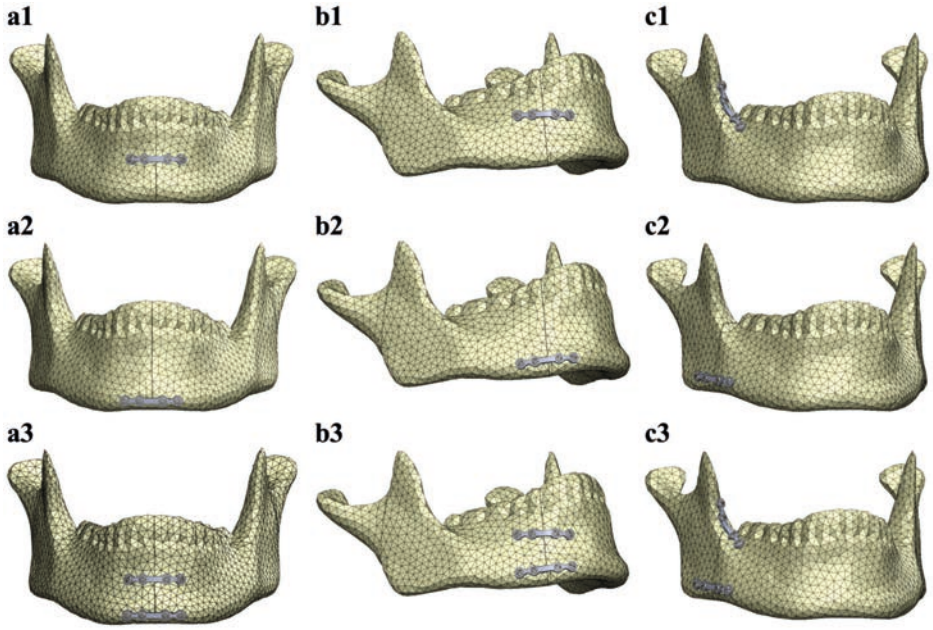

Figure 2. Plate positioning for mandibular (**a**) symphysis, (**b**) parasymphysis, and (**c**) angle fractures: (**1**) miniplate positioned at the superior border, (**2**) at the inferior border, and (**3**) the two plate combination.

Polymeric mandible mechanical testing (PMMT)

Various Synbone mandible (symphysis, parasymphysis, and angle) fractures were fixated with KLS Martin 2.0 mm 4-hole miniplates by an experienced OMF surgeon, using the LevelOne 2.0 mm KLS Martin surgical mini instrument system (2.0 mm Mini Module Regular Trauma set, KLS Martin, Gebrüder Martin GmbH & Co., Tuttlingen, Germany) (Supplementary Fig. S1). The miniplates were bent according to the shape of the mandible. The superior

miniplates were placed at the ideal line of osteosynthesis, and the inferior miniplates at the lower border. Positioning the miniplate on the mandible (e.g., bending, drilling, and screwing) was performed with the manufacturer's original instruments (KLS Martin, GmbH & Co., Tuttlingen, Germany).

An Instron mechanical test bench was used for conducting the PMMT (Instron 3400, 34TM-5 dual column table model, Norwood, USA) (Fig. 3a). The mechanical test bench was calibrated in advance, with a precision and accuracy of less than 1%. The PMMT was performed three times for each of the mandible replicas and each of the plate configurations whereupon a total of twenty-seven models were tested. This eliminated the risk of measurement bias. An automated test protocol was created inside the Instron's software (BlueHill Universal) to get an identical test set-up for all the mandible replicas.

An apparatus was custom fabricated so that the mandible could be placed onto the mechanical test bench (Fig. 3b), made of AISI (the American Iron and Steel Institute) 316 stainless steel (screws and two rod bars) and aluminium alloy (rest of the apparatus). Each mandible was secured inside the custom apparatus by 3D printed mandible holders made of Nylon (polyamide type 12), from the condyle to mid-ramus, just before the mandibular foramen (Fig. 3c). The two holes in each mandible holder were the same size as the stainless steel rod bars of the custom made apparatus which held the mandible in a fixed position. This eliminated movement, rotation, or translation of the mandible during mechanical testing. Furthermore, since Nylon can deform during multiple loading, the mandible holders were replaced after 9 tests, resulting in a total of 3 mandible holders being used during the PMMT.

The force on the mandible was applied by a custom 3D printed part, which was mounted on the mechanical test bench load cell (capable of a maximum of 5 kilonewtons [kN]) (Fig. 3d). The custom 3D printed part was made of Nylon (polyamide type 12) reinforced with an AISI 316 stainless steel ring in the centre hole that was mounted on the mechanical test bench load cell.

The mandibles were placed at an identical position inside the mechanical bench for each test. The load cell was automatically positioned at a predefined zero position. When the testing started, the mandible was set at a preload of 5 Newtons [N]. Then the load started to increase continuously at a rate of 1 Newton per second [N/s] until the failure point where the mandible's breaking point was reached. The mechanical test bench could only measure the displacement as an outcome. The displacement was recorded according to the mechanical test bench's load cell movement from the zero-position until reaching the failure point (Appendix 1: PMMT outcomes at the failure point).

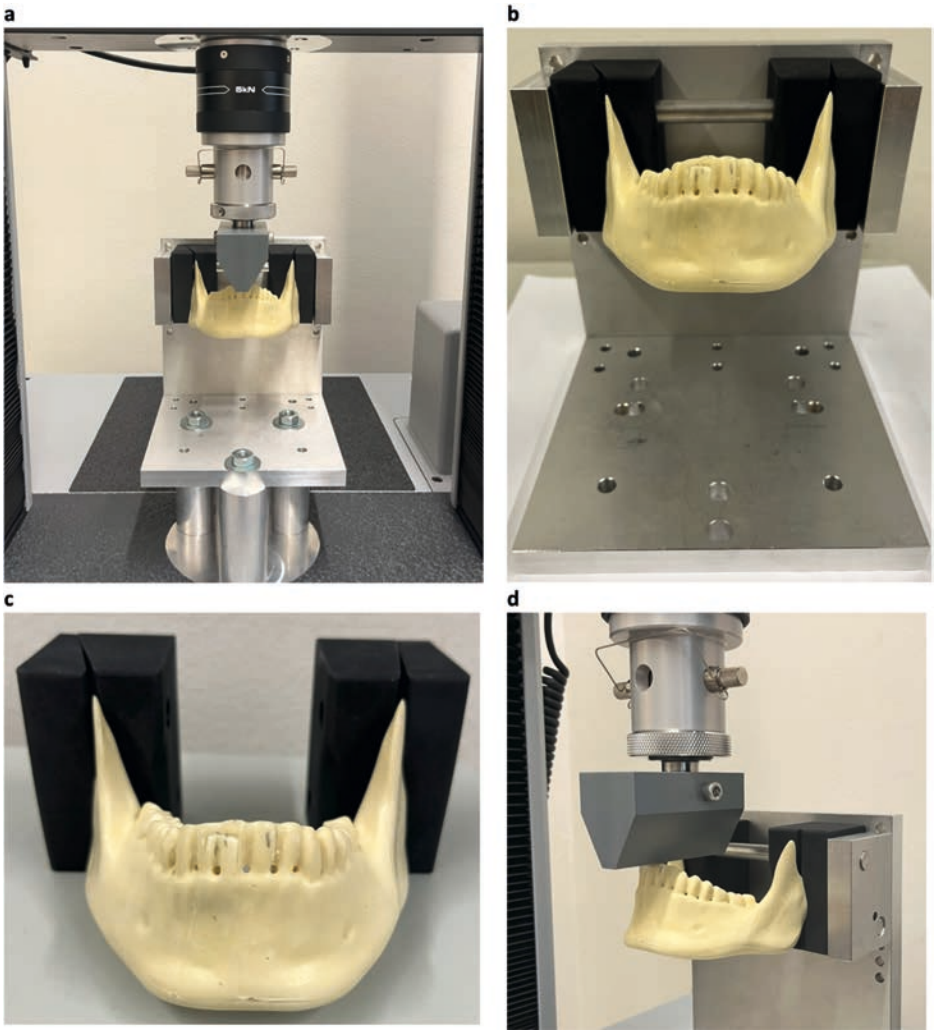

Figure 3. Polymeric mandible mechanical testing (PMMT). (**a**) The test set-up for positioning the mandible inside the mechanical test bench. (**b**) Custom fabricated apparatus for placing the mandible onto the mechanical test bench. (**c**) Custom 3D printed mandible holders for fixating the mandible inside the custom fabricated apparatus. (**d**) Load applied on the anterior of the mandible via a custom 3D printed part mounted on the mechanical test bench load cell.

Finite element analysis (FEA)

Assembly modelling

The FEA analysis started with positioning the 2.0 mm osteosynthesis miniplate at the fracture site. The miniplates were positioned at three configurations, namely: one superior plate, one inferior plate, and a two plate combination method with one miniplate located superiorly and the other inferiorly (Fig. 2).

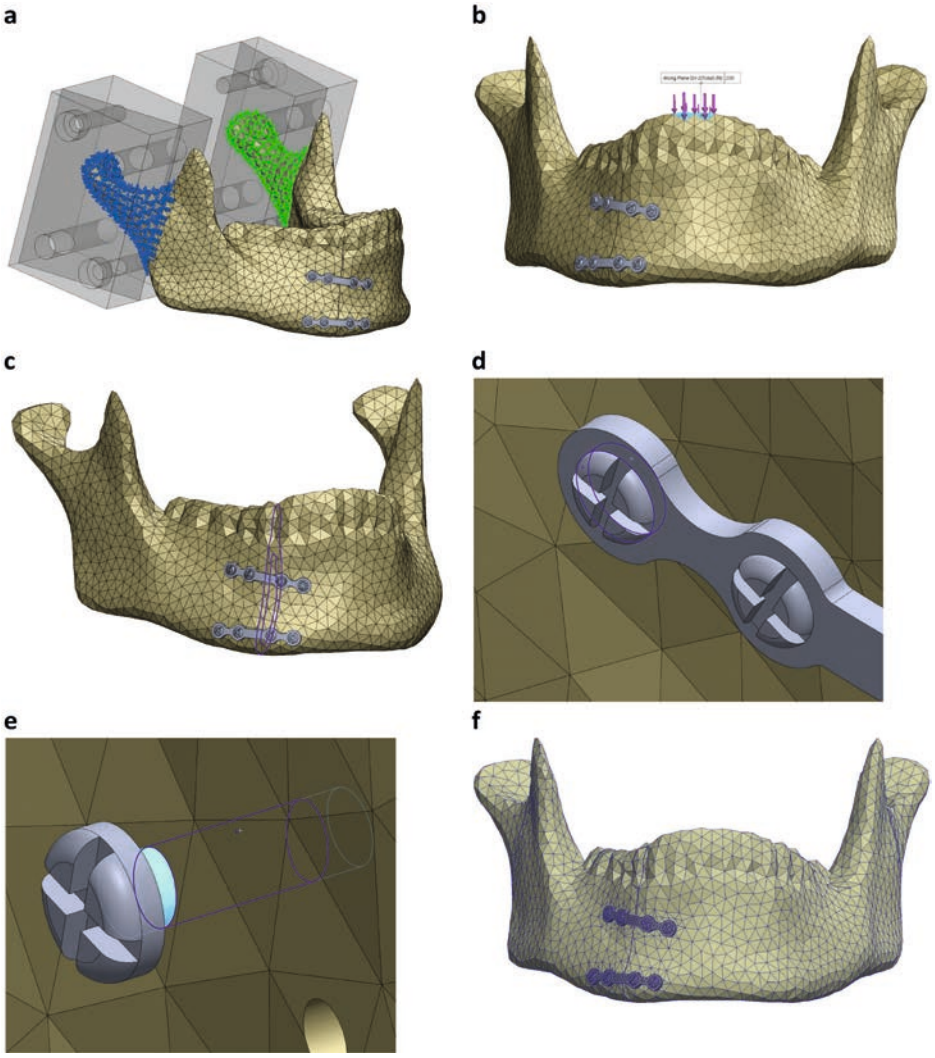

Figure 4. FEA set up in Solidworks. (**a**) Mandible fixation using fixed geometry (from the condyle to mid-ramus, just before the mandibular foramen), identical to fixation with the mandible holder in the PMMT. (**b**) Mastication force of 200 N applied downwards on the anterior of the mandible, identical to the load application in the PMMT. (**c**) Contact-Set boundaries between the fracture surfaces with a fracture distance of 0.1 mm and no penetration. (**d**) Contact boundary condition between the miniplate and screws. (**e**) Contact-Set boundary condition between the mandible and osteosynthesis. (**f**) Impression of the used converged mesh.

Force and fixation

The mandible fixation and load application in the FEA was identical to the PMMT set-up (Fig. 3). The FEA fixation configuration was matched to the mandible holder's fixation clamp system used in the PMMT (Fig. 4a). This was achieved by first placing the mandible holders on the mandible at the identical position as in the PMMT (from the condyle to mid-ramus, just before the mandibular foramen). Afterwards, the mandible fixation nodes were

selected based on the mandible holder reference lines. The line indicates the border where the mandible is not being held anymore by the mandible holder. Furthermore, the fixation was defined by using the fixed geometry option in Solidworks.

An average mastication force of 200 N was applied downwards on the mandible at the two incisor teeth, corresponding to the exact same location as the force applied in the PMMT (Fig. 4b). The 200 N force was chosen for two reasons, namely: (1) it is an average mastication force based on the literature[25–28]; and (2) this force is the best for comparing the FEA outcomes with those of the PMMT since, beyond this force, some of the mandible samples started to break during the mechanical testing (Appendix 1).

Synbone mandible material properties

The study used Synbone polymeric mandibles for both the mechanical testing and creating a 3D mandible model. Synbone is made of polyurethane (PU) synthetic foam with varying density, mimicking cortical and trabecular bone.[29–31] A few studies in the literature have evaluated the material properties of Synbone and all these studies show differences in mechanical properties.[29–33] Therefore, to increase the accuracy of this study, it was decided to determine the mechanical material properties of the Synbone mandible. This was achieved by a series of mechanical tests of Synbone foam blocks, namely: Generic Block (GB) and Generic Block High Density (GBHD). The decision to use these foam blocks was taken because, according to the manufacturer, their PU density is similar to that of the cortical and trabecular bone sections of Synbone mandibles. Test strip samples were made from the foam blocks for mechanical testing according to the American Society for Testing and Materials (ASTM) dimensions (Appendix 2 Fig. 1a). A calibrated Zwich/Roell mechanical test bench (TC-FR2, 5TS.D09, Z2.5 kN model; positioning accuracy 0.0001 mm, force accuracy 0.2%; Zwick/Roell, Venlo, the Netherlands) was used for the mechanical testing. The test strip samples were clamped onto the mechanical test bench using 3D printed grips made of Nylon (polyamide type 12) that were attached to the machine using screws (Appendix 2 Fig. 1b). The speed during the testing was set at 10 mm/min. The size of the test strips was measured before, during (at intervals of 20 N), and after testing. Multiple strips from each block were tested to get an accurate outcome measure and to eliminate measurement errors (Appendix 2 Fig. 1c-d). The mechanical properties were calculated for each test strip. Finally, all the data were analysed by a statistical expert with analysis of variance (Appendix 2 Table 1). The observed standard error was 3.47 for the cortical bone and 1.12 for the trabecular bone.

Finally, the material properties of the mandible were set according to the Synbone's material property testing outcomes. The cortical mandible's material properties were set at an elastic modulus of 196.86 megapascals [MPa], tensile strength of 6.68 MPa, yield strength of 48.12 MPa, mass density of 0.35 g/cm3, and Poisson's ratio of 0.10. The trabecular mandible's material properties were set at an elastic modulus of 60.98 MPa, tensile strength of 3.31 MPa, yield strength of 23.80 MPa, mass density of 0.19 g/cm3, and Poisson's ratio of 0.09.

Osteosynthesis material properties

The titanium osteosynthesis' (miniplate and screws) properties were: elastic modulus of 104800 MPa, tensile strength of 1100 MPa, yield strength of 827.40 MPa, mass density of 4.43 g/cm3, and Poisson's ratio of 0.31.[34]

Boundary conditions

The Solidworks contact-sets property manager tab enabled defining the boundary conditions and interactions between the mandible, miniplate, and screws (Fig. 4c-e). The interactions between the components were in accordance with the current opinion of mandibular fracture stabilisation based on a non-locking compression plate.[25–28] The cortical and trabecular bone segments were set as bounded with a 0 mm gap range using the component interaction tab in Solidworks. This meant the two fixed mandible bone segments behaved as one segment but, at the same time, kept their own identical mechanical behaviours during the simulation.

The rest of the component interactions were set by using the local interaction tab in Solidworks. The mandible fracture surfaces were defined by using contact-sets with a 0.1 mm fixed distance between the surfaces (Fig. 4c), representing optimal fracture reduction, and was in line with polymeric model testing. When fracture surfaces touch under loading, there was no friction and only forces normal to the surfaces could be exchanged. The connection between the miniplate and the screws were set as a contact in the contact-set properties (Fig. 4d). There was no friction between these components and only normal forces were exchanged between the components. The interaction between the screws and the mandible screw holes were defined as bounded (Fig. 4e). This means that the screw was tightened inside the screw hole in the mandible, keeping the miniplate fixed against the mandible surface. Finally, the connection between the mandible and the miniplate was set as the contact. This means that the miniplate was in contact with the surface of the mandible and was held firmly by the miniplate screws (the so called non-locking compression plating method).

FEA mesh convergence

The mesh size was investigated prior to running the FEA simulation analysis. Convergence of the solution was reached by reducing the mesh until the peak Von-Mises stress, in megapascals [MPa], became independent of the mesh size (Supplementary Fig. S2: mesh convergence plot). This led to a controlled mesh with a minimum element size of 1.68 mm and a maximum element size of 5 mm, which was used for the FEA studies (Fig. 4f).

Data analysis

The FEA outcomes were evaluated by firstly investigating the stress distribution, the maximum Von-Mises stress and its location (Table 1, Fig. 5-7, Fig. 9a). Secondly, the displacement was investigated in the FEA (Table 2). Furthermore, the outcomes of the mechanical testing were evaluated in terms of displacement in the PMMT (Table 2). Finally, the FEA outcomes were compared with the PMMT's displacement patterns for the various fracture types and plate configurations under a 200 N force (Table 2, Fig. 9c-d). The FEA's displacement in the

Z-axis (same axis as the force applied in the mechanical testing) was used for comparison purposes with the PMMT's displacement.

In terms of statistics, the FEA and the PMMT outcomes were analysed by statistical experts, using SPSS (version 26, IBM corporation, Armonk, New York). First, analysis of variance was applied to the Synbone material properties' testing outcomes. This determined the mean, standard deviation, and standard error of each material property parameter (Appendix 2 Table 1). Secondly, descriptive statistics was applied to determine the mean displacement, standard deviation, and 95% confidence interval of the repeated PMMT (Table 2). Furthermore, the displacement difference between the FEA and the PMMT testing was calculated (Table 2, Fig. 9c-d). Finally, other statistics was not applicable, because the sample size was not big enough for a sensible statistical analysis.

RESULTS

Finite element analysis (FEA)

The FEA outcomes illustrate the maximum Von-Mises stress in megapascals [MPa] (Table 1) and displacement in millimetres [mm] (Table 2). The stress distribution and the maximum stress varied according to the different fracture types and plate configurations (Fig. 5 and 9a). In all cases, the maximum stress was located on the osteosynthesis miniplate (see Fig. 6 and 7 for detailed frontal and back views of stress distribution on the miniplate). The Von-Mises stress was lower in the two plate combination for all the fracture types (symphysis, parasymphysis, and angle) compared to the single superior or inferior plate positioning (Fig. 5a3-c3, Fig. 9a). Compared to the single superior border (Fig. 5a1-c1), the single inferior border (Fig. 5a2-c2) plate positioning outcomes were not so satisfactory as the Von-Mises stress had increased, the fracture surfaces tended to open, and the fixation became unstable during loading. This effect was more visible for the angle fracture, where the amount of stress had increased dramatically compared to the symphysis and parasymphysis fractures.

In terms of displacement, the outcome patterns were similar to the stress outcomes (Table 2, Fig. 8, Fig. 9b-d). The displacement of the two plate combination was marginally lower compared to the single superior and the single inferior plate positioning in all the fracture types (Fig. 9b-d). Regarding the symphysis fracture, the superior border plate demonstrated slightly higher displacement compared to the inferior border plate (difference of 0.14 mm). Regarding the parasymphysis fracture, the inferior border plate exhibited slightly higher displacement than the superior plate (difference of 0.03 mm). Regarding the angle fracture, the difference became more obvious, where the superior border plate's displacement was much lower than that of the inferior border plate (difference of 0.89 mm).

Table 1. The FEA maximum Von-Mises stress and displacement outcomes.

Mandibular fracture	Miniplate configuration	Von-Mises stress [MPa]
Symphysis	Superior	711.31
	Inferior	745.00
	Two plate	690.16
Parasymphysis	Superior	856.33
	Inferior	883.07
	Two plate	541.68
Angle	Superior	1521.62
	Inferior	1588.13
	Two plate	1210.08

Table 2. Polymeric mandible mechanical testing (PMMT) displacement compared to FEA displacement at 200 N force.

Mandibular fracture	Miniplate configuration	Test number PMMT*	Displacement [mm] at 200 N		Displacement Difference ***
			PMMT*	FEA**	
Symphysis	**Superior**	1	3.82		
		2	5.33		
		3	5.18		
		Mean ± SD [95%CI]	4.78 ± 0.83 [0.94]	5.82	1.05
	Inferior	1	5.06		
		2	3.99		
		3	4.44		
		Mean ± SD [95%CI]	4.50 ± 0.54 [0.61]	5.68	1.19
	Two plate	1	4.80		
		2	4.66		
		3	3.87		
		Mean ± SD [95%CI]	4.44 ± 0.50 [0.57]	5.55	1.11
Parasymphysis	**Superior**	1	4.92		
		2	4.93		
		3	4.64		
		Mean ± SD [95%CI]	4.83± 0.16 [0.18]	6.03	1.20
	Inferior	1	4.27		
		2	6.06		
		3	4.56		
		Mean ± SD [95%CI]	4.96 ± 0.96 [1.09]	6.06	1.10
	Two plate	1	3.96		
		2	4.55		
		3	4.54		
		Mean ± SD [95%CI]	4.35± 0.34 [0.39]	5.51	1.16

[continued on next page]

Table 2. *[continued]*

Mandibular fracture	Miniplate configuration	Test number PMMT*	Displacement [mm] at 200 N		Displacement Difference ***
			PMMT*	FEA**	
Angle	**Superior**	1	5.16		
		2	4.78		
		3	6.33		
		Mean ± SD [95%CI]	5.42 ± 0.81 [0.92]	7.25	1.83
	Inferior	1	7.08		
		2	6.50		
		3	7.18		
		Mean ± SD [95%CI]	6.92± 0.37 [0.42]	8.14	1.22
	Two plate	1	5.39		
		2	5.33		
		3	4.83		
		Mean ± SD [95%CI]	5.18 ± 0.31 [0.35]	5.48	0.30

* For the PMMT: each plate configuration was repeated three times for each fracture under exact conditions (Test numbers 1-3). Furthermore, the mean, standard deviation (SD), and 95% confidence interval (CI) of the three repeated tests are shown.
** The FEA displacements are the exact values from the computer simulation at 200 N force.
*** Displacement difference between the FEA and PMMT in millimetres.

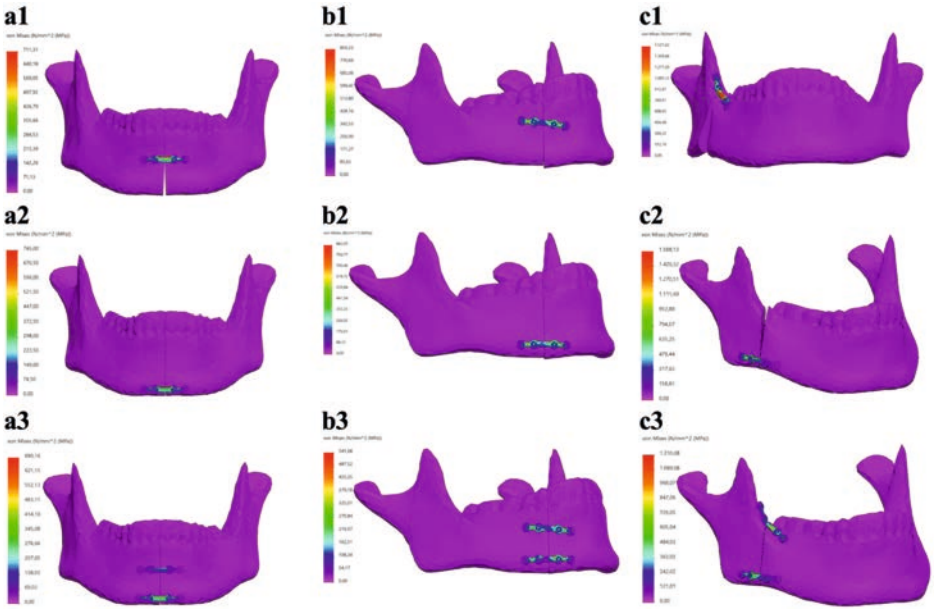

Figure 5. FEA Von-Mises stress pattern at 200 N load for (**a**) symphysis, (**b**) parasymphysis, and (**c**) angle fractures; with the miniplate positioned respectively at (**1**) the superior border, (**2**) inferior border, and (**3**) the two plate combination.

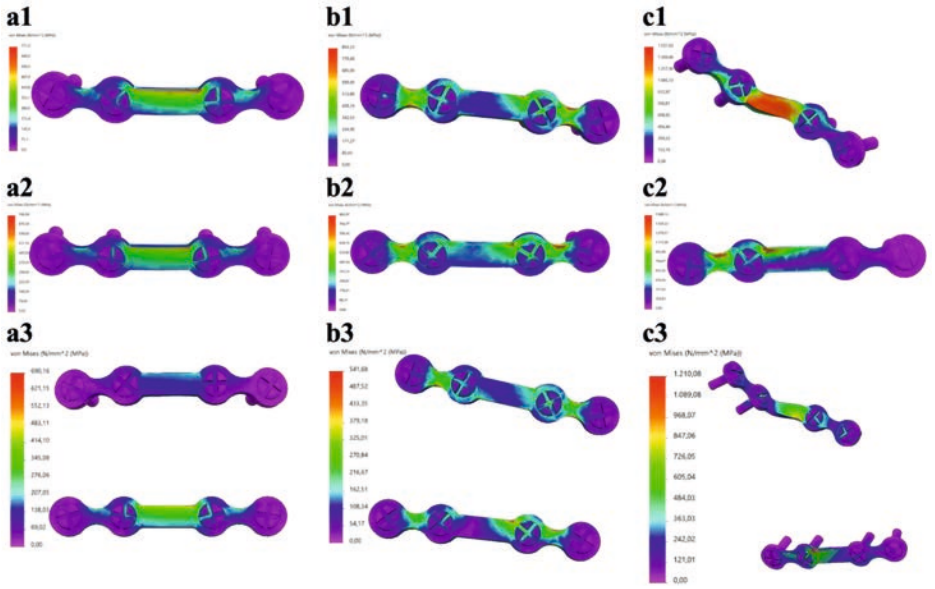

Figure 6. Frontal view of the FEA Von-Mises stress pattern on the osteosynthesis at 200 N load for: (**a**) symphysis, (**b**) parasymphysis, and (**c**) angle fractures; with the miniplate positioned respectively at (**1**) the superior border, (**2**) inferior border, and (**3**) the two plate combination.

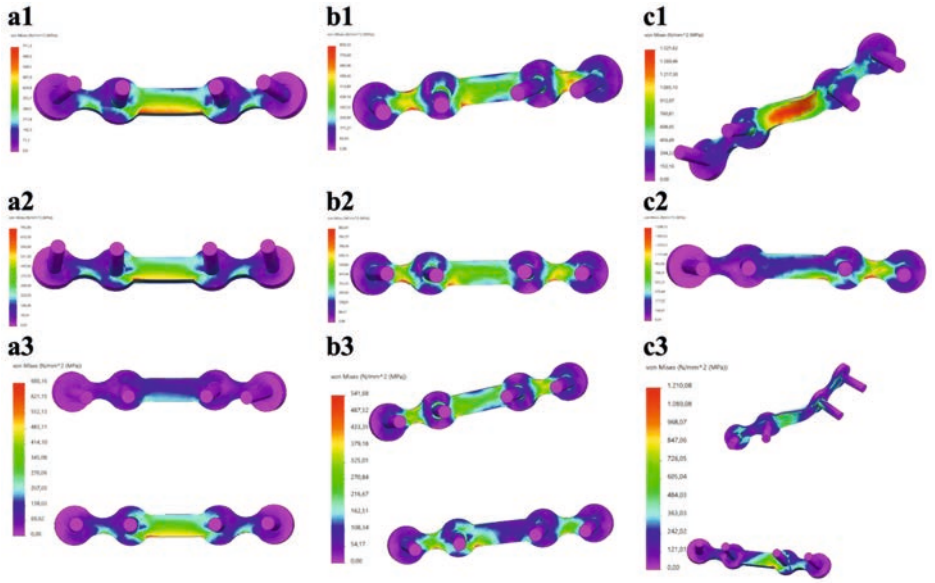

Figure 7. Back view of the FEA Von-Mises stress pattern on the osteosynthesis at 200 N load for: (**a**) symphysis, (**b**) parasymphysis, and (**c**) angle fractures; with the miniplate positioned respectively at (**1**) the superior border, (**2**) inferior border, and (**3**) the two plate combination.

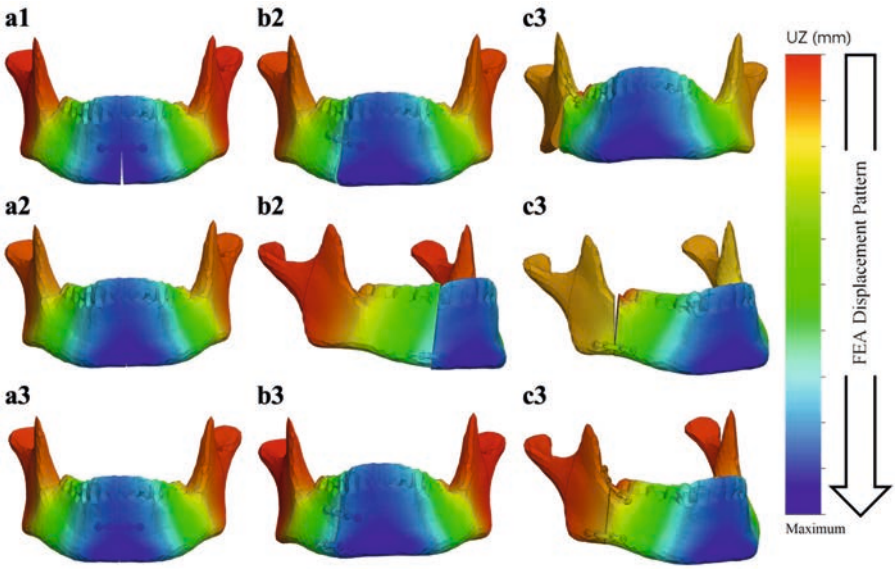

Figure 8. FEA displacement pattern with a 200 N load for (**a**) symphysis. (**b**) parasymphysis, and (**c**) angle fractures; with the miniplate positioned respectively at (**1**) the superior border, (**2**) inferior border, and (**3**) the two plate combination.
Note: The colour legend on the right side illustrates the assembly displacement pattern (with the blue colour representing the maximum displaced region).

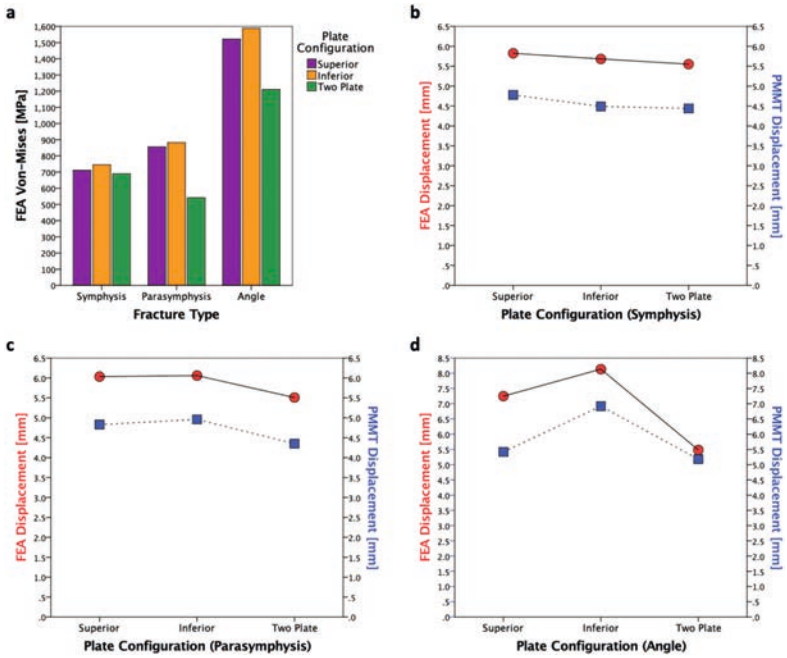

Figure 9. (**a**) FEA Von-Mises stress in [MPa]. (**b-d**) FEA (red) versus PMMT (blue) displacement for the three different plate configurations in [mm]: (**b**) symphysis, (**c**) parasymphysis, and (**d**) angle fractures.

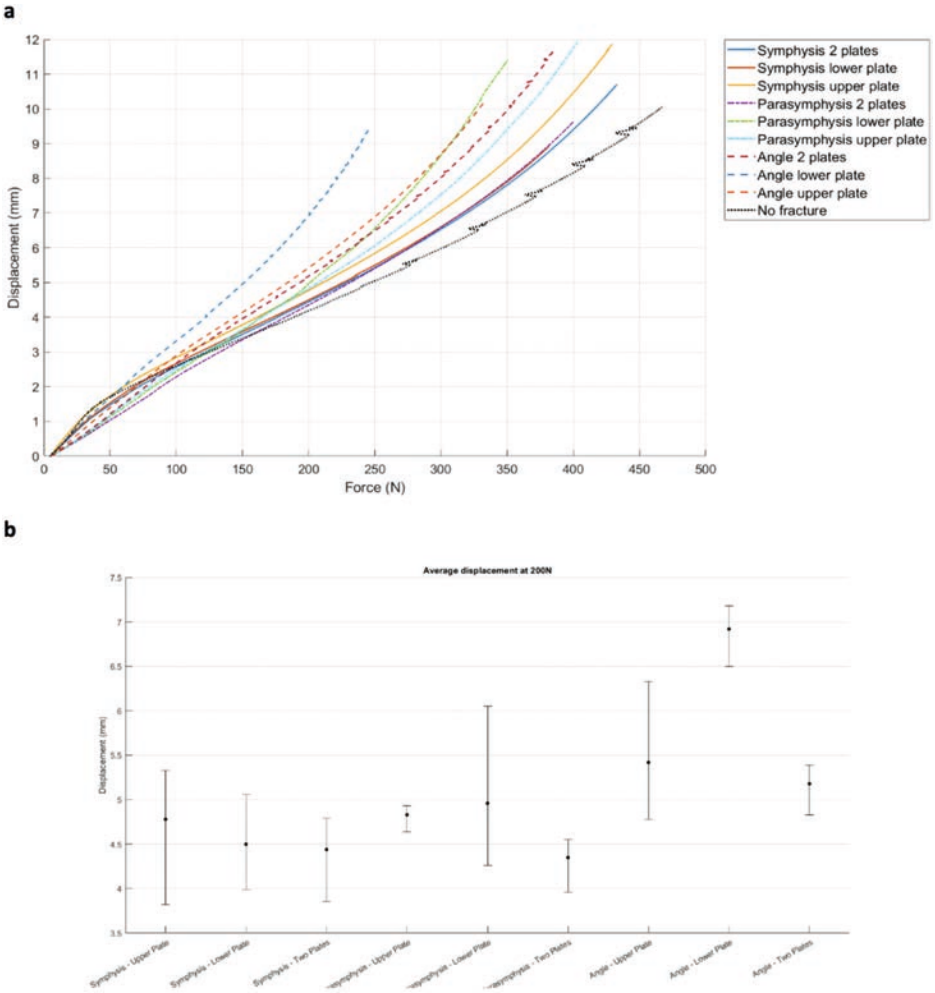

Figure 10. (**a**) Average force (x-axis) versus displacement (y-axis) of the PMMT for each mandible configuration. (**b**) Mean displacement and range for the 3 repeated tests at 200 N force.
Abbreviation: Upper plate (superior border), Lower plate (inferior border), Two plates (superior and inferior border plate combination), and Average (mean).

Polymeric mandible mechanical testing (PMMT)

The PMMT outcomes are shown in table 2 in terms of displacement [mm] on applying a 200 N force compared to the FEA displacement. The mechanical testing was performed until failure point was reached, where the polymeric mandible broke when applying the load (Fig. 10: PMMT load-displacement graph). At the failure point, all the mandible's broke at the region where the mandible was fixated with the 3D printed Nylon mandible holders (Appendix 1 Fig. 1-3: the PMMT break pattern at the failure point). In all cases, the mandible broke at a much higher force than 200 N, with some cases at just above a 200 N load (Appendix 1 Table 1: the PMMT failure force [N] and the maximum displacement [mm]). Therefore, displacement

at a force of 200 N was chosen for comparison purposes between the mechanical testing versus FEA in the Z-axis (same direction as the force applied during the mechanical testing).

In the PMMT, the two plate combination displayed the lowest displacement of all the fractures (Fig. 9b-d). Regarding the symphysis fractures, the superior border plate position demonstrated slightly higher displacement compared with the inferior border plate position (difference of 0.29 mm). Displacement was slightly lower for the parasymphysis fractures when the plate was in a superior border plate position compared to an inferior border position (difference of 0.13 mm). Regarding angle fractures, the displacement was much smaller for the superior border plate position than the inferior border plate position (a difference of 1.50 mm).

FEA versus PMMT

The displacement outcome differences between the FEA and the PMMT are shown in table 2. In all the cases, the FEA displacement was higher compared to the PMMT displacement (a total mean difference of 1.13 mm); however, the displacement patterns of both testing methods were similar for the different fracture types and plate configurations (Fig. 9b-d).

DISCUSSION

This study strived to create a validated 3D modelling and FEA numerical simulation principle for mandibular fracture management. In the study, we observed four major outcomes. First, the FEA outcomes are in line with the current understating of mandibular fracture fixation. Earlier literature suggested that the use of a single superior border miniplate may result in the least morbidity based on fracture distraction tension lines.[2,35] However, this may become a problem during functional loading due to the anatomy and biomechanics of the mandible, whereas a second inferior border miniplate would be necessary to protect the fracture site against the bending and torsional movement forces.[36–43] Such an effect was observed in our study, where the two miniplate combination generated more stability compared to a single miniplate (Table 1, Fig. 9). In the FEA, the stress on the miniplate resulted from the mandible deformities caused by the fracture. This means the miniplate(s) must hold the fracture surfaces in a stable anatomical position when a load is applied, and therefore it must withstand a huge amount of stress (Fig. 5). In the two plate method, the superior border miniplate neutralised the tension forces whereas the inferior border miniplate stabilised the compression forces (Fig. 5-8). Conversely, placing a single inferior border plate generated the least fracture stability during functional loading (Fig. 5-8).

The FEA stress outcomes (Fig. 5) suggest that all the deformations occurred on the miniplate(s), since we observed that the stress distribution in the mandible was almost constant. This may insinuate that the whole or part of the mandible can be treated as a rigid body. However, the former can be excluded by the fact that a completely rigid mandible would lead to zero stresses in the plates. To get a first impression of where the mandible can be treated as a

rigid body, we applied a 200 N load to a non-fractured mandible (Supplementary Fig. S3). The first observation was that the maximum peak Von-Mises stress of the non-fractured mandible was about 101.14 MPa (Supplementary Fig. S3a), which in Fig. 5 is in the lower range of the colour bar and hence hardly visible in those plots. However, carful observation of Fig. S3a1 illustrates that the stress in the red range of the colour bar can be traced in the exact spot in the blue range of the colour bar in Fig. 5. Secondly, the maximum stresses occurred at the fixation border with the mandible holders (Supplementary Fig. S3a1), indicating that this is the most vulnerable spot of the mandible in the study set-up. Using section clipping allows one to create a contour of the mandible regions, with the Von-Mises being equal or greater than 10 MPa (Supplementary Fig. S3a2). This shows that the stresses were smaller than in the remainder of the mandible which suggests that, apart from the fixation border area (in the mandibular ramus near the foreman mandibula) and possibly the area around the miniplate(s) regions, one could model the mandible with rigid bodies. [44–47] Therefore, we will investigate the possibilities in future studies regarding reducing the complexity of the FEA model.

Second, the outcomes of the FEA and the PMMT were consistent and comparable. The PMMT was used to verify the FEA outcomes. The study set-ups were identical in both the FEA and PMMT (e.g., identical miniplate positioning, load application, fixation location, and boundary conditions). Furthermore, the mechanical test bench in the study could only calculate the displacement as the output outcome. Therefore, only the FEA displacement in the Z-axis (same direction as the applied force in the mechanical testing) could be compared to the displacement outcome of the PMMT. However, both studies' outcomes showed a similar displacement pattern (Table 2, Fig. 9b-d). In all the fracture scenarios, displacement of the two miniplate combination was lower compared to the single superior or inferior border plate (Fig. 9b-d). Furthermore, there was a small consistent displacement difference between the FEA (slightly higher) versus the PMMT (Table 2). In the symphysis and parasymphysis fracture cases, there was an average displacement difference of 1.10 mm between the FEA versus the PMMT. In the angle fracture cases, the displacement varied marginally more between the FEA versus the PMMT; namely: 0.30 mm for the two miniplate combination, 1.83 mm for the superior border plate, and 1.22 mm for the inferior border plate.

The displacement difference between the FEA and the PMMT seems to be due to structural differences caused possibly by several factors. The first is the environmental differences between the FEA and the PMMT. FEA applies a numerical simulation to calculate the amount of stress or displacements (Fig. 5-8). Displacement in the PMMT, on the other hand, is measured according to the movement of the mechanical test bench load bar from the pre-determined zero position to the end position where the failure point is reached (Fig 10, Appendix 1). Secondly, fracture reduction may influence the outcomes. In the FEA studies, a gap of 0.1 mm was used based on the measured fracture surfaces distance from the fixated mandible replicas used in the PMMT. Regarding the PMMT, mandible fracture reduction and fixation with a miniplate was done by an expert surgeon; however, in the Synbone

models, the fracture resembled a saw cut instead of a true fracture. This may complicate the comparison with a true fracture reduction in the models. In addition, during the PMMT, the mandible was fixated using custom 3D printed mandible holders and placed in the custom apparatus for correct exact placement of the mandible onto the mechanical test bench (Fig. 3). This process might cause a minor alteration in the fracture surfaces distance in the different mandible replicas. We recommend that future studies should, if possible, measure the fracture gap after placing the mandible onto the mechanical test bench and use the corresponding distance in the FEA model. Thirdly, the composition of compact and trabecular bone may influence the outcomes. This is illustrated by the 95% confidence interval of the three repeated tests from each scenario (Table 2), illustrating a wide range in the PMMT sample data. Finally, we considered applying statistics for displacement comparison purposes between the FEA and the PMMT; however, it was not applicable due to the small sample size. Perhaps future studies could use a larger sample size.

Third, many studies in the literature have tested the Synbone mandible replicas mechanically to validate their FEA model [27,48,49] ; however, Synbone mandible replicas might not be a suitable material for FEA model validation through mechanical testing. First of all, Synbone does not provide information regarding the exact material properties of their mandible replicas of the cortical and trabecular bone sections. Secondly, investigation of the Synbone material properties in the literature illustrates different values in the studies. [27,48,49] , causing confusion regarding the true biomechanical material property values of Synbone mandible replicas. [27,48,49] Thirdly, this study's investigation of the material properties of Synbone foam blocks with densities close to the cortical and trabecular bone segments (provided by the manufacturer) illustrates that the SD and the SE of the material properties (e.g., elastic modulus) are not close enough to say whether it can be applied in FEA studies (Appendix 2 Table A1). Finally, it seems that the moulding process of making the mandible replicas creates a marginal error in the composition of the cortical and trabecular bone sections, as observed in our mandible replicas during the PMMT. This means that the biomechanical behaviour of the mandible during mechanical testing may not be identical between each mandible replica. Therefore, in future studies, we aim to use 3D printed mandibles made of a material with known properties that are comparable to real human bone instead of Synbone mandible replicas.

Finally, according to the literature, FEA is a promising tool in the OMF surgery for investigating different types of fracture management and different osteosynthesis systems or implants.[6–24,50] This study shows that our FEA model is an applicable tool for analysing simple mandibular fracture problems; therefore, the outcome of this study is a promising step towards developing a validated FEA model suitable for many different situations (e.g., complex mandibular fractures or other bone fractures in the OMF region).

In conclusion, this study illustrates that the application of the FEA principle in OMF surgery has a lot of protentional. The surgeon can take a leap of faith in the FEA's capabilities for

analysing mandibular fractures (e.g., atrophic or comminuted) as well as for studying or developing new types of osteosynthesis implants (e.g., patient specific 3D printed or biodegradable). However, there is a need for more extensive studies to conclude whether FEA alone is sufficient without having to undertake mechanical testing and whether it can be standardly applied in the clinical setting.

REFERENCES

1. Bohner, L. *et al.* Treatment of Mandible Fractures Using a Miniplate System: A Retrospective Analysis. *J Clin Med* **9**, 2922 (2020).
2. Champy, M. & Lodde, J. P. Synthèses mandibulaires. Localization des axilla en axilla des contraintes mandibulaires [Mandibular synthesis. Placement of the synthesis as a function of mandibular stress]. *Rev Stomatol Chir Maxillofac* **77**, 971–976 (1976).
3. Haerle, F., Champy, M. & Terry, B. C. *Atlas of Craniomaxillofacial Osteosynthesis*. (Georg Thieme Verlag, Stuttgart, 2009). Doi:10.1055/b-002-72255.
4. Ehrnfeld, M., Manson, P. N. & Perin, J. *Principles of Internal Fixation of the Craniomaxillofacial Skeleton*. (Georg Thieme Verlag, Stuttgart, 2012). Doi:10.1055/b-002-85491.
5. Sittitavornwong, S. *et al.* Integrity of a Single Superior Border Plate Repair in Mandibular Angle Fracture: A Novel Cadaveric Human Mandible Model. *J Oral Maxillofac Surg* **76**, 2611.e1-2611.e8 (2018).
6. Huang, C.-M., Chan, M.-Y., Hsu, J.-T. & Su, K.-C. Biomechanical analysis of subcondylar fracture fixation using miniplates at different positions and of different lengths. *BMC Oral Health* **21**, 543 (2021).
7. Trainotti, S. *et al.* Locking versus nonlocking plates in mandibular reconstruction with fibular graft-a biomechanical ex vivo study. *Clin Oral Investig* **18**, 1291–1298 (2014).
8. Hart, R. T., Hennebel, V. V., Thongpreda, N., Van Buskirk, W. C. & Anderson, R. C. Modeling the biomechanics of the mandible: A three-dimensional finite element study. *J Biomech* **25**, 261–286 (1992).
9. Anthrayose, P., Nawal, R. R., Yadav, S., Talwar, S. & Yadav, S. Effect of revascularisation and apexification procedures on biomechanical behaviour of immature maxillary central incisor teeth: a three-dimensional finite element analysis study. *Clin Oral Investig* **25**, 6671–6679 (2021).
10. Park, B. *et al.* The Stability of Hydroxyapatite/Poly-L-Lactide Fixation for Unilateral Angle Fracture of the Mandible Assessed Using a Finite Element Analysis Model. *Materials* **13**, 228 (2020).
11. Lisiak-Myszke, M. *et al.* Application of Finite Element Analysis in Oral and Maxillofacial Surgery—A Literature Review. *Materials* **13**, 3063 (2020).
12. Limjeerajarus, N. *et al.* Comparison of ultimate force revealed by compression tests on extracted first premolars and FEA with a true scale 3D multi-component tooth model based on a CBCT dataset. *Clin Oral Investig* **24**, 211–220 (2020).
13. Merema, B. B. J., Kraeima, J., Glas, H. H., Spijkervet, F. K. L. & Witjes, M. J. H. Patient-specific finite element models of the human mandible: Lack of consensus on current set-ups. *Oral Dis* **27**, 42–51 (2021).
14. Aftabi, H. *et al.* Computational models and their applications in biomechanical analysis of mandibular reconstruction surgery. *Comput Biol Med* **169**, 107887 (2024).
15. Sancar, B., Çetiner, Y. & Dayı, E. Evaluation of the pattern of fracture formation from trauma to the human mandible with finite element analysis. Part 1: Symphysis region. *Dental Traumatology* **39**, 352–360 (2023).
16. Sancar, B., Çetiner, Y. & Dayı, E. Evaluation of the pattern of fracture formation from trauma to the human mandible with finite element analysis. Part 2: The corpus and the angle regions. *Dental Traumatology* **39**, 437–447 (2023).
17. Xue, R. *et al.* Finite element analysis and clinical application of 3D-printed Ti alloy implant for the reconstruction of mandibular defects. *BMC Oral Health* **24**, 95 (2024).
18. Dario, V., Michelangelo-Santo, G., Roberto, B. & Fabio, F. Is All-on-four effective in case of partial mandibular resection? A 3D finite element study. *J Stomatol Oral Maxillofac Surg* **124**, 101463 (2023).
19. Maintz, M. *et al.* Parameter optimization in a finite element mandibular fracture fixation model using the design of experiments approach. *J Mech Behav Biomed Mater* **144**, 105948 (2023).
20. Falcinelli, C., Valente, F., Vasta, M. & Traini, T. Finite element analysis in implant dentistry: State of the art and future directions. *Dental Materials* **39**, 539–556 (2023).
21. Schönegg, D., Koch, A., Müller, G. T., Blumer, M. & Wagner, M. E. H. Two-screw osteosynthesis of the mandibular condylar head with different screw materials: a finite element analysis. *Comput Methods Biomech Biomed Engin* 1–5 (2023) doi:10.1080/10255842.2023.2209247.
22. Altuncu, F., Kazan, D. & Özden, B. Comperative evaluation of the current and new design miniplate fixation techniques of the advanced sagittal split ramus osteotomy using three-dimensional finite element analysis. *Med Oral Patol Oral Cir Bucal* **28**, 0–0 (2020).
23. Gupta, A., Dutta, A., Dutta, K. & Mukherjee, K. Biomechanical influence of plate configurations on mandible subcondylar fracture fixation: a finite element study. *Med Biol Eng Comput* **61**, 2581–2591 (2023).

24. Daqiq, O., Roossien, C. C., Wubs, F. W., Bos, R. R. M. & van Minnen, B. Optimisation of osteosynthesis positioning in mandibular body fracture management using finite element analysis. *Eur J Transl Clin Med* **6**, 10–25 (2023).
25. Rentes, A. M., Gavião, M. B. D. & Amaral, J. R. Bite force determination in children with primary dentition. *J Oral Rehabil* **29**, 1174–1180 (2002).
26. Ahmed, S. *et al.* A comparative study on evaluation of role of 1.5 mm microplates and 2.0 mm standard miniplates in management of mandibular fractures using bite force as indicator of recommendation. *Natl J Maxillofac Surg* **7**, 39 (2016).
27. Schupp, W., Arzdorf, M., Linke, B. & Gutwald, R. Biomechanical Testing of Different Osteosynthesis Systems for Segmental Resection of the Mandible. *Journal of Oral and Maxillofacial Surgery* **65**, 924–930 (2007).
28. Kumar, S. *et al.* Comparative evaluation of bite forces in patients after treatment of mandibular fractures with miniplate osteosynthesis and internal locking miniplate osteosynthesis. *J Int Soc Prev Community Dent* **4**, 26 (2014).
29. Aymach, Z., Nei, H., Kawamura, H. & Bell, W. Biomechanical evaluation of a T-shaped miniplate fixation of a modified sagittal split ramus osteotomy with buccal step, a new technique for mandibular orthognathic surgery. *Oral Surgery, Oral Medicine, Oral Pathology, Oral Radiology, and Endodontology* **111**, 58–63 (2011).
30. Bredbenner, T. L. & Haug, R. H. Substitutes for human cadaveric bone in maxillofacial rigid fixation research. *Oral Surg Oral Med Oral Pathol Oral Radiol Endod* **90**, 574–580 (2000).
31. Brown, A. D. *et al.* The mechanical response of commercially available bone simulants for quasi-static and dynamic loading. *J Mech Behav Biomed Mater* **90**, 404–416 (2019).
32. Zdero, R., Djuricic, A. & Schemitsch, E. H. Mechanical Properties of Synthetic Bones Made by Synbone: A Review. *J Biomech Eng* **145**, 121003 (2023).
33. Park, Y.-C. *et al.* Comparative Pull-Out Performances of Cephalomedullary Nail with Screw and Helical Blade According to Femur Bone Densities. *Applied Sciences* **11**, 496 (2021).
34. Gareb, B. *et al.* Comparison of the mechanical properties of biodegradable and titanium osteosynthesis systems used in oral and maxillofacial surgery. *Sci Rep* **10**, 18143 (2020).
35. Michelet, F. X., Deymes, J. & Dessus, B. Osteosynthesis with miniaturized screwed plates in axilla-facial surgery. *J Maxillofac Surg* **1**, 79–84 (1973).
36. Kroon, F. H. M., Mathisson, M., Cordey, J. R. & Rahn, B. A. The use of miniplates in mandibular fractures. *Journal of Cranio-Maxillofacial Surgery* **19**, 199–204 (1991).
37. Choi, B. H., Yoo, J. H., Kim, K. N. & Kang, H. S. Stability testing of a two miniplate fixation technique for mandibular angle fractures. An in vitro study. *Journal of Cranio-Maxillofacial Surgery* **23**, 122–125 (1995).
38. Braasch, D. C. & Abubaker, A. O. Management of Mandibular Angle Fracture. *Oral Maxillofac Surg Clin North Am* **25**, 591–600 (2013).
39. Madsen, M. J., McDaniel, C. A. & Haug, R. H. A Biomechanical Evaluation of Plating Techniques Used for Reconstructing Mandibular Symphysis/Parasymphysis Fractures. *Journal of Oral and Maxillofacial Surgery* **66**, 2012–2019 (2008).
40. Raut, R., Keerthi, R., Vaibhav, N., Ghosh, A. & Kamath Kateel, S. Single Miniplate Fixation for Mandibular Symphysis and Parasymphysis Fracture as a Viable Alternative to Conventional Plating Based on Champy's Principles: A Prospective Comparative Clinical Study. *J Maxillofac Oral Surg* **16**, 113–117 (2017).
41. Tams, J., van Loon, J.-P., Otten, E., Rozema, F. R. & Bos, R. R. M. A three-dimensional study of bending and torsion moments for different fracture sites in the mandible: an in vitro study. *Int J Oral Maxillofac Surg* **26**, 383–388 (1997).
42. Siddiqui, A., Markose, G., Moos, K. F., McMahon, J. & Ayoub, A. F. One miniplate versus two in the management of mandibular angle fractures: A prospective randomised study. *British Journal of Oral and Maxillofacial Surgery* **45**, 223–225 (2007).
43. Gear, A. J. L., Apasova, E., Schmitz, J. P. & Schubert, W. Treatment Modalities for Mandibular Angle Fractures. *Journal of Oral and Maxillofacial Surgery* **63**, 655–663 (2005).
44. Lloyd, J. E. *et al.* New Techniques for Combined FEM-Multibody Anatomical Simulation. In *New Developments on Computational Methods and Imaging in Biomechanics and Biomedical Engineering* (eds. Tavares, J. M. R. S. & Fernandes, P. R.) 75–92 (Springer International Publishing, Cham, 2019). Doi:10.1007/978-3-030-23073-9_6.
45. Rzymkowski, C. "Hybrid" Approach to Modelling of Biomechanical Systems. In *Human Biomechanics and Injury Prevention* 59–64 (Springer Japan, Tokyo, 2000). Doi:10.1007/978-4-431-66967-8_7.
46. Nispel, K., Lerchl, T., Senner, V. & Kirschke, J. S. Recent Advances in Coupled MBS and FEM Models of the Spine—A Review. *Bioengineering* **10**, 315 (2023).
47. Putame, G., Pascoletti, G., Terzini, M., Zanetti, E. M. & Audenino, A. L. Mechanical Behavior of Elastic Self-Locking Nails for Intramedullary Fracture Fixation: A Numerical Analysis of Innovative Nail Designs. *Front Bioeng Biotechnol* **8**, (2020).

48. Koper, D. C. *et al.* Topology optimization of a mandibular reconstruction plate and biomechanical validation. *J Mech Behav Biomed Mater* **113**, 104157 (2021).

49. van Kootwijk, A. *et al.* Semi-automated digital workflow to design and evaluate patient-specific mandibular reconstruction implants. *J Mech Behav Biomed Mater* **132**, 105291 (2022).

50. Patussi, C. *et al.* Evaluation of different stable internal fixation in unfavorable mandible fractures under finite element analysis. *Oral Maxillofac Surg* **23**, 317–324 (2019).

DECLARATIONS

Acknowledgment
The authors would like to thank Gerton A. Lunter (Professor of medical statistics, Faculty of medical sciences, University Medical Center Groningen), and Wim P. Krijnen (Statistics and probability, Faculty of science and engineering, University of Groningen) for their help with the statistics.

Author contributions
O.D. conducted the study design, 3D modelling, FEA computer studies, polymeric mandible mechanical testing (PMMT), and writing the manuscript. F.W.W., C.C.R, and B.v.M. were responsible for supervision, helping with data analysis, and provided continuous guidance. The authors approve the manuscript.

Competing interests
The authors have no competing interests.

Funding
No funding was obtained for this study.

Ethical approval
Not applicable. This study does not contain any procedure with human participants or animals performed by any of the authors. All applicable international, national, and/or institutional guidelines were followed.

Informed consent
Not applicable. For this type of study, formal consent is not required.

Data availability
Data is provided within the supplementary information files. Furthermore, all data are available from corresponding author upon reasonable request.

SUPPLEMENTARY MATERIAL

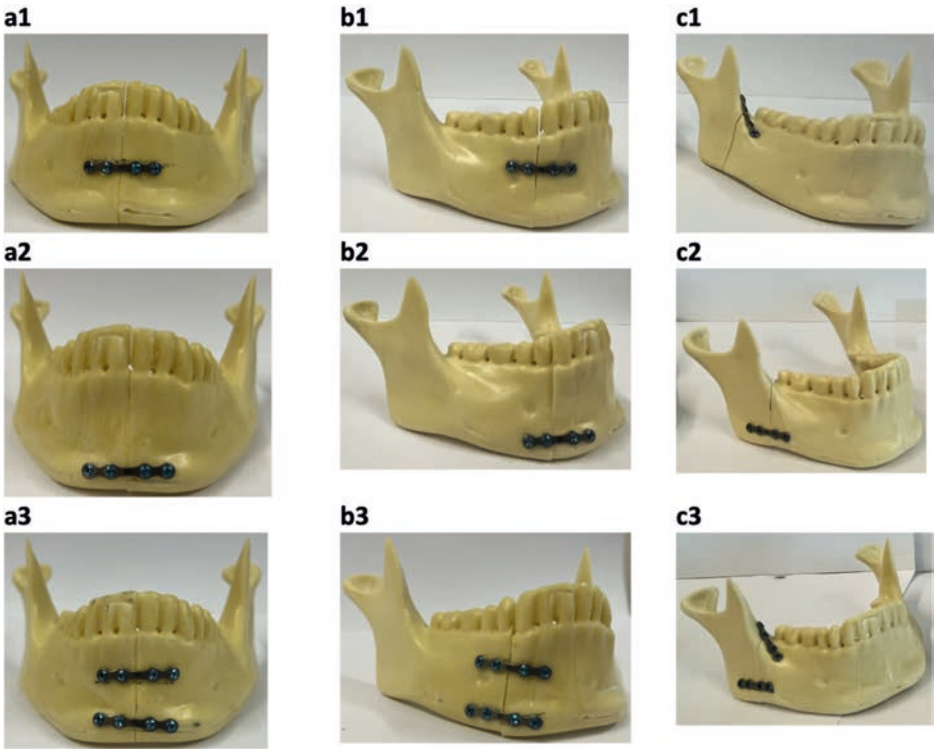

Supplementary Figure S1. PMMT miniplate positioning for mandibular (**a**) symphysis, (**b**) parasymphysis, and (**c**) angle fractures: with the miniplate positioned respectively at (**1**) the superior border, (**2**) inferior border, and (**3**) the two plate combination.

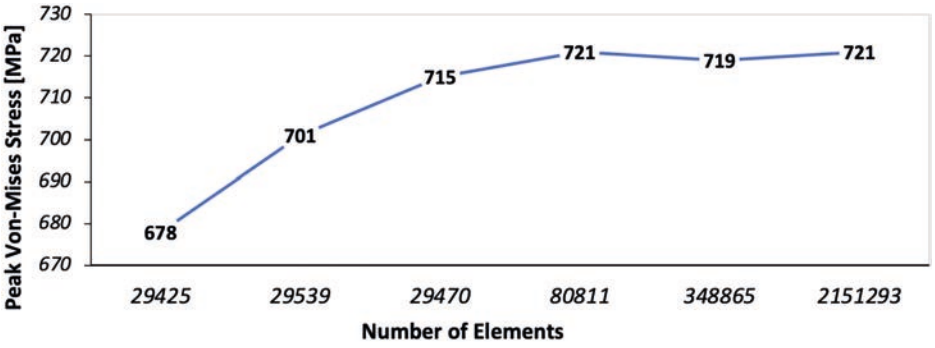

Supplementary Figure S2. Mesh convergence: X-axis the number of elements and Y-axis peak Von-Mises stress in MPa. Note: The applied mesh had a minimum element size 1.68 mm and a maximum element size of 5 mm.

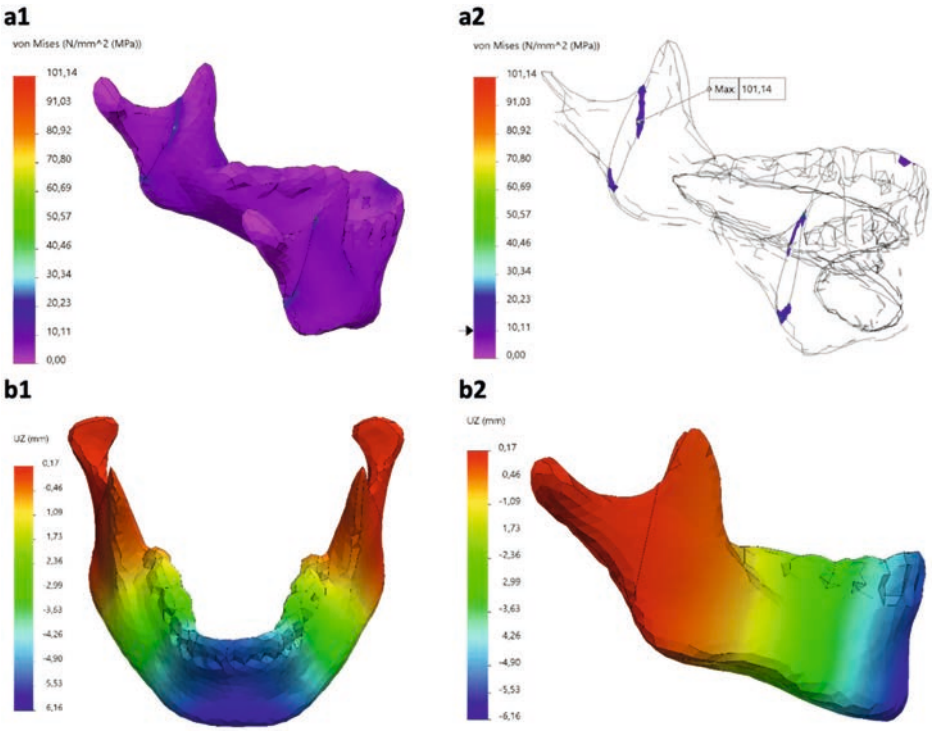

Supplementary Figure S3. FEA outcomes of a non-fractured mandible on applying a 200 N load. (**a**) Von-Mises stress in MPa: (**a1**) illustrating the stress pattern in the non-fractured mandible; (**a2**) focusing on the maximum stress region using the section clipping option in Solidworks (stress contour ≥ 10 MPa), illustrating the peak stress at the border of the fixation side with the mandible holders. (**b**) Illustrating the displacement pattern of the non-fractured mandible.

Appendix 1: Polymeric mandible mechanical testing (PMMT) outcomes at the failure point.

Appendix 1 Table A1. Polymeric mandible mechanical testing (PMMT) displacement at the failure force.

Mandibular fracture	Miniplate configuration	Test number*	Failure force [N]	Displacement [mm] at failure force
Symphysis	**Superior**	1	504	12.48
		2	429	14.31
		3	507	16.89
		Mean	*480*	*14.56*
	Inferior	1	381	10.03
		2	525	12.68
		3	425	11.59
		Mean	*443.67*	*11.43*
	Two-plate	1	467	12.38
		2	433	12.27
		3	522	12.80
		Mean	*474*	*12.48*
Parasymphysis	**Superior**	1	455	14.82
		2	403	11.85
		3	435	14.37
		Mean	*431*	*13.68*
	Inferior	1	395	12.89
		2	350	13.96
		3	454	16.06
		Mean	*399.67*	*14.30*
	Two-plate	1	400	9.41
		2	508	15.44
		3	464	12.62
		Mean	*457.33*	*12,49*
Angle	**Superior**	1	419	14.25
		2	402	11.93
		3	333	12.70
		Mean	*384.67*	*12.96*
	Inferior	1	245	9.82
		2	307	13.91
		3	250	10.13
		Mean	*267.33*	*11.29*
	Two-plate	1	384	12.41
		2	410	13.88
		3	449	14.08
		Mean	*414.33*	*13.46*

* For the PMMT: each plate configuration was repeated three times for each fracture under exact conditions (Test numbers 1-3).
Italics: mean values.

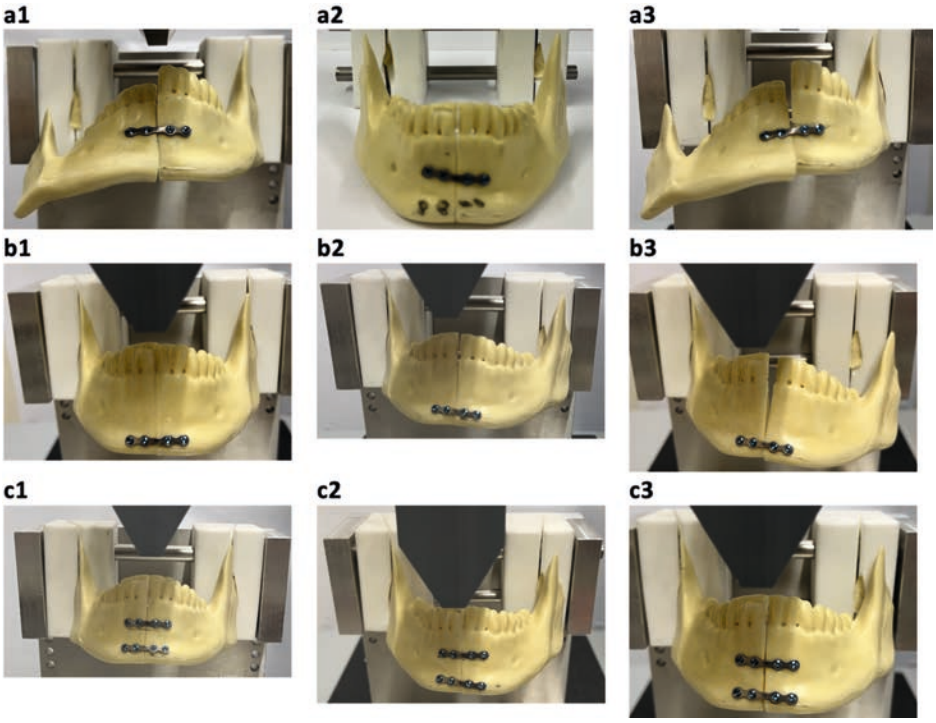

Appendix 1 Figure A1. The break pattern of mandible replicas with a symphysis fracture at the peak maximum force.
In all cases, the mandible broke at the fixated side where the mandible was fixed using the 3D printed Nylon (polyamide type 12) mandible holders inside the mechanical test bench. In all cases, the miniplate and screws remained intact on the mandible.
(**a**) Superior miniplate configuration: (a1, a2) broke on the right side (a1, a3), and (a2) broke on both fixation sides with the mandible holders.
(**b**) Inferior miniplate configuration: all the mandibles broke on the left side where the mandible was fixated by the 3D printed mandible holders inside the mechanical test bench
© Two miniplate configuration: all the mandibles broke on the left side where the mandible was fixated by the 3D printed mandible holders inside the mechanical test bench.

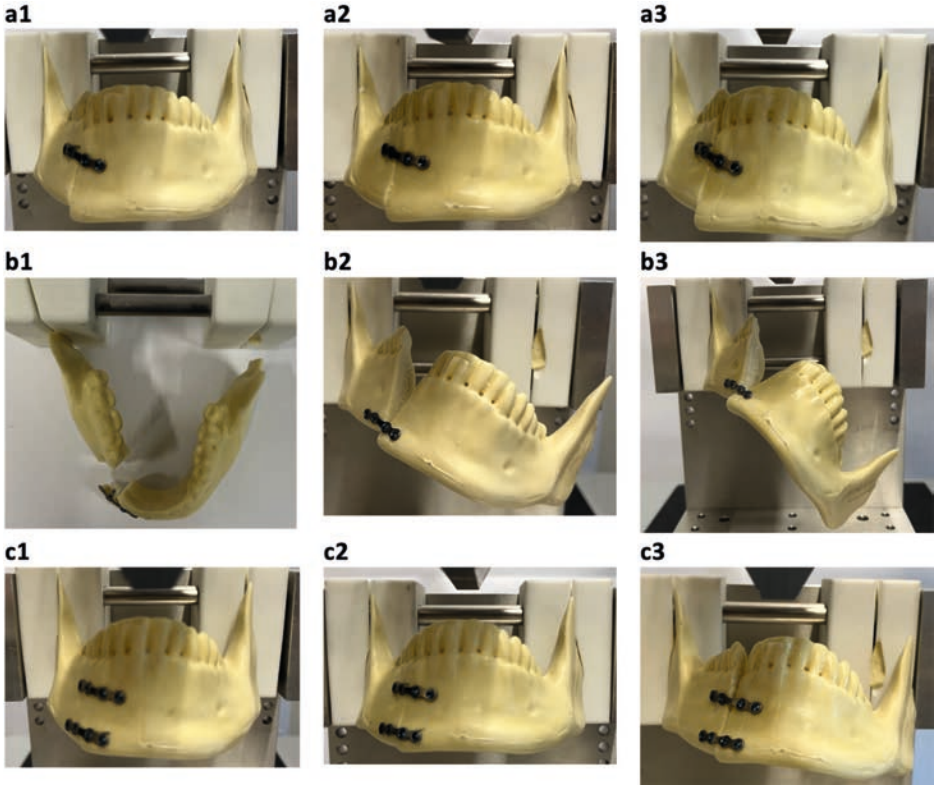

Appendix 1 Figure A2. The break pattern of mandible replicas with a parasymphysis fracture at the peak maximum force.
(**a**) Superior miniplate configuration: all the mandibles broke on the left fixated side where the mandible was fixated by the 3D printed mandible holders inside the mechanical test bench.
(**b**) Inferior miniplate configuration: all the mandibles broke on the left fixated side where the mandible was fixated by the 3D printed mandible holders inside the mechanical test bench. (b1) additional breakage at the parasymphysis fracture site into three fragments, and one screw was lost.
(**c**) Two miniplate configuration: all the mandibles broke on the left fixated side where the mandible was fixated by the 3D printed mandible holders inside the mechanical test bench.

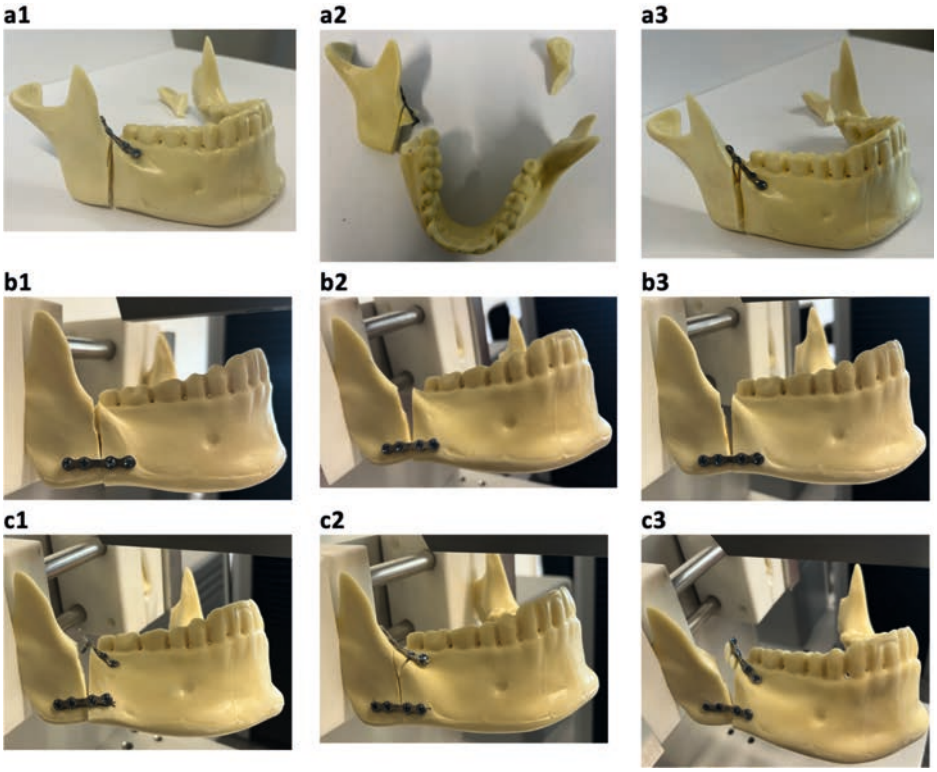

Appendix 1 Figure A3. The break pattern of mandible replicas with an angle fracture at the peak maximum force. (**a**) Superior miniplate configuration: all the mandibles broke on the left fixated side where the mandible was fixated by the 3D printed mandible holders inside the mechanical test bench. (a2) second accrued break in the angle fracture region into three fracture fragments, and one screw was loose. (a3) second accrued break on the angle fracture side into three fragments and no loose screws.
(**b**) Inferior miniplate configuration: all the mandibles broke on the left fixated side where the mandible was fixated by the 3D printed mandible holders inside the mechanical test bench.
(**c**) Two miniplate configuration: all the mandibles broke on the left fixated side where the mandible was fixated by the 3D printed mandible holders inside the mechanical test bench. (c1) two screws from the superior miniplate became loose. (c2) second breakage on the angle fracture site resulting into three total fragments with no loose screws. The fragments accrued between the second and third screws. (c3) second accrued breakage on the angle fracture side, creating four total fragments.

Appendix 2: Synbone material property testing

Appendix 2 Table A1. Outcomes of the Synbone mechanical material properties chosen for the cortical and trabecular bone properties in the FEA.

Bone	Properties	Mean	SD	SE	SE-	SE+
Cortical (GBHD)	**Elastic modulus [MPa]**	196.86	27.20	12.16	173.02	220.70
N = 5	**Tensile strength [MPa]**	6.68	0.50	0.21	6.28	7.08
	Yield strength [MPa]	48.12	3.61	1.47	45.23	51.00
	Poisson's ratio	0.01	0.11	0.05	0.01	0.19
	Mass Density (g/cm3)	0.35	-	-	-	-
Trabecular (GB)	**Elastic modulus [MPa]**	60.97	9.36	3.82	53.48	68.46
N = 6	**Tensile strength [MPa]**	3.31	0.19	0.08	3.15	3.46
	Yield strength [MPa]	23.80	1.35	0.55	22.72	24.88
	Poisson's ratio	0.09	0.07	0.03	0.04	0.14
	Mass Density (g/cm3)	0.19	-	-	-	-

Abbreviations: SD (standard deviation), SE (standard error), SE+ (standard error upper limit), SE- (standard error lower limit), and N (number of samples).
Note: the mass density was provided by the Synbone manufacturer.

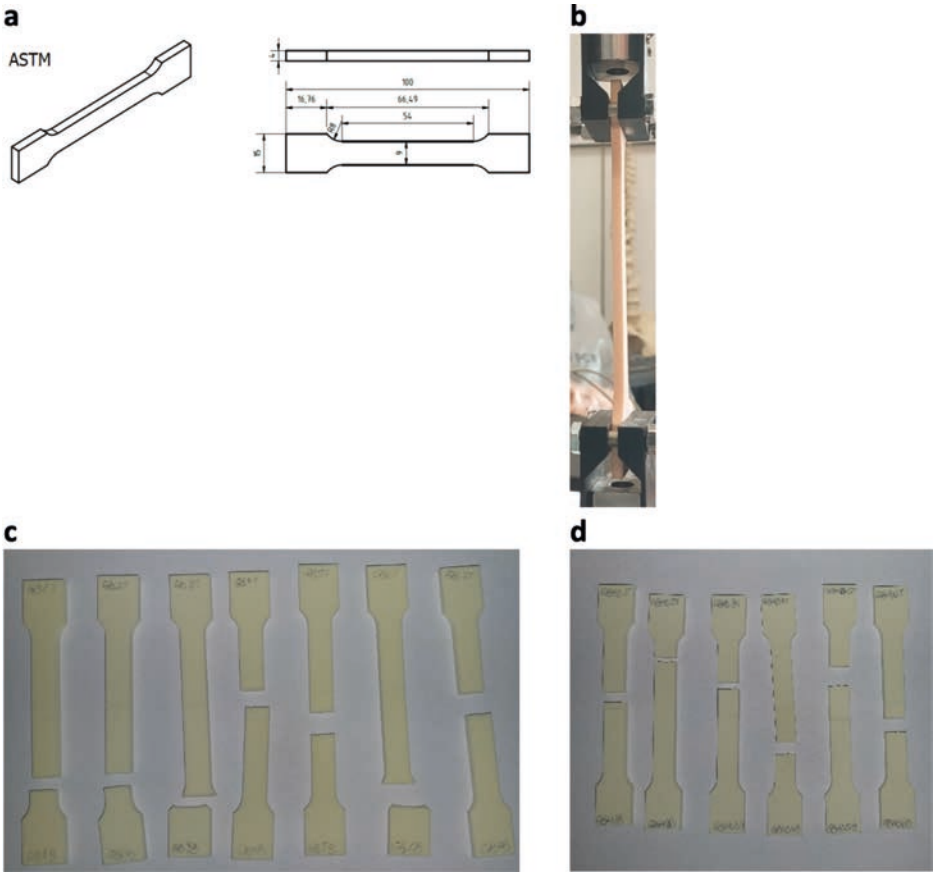

Appendix 2 Figure A1. (**a**) Test strips sizes according to the ASTM dimensions. (**b**) Test setup where the test strip was clamped inside the mechanical test bench. (**c-d**) Break pattern of the test strips: (**c**) GB, and (**d**) GBHD. *Abbreviations*: ASTM (American Society for Testing and Materials), GB (Generic Block), and GBHD (Generic Block High Density).

Additional appendix: Test setup 3D drawings and dimensions

Total assembly

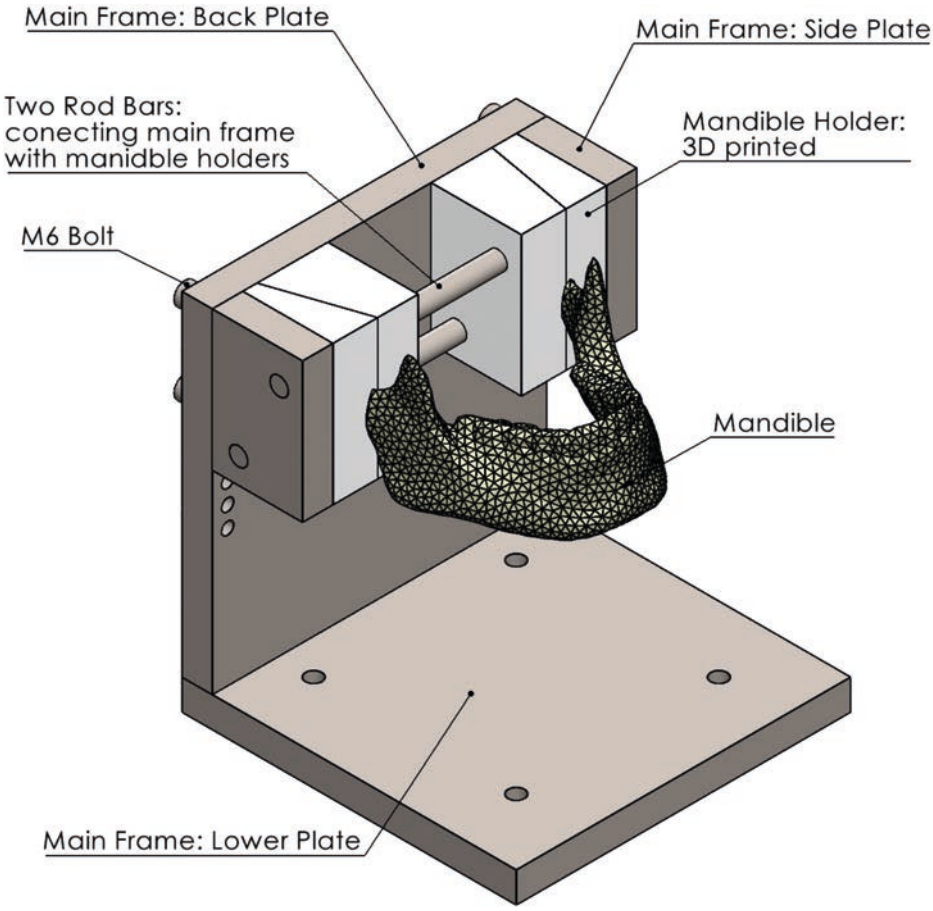

Main frame

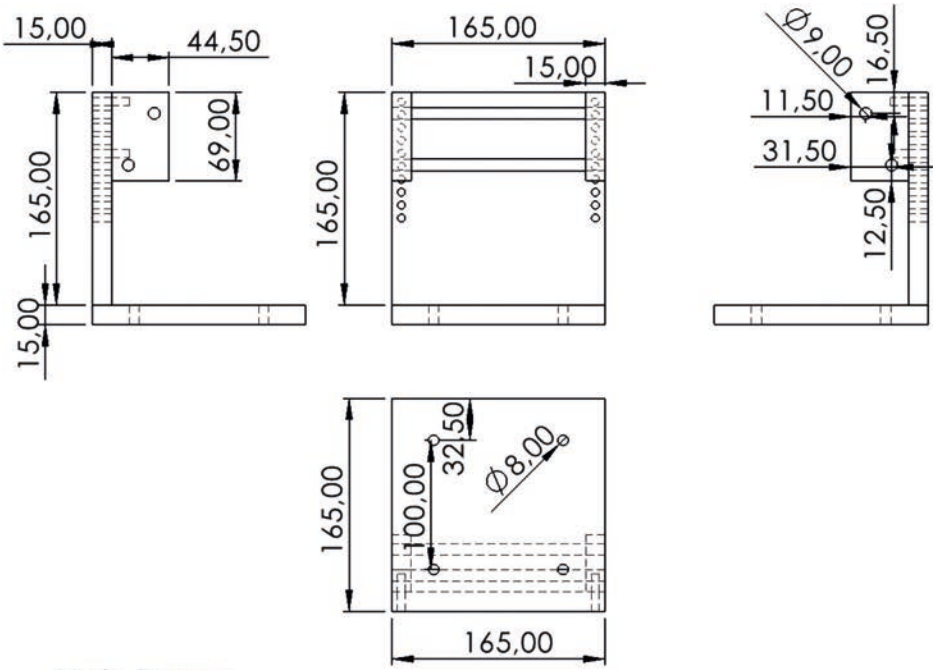
15,00
44,50
165,00
69,00
165,00
15,00
165,00
15,00
165,00
Ø9,00
16,50
11,50
31,50
12,50
165,00
32,50
Ø8,00
100,00
165,00

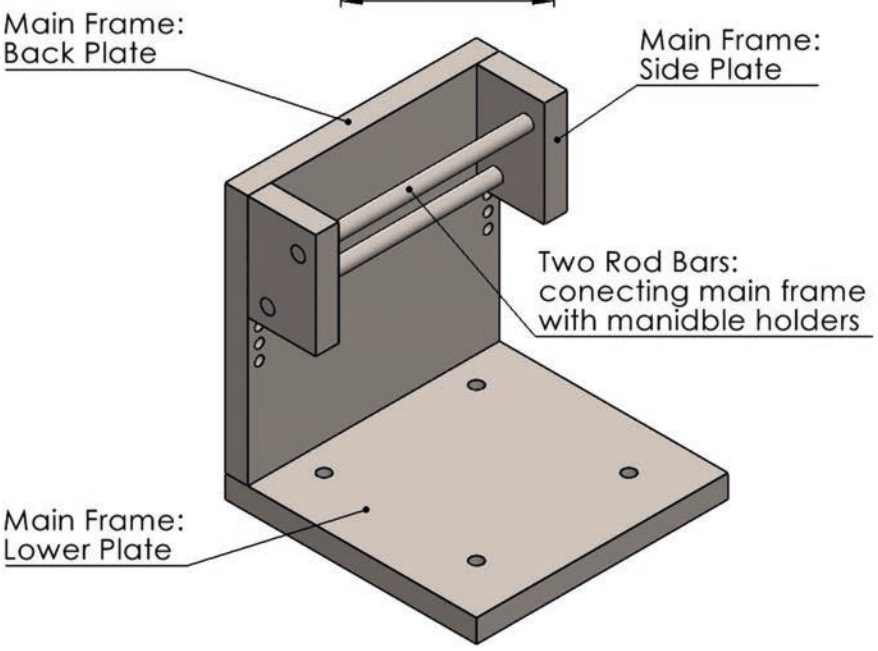
Main Frame:
Back Plate
Main Frame:
Side Plate
Two Rod Bars:
conecting main frame
with manidble holders
Main Frame:
Lower Plate

Mandible holders

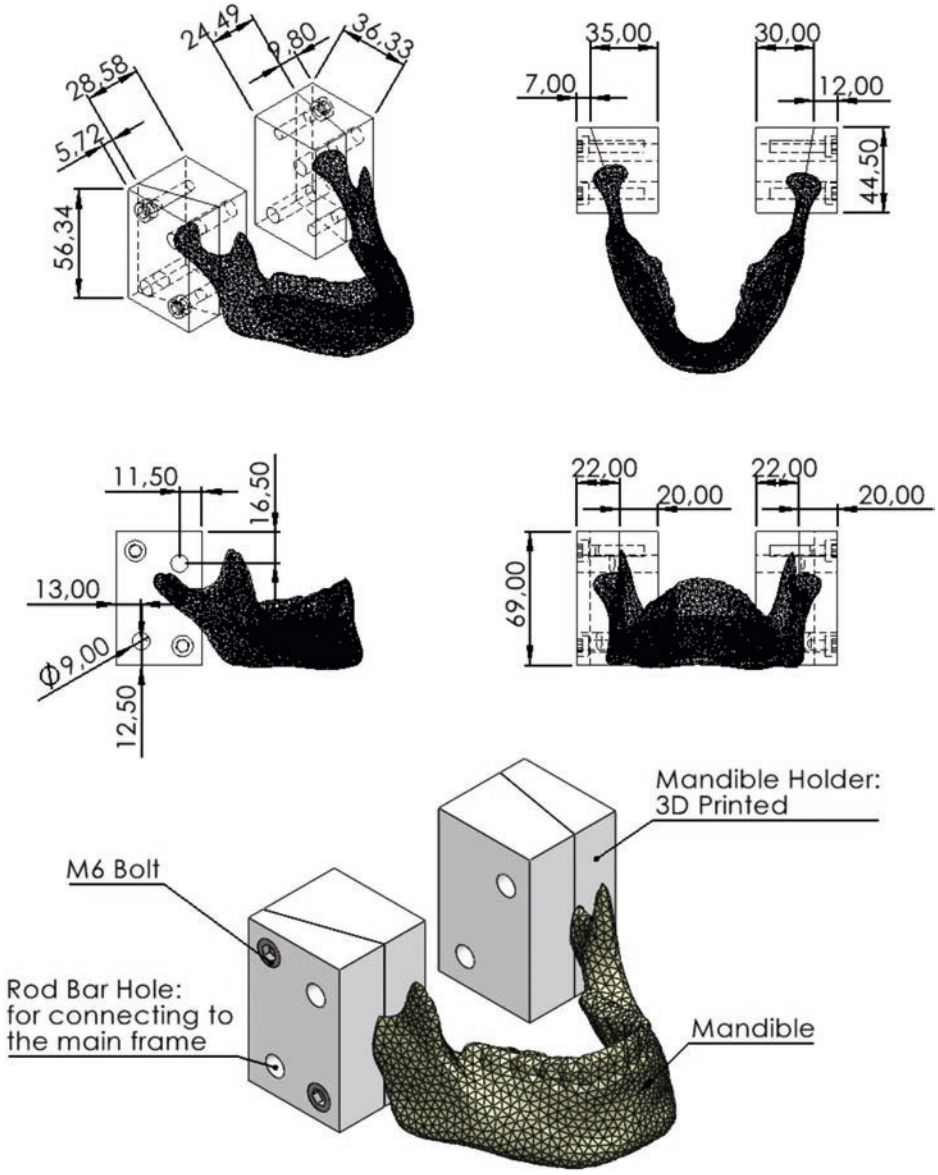

CHAPTER 5

Finite element analysis of mandibular fracture fixation authenticated by 3D printed mandible mechanical testing

Omid Daqiq[1]*, Baucke van Minnen[1], Frederik Karst Lucien Spijkervet[1], Friederik Wilhelm Wubs[2], Gerton Lunter[3], & Charlotte Christina Roossien[4]

[1] *Department of Oral and Maxillofacial Surgery, University Medical Center Groningen, University of Groningen, Hanzeplein 1, 9713 GZ, Groningen, The Netherlands.*
[2] *Bernoulli Institute for Mathematics, Computer Science and Artificial Intelligence, University of Groningen, Nijenborgh 9, 9713 GZ, Groningen, The Netherlands.*
[3] *Unit Medical Statistics and Machine Learning, Department of Epidemiology, University Medical Center Groningen, University of Groningen, Hanzeplein 1, 9700 RB, Groningen, The Netherlands.*
[4] *Engineering and Technology Institute Groningen, Department of Bio-Inspired MEMS and Biomedical Devices, University of Groningen, Nijenborgh 4, 9747 AG, Groningen, The Netherlands.*

Accepted 14 April 2025 & Published: 26 April 2025
Journal: Nature Scientific Reports
Cite: Daqiq O, van Minnen B, Spijkervet FKL, Wubs FW, Lunter G, Roossien CC. Finite element analysis of mandibular fracture fixation authenticated by 3D printed mandible mechanical testing. Sci Rep. 2025 Apr 26;15(1):14655. doi: 10.1038/s41598-025-98732-3. PMID: 40287549.

Link: https://www.nature.com/articles/s41598-025-98732-3

ABSTRACT

Finite element analysis (FEA) for mandibular fracture fixation in craniomaxillofacial surgery remains promising but has been restricted due to the absence of an authenticated FEA model. This study aims to create an authenticated FEA model. This model was verified through a series of 3D printed mandible mechanical testing (3D-MMT) in a universal tensile machine using an indistinguishable set-up. Non-comminuted mandibular symphysis, parasymphysis, and angle fracture fixation stability were evaluated using a 2.0 mm 4-hole miniplate in three different plate configurations. Both FEA and 3D-MMT outcomes were reproducible and in agreement with the present understanding of stable mandibular fracture treatment. The results show favourable fracture stability with the dual plating, followed by the superior border, with the least stability observed in the inferior border plating. Furthermore, the FEA and the 3D-MMT outcomes were consistently similar, with a systematic 0.56 ± 0.12 mm total displacement difference (standard deviation). An excellent interclass relation coefficient (0.93, 95% confidence interval: 0.80-0.96) was found between the FEA model and the 3D-MMT mechanical test, indicating that both results were consistent with each other. The authenticated FEA can accurately study the recognised biomechanical behaviour of non-comminuted mandibular fractures and shows a potential application for complex fracture fixation analysis.

INTRODUCTION

The application of three-dimensional (3D) modelling and finite element analysis (FEA) in craniomaxillofacial surgery (CMF) has been promising, particularly for mandibular fracture fixation[1–13]. FEA is a powerful non-invasive tool known for its high precision, which can effectively replace the time-consuming and costly *in vivo* studies, such as mechanical testing of polymeric or cadaveric mandibles[14–18]. As a flexible *in silico* instrument, FEA can enhance the understanding of fracture treatment by: (1) evaluating the distribution of stress, strain, displacement, or forces; and (2) providing a direct visual overview of what is happening to the fracture stability in terms of reduction and fixation[1–3,9–14,19,20]. Especially, in case of complex fractures (e.g., severely atrophic or comminuted), FEA can enhance the optimal fracture treatment (e.g., visualisation and localisation of the forces, stress, or displacement), and lead to improvement of the existing osteosynthesis or development of new implants (e.g., patient-tailored 3D printed implant)[1,2,21–23]. However, FEA applicability for mandibular fracture treatment has been limited due to the lack of an available authenticated model that could be routinely utilised in the clinical setting[1,2,14,21,24].

In our previous studies, we systematically took the steps towards developing an FEA model authenticated by a series of polymeric mandible mechanical tests[1,2]. We observed that the developed FEA model was a proper tool to evaluate non-comminuted mandibular fracture fixation stability; however, optimised adjustments were necessary in both the FEA model and the authentication process to achieve an excellent agreement between the FEA and the mechanical test setup (e.g., mandibular material properties, fracture reduction, and mechanical test configuration).

The aim of this study is to develop an authenticated *in silico* FEA model principle for mandibular fracture fixation. This will be investigated by evaluating common mandibular fracture treatment using a precisely fine-tuned FEA model, authenticated through a series of 3D printed mandible mechanical testing (3D-MMT). First, we hypothesise that our FEA principle is a valid tool for evaluating mandibular fracture fixations (e.g., in case of complex fractures), and can assist in optimal selection or development of osteosynthesis materials. This may reduce the future need for the use of costly and time-consuming model experiments and *in vivo* physical tests. Second, we hypothesise that the current FEA model is significantly improved compared to our previous model by substantially reducing the displacement difference between the FEA and 3D-MMT outcomes.

MATERIAL AND METHODS

Study outline

The FEA principle was applied to evaluate the fixation of the mandibular symphysis, parasymphysis, and angle fracture using different miniplate configurations. For the fracture

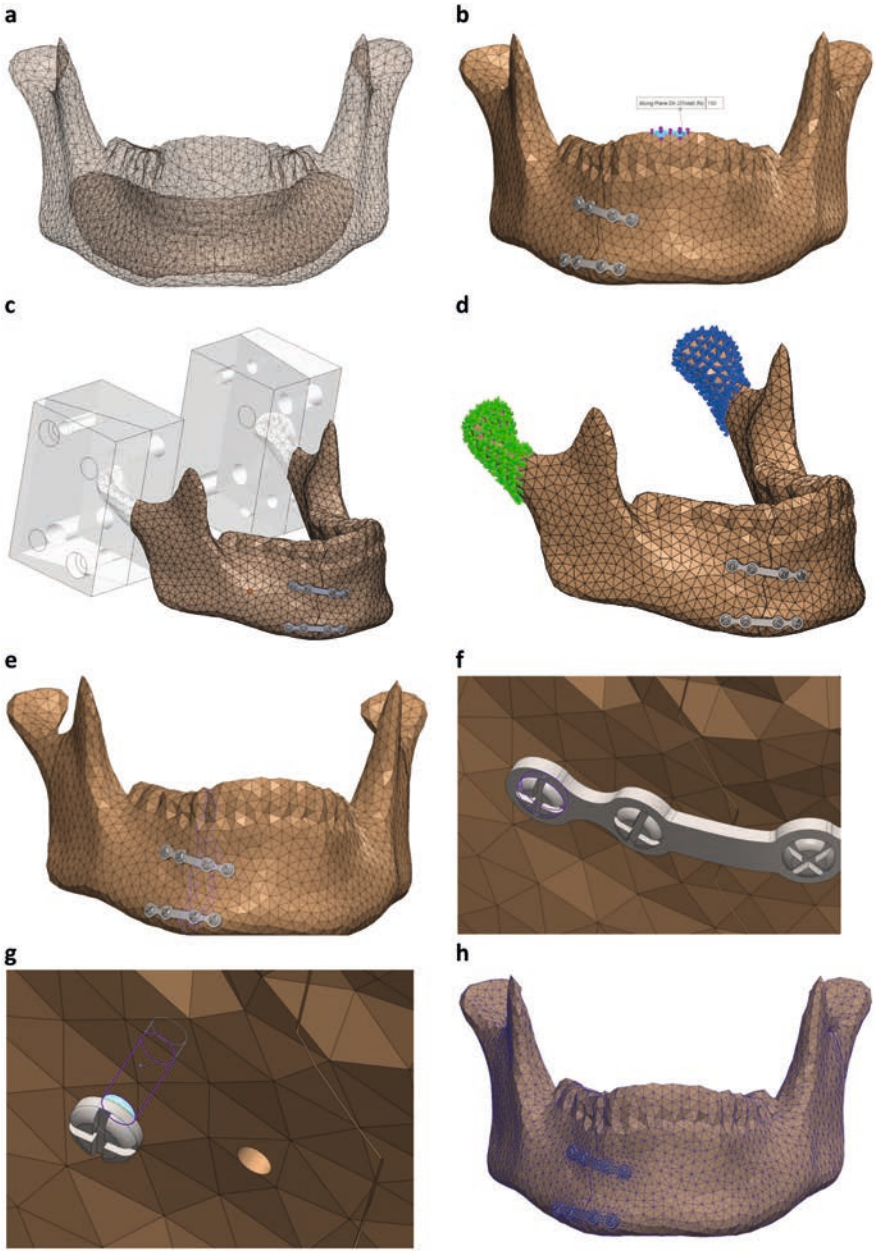

Figure 1. 3D model assembly and FEA set up in Solidworks. (**a**) Mandible 3D model with the segmented cortical bone and trabecular cavity. (**b**) Bite load of 150 N applied downward on the two frontal incisor teeth of the mandible, identical to the 3D-MMT load application. (**c-d**) Mandibular fixtures at the condylar region using fixed geometry, identical to the mandible holder's fixation used in the 3D-MMT: (**c**) defining the regions where fixtures are applied, and (**d**) the applied fixtures on the right and left condylar regions. (**e**) Fracture surfaces constraints using contact sets with no penetration and a fracture distance of 0.1 mm. (**f**) Contact connection interaction between the screw and the miniplate. (**g**) Bounded connection constraints between the screw and the mandible. (**h**) Illustrating the applied converged mesh.

fixation, the study used a 2.0 mm 4-hole 1.0 mm thick titanium miniplate (reference nr. 25-551-04-09) and the maxDrive 2.0 x 6 mm screws (reference nr. 25-872-05-09) (KLS-Martin, Gebrüder Martin GmbH & Co., Tuttlingen, Germany). Three different miniplate configurations were tested, namely: superior border (in accordance with the ideal line of osteosynthesis), inferior border (the lower mandibular border), and dual plating (using two miniplates at the mandibular superior and inferior border). Solidworks software (version SP5.0, 2021, Waltham, Massachusetts, USA) was used for the *in silico* numerical simulations. FEA authentication was attained by conducting the 3D mandible mechanical testing (3D-MMT), which used 3D printed polymeric mandibles placed in a universal tensile machine using a custom-made fixture device. Both FEA and 3D-MMT were conducted under identical conditions, specifically identically matched: fracture type, fracture reduction, miniplate configuration, miniplate location, applied load, mandibular condylar fixture region, connections, and constraints.

Creating 3D model

The study contains the same geometrically shaped mandible model as used in our previous study[1]. The 3D mandible model was obtained by a cone beam computed tomography (CBCT) scan (Planmeca Promax dental imaging device, 3D-Max ProFace, Helsinki, Finland) of a polymeric mandible (bone setting, 120 kVp tube potential, 2.5 mAs tube current, and 400 µm voxel size). Mimics software (version 20.0, Materialise, Leuven, Belgium) enabled cortical and trabecular mandibular bone segmentation using different Hounsfield units (HU) thresholds. Further, 3-Matic software (version 15, Materialise, Leuven, Belgium) was used to smooth and wrap the 3D model. Afterwards, Geomagic (Solidworks 2021 add-in, 3D systems, Rock Hill, South Carolina, USA) was used to create a single mandible assembly file by adding the cortical and trabecular bone segments. This way the segmentation geometrical mesh errors were resolved, and an organic functional file was made to import to Solidworks in a stereolithography (STL) file format (Fig. 1a). The rest of the analysis was conducted in Solidworks.

In the study, three clinically realistic non-comminuted jagged line fractures were created in the mandibular symphysis, parasymphysis, and angle regions (Fig. 2). The fracture surface distance was set at 0.1 mm, identical to the fracture surface distance measured from the fixated 3D printed mandibles used in the 3D-MMT. For the fracture fixation, a precise model of a 2.0 mm 4-hole titanium miniplate (1 mm thickness, 26 mm length, and 4.3 mm width) and 6 mm titanium screw (6 mm length and 2 mm diameters) was created in Solidworks. These were applied for the *in silico* fracture fixation in three different configurations (Fig. 2).

Finite element analysis (FEA)

Creating assembly

The 2.0 mm miniplate was positioned at the fracture site in three different plating configurations (Fig. 2). The miniplate was held against the mandibular surface using the maxDrive screws

tightened in the mandibular screw holes, in accordance with the non-locking compression plating system. The assembling setup in the *in silico* study was identical to the 3D-MMT study, ensuring matched fracture configurations and fixation setups in both studies (Fig. 2).

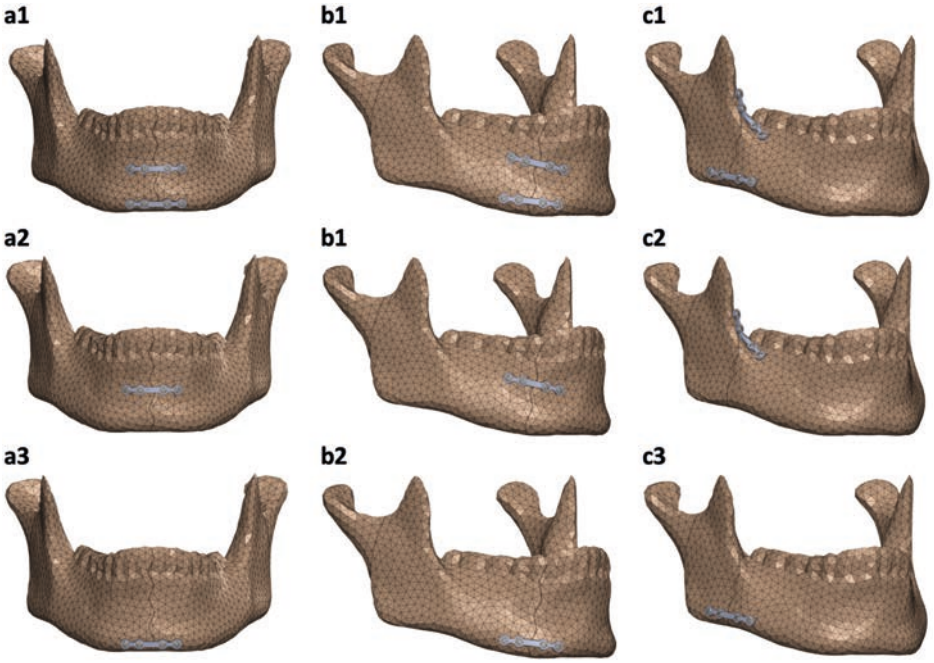

Figure 2. *In silico* mandibular fracture fixation in the region of (**a**) symphysis, (**b**) parasymphysis, and (**c**) angle using the following miniplate configurations: (**1**) dual plating configuration, (**2**) superior border plating, and (**3**) inferior border plating.

Load and fixture

The applied load and fixtures were matched to the setup used in the 3D-MMT. A load of 150 N was inserted on the two mandibular frontal incisor teeth, corresponding to the identical position of the applied load in the 3D-MMT (Fig. 1b). The 150 N load was selected for two reasons, namely: first, it is the average postoperative incisal maximum bite force according to the literature for a non-comminuted mandibular fracture treated with miniplate osteosynthesis[25,26]; and second, at this load, the FEA results can be best compared to the 3D-MMT outcomes.

Theixturees were precisely matched to the custom-made mandible holder clamp system used in the 3D-MMT (Fig 3). This was done by first positioning the 3D modelled mandible clamp system on the 3D mandible model at an exact location as applied in the 3D-MMT (Fig. 1c). Next, the fixture nodes were selected according to the reference lines from the mandible holders (Fig. 1d). Finally, the fixed geometry option in Solidworks was used for defining the fixtures at the selected regions (Fig. 1d).

Material properties

The material model used is linear elastic isotropic. The mechanical material properties of the material, used for 3D printing the mandible replicas, was provided by the manufacturer's datasheet[27,28]. The material properties of the cortical bone segment were set at an elastic modulus of 1700 megapascal [MPa], mass density of 0.93 g/cm^3, and Poisson's ratio of 0.34[27,28]. Though not used in the model but relevant in the interpretation of the results, we mention that the yield strength is 40 MPa. The trabecular bone segment was set as a cavity, identical to the 3D printed mandibles used in the 3D-MMT. Therefore, there was no need to define the material properties of the trabecular bone.

The titanium osteosynthesis (miniplate and screws) mechanical properties were defined with an elastic modulus of 104,800 MPa, yield strength of 827.40 MPa (not used in the model), mass density of 4.43 g/cm^3, and Poisson's ratio of 0.31[29].

Connections and constraints

The constraints between the mandible and osteosynthesis were defined by using the local interactions property manager in Solidworks. This was achieved based on the present knowledge of mandibular fracture fixation in accordance with non-locking compression osteosynthesis plating[1,30–33], identical to the setup used in the 3D-MMT. The constraints between most of the assembly parts were set as contact, namely the connection between the fracture surfaces (Fig. 1e), the miniplate and the mandible, and the miniplate and the screws (Fig. 1f). Contact was defined without friction, whereupon a load application, only normal forces would be exchanged between the surfaces of the components. Further, the fracture surfaces were set at a fixed distance of 0.1 mm, illustrating optimal reduction and in line with the measured fracture surfaces in the 3D-MMT after placing the mandible onto the universal tensile machine. Finally, the interactions between the screws and the mandible screw holes were set as bonded (Fig. 1g). This means that the screw is tight inside the mandible screw hole, holding the miniplate fixed against the mandibular surface.

FEA mesh convergence

Sensitivity analyses were conducted to determine the proper mesh size for the FEA. Convergence of the solution was attained by progressively reducing the mesh size until the peak Von-Mises stress [MPa] became independent of the mesh size (Supplementary Fig. S1: mesh convergence plot). This advanced to a controlled mesh which was used in the FEA simulations. The applied mesh was set at a 0.15 mm minimum and 5 mm maximum element size (Fig. 1h). The applied mesh had an average computation time of 45 minutes per simulation run, on a 12th Gen Intel Core i9-12950HX CPU 2.30 GHz processor with 32 GB RAM memory.

3D printed mandible mechanical testing (3D-MMT)

Solidworks mandibular 3D models with three different fractures were used for 3D printing the polymeric mandible replicas (Fig. 1a, Supplementary Figure S2). The study used 3D

printed mandibles made from a substance with known mechanical material properties. The fractured mandible replicas were 3D printed based on selective laser sintering (SLS) method in an EOS-P-369 printer (Electro Optical System, model P 369, EOS GmbH, Munich, Germany) using polyamide 12 (PA12) (EOS fine polymer powder, trade name: PA 2200 Performance, PA12 medical grade) material. The 3D printer could only print the cortical section of the mandible due to the limitations of the available 3D printer. The trabecular section was left empty as a cavity inside the cortical bone segment (Fig. 1). Hence, this was also applied in the FEA mandibular 3D model. Afterwards, assemblies of the fractured mandibles with the miniplates were created with the assistance of an experienced OMF surgeon; however, only one person did the assembling process (e.g., miniplate bending, drilling screw holes, and screwing) to eliminate any interindividual variations. The assembling process was done by using the manufacturer's original tools (Supplementary Fig. S2).

For the mechanical testing, a calibrated Instron 3400 universal tensile machine (Instron, 3400 series, dual column table 34TM-5 model, Norwood, USA) was used. A computerised test protocol was meticulously predefined using Instron's mechanical test bench software (version 4.34, BlueHill Universal, Illinois Tool Working Inc.) to establish an identical testing condition for all the mechanical experiments.

The study used a custom-made device for positioning the mandible onto the universal tensile machine, similar to the device used in Daqiq et al. (2024)[1]; however, the mandible holders were significantly improved (Fig. 3a-d). The redesigned mandible holders were constructed of outer frame blocks made of A6061 aluminium alloy with 3D printed inner inserts from nylon (polyamide type 6, PA6) (Fig. 3c-d). This design allowed the holders to function as a clamp system, securely holding the mandible at the mandibular condylar region (Fig. 3c-d). Each mandible holder frame consisted of two individual blocks connected by four M6 stainless-steel bolts, ensuring a fixed tight clamp system that facilitated easy placement and removal of the mandible onto the device (Fig. 3d). The outer frame of the mandible holders was securely fixed tight to the front plate of the custom-made device using M6 bolts, effectively eliminating any movement, translation, or rotation of the mandible (Fig. 3e). The nylon inner inserts (Fig. 3c) were replaced after every nine tests due to the potential of deformation from repeated use, with a total of four pairs of inserts used for each side.

To apply load on the mandible, a custom 3D printed adaptor was mounted on the load cell of the universal tensile machine (Fig. 3f). This adaptor, made of nylon (PA6), was further strengthened by an AISI 316 stainless-steel flat ring inserted into the centre hole where it was connected to the load cell of the tensile machine. The load cell was capable of 5 kilonewtons [kN] maximum load. The mechanical load was applied on the two mandibular frontal incisors via the 3D printed adaptor (Fig. 3f).

Prior to the start of each test, the mandibles were positioned onto the universal tensile machine at an identical location using the custom-made device with mandible holders

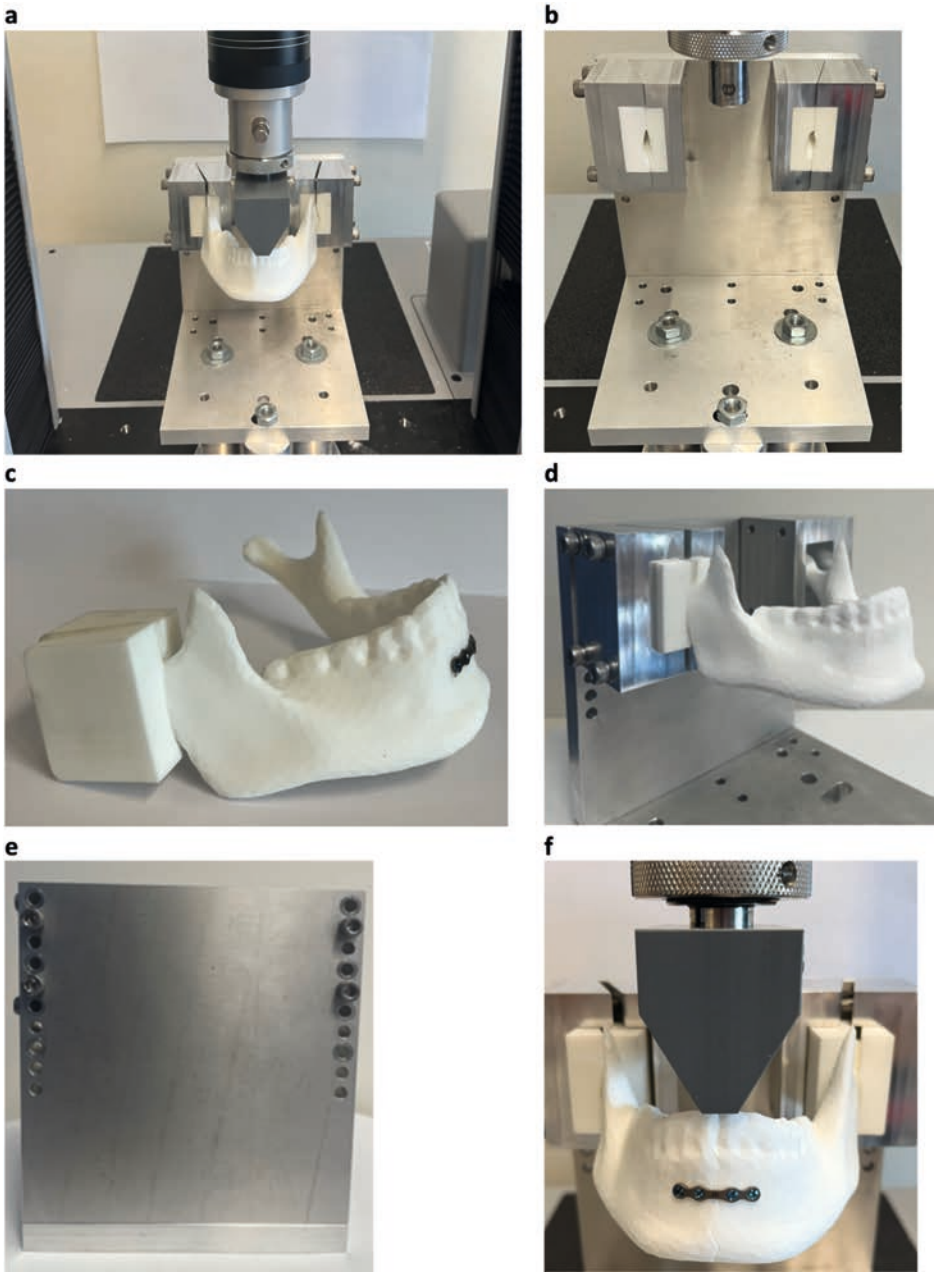

Figure 3. 3D printed mandible mechanical testing (3D-MMT). (**a**) Total overview of test setup used in the 3D-MMT. (**b**) Overview of the custom-made device including the mandible holders for positioning the mandible onto the mechanical test bench. (**c**) The 3D printed mandible inserts used for positioning the mandible inside the aluminium mandible holder frames. (**d**) Overview of how mandible inserts are positioned inside the mandible holder aluminium frames. (**e**) The back view of the custom-made device front plate, showing four M6 bolts used for tightening the mandible holder aluminium frames to the frontal plate of custom-made device. (**f**) Applied load through a custom 3D printed adaptor attached to the load cell of the universal tensile machine.

(Fig. 3). Before starting with the experiments, the load cell was calibrated to a predefined zero position. The testing started by running the pre-programmed test protocol in the universal tensile machine software. A preload of 5 Newton [N] was applied, after which the load increased continuously at the rate of 1 Newton per second [N/s]. Each test was automatically terminated upon reaching the failure point (e.g., mandible breaks, or the fixation fails), defined at a load drop threshold of 40%. In the study, only the compressive displacement in relation to the applied load could be measured by the tensile machine. The compressive displacement in the downward direction was registered based on the movement of the load cell from the initial zero position up to the failure point (Appendix: 3D-MMT results at the failure load). All the test data were logged in the tensile machine software and were exported for further analysis.

Finally, the mechanical testing was performed three times for each of the fractures and each of the plate configurations with a total of twenty-seven tests (e.g., angle fracture with dual plating was tested three times). Furthermore, an additional three tests were conducted for non-fractured mandible replicas for the comparison.

Data analysis

Firstly, in the FEA simulations: the Von-Mises stress distribution and the maximum Von-Mises stress in megapascal [MPa] (Table 1, Fig. 4-6) as well as the displacement in millimetre [mm] were assessed (Table 2, Fig. 7). The presence of small amount of stress at the fixture regions was visualised by applying iso clipping property manager option (set at 4 or 40 MPa), which is the smallest stress value that could be chosen to properly show the stress around the fixture sites in the figures (Supplementary Figure S3b-c and S4). Secondly, the 3D-MMT displacement [mm] outcomes were evaluated (Table 2). Lastly, the displacement results of the FEA were compared to the outcomes from the 3D-MMT. This was achieved by comparing the displacement pattern for the different fracture types and miniplate configurations at 150 N load (Table 2, Fig. 8). For displacement comparison, the FEA displacement in the Z-axis was used, as this corresponds to the direction of applied load in the 3D-MMT.

The outcomes of the FEA and the 3D-MMT were evaluated using IBM SPSS (version 28, IBM Corporation, Chicago, IL, USA) and R (version 4.1.1, r-project.org) with NLME package (version 3.1.166, Mixed Effects Models package). Firstly, descriptive statistics were used to determine the mean displacement and standard deviation (SD) of the three repeated 3D-MMT tests. Secondly, the FEA versus the 3D-MMT displacement differences were calculated for each fracture type and miniplate configuration as well as determining the total mean displacement difference. Finally, the interclass correlation coefficient (ICC) was calculated by estimating variance components in a mixed effect model, allowing for different variances for the experiment (σ^2_e) and the simulation (σ^2_s), as well as a fixed (systematic) difference between these modes; the ICC was then calculated as the correlation between simulation and experimental measurements, $\sigma^2_t / \sqrt{(\sigma^2_t + \sigma^2_s)(\sigma^2_t + \sigma^2_e)}$, where σ^2_t is the estimated true variance of the displacement, and confidence intervals were estimated from the variance-

covariance matrix of the variance estimates. ICC values were interpreted as follows: 0.00-0.20 is poor, 0.20-0.40 is fair, 0.40-0.60 is moderate, 0.60-0.80 is good, and 0.80-1.00 is excellent agreement[34].

RESULTS

Finite element analysis (FEA)

The Von-Mises stress outcomes [MPa] are presented in Table 1. Different fracture types and miniplate configurations led to the variation in the Von-Mises stress distributions and the maximum Von-Mises stress location (Fig. 4-6 and Fig. 8a). In all the FEA models, the maximum stress (267.70 to 1511.57 MPa) remains on the miniplate which is responsible for holding the fracture segments into a fixed stable position (Fig. 4-6). In terms of miniplate configurations, the dual plating method exhibited the lowest Von-Mises stress (267.70 to 802.90 MPa) (Fig. 4a1-c1), followed by superior border plating (373.43 to 1163.67 MPa) (Fig. 4a2-c2), and the highest stress was observed in the inferior border plate positioning (450.51 to 1511.57 MPa) (Fig. 4a3-c3). Regarding the fracture type, the angle fracture produced the highest stress (802.90 to 1511.57 MPa), followed by the parasymphysis fracture (512.38 to 854.16 MPa), with the lowest stress observed in the symphysis fracture (267.70 to 450.51 MPa). Further, a non-fractured mandible illustrates much lower stress (129.98 MPa) compared to a fractured mandible (Table 1, Supplementary Fig. S3). Furthermore, a small stress distribution was observed along the condylar fixture region where the mandible is held tight using the mandible holders (Supplementary Fig. S4). However, the stress is much lower at this condylar fixture region compared to the stress located on the miniplate.

Table 2 and Figure 7 present the FEA displacement results [mm]. The displacement varied for different fracture types and miniplate configurations, revealing a similar pattern compared to the Von-Mises stress results (Table 1, Fig. 8). In all the fractures, the dual plating method demonstrated smaller displacements compared to a single plating (Table 2, Fig. 8.b-d). Additionally, the displacement is greater in the inferior border compared to the superior border plating in all the fracture types, with displacement differences of 0.17, 0.64, and 0.43 mm (respectively for the symphysis, parasymphysis, and angle fracture) (Fig. 8b-d). Furthermore, displacement observed in a non-fractured mandible remains lower compared to the fractured mandibles (Table 2, Supplementary Fig. S3).

Third, the fracture stability using different miniplate configurations is illustrated (Fig. 5 and Fig. 7). Placement of the miniplate at the lower border results in the least stability, as the fracture faces tend to open, leading to reduced fixation stability. This effect is more visible in the angle fracture compared to the parasymphysis and the symphysis fractures. In contrast, dual plating demonstrates the most optimal fracture stability, maintaining intact and stable fracture surfaces.

Table 1. FEA maximum Von-Mises stress [MPa] outcomes.

Mandibular fracture	Miniplate configuration	Von-Mises stress [MPa]
Symphysis	Dual plating	267.70
	Superior border	373.43
	Inferior border	450.51
Parasymphysis	Dual plating	612.38
	Superior	781.84
	Inferior	854.16
Angle	Dual plating	802.90
	Superior	1163.67
	Inferior	1511.57
Non-Fractured mandible*	Not applicable	129.98

* Non-Fractured mandible: as a baseline for comparison.

Table 2. The 3D-MMT displacement compared to the FEA displacement in mm at 150 N load.

Mandibular fracture	Miniplate configuration	Test number	Displacement [mm] at 150 N		Displacement Difference***
		3D-MMT*	3D-MMT*	FEA**	
Symphysis	**Dual plating**	1	2.65		
		2	2.99		
		3	3.59		
		Mean ± SD	*3.07 ± 0.39*	2.52	0.55
	Superior border	1	3.37		
		2	3.39		
		3	2.93		
		Mean ± SD	*3.23 ± 0.21*	2.63	0.60
	Inferior border	1	3.26		
		2	3.43		
		3	3.31		
		Mean ± SD	*3.33 ± 0.07*	2.80	0.53
Parasymphysis	**Dual plating**	1	3.96		
		2	3.48		
		3	3.53		
		Mean ± SD	*3.65 ± 0.22*	3.05	0.60
	Superior border	1	3.95		
		2	3.47		
		3	4.48		
		Mean ± SD	*3.97 ± 0.41*	3.21	0.76
	Inferior border	1	4.05		
		2	4.39		
		3	4.31		
		Mean ± SD	*4.25 ± 0.15*	3.85	0.40

[continued on next page]

Table 2. *[continued]*

Mandibular fracture	Miniplate configuration	Test number 3D-MMT*	Displacement [mm] at 150 N		Displacement Difference***
			3D-MMT*	FEA**	
Angle	**Dual plating**	1	4.26		
		2	4.47		
		3	4.28		
		Mean ± SD	*4.34 ± 0.10*	3.59	0.75
	Superior border	1	4.77		
		2	4.16		
		3	4.63		
		Mean ± SD	*4.52 ± 0.26*	3.90	0.62
	Inferior border	1	4.76		
		2	4.71		
		3	4.77		
		Mean ± SD	*4.75 ± 0.02*	4.33	0.42
Non-Fractured		1	2.96		
		2	3.36		
		3	2.99		
		Mean ± SD	*3.10 ± 0.18*	2.41	0.69

* 3D-MMT (3D printed mandible mechanical testing) displacement: each scenario (fracture mandible with three different miniplate configurations and non-fractured mandible) was repeated three times under identical conditions (Test number 1-3). *Italic*: mean and standard deviation (SD) of the three repeated tests.
** FEA displacement represents the exact values from the numerical simulations at 150 N load.
*** Displacement differences between the FEA versus the 3D-MMT at 150 N load.

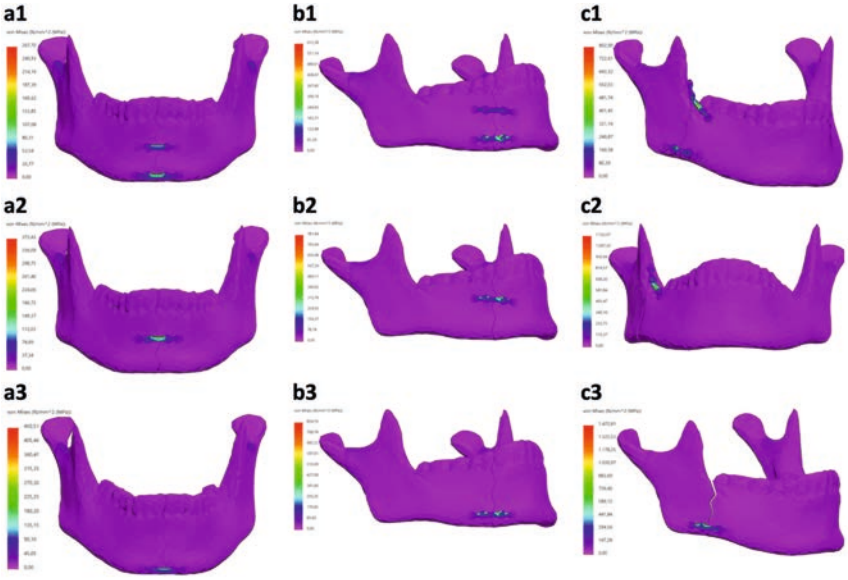

Figure 4. FEA Von-Mises stress distribution at 150 N load for the mandibular (**a**) symphysis, (**b**) parasymphysis, and (**c**) angle fracture fixated using the following miniplate configurations: (**1**) dual plating, (**2**) superior border plating, and (**3**) inferior border plating.
Colour coding: the minimum stress is indicated by bright pink colour; and the maximum, as indicated in Table 1, by red colour.

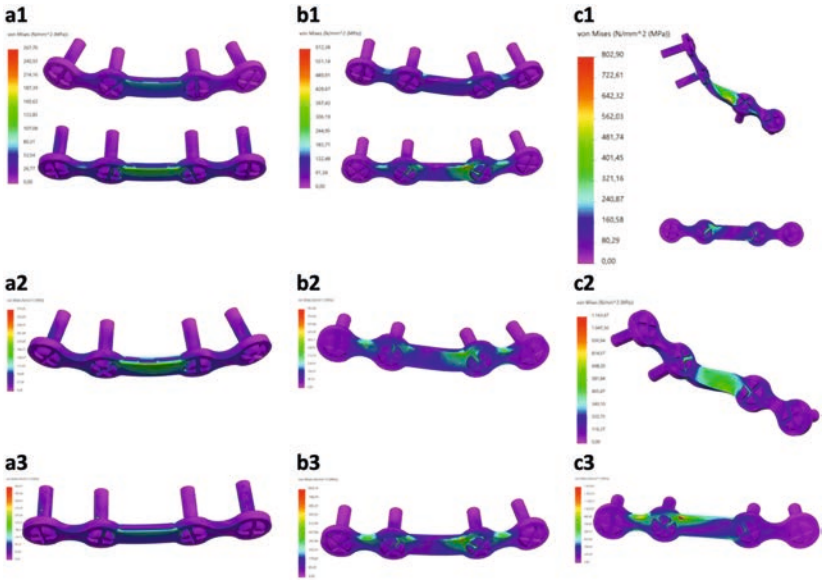

Figure 5. Anterior overview of the osteosynthesis (miniplate and screws) FEA Von-Mises stress distribution at 150 N load for the mandibular (**a**) symphysis, (**b**) parasymphysis, and (**c**) angle fracture using the following fixation configurations: (**1**) dual plating, (**2**) superior border plating, and (**3**) inferior border plating.
Colour coding: the minimum stress is indicated by bright pink colour; and the maximum, as indicated in Table 1, by red colour.

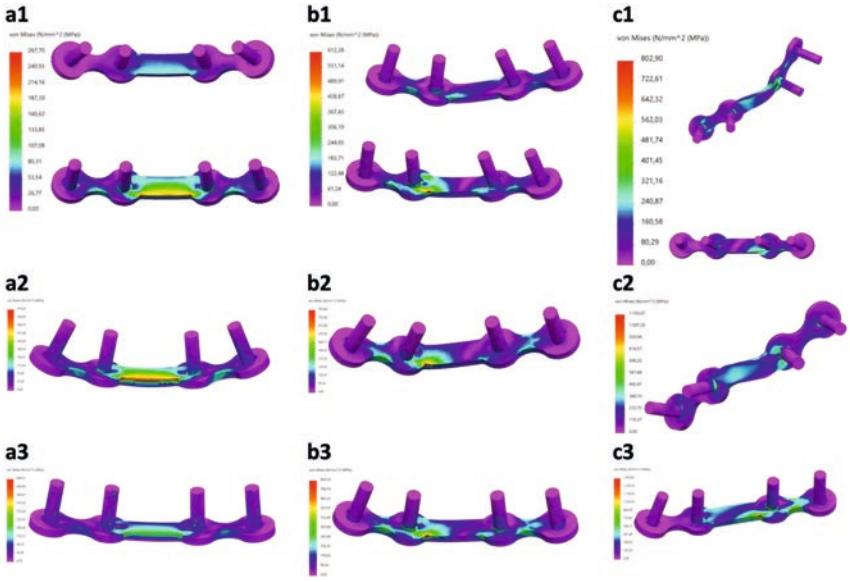

Figure 6. Posterior overview of the osteosynthesis (miniplate and screws) FEA Von-Mises stress distribution at 150 N load for the mandibular (**a**) symphysis, (**b**) parasymphysis, and (**c**) angle fracture using the following fixation configurations: (**1**) dual plating, (**2**) superior border plating, and (**3**) inferior border plating.
Colour coding: the minimum stress is indicated by bright pink colour; and the maximum, as indicated in Table 1, by red colour.

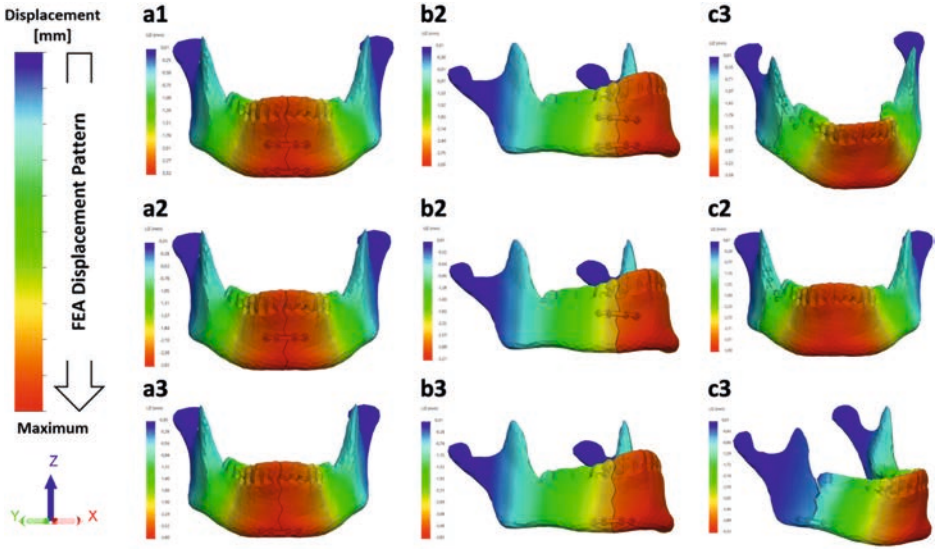

Figure 7. FEA displacement distribution in the Z-axis (same direction as the applied force) at 150 N load for the mandibular (**a**) symphysis, (**b**) parasymphysis, and (**c**) angle fracture with the following miniplate configurations: (**1**) dual plating, (**2**) superior border plating, and (**3**) inferior border plating.
Colour coding: on the left side showing the displacement pattern (with the red colour representing the maximum displacement), and the coordinate axis.

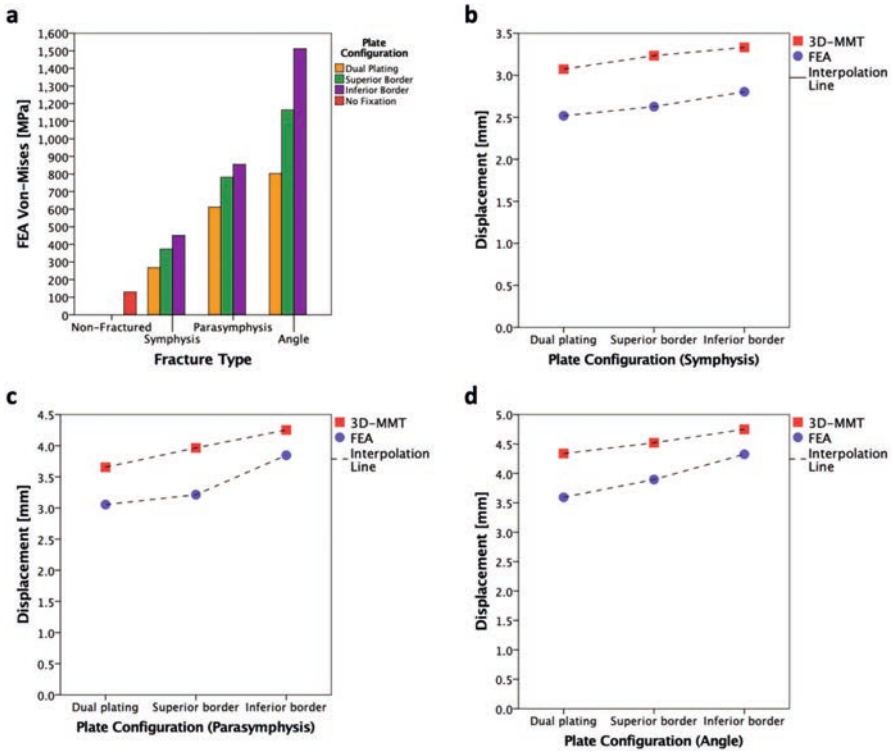

Figure 8. (**a**) FEA simulation maximum Von-Mises stress outcomes [MPa] at 150 N load. (**b-d**) Displacement [mm] pattern of 3D-MMT (red) versus FEA (blue) of each fracture fixated with three different miniplate configurations at 150 N load; respectively: (**b**) symphysis, (**c**) parasymphysis, and (**d**) angle fracture.

Three-dimensional mandible mechanical testing (3D-MMT)

The 3D-MMT compressive displacement [mm] outcomes at a 150 N load are presented in Table 2 which is compared to the FEA displacement. In the mechanical tests, the load was gradually increased until reaching the failure point, which resulted in either the mandible breaking or the fixation failure (Fig. 9, Appendix: 3D-MMT outcomes at the failure load). Hence, at this failure point, all the mandible assemblies broke at the condylar fixture region (Appendix: Fig. A1-A4). The lowest displacement is found in the dual plate combination for all the fractures compared to the single plating (Table 2, Fig. 8b-d). In the single plate positioning, the displacement in the superior border plating was lower compared to the inferior border plating with the displacement difference of 0.10, 0.28, and 0.23 mm (respectively for the symphysis, parasymphysis, and angle fracture).

FEA versus 3D-MMT

Table 2 illustrates the displacement variations between the 3D-MMT and the FEA. The 3D-MMT demonstrates slightly higher displacement compared to the FEA, with a mean total displacement difference and SD of 0.59 ± 0.12 mm. Furthermore, the displacement patterns for different miniplate configurations across the various fracture types remain comparable

and similar in both studies (Fig. 8b-d). Finally, the displacement ICC between the 3D-MMT and the FEA was 0.93 (95% CI: 0.80-0.96) indicating excellent correlation between the two analyses. Note that ICC is based on covariances; thus, subtracting the displacement difference 0.59 mm or any other number will give the same result.

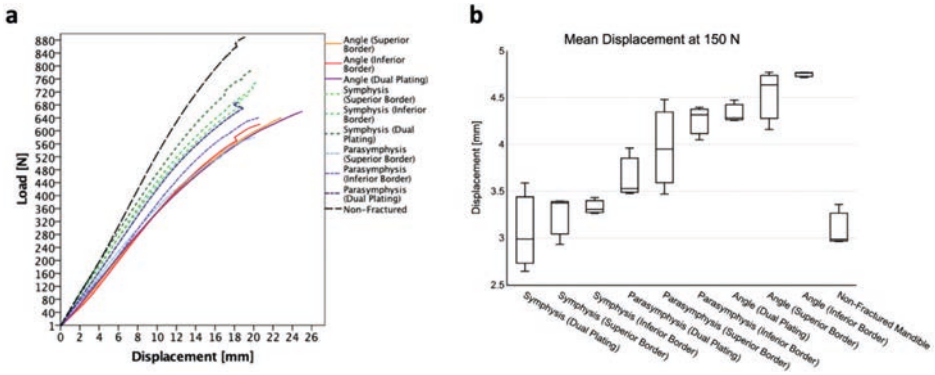

Figure 9. (**a**) Load (Y-coordinate) and displacement (X-coordinate) curve of the 3D-MMT mechanical tests from the start to the breakage load; and (**b**) displacement boxplot at 150 N load. The plots are based on the mean displacement of the three repeated tests conducted under identical conditions.

DISCUSSION

The purpose of this study was to develop an authenticated 3D FEA model principle for the simulation of mandibular fracture treatment. This was achieved through a systematic approach to enhance our previous attempt to develop such a model by improving both the FEA methodology and the mechanical testing authentication process[1].

Three major outcomes were observed. Firstly, the results of mandibular FEA were similar to the present interpretations of mandibular fracture treatment. As the literature demonstrates, superior border plating results in eliminating the tensile forces on the mandible[35–38], while inferior border plating is necessary during functional load movements to stabilise the fracture against the torsional and bending forces[31,33,39–44]. This study confirms these effects, showing that dual plating provides the most optimal fracture stability, followed by superior border plating, and the least stability was observed in inferior border plating (Fig. 8). In a dual plating method (Fig. 8, Fig. 4a1-a3), tensile forces are neutralised by the superior border miniplate, while the inferior border miniplate counterbalances compression forces during the application of a load. Furthermore, applying a single miniplate at the inferior border results in the least fracture stability (Fig. 4a3-c3). A similar effect was observed in our previous study, only with less correlation between the FEA and the 3D-MMT outcomes[1].

A key point to discuss is that the stress results show that the stress distribution on the fractured mandibles is almost constant, with most deformations occurring at the miniplate

region. Using the Solidworks iso clipping property manager set at 40 MPa reveals a small amount of stress around the mandibular condylar fixture site (replicating the mandible holders used in the 3D-MMT) (Supplementary Fig. S4). This effect is more visible when examining a non-fractured mandible (Supplementary Fig. S3). The maximum stress observed in the non-fractured mandible is 129.98 MPa, located at the condylar fixture site (Supplementary Fig. S3a-c). However, this peak stress occurs in the outer mandibular bone surface region, while the stress in the rest of the mandible remains below 4 MPa (Supplementary Fig. S3c). When observing the colour bar stress pattern between the fractured and non-fractured mandibles (Fig. 4, Supplementary Fig. S3c and Fig. S4), it is evident that the stress in the remainder of the mandible (except the condylar fixture region and the osteosynthesis fixation site) is less than 4 MPa, illustrating that the mandible possibly can be considered as a rigid body[45–50]. Currently, a single simulation run takes approximately 45 minutes using the converged mesh, with multiple runs often required to achieve accurate outcomes for clinical practice. This extended duration can lead to a lengthy decision-making process. To speed up the performance, one possibility is to model certain parts of the mandible as a rigid body, thereby reducing the degrees of freedom and, consequently, the computation time.

Secondly, the 3D-MMT results were consistently in line with the FEA outcomes and comparable (Fig. 8c-d). Both had an identical setup, each containing the same fracture type, fracture reduction, miniplate configuration, miniplate positioning, load application on the mandible, condylar fixture, and connections or interactions between the components. The universal tensile machine used in the 3D-MMT could only generate load-displacement relationships as output. This means that in the mechanical tests, the load was applied downward in the gravitational direction on the mandibular frontal incisors (Fig. 3f), with displacement changes measured in the same direction (Fig. 3, Fig. 9a). For this reason, the FEA displacement in the Z-axis (same direction as mechanical tests) was used for comparison with the 3D-MMT displacement. The displacement patterns in both studies were consistently similar (Table 2, Fig. 8): the dual plating system resulted in a lower displacement compared to single plating, followed by superior border plating, and most displacement was observed in the inferior border plating. This agreement resulted in an excellent interclass correlation (ICC between the FEA and the 3D-MMT displacement, 0.93; 95% CI: 0.80-0.96), where the ICC is based on covariances and will not change by a systematic error. The absolute displacement difference between the FEA and the 3D-MMT was consistently low, with a mean difference and SD of 0.59 ± 0.12 mm. This systematic error is substantially lower compared to our previous study[1] (1.13 mm).

Several biomechanical factors likely contribute to the remaining small but consistent displacement difference between the FEA and the 3D-MMT. First, in this study, Solidworks software was used to best compare the outcomes with our previous publication[1], which used the same software. In the follow-up studies, we will consider using software programs that may be more suitable for complex FEA models and could filter out small mismatches (e.g., Abaqus, Ansys, or Comsol). Second, we used bonded condition between the screws and the mandible screw hole connection (Fig. 1g), while a friction condition might be more correct. However, in

a clinical setting, it is impossible to measure this; therefore, the assumption of bondedness is reasonable. Third, a substantial fraction of the systematic error is likely due to the mandible holders (Fig. 1c and Fig. 3). We modelled rigid mandible holders with zero displacement at the interface with the mandible. Both are approximations of reality since the holder will deform too, and the holder-mandible interface is a friction boundary (see Appendix 2). So due to the force acting at the incisal teeth region (Fig. 2b and Fig. 3f), the moment at the mandible holder is at its maximum and a non-negligible strain may occur there. The largest differences occur when the peak stress is about the yield stress or higher. Hence, plasticity is expected to play a role in the measurements too, whereas this was not taken into account in the FEA model. Recall that we set the mandibular material model as linear elastic isotropic, which neglects the nonlinear effect of large deformations. It is only valid as long as the stresses remain below the yield stress. This is a limitation of the present model which is to be relaxed in a next model. Furthermore, in future studies, we recommend using stress-strain sensor gauges during mechanical testing (e.g., at the peak strain zone predicted in the FEA) to quantify the stress or strain on the miniplate and the fixtures. Further, if possible, more studies should be conducted to measure friction and define its effect on the fixation and fixture regions as well as between the fracture fragments. Because of the numerous potential causes of the systematic error, it will likely be difficult to fully account for this systematic error. However, for clinical practice a small systematic error is not truly relevant. The computational model clearly shows which fixation configuration is most favourable for each fracture. A practical solution is to subtract 0.59 from all predicted "displacement difference" values in Table 2, making the new difference always less than 5% of the computed value.

Thirdly, using 3D printed mandibles made from materials with known mechanical properties appears to be the best replacement of the commercially available mandible replicas (e.g., Synbone, Sawbone). This enables a more accurate and precise comparison between the FEA and the 3D-MMT. The primary challenge of 3D printing lies in replicating the mandibular trabecular region. In our study, it was only possible to print the mandibular cortical segment with the trabecular segment being an empty cavity. However, the influence of trabecular bone on fracture stability is very limited; therefore, it is doubtful whether a precise simulation of the trabecular part contributes to an even more reliable FEA model. Additionally, it remains crucial that the mechanical testing process aligns precisely with the FEA setup for effective validation; therefore, the mandibles in the FEA and the 3D-MMT studies were identical. Furthermore, in future studies, it would be valuable to explore 3D printable materials with mechanical material properties identical to those of human mandibular bone. Finally, both *in silico* and experimental analyses were conducted using a polymeric material, which is inherently isotropic. However, cortical bone exhibits highly anisotropic behaviour, and when combined with the influence of the trabecular structures, differing mechanical responses from the miniplates are to be expected in clinical settings.

The strength of this study is the improvements over our previous study[1] and the inclusion of new scientific findings. Compared to the earlier model[1], this study includes five significant

adjustments: 1) Synbone mandible replicas were used in our previous study[1]. We tried to determine the Synbone mandibular cortical and trabecular mechanical properties by mechanical experiments using Synbone specimens, as these properties were not provided by the manufacturer. The found material properties (e.g., elastic modulus) were in line with earlier studies[51–53], with a slight variation observed in the composition of the Synbone trabecular and cortical segments at the end of the experiments, probably caused by the moulding process. Such variations could lead to differences in the biomechanical behaviour of the mandible replica. In contrast, the current study used 3D printed mandible replicas made from PA12, a material with exactly known mechanical properties. This approach ensured that the geometrical shape, composition, and mechanical material properties of the mandible were identical in both FEA and 3D-MMT. 2) In our earlier study, we could not say for sure whether the fracture reduction in both the FEA and the 3D-MMT were identical[1]. Therefore, in the current study, the fracture surface distance in the 3D-MMT was measured, and a similar reduction was created in the FEA (Fig. 1e and Fig. 2). 3) The previous study contained mandibles with a non-comminuted straight-line fracture, resembling a saw cut rather than a realistic fracture[1]; therefore, this study used true jagged-line fractures, which more accurately resemble the non-comminuted clinical fractures (Fig. 2). 4) The mandibular clamp system used in the earlier study was entirely made of nylon (PA6) and it was secured in the custom-made device using two stainless-steel rod bars[1]. This setup might have led to non-observable mandibular movements at the fixture regions during the application of load, slight alterations in the positioning of the new mandible replica due to the sliding mechanism, and in a too rigid fixture since the mandible was fixed from the condyle to the mid-ramus region. In response, the current study redesigned and significantly optimised the mandible holders. This was achieved by creating aluminium frame blocks with nylon inserts, with the outer frame blocks fixed tight to the front plate of the custom-made device (Fig. 3). This design effectively eliminated any mandibular movement, translation, or rotation at the fixture region. Further, it ensured the precise placement of each mandible replica onto the mechanical test bench without any variations. Furthermore, this setup is considerably more realistic, as it holds the mandible only in the condylar region (Fig. 3c-d). 5) The previous study used a 200 N load in the FEA simulations and displacement comparisons[1]. In contrast, this study applied a more realistic load of 150 N (Fig. 1b), based on literature reporting the maximum incisal bite force following surgery for a non-comminuted mandibular fracture fixated with miniplate osteosynthesis[25,26].

In conclusion, this study presents our authenticated and accurate FEA model for the assessment of mandibular fracture fixation. The *in silico* FEA outcomes of the non-comminuted fractures are in line with the present understanding of the mandibular fracture treatment and authenticated with the *in vivo* mechanical experiments. This means that the *in silico* FEA model can be used to analyse complex fractures (e.g., comminuted, or atrophic), compare or improve the current osteosynthesis (e.g., titanium versus biodegradable miniplates), and develop new implants (e.g., 3D printed patient specific implants), without the need for costly or time-consuming models and *in vivo* experiments. Therefore, the next step would be to use

this model to study complex mandibular fracture fixations and compare the simulation results with the clinical outcomes. Perhaps, ultimately it can be routinely used as a tool in the clinical setting for enhancing the treatment approach of complex mandibular fractures.

REFERENCES

1. Daqiq, O., Roossien, C. C., Wubs, F. W. & van Minnen, B. Biomechanical assessment of mandibular fracture fixation using finite element analysis validated by polymeric mandible mechanical testing. *Sci Rep* **14**, 11795 (2024).
2. Daqiq, O., Roossien, C. C., Wubs, F. W., Bos, R. R. M. & van Minnen, B. Optimisation of osteosynthesis positioning in mandibular body fracture management using finite element analysis. *Eur J Transl Clin Med* **6**, 10–25 (2023).
3. Aftabi, H. *et al.* Computational models and their applications in biomechanical analysis of mandibular reconstruction surgery. *Comput Biol Med* **169**, 107887 (2024).
4. Altuncu, F., Kazan, D. & Özden, B. Comperative evaluation of the current and new design miniplate fixation techniques of the advanced sagittal split ramus osteotomy using three-dimensional finite element analysis. *Med Oral Patol Oral Cir Bucal* **28**, 0–0 (2020).
5. Dario, V., Michelangelo-Santo, G., Roberto, B. & Fabio, F. Is All-on-four effective in case of partial mandibular resection? A 3D finite element study. *J Stomatol Oral Maxillofac Surg* **124**, 101463 (2023).
6. Falcinelli, C., Valente, F., Vasta, M. & Traini, T. Finite element analysis in implant dentistry: State of the art and future directions. *Dent Mater* **39**, 539–556 (2023).
7. Gupta, A., Dutta, A., Dutta, K. & Mukherjee, K. Biomechanical influence of plate configurations on mandible subcondylar fracture fixation: a finite element study. *Med Biol Eng Comput* **61**, 2581–2591 (2023).
8. Maintz, M. *et al.* Parameter optimization in a finite element mandibular fracture fixation model using the design of experiments approach. *J Mech Behav Biomed Mater* **144**, 105948 (2023).
9. Sancar, B., Çetiner, Y. & Dayı, E. Evaluation of the pattern of fracture formation from trauma to the human mandible with finite element analysis. Part 1: Symphysis region. *Dental Traumatology* **39**, 352–360 (2023).
10. Sancar, B., Çetiner, Y. & Dayı, E. Evaluation of the pattern of fracture formation from trauma to the human mandible with finite element analysis. Part 2: The corpus and the angle regions. *Dental Traumatology* **39**, 437–447 (2023).
11. Schönegg, D., Koch, A., Müller, G. T., Blumer, M. & Wagner, M. E. H. Two-screw osteosynthesis of the mandibular condylar head with different screw materials: a finite element analysis. *Comput Methods Biomech Biomed Engin* **27**, 878–882 (2024).
12. Adamović, P., Matoc, L., Knežević, P., Sabalić, S. & Kodvanj, J. Biomechanical analysis of a novel screw system with a variable locking angle in mandible angle fractures. *Med Biol Eng Comput* **61**, 2951–2961 (2023).
13. Xue, R. *et al.* Finite element analysis and clinical application of 3D-printed Ti alloy implant for the reconstruction of mandibular defects. *BMC Oral Health* **24**, 95 (2024).
14. Lisiak-Myszke, M. *et al.* Application of Finite Element Analysis in Oral and Maxillofacial Surgery-A Literature Review. *Materials (Basel)* **13**, (2020).
15. Sittitavornwong, S. *et al.* Integrity of a Single Superior Border Plate Repair in Mandibular Angle Fracture: A Novel Cadaveric Human Mandible Model. *Journal of Oral and Maxillofacial Surgery* **76**, 2611.e1-2611.e8 (2018).
16. Huang, C.-M., Chan, M.-Y., Hsu, J.-T. & Su, K.-C. Biomechanical analysis of subcondylar fracture fixation using miniplates at different positions and of different lengths. *BMC Oral Health* **21**, 543 (2021).
17. Trainotti, S. *et al.* Locking versus nonlocking plates in mandibular reconstruction with fibular graft-a biomechanical ex vivo study. *Clin Oral Investig* **18**, 1291–1298 (2014).
18. Hart, R. T., Hennebel, V. V, Thongpreda, N., Van Buskirk, W. C. & Anderson, R. C. Modeling the biomechanics of the mandible: a three-dimensional finite element study. *J Biomech* **25**, 261–86 (1992).
19. Anthrayose, P., Nawal, R. R., Yadav, S., Talwar, S. & Yadav, S. Effect of revascularisation and apexification procedures on biomechanical behaviour of immature maxillary central incisor teeth: a three-dimensional finite element analysis study. *Clin Oral Investig* **25**, 6671–6679 (2021).
20. Park, B. *et al.* The Stability of Hydroxyapatite/Poly-L-Lactide Fixation for Unilateral Angle Fracture of the Mandible Assessed Using a Finite Element Analysis Model. *Materials* **13**, 228 (2020).
21. Merema, B. B. J., Kraeima, J., Glas, H. H., Spijkervet, F. K. L. & Witjes, M. J. H. Patient-specific finite element models of the human mandible: Lack of consensus on current set-ups. *Oral Dis* **27**, 42–51 (2021).
22. Patil, P. G., Seow, L. L., Uddanwadikar, R., Pau, A. & Ukey, P. D. Different implant diameters and their effect on stress distribution pattern in 2-implant mandibular overdentures: A 3D finite element analysis study. *J Prosthet Dent* **131**, 675–682 (2024).
23. Ruf, P. *et al.* Biomechanical evaluation of CAD/CAM magnesium miniplates as a fixation strategy for the treatment of segmental mandibular reconstruction with a fibula free flap. *Comput Biol Med* **168**, 107817 (2024).

24. Limjeerajarus, N. *et al.* Comparison of ultimate force revealed by compression tests on extracted first premolars and FEA with a true scale 3D multi-component tooth model based on a CBCT dataset. *Clin Oral Investig* **24**, 211–220 (2020).
25. Kshirsagar, R., Jaggi, N. & Halli, R. Bite Force Measurement in Mandibular Parasymphyseal Fractures: A Preliminary Clinical Study. *Craniomaxillofac Trauma Reconstr* **4**, 241–244 (2011).
26. Ahmed, S. *et al.* A comparative study on evaluation of role of 1.5 mm microplates and 2.0 mm standard miniplates in management of mandibular fractures using bite force as indicator of recommendation. *Natl J Maxillofac Surg* **7**, 39 (2016).
27. EOS GmbH – Electro Optical Systems. Matreial Data Sheet PA 2200. www.epfl.ch/schools/sti/ateliers/wp-content/uploads/2018/05/sls_PA2200_EOS.pdf (2024).
28. Materialise Manufacturing. Datasheets 3D Printing Materials: PA12 Medical Grade. www.materialise.com/en/industrial/3d-printing-materials/pa12-medical-grade?utm_source=datasheet&utm_medium=referral&utm_campaign=man-datasheets-pdf (2024).
29. Gareb, B. *et al.* Comparison of the mechanical properties of biodegradable and titanium osteosynthesis systems used in oral and maxillofacial surgery. *Sci Rep* **10**, 18143 (2020).
30. Bohner, L. *et al.* Treatment of Mandible Fractures Using a Miniplate System: A Retrospective Analysis. *J Clin Med* **9**, 2922 (2020).
31. Madsen, M. J., McDaniel, C. A. & Haug, R. H. A Biomechanical Evaluation of Plating Techniques Used for Reconstructing Mandibular Symphysis/Parasymphysis Fractures. *Journal of Oral and Maxillofacial Surgery* **66**, 2012–2019 (2008).
32. Braasch, D. C. & Abubaker, A. O. Management of Mandibular Angle Fracture. *Oral Maxillofac Surg Clin North Am* **25**, 591–600 (2013).
33. Raut, R., Keerthi, R., Vaibhav, N., Ghosh, A. & Kamath Kateel, S. Single Miniplate Fixation for Mandibular Symphysis and Parasymphysis Fracture as a Viable Alternative to Conventional Plating Based on Champy's Principles: A Prospective Comparative Clinical Study. *J Maxillofac Oral Surg* **16**, 113–117 (2017).
34. Landis, J. R. & Koch, G. G. The measurement of observer agreement for categorical data. *Biometrics* **33**, 159–74 (1977).
35. Champy, M. & Lodde, JP. Localization des axilla en axilla des contraintes mandibulaires [Mandibular synthesis. Placement of the synthesis as a function of mandibular stress]. *Rev Stomatol Chir Maxillofac* **77**, 971–976 (1976).
36. Michelet, F. X., Deymes, J. & Dessus, B. Osteosynthesis with miniaturized screwed plates in axilla-facial surgery. *J Maxillofac Surg* **1**, 79–84 (1973).
37. Haerle, Franz., Champy, M. & Terry, B. C. *Atlas of Craniomaxillofacial Osteosynthesis*. (Georg Thieme Verlag, Stuttgart, 2009). Doi:10.1055/b-002-72255.
38. Ehrnfeld, M., Manson, PN. & Perin, J. *Principles of Internal Fixation of the Craniomaxillofacial Skeleton: Trauma and Orthogenetic Surgery.* (Georg Thieme Verlag, 2012).
39. Kroon, F. H. M., Mathisson, M., Cordey, J. R. & Rahn, B. A. The use of miniplates in mandibular fractures. *Journal of Cranio-Maxillofacial Surgery* **19**, 199–204 (1991).
40. Choi, B. H., Yoo, J. H., Kim, K. N. & Kang, H. S. Stability testing of a two miniplate fixation technique for mandibular angle fractures. An in vitro study. *Journal of Cranio-Maxillofacial Surgery* **23**, 122–125 (1995).
41. Braasch, D. C. & Abubaker, A. O. Management of Mandibular Angle Fracture. *Oral Maxillofac Surg Clin North Am* **25**, 591–600 (2013).
42. Tams, J., van Loon, J.-P., Otten, E., Rozema, F. R. & Bos, R. R. M. A three-dimensional study of bending and torsion moments for different fracture sites in the mandible: an in vitro study. *Int J Oral Maxillofac Surg* **26**, 383–388 (1997).
43. Siddiqui, A., Markose, G., Moos, K. F., McMahon, J. & Ayoub, A. F. One miniplate versus two in the management of mandibular angle fractures: A prospective randomised study. *British Journal of Oral and Maxillofacial Surgery* **45**, 223–225 (2007).
44. Gear, A. J. L., Apasova, E., Schmitz, J. P. & Schubert, W. Treatment Modalities for Mandibular Angle Fractures. *Journal of Oral and Maxillofacial Surgery* **63**, 655–663 (2005).
45. Rzymkowski, C. "Hybrid" Approach to Modelling of Biomechanical Systems. In *Human Biomechanics and Injury Prevention* 59–64 (Springer Japan, Tokyo, 2000). Doi:10.1007/978-4-431-66967-8_7.
46. Lloyd, J. E. *et al.* New Techniques for Combined FEM-Multibody Anatomical Simulation. In *New Developments on Computational Methods and Imaging in Biomechanics and Biomedical Engineering* (eds. Tavares, J. M. R. S. & Fernandes, P. R.) 75–92 (Springer International Publishing, Cham, 2019). Doi:10.1007/978-3-030-23073-9_6.
47. Nispel, K., Lerchl, T., Senner, V. & Kirschke, J. S. Recent Advances in Coupled MBS and FEM Models of the Spine—A Review. *Bioengineering* **10**, 315 (2023).
48. Putame, G., Pascoletti, G., Terzini, M., Zanetti, E. M. & Audenino, A. L. Mechanical Behavior of Elastic Self-Locking Nails for Intramedullary Fracture Fixation: A Numerical Analysis of Innovative Nail Designs. *Front Bioeng Biotechnol* **8**, (2020).

49. Gallo, L. M. Modeling of Temporomandibular Joint Function Using MRI and Jaw-Tracking Technologies – Mechanics. *Cells Tissues Organs* **180**, 54–68 (2005).

50. Gallo, L. M., Airoldi, G. B., Airoldi, R. L. & Palla, S. Description of Mandibular Finite Helical Axis Pathways in Asymptomatic Subjects. *J Dent Res* **76**, 704–713 (1997).

51. Koper, D. C. *et al.* Topology optimization of a mandibular reconstruction plate and biomechanical validation. *J Mech Behav Biomed Mater* **113**, 104157 (2021).

52. van Kootwijk, A. *et al.* Semi-automated digital workflow to design and evaluate patient-specific mandibular reconstruction implants. *J Mech Behav Biomed Mater* **132**, 105291 (2022).

53. Schupp, W., Arzdorf, M., Linke, B. & Gutwald, R. Biomechanical Testing of Different Osteosynthesis Systems for Segmental Resection of the Mandible. *Journal of Oral and Maxillofacial Surgery* **65**, 924–930 (2007).

DECLARATIONS

Acknowledgment
The authors would like to thank dr. Konstantina Delli (oral medicine specialist and clinical epidemiologist) at the University Medical Center Groningen for her help with the statistics.

Author contribution
O.D. conducted the study design, 3D modelling, FEA computer studies, 3D printed mandible mechanical testing (3D-MMT), and wrote the manuscript. F.W.W., C.C.R, F.K.L.S and B.v.M. were responsible for supervision, helping with data analysis, and providing guidance. G.L. assisted with the interclass correlation coefficient statistical analysis. The authors approve the manuscript.

Conflict of interest
The authors declare that they have no conflict of interest.

Funding
The materials used for the three-dimensional mandible mechanical testing (3D-MMT) were funded by the Maxim Champy research grant awarded by S.O.R.G. (Strasburg Osteosynthesis Research Group). The funding organisation had no influence on the study design, conducting the study (including collection, management, evaluation, and interpretation of the data), and the writing of the manuscript.

Ethical approval
Not applicable. This study does not contain any procedure with human participants or animals performed by any of the authors. All applicable international, national, and/or institutional guidelines were followed.

Informed consent
Not applicable. For this type of study, formal consent is not required.

Data availability
All data are available from corresponding author upon reasonable request.

SUPPLEMENTARY MATERIAL

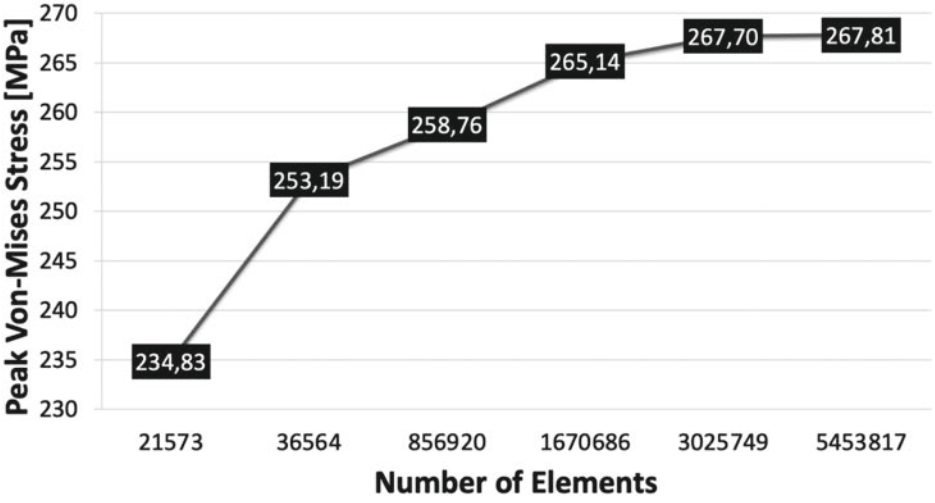

Supplementary Figure S1. Mesh convergence plot with the X-coordinate representing the number of mesh elements and Y-coordinate representing the peak Von-Mises stress [MPa]. The converged mesh had a minimum 0.15 and a maximum 5 mm element size, with an average computation time of 45 minutes per simulation run (using a 12th Gen Intell Corel i9-12950HX CPU @ 2.30 GHz processor with 32 GB RAM memory).

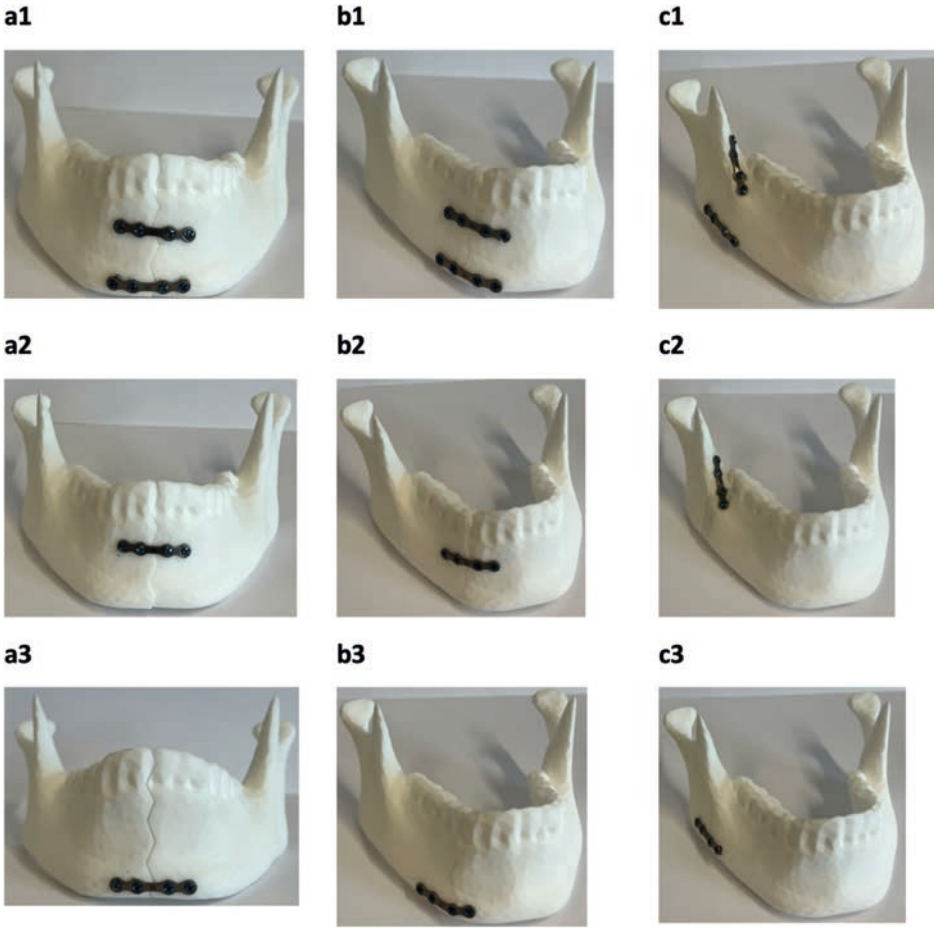

Supplementary Figure S2. Configuration of the 2.0 mm 4-hole 1 mm thick titanium miniplate on the mandibular (**a**) symphysis, (**b**) parasymphysis, and (**c**) angle fractures; with the following miniplate configuration: (**1**) dual plating (**2**), superior border plating, and (**3**) inferior border plating.

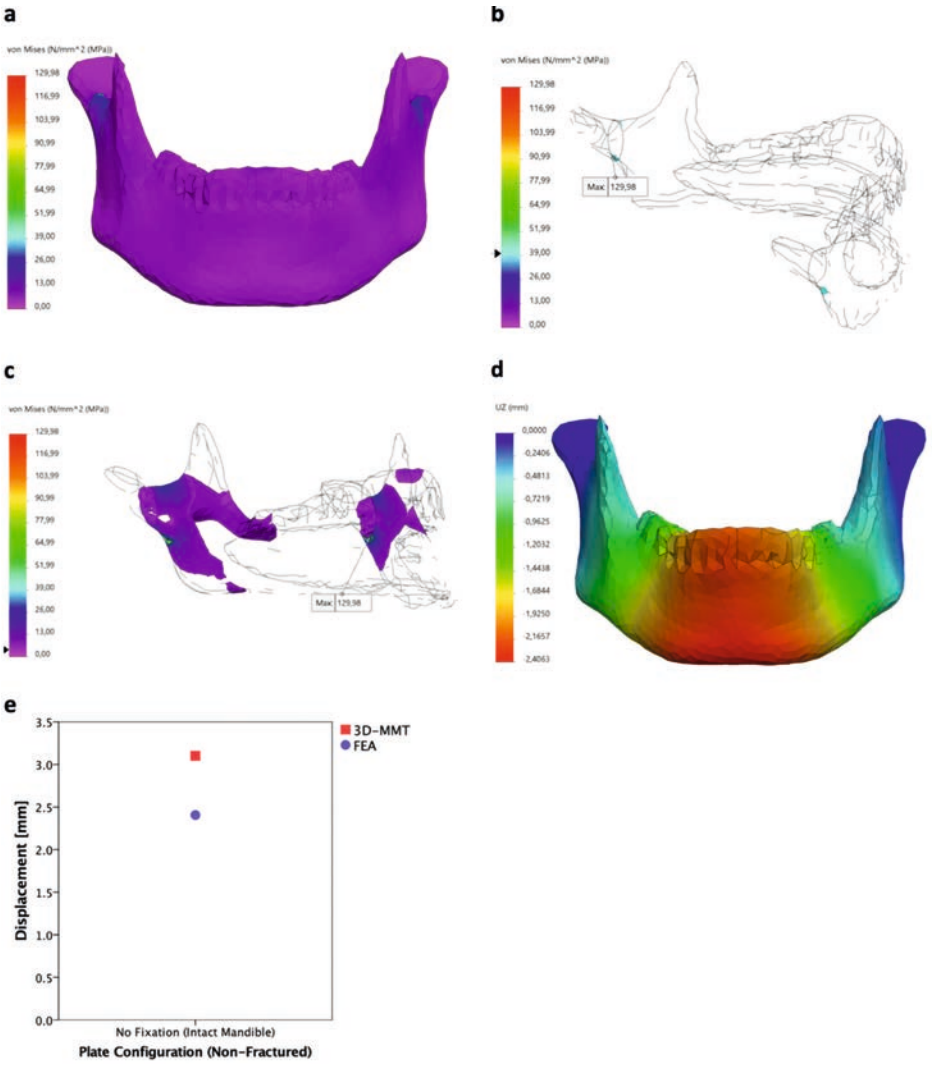

Supplementary Figure S3. Outcomes of non-fracture mandible at 150 N load. (**a**): FEA Von-Mises stress [MPa] pattern. (**b-c**) Stress visualisation at the mandibular condylar fixture site, using the iso clipping: (**b**) set at 40 MPa, and (**c**) set at 4 MPa. (**d**) Displacement [mm] pattern. (**e**) Displacement between the 3D-MMT versus the FEA with a difference of 0.69 mm.

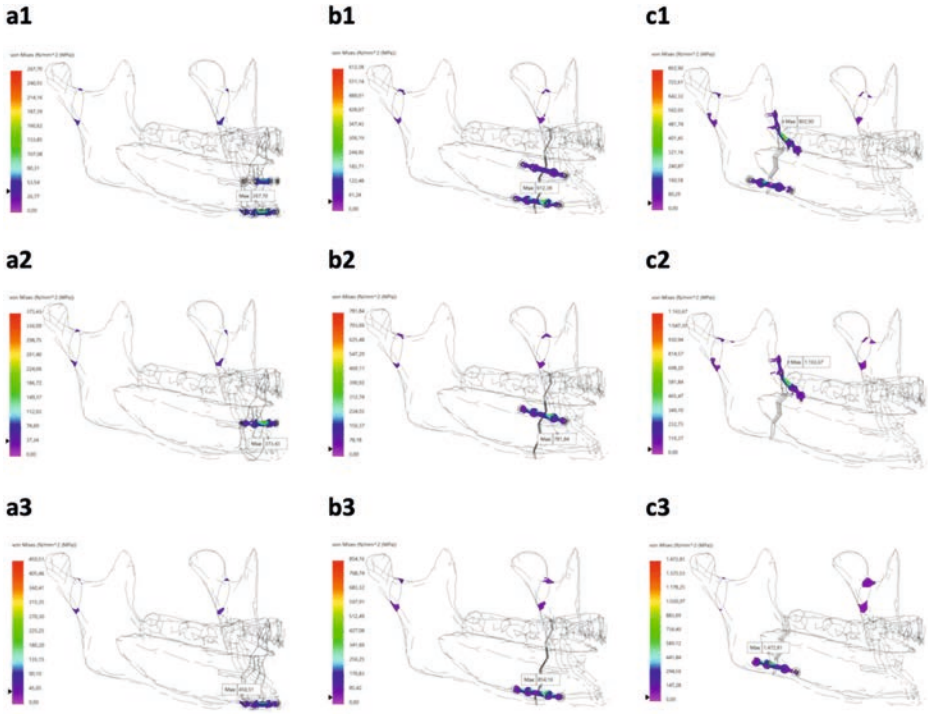

Supplementary Figure S4. Illustrating the Von-Mises stress pattern at the fixture site using iso clipping set at 40 MPa for the mandibular: (**a**) symphysis, (**b**) parasymphysis, and (**c**) angle fractures; with the following miniplate configurations: (**1**) dual plating, (**2**) superior border plating, and (**3**) inferior border plating.

Appendix 1: 3D printed mandible mechanical testing (3D-MMT) outcomes at the failure load.

Appendix 1 Table A1. Failure load and displacement at the failure point from each of the three repeated 3D printed mandible mechanical testing (3D-MMT).

Mandibular fracture	Miniplate configuration	Test number*	Failure load [N]	Displacement [mm] at failure load
Symphysis	**Dual plating**	1	762.08	18.73
		2	721.24	18.84
		3	800.22	20.47
		Mean	*761.18 ± 39.50*	*19.35 ± 0.98*
	Superior border	1	681.62	19.31
		2	688.98	20.50
		3	714.66	19.65
		Mean	*695.09 ± 17.35*	*19.82 ± 0.61*
	Inferior border	1	669.06	22.75
		2	738.05	20.97
		3	755.37	20.62
		Mean	*720.83 ± 45.66*	*21.45 ± 1.14*
Parasymphysis	**Dual plating**	1	675.51	19.85
		2	681.77	20.89
		3	700.70	19.52
		Mean	*685.99 ± 13.11*	*20.09 ± 0.71*
	Superior border	1	582.30	20.15
		2	522.70	17.76
		3	533.41	17.45
		Mean	*546.13 ± 31.77*	*18.45 ± 1.48*
	Inferior border	1	640.27	19.68
		2	645.57	20.81
		3	590.27	17.29
		Mean	*625.37 ± 30.51*	*19.26 ± 1.80*

[continued on next page]

Appendix 1 Table A1. *[continued]*

Mandibular fracture	Miniplate configuration	Test number*	Failure load [N]	Displacement [mm] at failure load
Angle	**Dual plating**	1	670.45	25.38
		2	669.12	26.19
		3	617.31	21.44
		Mean	*652.30 ± 30.31*	*24.34 ± 2.54*
	Superior border	1	643.55	22.94
		2	608.48	20.71
		3	610.72	20.92
		Mean	*620.92 ± 19.63*	*21.52 ± 1.23*
	Inferior border	1	625.89	21.09
		2	623.50	20.78
		3	573.58	19.83
		Mean	*607.65 ± 29.54*	*20.57 ± 0.66*
Non-Fractured		1	863.60	18.88
		2	892.11	19.13
		3	844.83	18.07
		Mean	*866.85 ± 23.80*	*18.69 ± 0.56*

* Test number: each scenario (fractured mandible with three different plate configurations and non-fractured mandible) was repeated three times under identical conditions (Test number 1-3).
Italic: mean and standard deviation (SD) of the three repeated tests.

Appendix 1 Figure A1. Breakage pattern of the mandibular symphysis fracture fixed with three different plate configurations at the maximum failure load. $
(**a**) Dual plating: (a1) broke at the right fixture side, (a2) at the left fixture side, and (a3) at both fixture sides.
(**b**) Superior border plating: all mandibles broke at the right fixture side (b1-b3).
(**c**) Inferior border plating: all mandibles broke at the left fixture side (c1-c3).
Hence: the fixture region is the location where the mandible is tightly fixed using the mandible holders inside the custom-made apparatus used for placing the mandible onto the mechanical test bench.

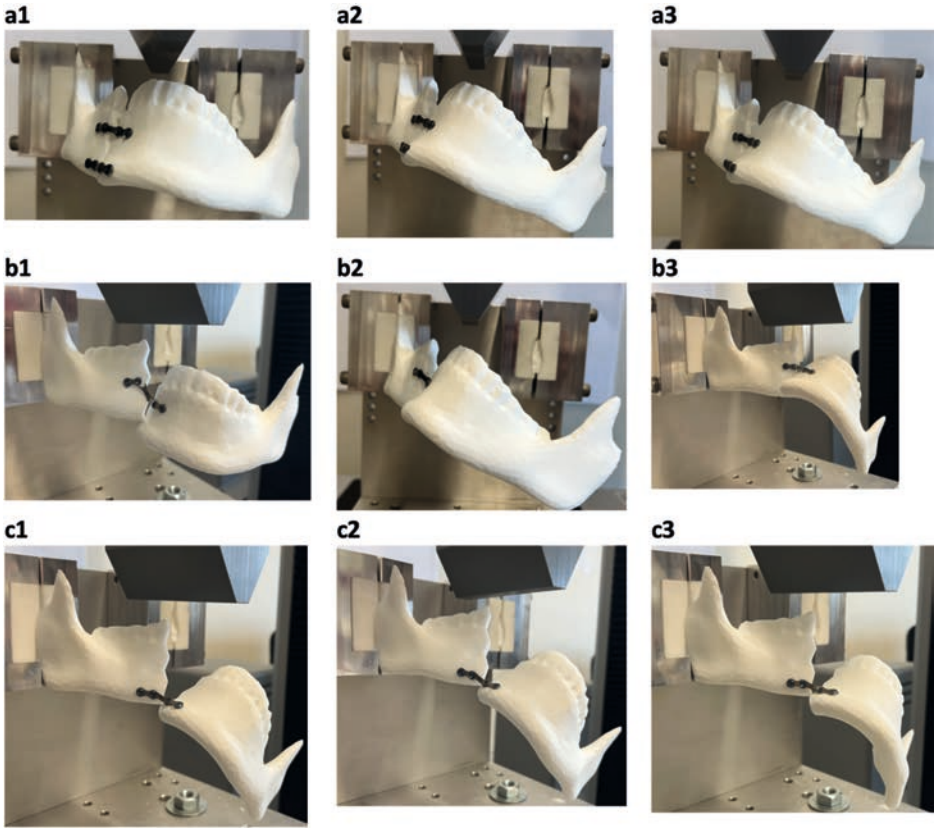

Appendix 1 Figure A2. Breakage pattern of the mandibular parasymphysis fracture fixed with three different plate configurations at the maximum failure load.
(**a**) Dual plating: all the mandibles broke at the left fixture side (a1-a3).
(**b**) Superior border plating: all the mandibles broke at the left fixture side (b1-b3).
(**c**) Inferior border plating: all the mandibles broke at the left fixture side (c1-c3)
Hence: the fixture region is the location where the mandible is tightly fixed using the mandible holders inside the custom-made apparatus used for placing the mandible onto the mechanical test bench.

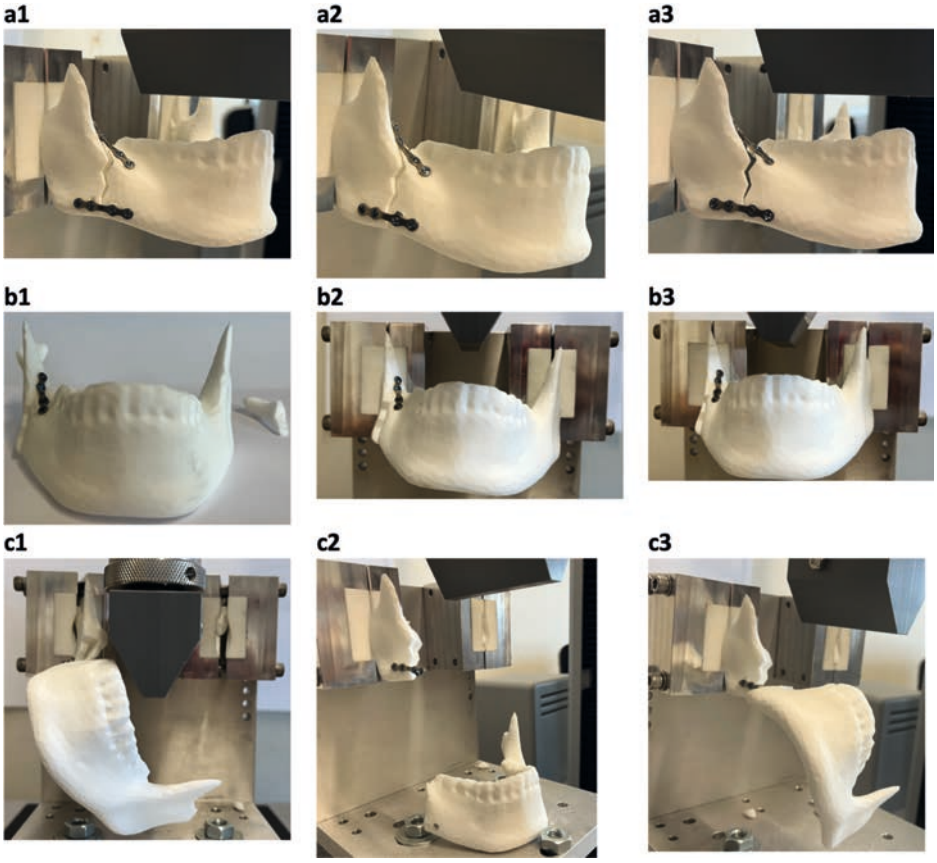

Appendix 1 Figure A3. Breakage pattern of the mandibular angle fracture fixed with three different plate configurations at the maximum failure load.
(**a**) Dual plating: all the mandibles broke at the left fixture side (a1-a3).
(**b**) Superior border plating: all the mandibles broke at the left fixture side (b1-b3).
(**c**) Inferior border plating: all the mandibles broke at the left fixture side (c1-c3). Further, there was an additional failure in the second test (c2), where the proximal screws were loosened from the mandible screw holes.
Hence: the fixture region is the location where the mandible is tightly fixed using the mandible holders inside the custom-made apparatus used for placing the mandible onto the mechanical test bench.

Appendix 1 Figure A4. The break pattern of non-fractured mandible replicas at the maximum failure load. (**a**) all the mandibles broke at the left fixture side (a1-a3).
Hence: the fixture region is the location where the mandible is tightly fixed using the mandible holders inside the custom-made apparatus used for placing the mandible onto the mechanical test bench.

Appendix 2: FEA evaluation of the effect of mandible holders.

Explanation FEA model:

In this section we evaluated the effect of mandible holders. Therefore, two cases were studied, namely: a mandible holder as one solid body and a mandible holder consisting of two components.

Regarding the 3D design of the mandible holders and the mandible (Appendix 2 Figure 1a):

- The mandible holders have the same dimensions as the holders used in the study. In here two different mandible holder setups were assessed, namely: a single block mandible holder and a mandible holder made of two components.
- The mandible self was simplified as a rod, with the same diameter dimension as the mandible holder hole (where the mandible is placed inside the mandible holders).

Regarding the FEA setup:

- Fixture: fixed geometry at the back side of the holders (the green dots) (Appendix 2 Figure 1b).
- Load: 75 N load applied on the rod bar (purple arrows) (Appendix 2 Figure 1b).
- Material: mandible holder set as Nylon 6, and the rod set as AISI 316 stainless steel.
- Contact between mandible holder and rod: set as contact with 0.05 friction.
- Contact mandible holder consisting of two components: the connection between the components was set as contact with 0.05 friction:

Explanation outcomes:

We observe some stress along the split for the two-components holder and at the tip of the rod 0,1 mm displacement (Appendix 2 Figure 1c-d). The latter is about 6 times smaller than the systematic error we have observed. The displacement will increase if we make the rod thinner, since the contact area will decrease. Because in the holder, the width of the mandible is lower than the height, we think that the displacement value will go up to the systematic error we observe.

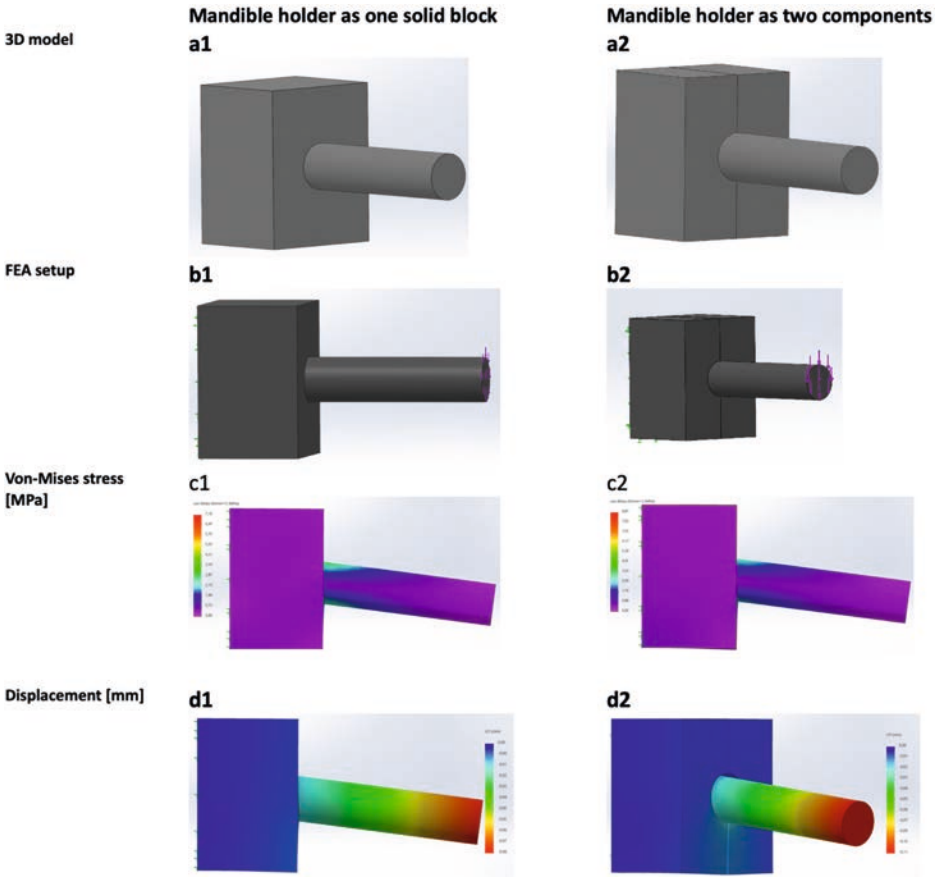

Appendix 2 Figure A1. FEA evaluation of simplified assembly containing two different mandible holder configurations (single block versus two separate blocks) and a rod bar resembling the mandible.

Additional appendix: Test setup 3D drawings and dimensions

Total assembly

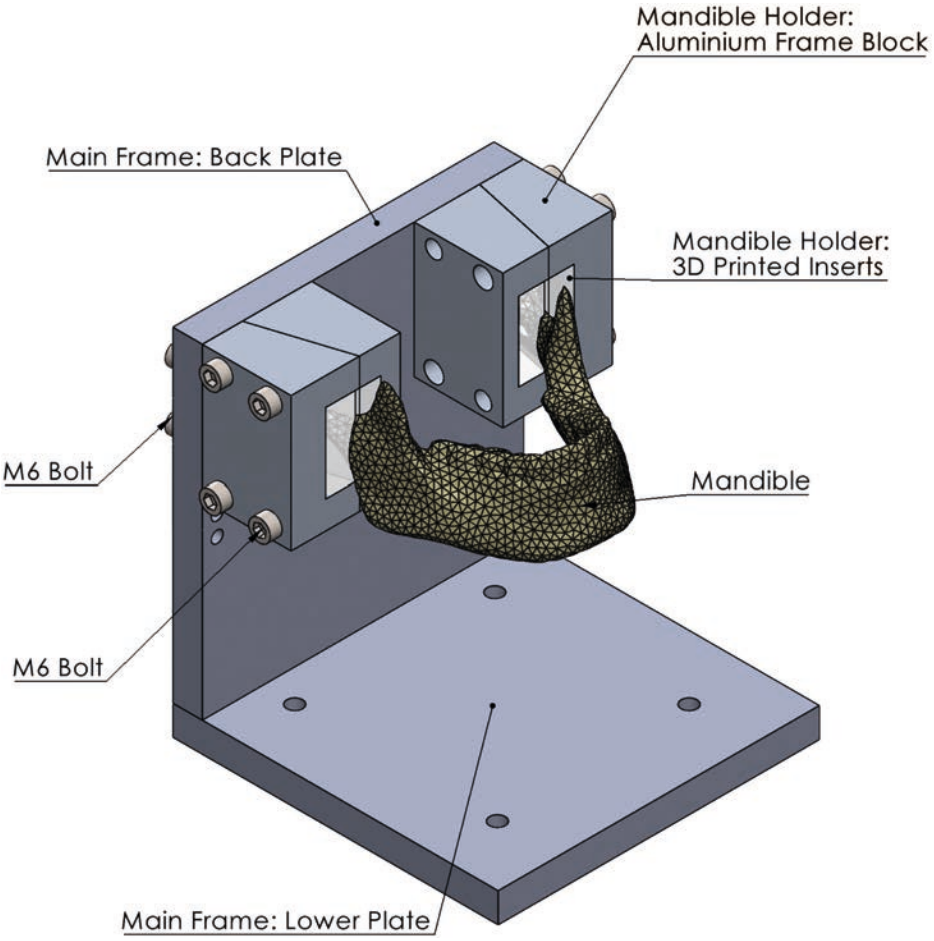

Main frame

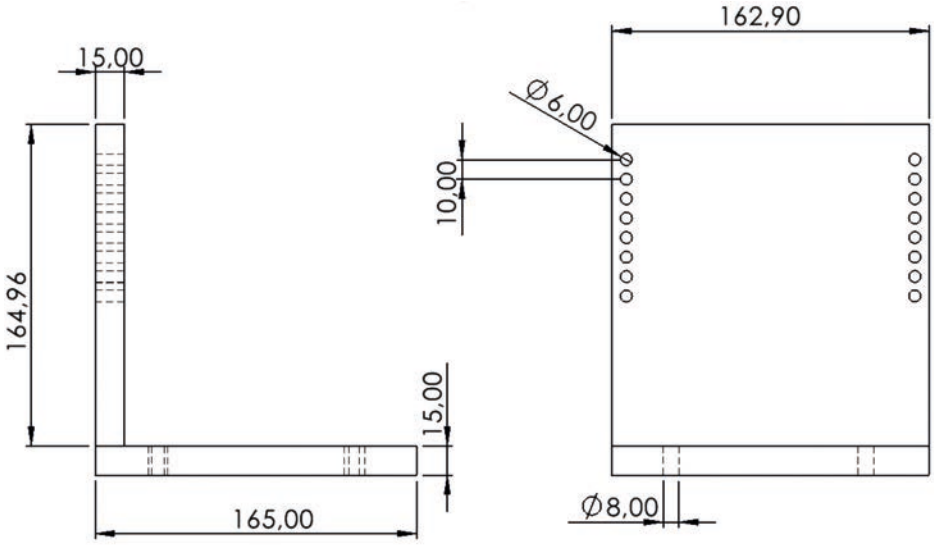
15,00
164,96
15,00
165,00
162,90
Ø6,00
10,00
Ø8,00

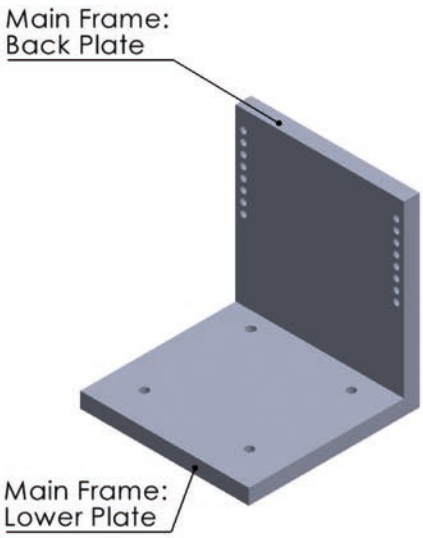
Main Frame:
Back Plate
Main Frame:
Lower Plate

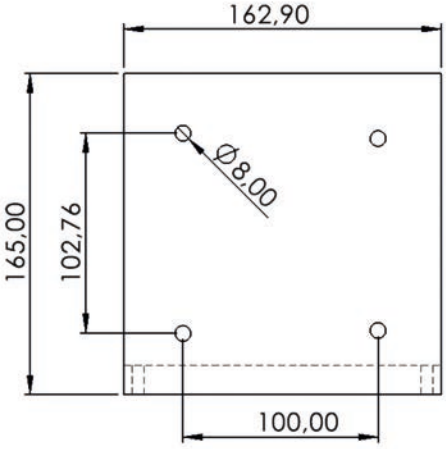
162,90
Ø8,00
165,00
102,76
100,00

Mandible holder frame blocks

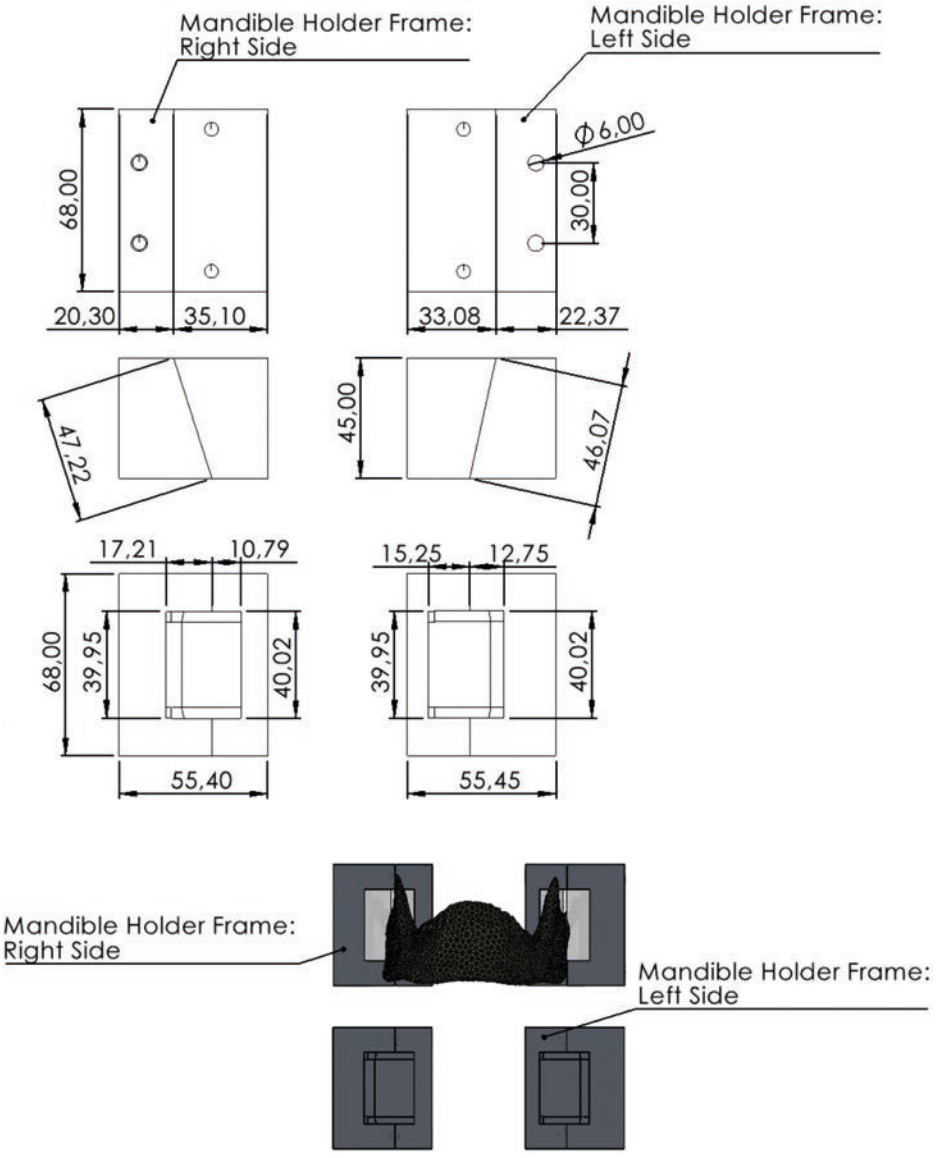

Mandible holder 3D printed inserts

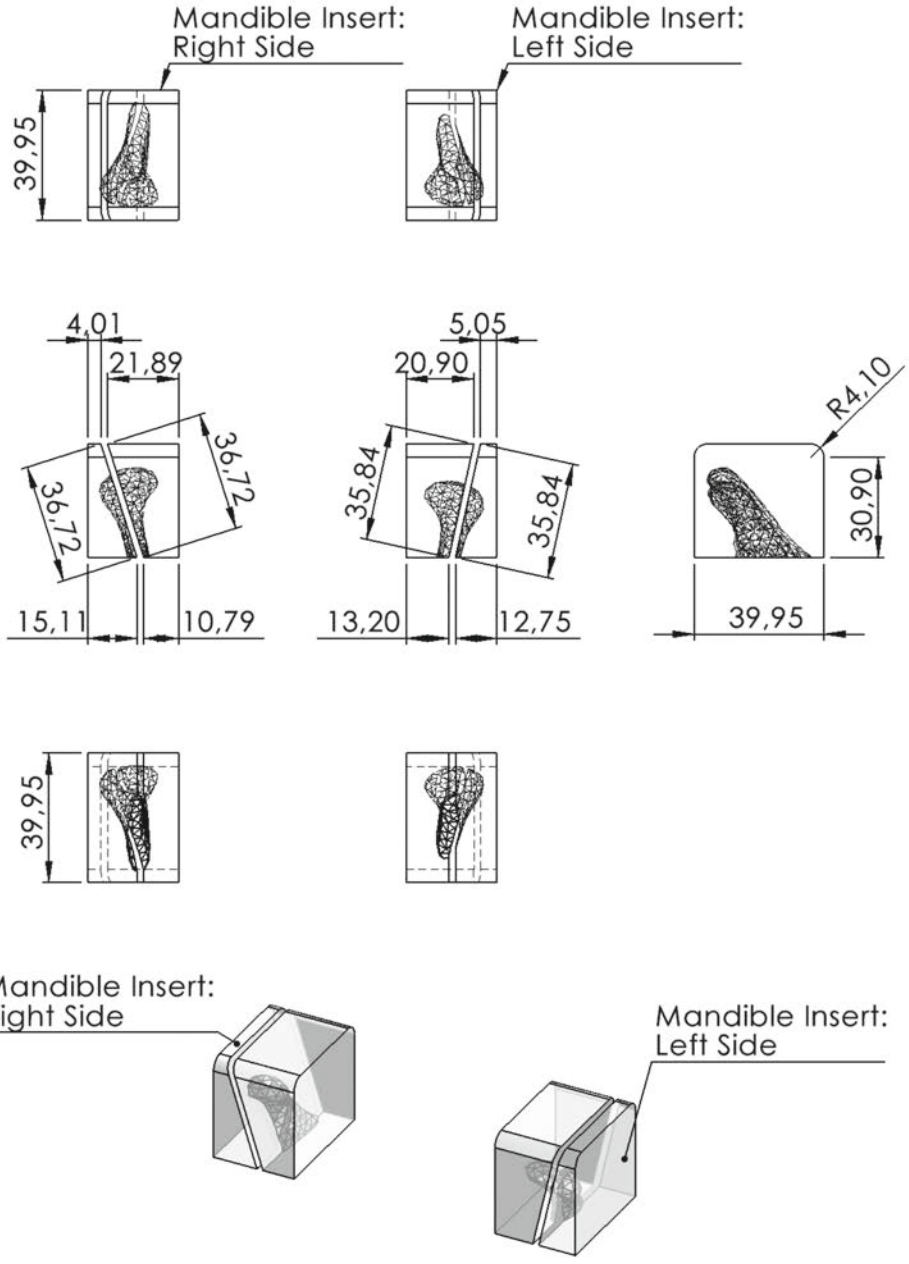

SECTION IV

Application of validated FEA in complex fracture

CHAPTER 6

In silico analysis of severely atrophic edentulous mandibular body and angle fracture fixation using a validated finite element analysis model

Omid Daqiq[1]*, Friederik Wilhelm Wubs[2], Frederik Karts Lucien Spijkervet[1], Charlotte Christina Roossien[3] & Baucke van Minnen[1]

[1] *Department of Oral and Maxillofacial Surgery, University Medical Center Groningen, University of Groningen, Hanzeplein 1, 9713 GZ, Groningen, The Netherlands.*

[2] *Bernoulli Institute for Mathematics, Computer Science and Artificial Intelligence, University of Groningen, Nijenborgh 9, 9747 AG, Groningen, The Netherlands.*

[3] *Bio-inspired MEMS and Biomedical Devices group, Engineering and Technology Institute Groningen, Faculty of Science and Engineering, University of Groningen, Nijenborgh 4, 9747 AG, Groningen, The Netherlands.*

Submitted: 25 August 2025
Journal: Journal of Cranio-Maxillofacial Surgery

ABSTRACT

The clinical controversies regarding the treatment of severely atrophic edentulous mandibular fractures can be further clarified by in silico analysis. This study aimed to assess the biomechanical aspects of their fixation by using a validated finite element analysis (FEA) model.

This was achieved by simulating a 3D digital twin of a Luhr class III severe atrophic edentulous mandible. First, the effects of the number of the fractures (unilateral versus bilateral), precision of fracture reduction (interfragmentary gap of 0.01, 0.1, and 1 mm), miniplate type (2.0 mm 4-hole versus 6-hole), and screw loosening (distal, mesial, and both side of fracture) were assessed for mandibular body fracture. Second, the influence of miniplate type and screw loosening were investigated for the angle fracture.

FEA simulations illustrated that the number of the fractures, fracture reduction, and screw loosening directly adjacent to the fracture have a major effect on fracture stability. Additionally, the outcomes supported the current understanding of atrophic mandibular fracture treatment and provided new biomechanical insights into its fixation.

In conclusion, the previously validated FEA model demonstrated promising results. As it effectively simulates fixation stability of these fractures, it can also be applied to study other complex mandibular fractures.

Keywords

Finite Element Analysis, Severely atrophic edentulous mandibular fracture, Miniplate osteosynthesis, Fixation stability and biomechanics, Computer-assisted surgery, Traumatology.

INTRODUCTION

FEA is a powerful in-silico tool that can enhance the evaluation of bone fractures (e.g., mandible) and fixations methods in the craniomaxillofacial (CMF) region (Altuncu et al., 2020; Daqiq et al, 2024; Daqiq et al., 2025a; Dario et al., 2023; Falcinelli et al., 2023; Gupta et al., 2023; Kahveci & Ayranci, 2023; Maintz et al., 2023; Schönegg et al., 2024; Xue et al., 2024). It is a precise non-invasive way of assessing fracture fixation under application of load, by visualising the amount of stress, strain, and displacement along with illustrating the fracture stability under various conditions (Adamović et al., 2023; Aftabi et al., 2024; Anthrayose et al., 2021; Lisiak-Myszke et al., 2020; Park et al., 2020; Patil et al., 2024; Ruf et al., 2024; Sancar et al., 2023; Xue et al., 2024). Therefore, in case of complex fractures, FEA can assist the surgeon in finding the best approach for fracture fixation, can improve the current osteosynthesis, and allow designing new type of implants (Daqiq et al, 2023, 2024, 2025a; Kahveci & Ayranci, 2023; Sugiura et al., 2009; Vajgel et al., 2013).

In previous studies we developed a validated FEA model for simulating mandibular fracture fixations by assessing non-comminuted fractures with a well-known clinical and biomechanical behaviour, using standard miniplate osteosynthesis (Daqiq et al., 2024, 2025a). The next step was to apply the FEA model to study the fixation of mandibular fractures with scientific controversy about the optimal fixation method and to assess its applicability in the clinical setting. In case of severely atrophic edentulous mandibular fractures literature indicates that there is insufficient evidence to definitively recommend any specific fixation (Bera & Tiwari, 2023). As for mandibular angle fractures there is controversy about the best method of fixation, as well. Even by choosing the often applied method of fixation along the oblique external line, the handbooks disagree on the number of screws (Ehrnfeld et al., 2012; Haerle et al., 2009). Additionally, clinical studies are often time-consuming or unfeasible without the required inclusions, while laboratory experiments can be resource-intensive and costly. In this context, the validated FEA model offers a valuable alternative, with the potential to generate novel biomechanical insights into the surgical management of these complex fractures. It can enhance the clinician's understanding of fracture fixation mechanics and support evidence-based advancements in surgical decision-making.

The aim of this study is to apply the validated FEA model to investigate clinically non-routine complex fractures by simulating the fixation of severely atrophic edentulous mandibular body and angle fractures. We hypothesized that our FEA model can accurately demonstrate the biomechanical behaviour of these fractures, fixated with different treatment scenarios, and, thereby, can give a new insight regarding fixation of these fractures. Second, we hypothesise that the fracture fixation stability is influenced by the number of the fractures, precision of fracture reduction, miniplate type, and screw loosening; therefore, the effect of these critical variables in severely atrophic edentulous mandibular fractures can be replicated using the FEA model.

MATERIAL AND METHODS

Study outline

In our previous studies, we developed a validated FEA model for studying mandibular fracture treatment (Daqiq et al., 2024, 2025a). In this study, the same FEA principle was applied to analyse the fixation of mandibular body and angle fracture in a Luhr class III (vertical body height of 10 mm or less) (Luhr et al., 1996) severely atrophic edentulous mandible with a mandibular body height of 5.7 mm (Fig. 1). The fractures were fixated using a 3D digital representation of either a 2.0 mm 4-hole 1.0 mm thick (reference nr. 25-551-04-09; dimension: 1 mm thickness, 26 mm length, and 4.3 mm width) or a 2.0 mm 6-hole 1.0 mm thick (reference nr. 25-550-06-91; dimension: 1 mm thickness, 31.8 mm length, and 4.3 mm width) titanium miniplate, along with maxDrive® 2.0 x 6 mm screws (reference nr. 25-872-05-09; dimension: 6 mm length and 2 mm diameters) (KLS-Martin, Gebrüder Martin GmbH & Co., Tuttlingen, Germany). The numerical FEA studies were conducted using Solidworks software (version SP5.0, 2021, Waltham, Massachusetts, USA) (Fig. 1).

The study focused on addressing key clinically relevant questions concerning the fixation of severely atrophic edentulous mandibular body and angle fractures. First, for mandibular body fractures, the effects of the number of the fractures (unilateral versus bilateral) (Fig. 2A), osteosynthesis fixation type (2.0 mm 4-hole versus 6-hole miniplate) (Fig. 2B-C), precision of fracture reduction (interfragmentary gap of 0.01, 0.1, and 1 mm) (Fig. 2D), and screw loosening (on the distal, mesial, and both sides of the fracture site) were evaluated (Fig. 2H). Second, for a mandibular angle fracture with 0.1 mm reduction (Fig. 2E), the influences of miniplate type (2.0 mm 4-hole versus 6-hole miniplate) (Fig. 2F-G) and screw loosening (on the distal, mesial, and both side of the fracture site) were assessed (Fig. 2I). The precision of the mandibular body fracture reduction was assessed based on the interfragmentary distance between the fracture surfaces, which was incrementally increased by factor of 10, starting from 0.01 (indicating good reduction), to 0.1 (moderate), and 1 mm (poor reduction) (Fig. 2D). In both mandibular body and angle simulations, screw loosening was defined by removing the studied screw positioned directly adjacent to the fracture site (on the mesial, distal, and both sides) (Fig. 2H-I) in the FEA simulation model.

Creating 3D models

Mandible

The 3D digital twin of the mandible was obtained by using computed tomography (CT) scan (Siemens, SOMATOM® Force model, Siemens Healthcare GmbH, Germany) of a severely atrophic edentulous cadaveric mandible with a 5.7 mm mandibular body height (Fig. 1A). The mandible was scanned using the 3D skull bone setting with a 0.6 mm slice size, 80 kV tube potential, 6.3 mA tube current, 473 MGy*cm3 DAP, 1.2 mGy CTDI, and 400 µm HD voxel size. The CT scan enabled obtaining the digital imaging and communication in medicine (DICOM) file for further image processing. The file was then imported into Mimics Medical

software (version 23.0, Materialise, Leuven, Belgium) for 3D segmentation, achieved by assigning masks and adjusting the Hounsfield unit (HU) threshold. Afterwards, the segmentation file was then exported as stereolithography (STL) file format and loaded into the Geomagic Freeform software (version 2021.0.56, 3D System, Rock Hill, South Carolina, USA). The trabecular bone was set as cavity, the model was smoothed, and the surfaces were closed or fixed if needed. Using the "remesh" function in Freeform, the STL file was brought to a fixed triangle size of 2.5 mm. The 3D part, containing the cortical bone and trabecular cavity, was exported without any reduction in the file size. These steps enabled creating a workable organic mandibular model, free from segmentation mesh errors, which could be flawlessly imported into Solidworks software (version SP5.0, 2021, Waltham, Massachusetts, USA) in STL file format (Fig. 1B).

The remainder of the study and analysis were conducted in Solidworks software, including the creation of the fractures in the mandible, 3D modelling of osteosynthesis (miniplates and screws), formation of the assemblies (fractured mandibles fixated with osteosynthesis), and FEA simulations.

Fractures

In the study, clinically realistic jagged line fractures were created in the mandibular body and angle regions (Fig. 2A and Fig. 2E). The mandibular body fracture 3D models included both unilateral and bilateral fractures (Fig. 2A). First, a unilateral fracture on the right side of the mandibular body was created. Then, in the bilateral body fracture 3D models, an additional fracture on the left side of mandibular body was introduced. For both unilateral and bilateral fractures, the fracture reduction or the interfragmentary gap between the fracture surfaces was set to 0.01, 0.1, and 1 mm (Fig. 2D). This was achieved by increasing the distance between the fracture surfaces, starting at 0.01 mm, and increasing it by a factor of 10 each time, without altering the fracture pattern or shape. For the mandibular angle fractures, a unilateral fracture was created on the left side of the mandibular angle region with a 0.1 mm fracture reduction (Fig. 2E). In both the mandibular body and angle fracture studies, the effect of loose screws was investigated by removing or excluding the studied screw(s) from the 3D FEA model (Fig. 2H-I).

Osteosynthesis

The precise 3D models of the titanium osteosynthesis components used for fracture fixation were designed in Solidworks, including 2.0 mm 4-hole and 6-hole miniplates along with a 2.0 × 6 mm screw (Fig. 2B-C and Fig. 2F-G).

Assembly

For the assembly process, the miniplate was positioned along the fracture line. The miniplates were then shaped (bent and/or twisted) based on the outer surface geometry of the mandible using the "Flex" option in the features tap of Solidworks. Afterwards, the miniplate was secured against the mandibular surface using the screws which were tightened into the

mandibular screw holes (Fig. 2B-C and Fig. 2F-G). This setup is in accordance with the non-locking compression plating system (Bohner et al., 2020; Braasch & Abubaker, 2013; Daqiq et al., 2024, 2025a; Madsen et al., 2008; Raut et al., 2017).

FEA setup

Load and fixture

A 150 N load was applied on the two mandibular incisal teeth regions positioned at the anterior mandibular symphysis (Fig. 1C). This was in accordance with the current literature's mean postoperative maximum incisal bite force for a mandibular fracture treated with miniplate osteosynthesis (Ahmed et al., 2016; Daqiq et al., 2025b; Kshirsagar et al., 2011). The load was applied downward, similar to the downward incisal mastication force, using "Force" option in Solidworks external load advisor. The applied load was identical across all the mandibular model simulations.

The mandibular fixture was set on the right and left mandibular condyle using "Fixed Geometry" option in Solidworks fixture advisor (Fig. 1C) (Daqiq et al., 2025a). The applied fixture was identical in all the mandible models.

Material properties

The material properties of the bone and the osteosynthesis materials were manually added to the custom materials in the Solidworks library. The bone material model used was linear elastic isotropic.

The material properties of the mandibular cortical bone were set at an elastic modulus of 29900 megapascal [MPa], mass density of 8.190 g/cm3, and Poisson's ratio of 0.13 (Daqiq et al., 2025b; Schwartz-Dabney & Dechow, 2003). The trabecular bone segment was set as a cavity, so there was no need to define the material properties for the trabecular bone.

The biomechanical properties of the titanium osteosynthesis (miniplate and screws) were set at an elastic modulus of 104800 MPa, tensile strength of 1100 MPa, yield strength of 827.40 MPa (not used in the model), mass density of 4.43 g/cm3, and Poisson's ratio of 0.31 (Gareb et al., 2020).

Boundary conditions

The boundary conditions between the mandible and osteosynthesis components were designated by using the "Contact Sets" property manager in the local interaction tab of Solidworks. This was according to the current knowledge of mandibular fracture fixation based on the non-locking compression osteosynthesis plating (Bohner et al., 2020; Braasch & Abubaker, 2013; Daqiq et al., 2024, 2025a; Madsen et al., 2008; Raut et al., 2017). The interaction between most of the parts were assigned as contact, including the constraints between the fracture surfaces (Fig. 1D), the miniplate and the screws (Fig. 1E), and the miniplate

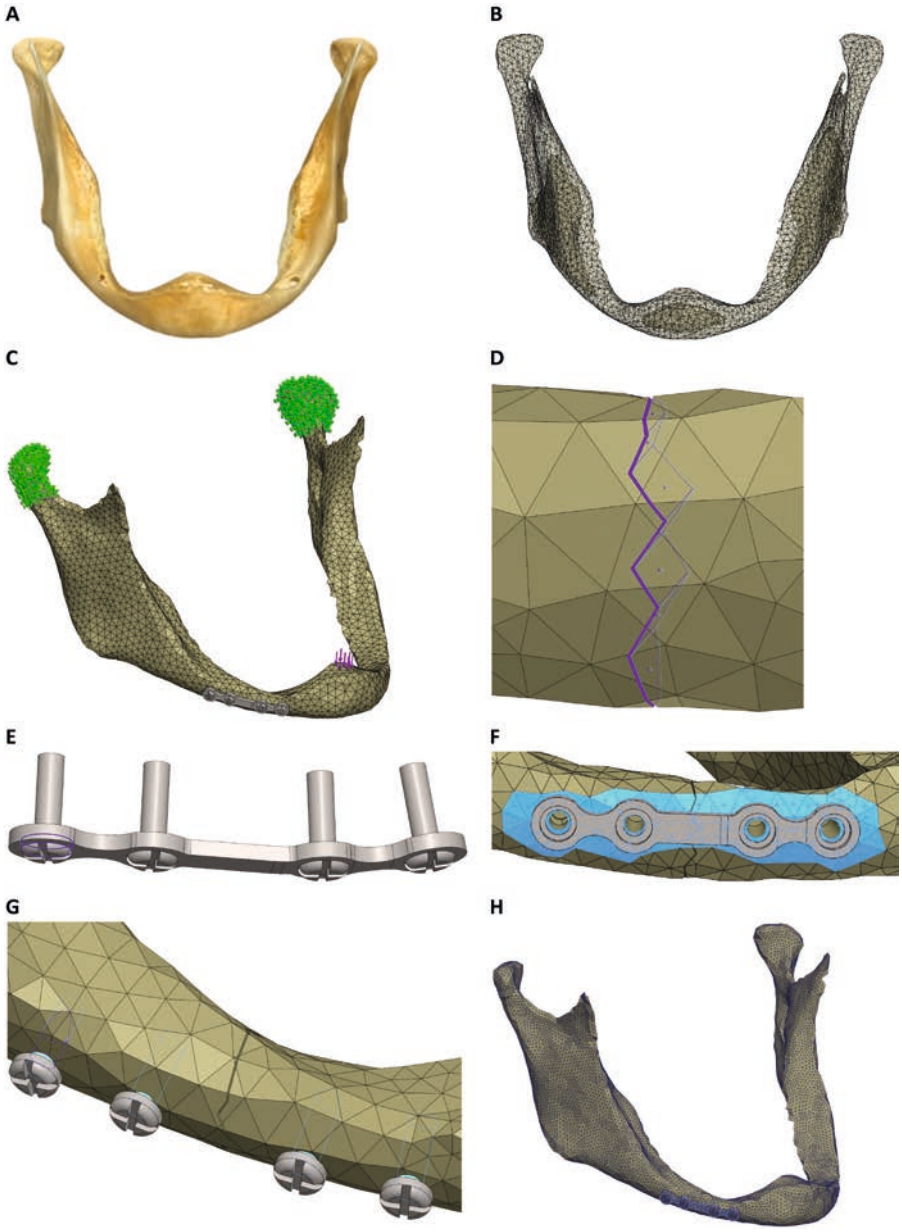

Fig. 1. Visualisation of the mandibular 3D modelling (**A-B**) and FEA setup in Solidworks (**C-H**), identical across all simulated studies. (**A)** Severely atrophic edentulous cadaveric mandible Luhr class III (5.7 mm vertical body height). (**B)** Reconstructed 3D mandible model comprising cortical bone and an internal trabecular cavity. (**C)** Applied 150 N downward load on the anterior of the mandible at the incisal region (indicated by pink arrows) and applied fixture at the condylar regions using fixed geometry (indicated by green arrows). (**D)** Fracture surfaces boundary condition using contact with no penetration. (**E)** Contact constraint between the miniplate and screw. (**F)** Surface contact boundary condition between the outer mandibular surface and the inner miniplate surface touching the mandible. (**G)** Bonded connection constraints between the screw and the mandible screw hole. (**H**) Impression of the applied mesh.

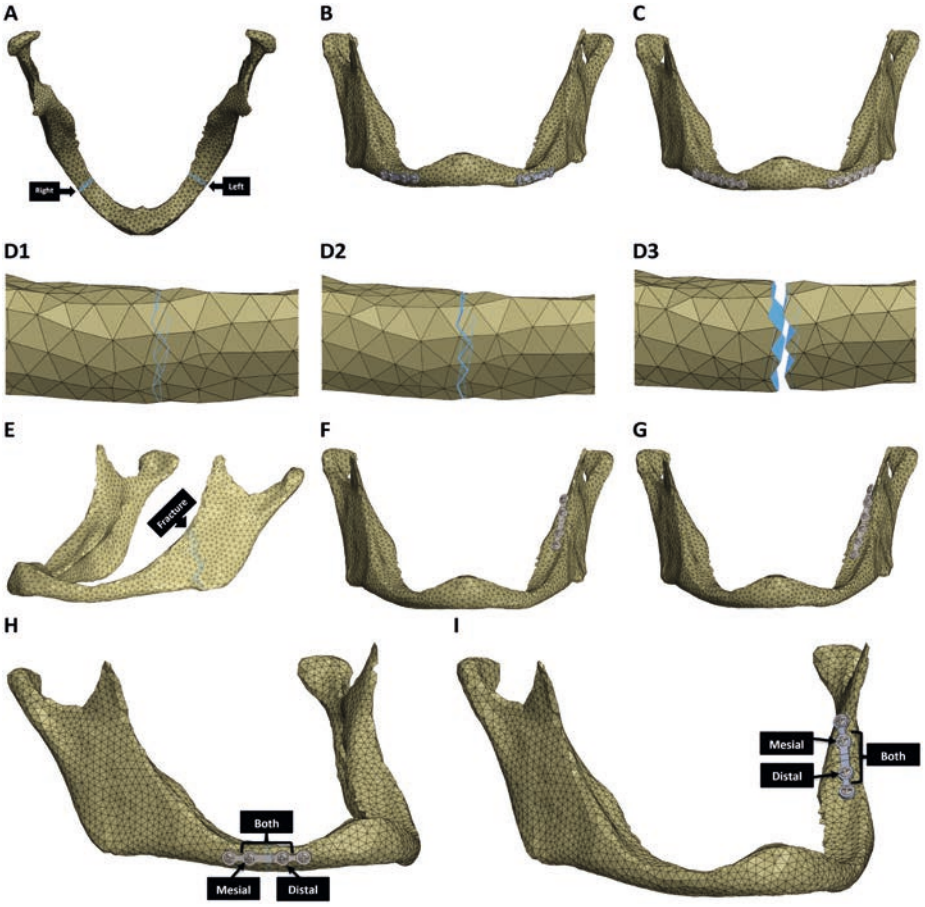

Fig. 2. Mandibular body (**A-D, H**) and angle (**E-G, I**) fracture scenarios investigated in a severely atrophic edentulous mandible. (**A**) Bilateral mandibular body fracture (hence unilateral body fracture contains a fracture only on the right mandibular body). (**B-C**) Positioning of the 2.0 mm 4-hole (**B**) and the 2.0 mm 6-hole (**C**) miniplate (hence the unilateral fracture fixation is only limited to the right side). (**D**) Detail of right mandibular body fracture reduction with interfragmentary gap of 0.01, 0.1, and 1 mm (resp. **1-3**) (hence identical reduction was applied for the left side fracture). (**E**) Unilateral mandibular angle fracture on the left side with 0.1 mm fracture reduction. (**F-G**) Location of the 2.0 mm 4-hole (**F**) and 2.0 mm 6-hole (**G**) miniplate. (**H-I**) Location of screw loosening directly adjacent to the fracture site in the 4-hole miniplate fixation for the unilateral body (**H**) and unilateral angle (**I**) fractures (with same screw loosening conditions applied to the 6-hole miniplate).

and the mandible (Fig. 1F). Contact was defined without presence of friction, whereupon a load application, only normal forces would be exchanged between the surfaces of the components. Additionally, the fracture surfaces were further defined by applying contact sets with a fixed distance, depending on the prespecified fracture reduction (interfragmentary gap of 0.01, 0.1, or 1 mm), with no penetration between the surfaces during loading (Fig. 1D). Lastly, connection between the screws and the mandible screw holes was set as bounded (Fig. 1G). This means that the screws are tightly fitted inside the mandible screw holes, securing the miniplate fixed against the mandibular surface.

Mesh

The study performed sensitivity analyses to determine the FEA optimal mesh size. Convergence of the solution was reached by continuously reducing the mesh size until the peak Von-Mises stress [MPa] became independent of the mesh size (Supplementary Fig. S1: mesh convergence plot). This led to a controlled mesh which was applied in the simulations (Fig. 1H). The used mesh has a minimum element size of 0.1 mm and a maximum element size of 5 mm. The mesh resulted in an average computation time of 30 minutes per simulation run, using a 12th Gen® Intel Core™ i9-12950HX CPU @ 2.30 GHz processor with 32 GB of RAM.

Data analysis

The FEA outcomes of Von-Mises stress [MPa] and displacement (the same direction as the applied load in the Y-axis) [mm] were obtained (Table 1-3, Fig. 3-5, and Supplementary Fig. S2-S7). First, the mandibular body fracture fixation was studied by assessing the effects of the number of the fractures, the precision of fracture reduction, and the type of osteosynthesis miniplate (Table 1, Fig. 3A-F, and Fig. 5A-B). Additionally, the influence of screw loosening on the stability of unilateral mandibular body fixation using 4-hole versus 6-hole miniplates was evaluated (Table 2, Fig. 3G-H, and Fig 5. C-D). Second, a mandibular angle fracture was simulated to analyse the effects of miniplate type and the presence of loose screw(s) on fixation stability (Table 3, Fig. 4, and Fig. 5E-F). It did not make sense to conduct statistical analysis due to the nature of the study and the small data size. However, numerical simulation constitutes a valid quantitative research methodology.

RESULTS

The FEA findings illustrate the maximum Von-Mises stress in megapascal [MPa] and displacement in millimetres [mm] for the different simulated scenarios in the severely atrophic edentulous mandible containing body or angle fractures (Table 1-3, Fig. 3-5) (Supplementary Fig. S2-S7: comprehensive FEA outcomes). In the FEA, the fracture fixation stability is assessed by observing the amount stress and displacement pattern along with illustrating the fracture fixation behaviour. The stability of fracture fixation varies across different studied scenarios, with the maximum stress consistently remaining on the miniplate in all the simulated cases.

Mandibular body fracture

The effect of number of the fractures, precision of fracture reduction, and miniplate type is presented (Table 1, Fig. 3C-F, and Fig. 5A-B) (Supplementary Fig. S2-5). First, regarding the number of the fractures, unilateral fracture results in much lower stress and displacement compared to bilateral fractures. Second, optimal fracture reduction or minimization of the interfragmentary gap between the fracture surfaces influences the amount of stress and displacement as well as fracture stability. Optimal fracture reduction was observed in the 0.01 mm, followed by 0.1 mm, with the least stability in cases with a 1 mm fracture distance.

Third, using a 2.0 mm 6-hole titanium miniplate results in lower stress and displacement compared to the 4-hole miniplate, leading to more stable fracture fixation.

Table 1. FEA outcomes of unilateral versus bilateral mandibular body fracture fixation using 2.0 mm 4-hole versus 6-hole miniplates for different fracture reductions.

		Mandibular Body Fracture Fixation			
		2.0 mm 4-hole Miniplate		2.0 mm 6-hole Miniplate	
Number of the Fractures*	Fracture Reduction**	Von-Mises Stress [MPa]	Displacement [mm]	Von-Mises Stress [MPa]	Displacement [mm]
Unilateral	**0.01**	558.86	1.74	459.01	1.68
	0.1	685.26	1.77	492.79	1.75
	1	896.06	1.81	508.69	1.75
Bilateral	**0.01**	1156.91	2.49	967.16	2.24
	0.1	1410.43	2.90	1290.15	2.75
	1	2418.30	4.35	1862.75	3.27

* Number of the fractures: (unilateral: right mandibular body fracture; bilateral: additional left mandibular body fracture.
**Fracture reduction: interfragmentary gap between the fracture surfaces in mm.

Furthermore, loose miniplate screw(s) directly adjacent to the unilateral fracture site adversely affected fixation stability (Table 2, Fig. 3G-H, and Fig. 5C-D) (Supplementary Fig. S2-S5). In both fixation methods, the stress and displacement increased in case of detached screw(s). The 4-hole miniplate exhibited higher stress and displacement compared to the 6-hole miniplate. The highest stress and displacement were observed for loose screws on both sides of the fracture site (on the mesial and distal regions), followed by the mesial side, and then the distal side.

Table 2. FEA outcomes of unilateral right mandibular body fracture fixation with 0.01 mm fracture reduction using 2.0 mm 4-hole versus 6-hole miniplate with various loose screw configurations.

	Mandibular Unilateral Body Fracture Fixation			
	2.0 mm 4-hole Miniplate		2.0 mm 6-hole Miniplate	
Screw Loosening*	Von-Mises Stress [MPa]	Displacement [mm]	Von-Mises Stress [MPa]	Displacement [mm]
None	558.86	1.75	459.01	1.68
Mesial side	1090.71	3.56	499.70	1.73
Distal side	1014.34	3.52	516.75	1.70
Both sides	1100.67	3.62	590.11	1.77

* Screw loosening refers to screws directly adjacent to the fracture site that hold the fracture fragment together: none (all screws remain intact in the mandible), mesial (on the mesial side of the fracture), distal (on the distal side of the fracture), and both (on both sides of fracture site).

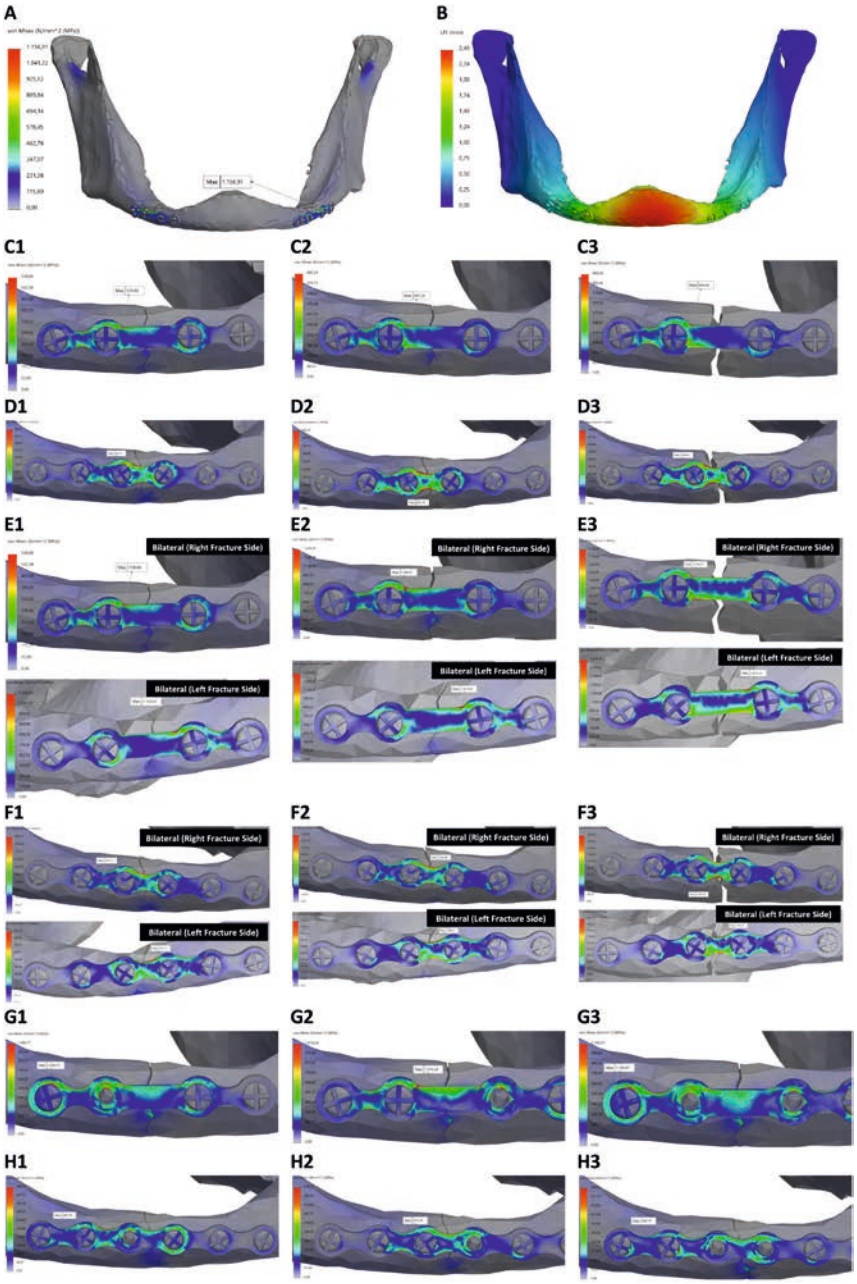

Fig. 3. General overview of Von-Mises stress (**A**) and displacement (**B**) distribution in the severe atrophic edentulous mandibular body fracture fixation (e.g., bilateral fracture case with 0.01 mm reduction fixated using two 2.0 mm 4-hole miniplates). (**C-F**) Magnified view of Von-Mises stress outcomes and fracture stability in the simulated cases. (**C-F**) Effect of fracture reduction with interfragmentary gap of 0.01, 0.1, and 1 mm (resp. **1-3**): (**C-D**) unilateral fracture, (**E-F**) bilateral fracture, (**C,E**) 2.0 mm 4-hole miniplate, and (**D-F**) 2.0 mm 6-hole miniplate fixation. (**G-H**) Effect of screw loosening directly adjacent to the fracture site (resp. **1-3**: on the mesial, distal, and both sides of fracture site): (**E**) 2.0 mm 4-hole miniplate, and (**F**) 2.0 mm 6-hole miniplate fixation.

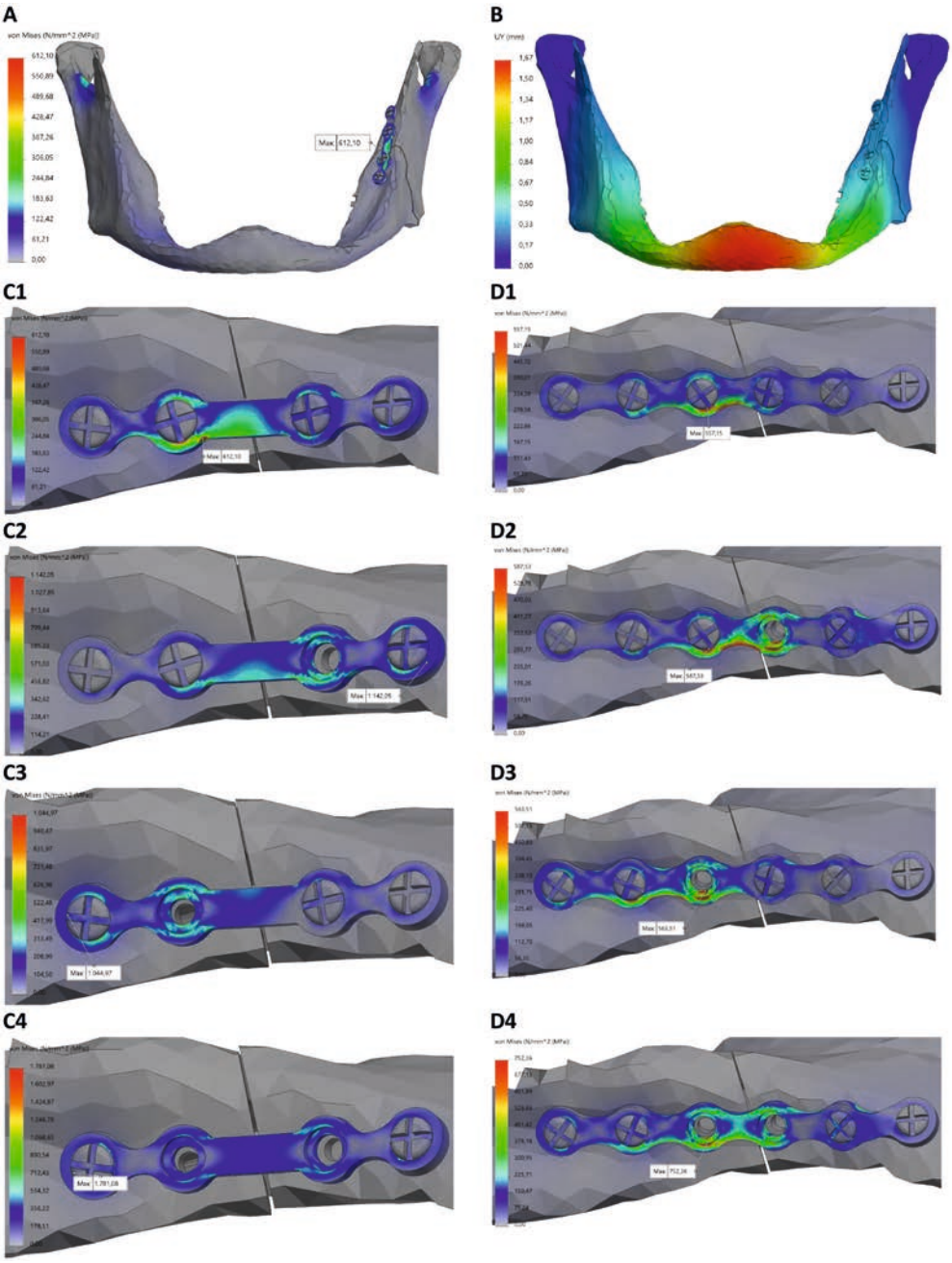

Fig. 4. General overview of Von-Mises stress (**A**) and displacement (**B**) distribution in the severe atrophic edentulous unilateral mandibular angle fracture fixation (e.g., fixated using two 2.0 mm 4-hole miniplates). (**C-D**) Magnified view of Von-Mises stress outcomes and fracture stability in the simulated cases, illustrating the influence of 2.0 mm 4-hole (**C**) versus 2.0 mm 6-hole miniplate, and the effect of screw loosening directly adjacent to the fracture site (**1**: none, **2**: on the mesial side, **3**: distal side, or **4**: both sides of the fracture site). Note: loosen screw causes visual misalignments.

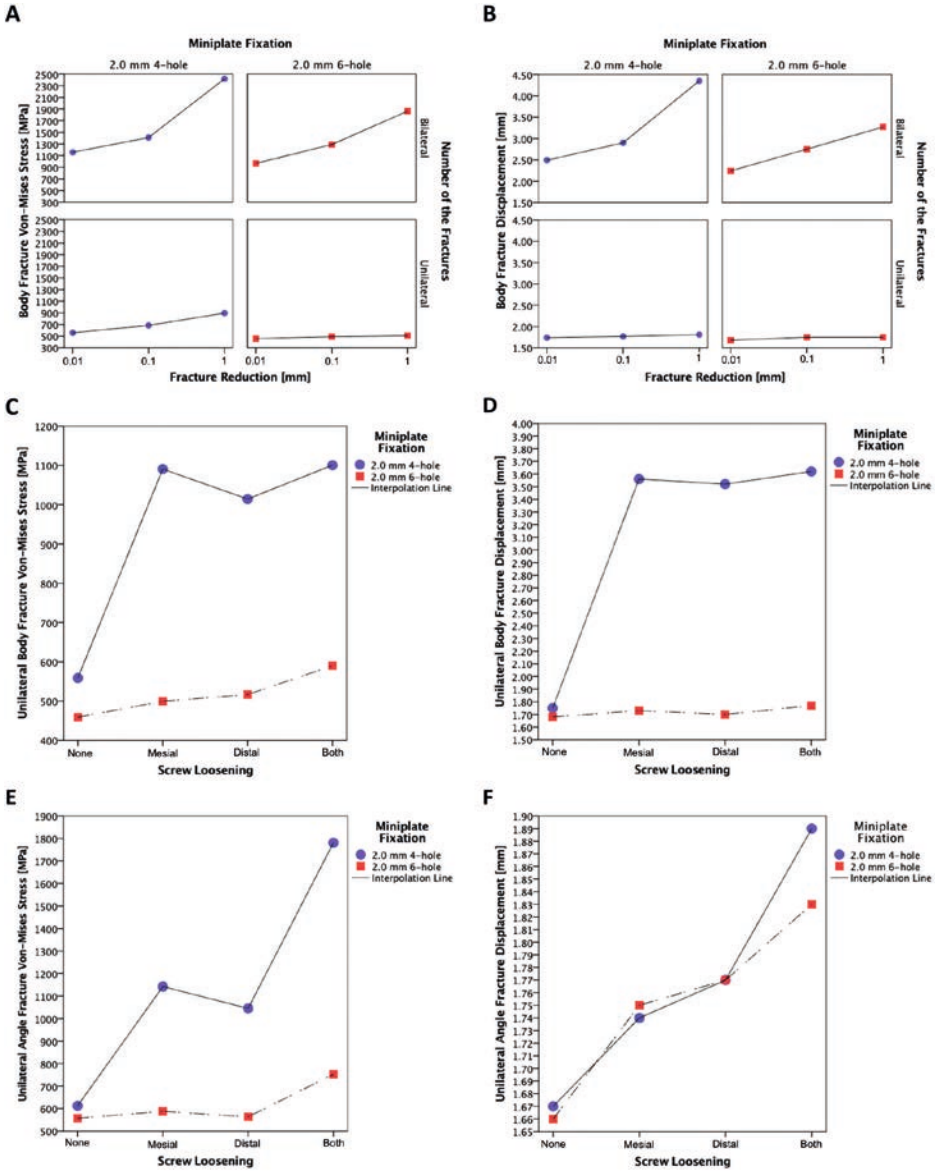

Fig. 5. Von-Mises stress (**A, C, E**) and displacement (**B, D, F**) outcomes of mandibular (**A-D**) body and (**E-F**) angle fractures. (**A-B**) Effect of fracture reduction precision and osteosynthesis miniplate type in the unilateral versus bilateral body fractures. (**C-E**) Influence of screw loosening directly adjacent to the fracture site and miniplate type in the unilateral body fracture (**C-D**) and in the unilateral angle fracture (**E-F**).
Color coding: represents the fixation method using 2.0 mm 4-hole (**blue**) versus 2.0 mm 6-hole (**red**) titanium miniplate.

Mandibular angle fracture

The effects of the osteosynthesis miniplate type and screw loosening were evaluated (Table 3, Fig. 4, and Fig. 5E-F) (Supplementary Fig. S6-S7). First, with respect to miniplate type,

the 6-hole miniplate demonstrates lower stress and displacement compared to the 4-hole miniplate system, resulting in a better fracture stability (Fig. 3C1-D1, Fig. 5E-F). Second, screw loosening directly adjacent to the fracture site leads to increased stress and displacement, thereby compromising fracture stability (Fig 3C2-D4, Fig. 5E-F). In all cases, the maximum stress and displacement were observed when both screws directly adjacent to the fracture line (mesial and distal) were loose, followed by single loose screw on the mesial side, and then on the distal side of the fracture line. The loose screw(s) causes movement of fracture segments, leading to fracture instability. This effect is the largest when both screws near the fracture site are loose for both fixation methods. Across all scenarios, the highest stress concentrations were consistently located on the miniplate.

Table 3. FEA outcomes of unilateral severe atrophic edentulous mandibular angle fracture fixation using 2.0 mm 4-hole versus 6-hole miniplates with various loose screw configurations.

	Mandibular Unilateral Angle Fracture Fixation			
	2.0 mm 4-hole Miniplate		2.0 mm 6-hole Miniplate	
	Von-Mises Stress	Displacement	Von-Mises Stress	Displacement
Screw Loosening*	[MPa]	[mm]	[MPa]	[mm]
None	612.10	1.67	557.15	1.66
Mesial side	1142.05	1.74	587.53	1.75
Distal side	1044.97	1.77	563.51	1.77
Both sides	1781.08	1.89	752.36	1.83

* Screw loosening refers to screws directly adjacent to the fracture site, holding the fracture fragment together: none (all screws intact in the mandible), mesial (on the mesial side of fracture), distal (on the distal side of the fracture), and both (on both sides of fracture site).

DISCUSSION

In our previous studies, we developed a validated FEA principle by simulating non-comminuted mandibular fractures, where the FEA model was authenticated by testing mandible replicas in a mechanical test bench under identical conditions as the FEA (Daqiq et al., 2024, 2025a). The aim of the present study was to apply the validated FEA model to investigate more clinically non-routine complex fractures. Therefore, fracture fixation in a severely atrophic edentulous mandible was simulated in the body and angle regions. In all studies, fracture stability was assessed in terms of stress and displacement along with illustrating the effect to the fracture fixation in the different simulated cases. The FEA setup was identical for all the simulations, including the applied load, condylar fixture region, mechanical material properties, and boundary conditions.

The study shows that our previously validated FEA model (Daqiq, 2025a) proved to be a suitable tool for in silico analysis of complex mandibular fractures, effectively simulating fracture fixation in a severely atrophic edentulous mandible (Table 1-3, Fig. 5). According

to the latest systematic review by Bera et al. (2023) on the management of unilateral and bilateral edentulous atrophic mandibular fractures, there is insufficient evidence to definitely recommend any specific treatment modality for this type of fractures (Bera & Tiwari, 2023). This challenge is further amplified in cases involving extremely atrophic mandibles, especially for the bilateral fractures which demand a more rigid fixation (Bera & Tiwari, 2023). The existing literature highlights considerable uncertainties regarding the optimal fixation of such fractures, making their management a complex task, even for experienced surgeons (Bera & Tiwari, 2023; Ellis & Price, 2008; Emam et al., 2018; Madsen et al., 2008; Mugino et al., 2005). Additionally, the literature suggests that the clinical decision-making should be based on surgeons past experience and the extent of bone resorption in the edentulous mandible, with particular consideration given to the location of fracture subsites (Brucoli et al., 2020; Ellis & Price, 2008; Madsen et al., 2008). Nonetheless, there remains a lack of consensus on the ideal surgical approach and the preferred plating system, largely attributed to reduced bone quantity and inadequate bone quality as well as limited bone to bone contact at the fracture site (Bera & Tiwari, 2023; Brucoli et al., 2020; Castro-Núñez et al., 2017; Mugino et al., 2005; Novelli et al., 2012; Wittwer et al., 2006). Furthermore, numerous studies suggest that both the positioning of osteosynthesis and the choice of plating technique significantly influence the stability of mandibular atrophic fracture (Choi et al., 2005; Chrcanovic, 2013; Kahveci & Ayranci, 2023; Mugino et al., 2005; Novelli et al., 2012; Sugiura et al., 2009). Additionally, while the fixation of an unilateral atrophic fracture can be challenging (Bera & Tiwari, 2023; Brucoli et al., 2020; Gerbino et al., 2018; Melo et al., 2011), it becomes more complex in bilateral cases (Benech et al., 2013; Bera & Tiwari, 2023; Gerbino et al., 2018; Melo et al., 2011; Roccia et al., 2024). Therefore, the in silico methodology used in the study allows to effectively assess these fractures, as studying them in the clinical settings remains challenging.

The following findings were observed regrading mandibular body fracture fixation (Table 1 and 2, Fig. 3, Fig. 5A-D). First, bilateral fracture fixation generates higher stress and displacement compared to unilateral fracture. This endorses the clinical complexity of bilateral fracture treatment and suggest that bilateral fractures may require a stronger or more rigid fixation to ensure adequate stability (Fig. 5A-B). Second, the 6-hole miniplate proves superior compared to the 4-hole miniplate, exhibiting lower stress and displacement (Fig. 5A-B); however, stronger reconstruction plates were not applied in the current simulation. Nevertheless, the study shows that, even in a severely atrophic edentulous mandible a small miniplate might by clinically acceptable in cases of a unilateral fracture (Fig. 3C1). Third, the precision of fracture reduction has a major impact on the fixation stability (Fig. 3C-F, Fig. 5A-B). Fracture reduction was most optimal at a 0.01 mm interfragmentary gap, with minimal displacement observed between fracture surfaces. A 0.1 mm gap exhibited slight displacement, indicating reduced but still acceptable stability. In contrast, a 1 mm gap resulted in the least stability, with pronounced displacement or misalignment of the fracture fragments. This indicates the critical importance of achieving perfect fracture reduction to ensure interfragmentary stability and to promote optimal bone healing, even in

resorbed mandibles with a small fracture contact area. Although we currently do not know what fracture distance can be achieved clinically with careful reduction, this study shows that it is worthwhile for the clinician to put effort and time in the reduction of the fracture, to favour treatment outcome. Fourth, screw loosening directly adjacent to the fracture site reduces fixation stability, resulting in increased stress and displacement (Table 2, Fig. 5B-C). In both 4-hole and 6-hole miniplates, maximum instability was observed when both screws directly adjacent to the fracture site were removed, followed by the distal side screw, and then the mesial side screw. Notably, the effect of screw detachment is much more prominent in the 4-hole miniplate (Fig. 3G) compared to the 6-hole miniplate (Fig. 3H). This may suggest that one should use a 6-hole miniplate instead of 4-hole miniplate, to ensure maximum fracture stability in case of possible screw loosening, especially in cases when the surgeon questions the bone quality or the compliance of the patient.

The following outcomes were observed in the fixation of unilateral mandibular angle fracture (Table 3, Fig. 4, Fig. 5E-F). First, a superiorly positioned 6-hole miniplate (Fig. 4D1) provides greater fracture stability compared to a 4-hole miniplate (Fig. 4C1), as evident by reduced stress distribution and displacement (Fig. 5E-F). This indicates that the 6-hole miniplate method can offers more stability in comparison to the 4-hole plating; however, the differences in peak stress and displacement between these two plating systems (respectively 54.94 MPa, and 0.01 mm) were relatively marginal, and probably not clinically relevant. This suggests that the use of a 4-hole miniplate may be still sufficient for the treatment of unilateral angle fractures, as is also advocated by the textbook of Haerle et al. (Haerle et al., 2009). Second, in case of screw loosening (Fig. 5E-F), if the 4-hole plate is used, this study shows that the stress on the rest of the screws increases directly. In contrast, one loose screw in the 6-hole plate configuration has only limited effects. For both miniplate systems (Fig. 4C2-D4), the least stability was observed when both screws directly adjacent to the fracture site were loose, followed by mesial screw, and then the distal screw. This might suggest that it is wise to use a 6-hole miniplate instead of a 4-hole miniplate to ensure optimal stability when the risk of screw loosening is high.

These findings illustrates that the in silico simulations using the validated FEA model provides new fresh insights into the treatment of the severe atrophic edentulous mandibular fracture fixation, as the study comprehensively assessed the influence of various critical factors that may affect fracture stability in both mandibular body and angle fractures. This makes this study essential and clinically relevant as the validated FEA can easily simulate the biomechanical behaviour of these fractures. Future studies are encouraged to extend the application of this FEA model to other atrophic mandibular fracture cases and other complex mandibular fractures (e.g., comminuted, or wedge fractures) as well as assessing the fixation strategies (e.g., 3D printed patient specific implants). Such investigations would further confirm the model's applicability in analysing non-routine complex fractures in the clinical setting.

The following limitations were observed. First, Solidworks was used for 3D modelling and FEA simulations, whereas other software's may be more suitable for complex FEA models (e.g., Abaqus, Ansys, or Comsol). Second, the FEA model used (linear) static analysis, in which a time-invariant load was applied to the 3D model, resulting in a linear relationship between load and induced responses. However, the biomechanical behaviour of the fixation may differ under dynamic cyclic loading conditions (e.g., during mastication), potentially increasing risk of complications (e.g., screw loosening). Therefore, in a clinical context, dynamic simulations may provide a more realistic representation of the cyclic nature of masticatory forces (Dicker et al., 2012; Djebbar et al., 2015; Kayabaşı et al., 2006; Kuntamukkula et al., 2018; Lanyon & Rubin, 1984; Tams et al., 1997, 1996). Third, the 3D digital twin mandible model only included the cortical bone segment, with the trabecular bone represented as cavity. The elastic modulus of cortical segments is much higher compared to trabecular bone segments (at least a factor 100) (Daqiq et al., 2025b), therefore one expects that the effect of the trabecular bone part is negligible. In addition, the severely resorbed mandible is nearly totally cortical, so in this study the presence of trabecular bone is of limited influence. However, incorporating the trabecular component in future simulations, especially in less resorbed cases, could provide a more comprehensive understanding of its biomechanical contribution. Fourth, the mandible material properties were added as linear elastic isotropic. This leads to disabling the tensile and yield strength in the simulations which leads to neglecting plastic deformations. This resulted the simulation to be conducted using the small strain assumption with the strain tensor being linearized, where the nonlinear coupling between the stretches and rotations could be ignored. Perhaps, in follow up studies, this effect can be further evaluated. Additionally, we acknowledge that for studying the occurrence of fractures one has to incorporate plastic deformation in the model. However, we studied fracture fixations stability, which can only occur if in both mandible and osteosynthesis the stresses are well below the respective yield stresses. If it would exceed the yield strength, the fixation configuration must be considered mechanically inadequate and consequently rejected. Fifth, the boundary conditions between the components were set in accordance with the non-locking compression plating system (Bohner et al., 2020; Braasch & Abubaker, 2013; Daqiq et al., 2024, 2025a; Madsen et al., 2008; Raut et al., 2017). A frictionless contact condition was used between the fracture surfaces, osteosynthesis parts (miniplate and screws), and between the miniplate and the mandible (Fig. 1E-G). This means upon a load application; only normal forces could be exchanged between the component surfaces. Additionally, a bonded interaction was set between the screws and the mandible screw holes (Fig. 1H), although a friction interaction may play a role. However, it would be impossible to measure this in the clinical setting; therefore, the defined boundary conditions are justifiable. Sixth, to say whether the FEA outcomes were fully valid, one might suggest performing a series of mechanical tests to authenticate it. However, since the study used an already validated FEA model, we can assume that the outcomes are correct as they are consistent with the current clinical understanding of the fracture management (Ehrnfeld et al., 2012; Haerle et al., 2009). Finally, the simulated cases were based on the commonly asked questions by the experienced CMF surgeons

regarding the fixation of severely atrophic edentulous mandibular fractures. Naturally, there are many other fractures, fixation systems, and factors that can be assessed in future studies (e.g., evaluating different degree of screw loosening due to micromotion caused by displacements due to mastication (Kohli et al., 2021)).

In conclusion, this study shows that the previously validated FEA model is an effective tool for evaluating fixation of mandibles. The applied FEA principle can accurately simulate the biomechanical behaviour of severe atrophic edentulous mandibular fracture treatment with osteosynthesis and gives new insights in the factors that may influence the fixation stability in the clinical setting. Fixation stability in severely atrophic edentulous mandibular fractures is critically influenced by factors examined in this study, including the number of fractures, the precision of fracture reduction, the type of miniplate, and the potential for screw loosening. FEA studies have demonstrated in how much these variables play a role in achieving optimal treatment outcomes and should therefore be carefully considered during clinical decision-making. Furthermore, as the FEA model can be used for in silico analysis of these fractures, it can also be applied to other complex mandibular fracture simulations. In future studies, it is recommended to use the FEA model to further investigate atrophic mandibles with other fractures (e.g., angle fractures combined with parasymphysis fractures, or different fracture patterns) or other fixation systems (e.g., stronger reconstruction plates). Additionally, studying other complex mandibular fractures (e.g., comminuted or wedge) and fixation methods (e.g., 3D printed patient specific implants versus conventional osteosynthesis).

REFERENCES

Adamović, P., Matoc, L., Knežević, P., Sabalić, S., & Kodvanj, J. (2023). Biomechanical analysis of a novel screw system with a variable locking angle in mandible angle fractures. *Medical & Biological Engineering & Computing*, *61*(11), 2951–2961. https://doi.org/10.1007/s11517-023-02895-y

Aftabi, H., Zaraska, K., Eghbal, A., McGregor, S., Prisman, E., Hodgson, A., & Fels, S. (2024). Computational models and their applications in biomechanical analysis of mandibular reconstruction surgery. *Computers in Biology and Medicine*, *169*, 107887. https://doi.org/10.1016/j.compbiomed.2023.107887

Ahmed, S., Rehman, S., Ansari, M., Khan, A., Farooq, O., & Khan, A. (2016). A comparative study on evaluation of role of 1.5 mm microplates and 2.0 mm standard miniplates in management of mandibular fractures using bite force as indicator of recommendation. *National Journal of Maxillofacial Surgery*, *7*(1), 39. https://doi.org/10.4103/0975-5950.196128

Altuncu, F., Kazan, D., & Özden, B. (2020). Comperative evaluation of the current and new design miniplate fixation techniques of the advanced sagittal split ramus osteotomy using three-dimensional finite element analysis. *Medicina Oral Patología Oral y Cirugia Bucal*, *28*(6), 0–0. https://doi.org/10.4317/medoral.25964

Anthrayose, P., Nawal, R. R., Yadav, S., Talwar, S., & Yadav, S. (2021). Effect of revascularisation and apexification procedures on biomechanical behaviour of immature maxillary central incisor teeth: a three-dimensional finite element analysis study. *Clinical Oral Investigations*, *25*(12), 6671–6679. https://doi.org/10.1007/s00784-021-03953-1

Benech, A., Nicolotti, M., Brucoli, M., & Arcuri, F. (2013). Intraoral extra-mucosal fixation of fractures in the atrophic edentulous mandible. *International Journal of Oral and Maxillofacial Surgery*, *42*(4), 460–463. https://doi.org/10.1016/j.ijom.2012.11.013

Bera, R. N., & Tiwari, P. (2023). Current Evidence for the Management of Edentulous Atrophic Mandible Fractures: A PRISMA-SWiM Guided Review. *Craniomaxillofacial Trauma & Reconstruction*, *16*(4), 317–332. https://doi.org/10.1177/19433875221115585

Bohner, L., Beiglboeck, F., Schwipper, S., Lustosa, R. M., Segura, C. P. M., Kleinheinz, J., & Jung, S. (2020). Treatment of mandible fractures using a miniplate system: A retrospective analysis. *Journal of Clinical Medicine*, *9*(9), 1–8. https://doi.org/10.3390/jcm9092922

Braasch, D. C., & Abubaker, A. O. (2013). Management of Mandibular Angle Fracture. *Oral and Maxillofacial Surgery Clinics of North America*, *25*(4), 591–600. https://doi.org/10.1016/j.coms.2013.07.007

Brucoli, M., Boffano, P., Romeo, I., Corio, C., Benech, A., Ruslin, M., … Starch-Jensen, T. (2020). Surgical management of unilateral body fractures of the edentulous atrophic mandible. *Oral and Maxillofacial Surgery*, *24*(1), 65–71. https://doi.org/10.1007/s10006-019-00824-8

Castro-Núñez, J., Cunningham, L. L., & Van Sickels, J. E. (2017). A historical perspective with current opinion on the management of atrophic mandibular fractures. *Oral Surgery, Oral Medicine, Oral Pathology and Oral Radiology*, *124*(6), e276–e282. https://doi.org/10.1016/j.oooo.2017.09.007

Choi, B.-H., Huh, J.-Y., Suh, C.-H., & Kim, K.-N. (2005). An in vitro evaluation of miniplate fixation techniques for fractures of the atrophic edentulous mandible. *International Journal of Oral and Maxillofacial Surgery*, *34*(2), 174–177. https://doi.org/10.1016/j.ijom.2003.10.024

Chrcanovic, B. R. (2013). Fixation of mandibular angle fractures: in vitro biomechanical assessments and computer-based studies. *Oral and Maxillofacial Surgery*, *17*(4), 251–268. https://doi.org/10.1007/s10006-012-0367-0

Daqiq, O., Gareb, B., Spijkervet, F. K. L., Wubs, F. W., Roossien, C. C., & van Minnen, B. (2025b). Finite element analysis of the human mandible: a systematic review with meta-analysis of the essential input parameters. *Scientific Reports*, *15*(1), 19582. https://doi.org/10.1038/s41598-025-03959-9

Daqiq, O., Roossien, C. C., Wubs, F. W., Bos, R. R. M., & van Minnen, B. (2023). Optimisation of osteosynthesis positioning in mandibular body fracture management using finite element analysis. *European Journal of Translational and Clinical Medicine*, *6*(2), 10–25. https://doi.org/10.31373/ejtcm/163427

Daqiq, O., Roossien, C. C., Wubs, F. W., & van Minnen, B. (2024). Biomechanical assessment of mandibular fracture fixation using finite element analysis validated by polymeric mandible mechanical testing. *Scientific Reports*, *14*(1), 11795. https://doi.org/10.1038/s41598-024-62011-4

Daqiq, O., van Minnen, B., Spijkervet, F. K. L., Wubs, F. W., Lunter, G., & Roossien, C. C. (2025a). Finite element analysis of mandibular fracture fixation authenticated by 3D printed mandible mechanical testing. *Scientific Reports*, *15*(1), 14655. https://doi.org/10.1038/s41598-025-98732-3

Dario, V., Michelangelo-Santo, G., Roberto, B., & Fabio, F. (2023). Is All-on-four effective in case of partial mandibular resection? A 3D finite element study. *Journal of Stomatology, Oral and Maxillofacial Surgery*, *124*(5), 101463. https://doi.org/10.1016/j.jormas.2023.101463

Dicker, G. J., Tuijt, M., Koolstra, J. H., Van Schijndel, R. A., Castelijns, J. A., & Tuinzing, D. B. (2012). Static and dynamic loading of mandibular condyles and their positional changes after bilateral sagittal split advancement osteotomies. *International Journal of Oral and Maxillofacial Surgery*, *41*(9), 1131–1136. https://doi.org/10.1016/j.ijom.2012.03.013

Djebbar, N., Serier, B., & Bouiadjra, B. B. (2015). Finite element analysis in static and dynamic behaviors of dental prosthesis. *Structural Engineering and Mechanics*, *55*(1), 65–78. https://doi.org/10.12989/sem.2015.55.1.065

Ehrnfeld, M., Manson, P., & Perin, J. (2012). *Principles of Internal Fixation of the Craniomaxillofacial Skeleton: Trauma and Orthogenetic Surgery* (1st ed.). Georg Thieme Verlag. Retrieved from https://www.aofoundation.org/cmf/clinical-library-and-tools/aocmf-manuals

Ellis, E., & Price, C. (2008). Treatment Protocol for Fractures of the Atrophic Mandible. *Journal of Oral and Maxillofacial Surgery*, *66*(3), 421–435. https://doi.org/10.1016/j.joms.2007.08.042

Emam, H. A., Ferguson, H. W., & Jatana, C. A. (2018). Management of atrophic mandible fractures: an updated comprehensive review. *Oral Surgery*, *11*(1), 79–87. https://doi.org/10.1111/ors.12300

Falcinelli, C., Valente, F., Vasta, M., & Traini, T. (2023). Finite element analysis in implant dentistry: State of the art and future directions. *Dental Materials : Official Publication of the Academy of Dental Materials*, *39*(6), 539–556. https://doi.org/10.1016/j.dental.2023.04.002

Gareb, B., Roossien, C. C., van Bakelen, N. B., Verkerke, G. J., Vissink, A., Bos, R. R. M., & van Minnen, B. (2020). Comparison of the mechanical properties of biodegradable and titanium osteosynthesis systems used in oral and maxillofacial surgery. *Scientific Reports*, *10*(1), 18143. https://doi.org/10.1038/s41598-020-75299-9

Gerbino, G., Cocis, S., Roccia, F., Novelli, G., Canzi, G., & Sozzi, D. (2018). Management of atrophic mandibular fractures: An Italian multicentric retrospective study. *Journal of Cranio-Maxillofacial Surgery*, *46*(12), 2176–2181. https://doi.org/10.1016/j.jcms.2018.09.020

Gupta, A., Dutta, A., Dutta, K., & Mukherjee, K. (2023). Biomechanical influence of plate configurations on mandible subcondylar fracture fixation: a finite element study. *Medical and Biological Engineering and Computing*, *61*(10), 2581–2591. https://doi.org/10.1007/s11517-023-02854-7

Haerle, F., Champy, M., & Terry, B. C. (2009). *Atlas of Craniomaxillofacial Osteosynthesis*. (F. Haerle, M. Champy, B. C. Terry, & A. Reinhardt, Eds.) (Second). Stuttgart: Georg Thieme Verlag. https://doi.org/10.1055/b-002-72255

Kahveci, K., & Ayranci, F. (2023). Finite element analysis of different internal fixation methods for the treatment of atrophic mandible fractures. *Journal of Stomatology, Oral and Maxillofacial Surgery*, *124*(1), 101276. https://doi.org/10.1016/j.jormas.2022.08.019

Kayabaşı, O., Yüzbasıoğlu, E., & Erzincanlı, F. (2006). Static, dynamic and fatigue behaviors of dental implant using finite element method. *Advances in Engineering Software*, *37*(10), 649–658. https://doi.org/10.1016/j.advengsoft.2006.02.004

Kohli, N., Stoddart, J. C., & van Arkel, R. J. (2021). The limit of tolerable micromotion for implant osseointegration: a systematic review. *Scientific Reports*, *11*(1), 10797. https://doi.org/10.1038/s41598-021-90142-5

Kshirsagar, R., Jaggi, N., & Halli, R. (2011). Bite Force Measurement in Mandibular Parasymphyseal Fractures: A Preliminary Clinical Study. *Craniomaxillofacial Trauma & Reconstruction*, *4*(4), 241–244. https://doi.org/10.1055/s-0031-1293521

Kuntamukkula, S., Sinha, R., Tiwari, P. K., & Paul, D. (2018). Dynamic Stability Assessment of the Temporomandibular Joint as a Sequela of Open Reduction and Internal Fixation of Unilateral Condylar Fracture. *Journal of Oral and Maxillofacial Surgery*, *76*(12), 2598–2609. https://doi.org/10.1016/j.joms.2018.06.014

Lanyon, L. E., & Rubin, C. T. (1984). Static vs dynamic loads as an influence on bone remodelling. *Journal of Biomechanics*, *17*(12), 897–905. https://doi.org/10.1016/0021-9290(84)90003-4

Lisiak-Myszke, M., Marciniak, D., Bieliński, M., Sobczak, H., Garbacewicz, Ł., & Drogoszewska, B. (2020). Application of Finite Element Analysis in Oral and Maxillofacial Surgery—A Literature Review. *Materials*, *13*(14), 3063. https://doi.org/10.3390/ma13143063

Luhr, H.-G., Reidick, T., & Merten, H.-A. (1996). Results of treatment of fractures of the atrophic edentulous mandible by compression plating: A retrospective evaluation of 84 consecutive cases. *Journal of Oral and Maxillofacial Surgery*, *54*(3), 250–254. https://doi.org/10.1016/S0278-2391(96)90733-8

Madsen, M. J., McDaniel, C. A., & Haug, R. H. (2008). A Biomechanical Evaluation of Plating Techniques Used for Reconstructing Mandibular Symphysis/Parasymphysis Fractures. *Journal of Oral and Maxillofacial Surgery*, *66*(10), 2012–2019. https://doi.org/10.1016/j.joms.2008.06.013

Maintz, M., Msallem, B., de Wild, M., Seiler, D., Herrmann, S., Feiler, S., … Thieringer, F. M. (2023). Parameter optimization in a finite element mandibular fracture fixation model using the design of experiments approach. *Journal of the Mechanical Behavior of Biomedical Materials*, *144*, 105948. https://doi.org/10.1016/j.jmbbm.2023.105948

Melo, A. R., de Aguiar Soares Carneiro, S. C., Leal, J. L. F., & Vasconcelos, B. C. do E. (2011). Fracture of the Atrophic Mandible: Case Series and Critical Review. *Journal of Oral and Maxillofacial Surgery*, *69*(5), 1430–1435. https://doi.org/10.1016/j.joms.2010.05.078

Mugino, H., Takagi, S., Oya, R., Nakamura, S., & Ikemura, K. (2005). Miniplate osteosynthesis of fractures of the edentulous mandible. *Clinical Oral Investigations*, *9*(4), 266–270. https://doi.org/10.1007/s00784-005-0012-5

Novelli, G., Sconza, C., Ardito, E., & Bozzetti, A. (2012). Surgical Treatment of the Atrophic Mandibular Fractures by Locked Plates Systems: Our Experience and a Literature Review. *Craniomaxillofacial Trauma & Reconstruction*, *5*(2), 65–74. https://doi.org/10.1055/s-0031-1300961

Park, B., Jung, B. T., Kim, W. H., Lee, J.-H., Kim, B., & Lee, J.-H. (2020). The Stability of Hydroxyapatite/Poly-L-Lactide Fixation for Unilateral Angle Fracture of the Mandible Assessed Using a Finite Element Analysis Model. *Materials*, *13*(1), 228. https://doi.org/10.3390/ma13010228

Patil, P. G., Seow, L. L., Uddanwadikar, R., Pau, A., & Ukey, P. D. (2024). Different implant diameters and their effect on stress distribution pattern in 2-implant mandibular overdentures: A 3D finite element analysis study. *The Journal of Prosthetic Dentistry*, *131*(4), 675–682. https://doi.org/10.1016/j.prosdent.2022.04.018

Raut, R., Keerthi, R., Vaibhav, N., Ghosh, A., & Kamath Kateel, S. (2017). Single Miniplate Fixation for Mandibular Symphysis and Parasymphysis Fracture as a Viable Alternative to Conventional Plating Based on Champy's Principles: A Prospective Comparative Clinical Study. *Journal of Maxillofacial and Oral Surgery*, *16*(1), 113–117. https://doi.org/10.1007/s12663-016-0919-1

Roccia, F., Cena, P., Cremona, G., Garzino Demo, P., & Sobrero, F. (2024). Characteristics and Surgical Management of Bilateral Body Mandibular Fractures: A 23-Year Experience. *Journal of Clinical Medicine*, *14*(1), 160. https://doi.org/10.3390/jcm14010160

Ruf, P., Orassi, V., Fischer, H., Steffen, C., Kreutzer, K., Duda, G. N., … Rendenbach, C. (2024). Biomechanical evaluation of CAD/CAM magnesium miniplates as a fixation strategy for the treatment of segmental mandibular reconstruction with a fibula free flap. *Computers in Biology and Medicine*, *168*, 107817. https://doi.org/10.1016/j.compbiomed.2023.107817

Sancar, B., Çetiner, Y., & Dayı, E. (2023). Evaluation of the pattern of fracture formation from trauma to the human mandible with finite element analysis. Part 2: The corpus and the angle regions. *Dental Traumatology*, *39*(5), 437–447. https://doi.org/10.1111/edt.12841

Schönegg, D., Koch, A., Müller, G. T., Blumer, M., & Wagner, M. E. H. (2024). Two-screw osteosynthesis of the mandibular condylar head with different screw materials: a finite element analysis. *Computer Methods in Biomechanics and Biomedical Engineering*, *27*(7), 878–882. https://doi.org/10.1080/10255842.2023.2209247

Schwartz-Dabney, C. L., & Dechow, P. C. (2003). Variations in cortical material properties throughout the human dentate mandible. *American Journal of Physical Anthropology*, *120*(3), 252–277. https://doi.org/10.1002/ajpa.10121

Sugiura, T., Yamamoto, K., Murakami, K., Kawakami, M., Kang, Y. B., Tsutsumi, S., & Kirita, T. (2009). Biomechanical Analysis of Miniplate Osteosynthesis for Fractures of the Atrophic Mandible. *Journal of Oral and Maxillofacial Surgery*, *67*(11), 2397–2403. https://doi.org/10.1016/j.joms.2008.08.042

Tams, J., van Loon, J.-P., Otten, E., Rozema, F. R., & Bos, R. R. M. (1997). A three-dimensional study of bending and torsion moments for different fracture sites in the mandible: an in vitro study. *International Journal of Oral and Maxillofacial Surgery*, *26*(5), 383–388. https://doi.org/10.1016/S0901-5027(97)80803-X

Tams, J., van Loon, J.-P., Rozema, F. R., Otten, E., & Bos, P. R. M. (1996). A three-dimensional study of loads across the fracture for different fracture sites of the mandible. *British Journal of Oral and Maxillofacial Surgery*, *34*(5), 400–405. https://doi.org/10.1016/S0266-4356(96)90095-9

Vajgel, A., Camargo, I. B., Willmersdorf, R. B., de Melo, T. M., Filho, J. R. L., & de Holanda Vasconcellos, R. J. (2013). Comparative Finite Element Analysis of the Biomechanical Stability of 2.0 Fixation Plates in Atrophic Mandibular Fractures. *Journal of Oral and Maxillofacial Surgery*, *71*(2), 335–342. https://doi.org/10.1016/j.joms.2012.09.019

Wittwer, G., Adeyemo, W. L., Turhani, D., & Ploder, O. (2006). Treatment of Atrophic Mandibular Fractures Based on the Degree of Atrophy—Experience With Different Plating Systems: A Retrospective Study. *Journal of Oral and Maxillofacial Surgery*, *64*(2), 230–234. https://doi.org/10.1016/j.joms.2005.10.025

Xue, R., Lai, Q., Xing, H., Zhong, C., Zhao, Y., Zhu, K., … Liu, C. (2024). Finite element analysis and clinical application of 3D-printed Ti alloy implant for the reconstruction of mandibular defects. *BMC Oral Health*, *24*(1). https://doi.org/10.1186/s12903-024-03857-y

DECLARATIONS

Acknowledgment
None.

Author contribution
O.D. conducted the study design, 3D modelling, FEA computer studies, data analysis, and wrote the manuscript. F.K.L.S, F.W.W., C.C.R, and B.v.M. were responsible for supervision, helping with data analysis, and providing guidance. The authors approve the manuscript.

Conflict of interest
The authors declare that they have no conflict of interest.

Funding
None.

Ethical approval
Not applicable. This study does not contain any procedure with human participants or animals performed by any of the authors. All applicable international, national, and/or institutional guidelines were followed.

Informed consent
Not applicable. For this type of study, formal consent is not required.

Data availability
All data are available from corresponding author upon reasonable request.

SUPPLEMENTARY DATA

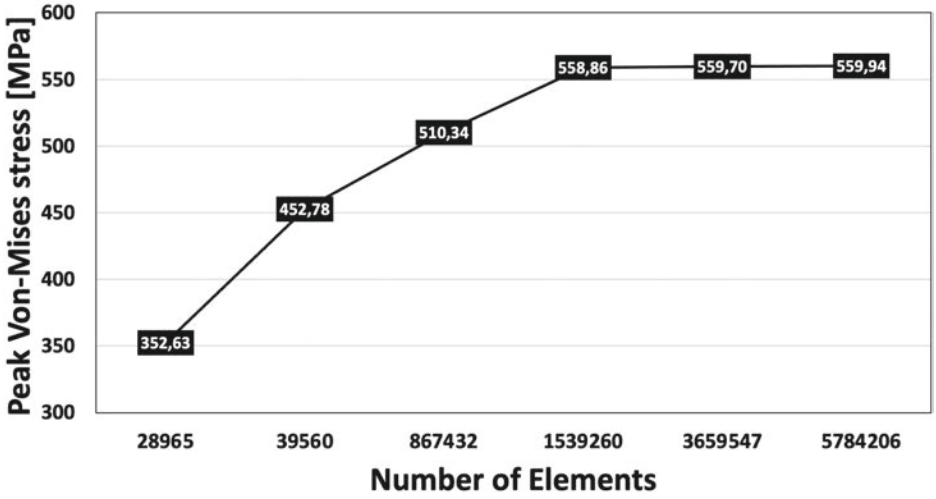

Supplementary Fig. S1. Mesh convergence plot with the X-coordinate representing the number of mesh elements and Y-coordinate representing the peak Von-Mises stress [MPa]. The used mesh has a minimum element size of 0.1 mm and a maximum element size of 5 mm. The mesh resulted in an average computation time of 30 minutes per simulation run, using a 12th Gen(R) Intel Core(TM) i9-12950HX CPU @ 2.30 GHz processor with 32 GB of RAM.

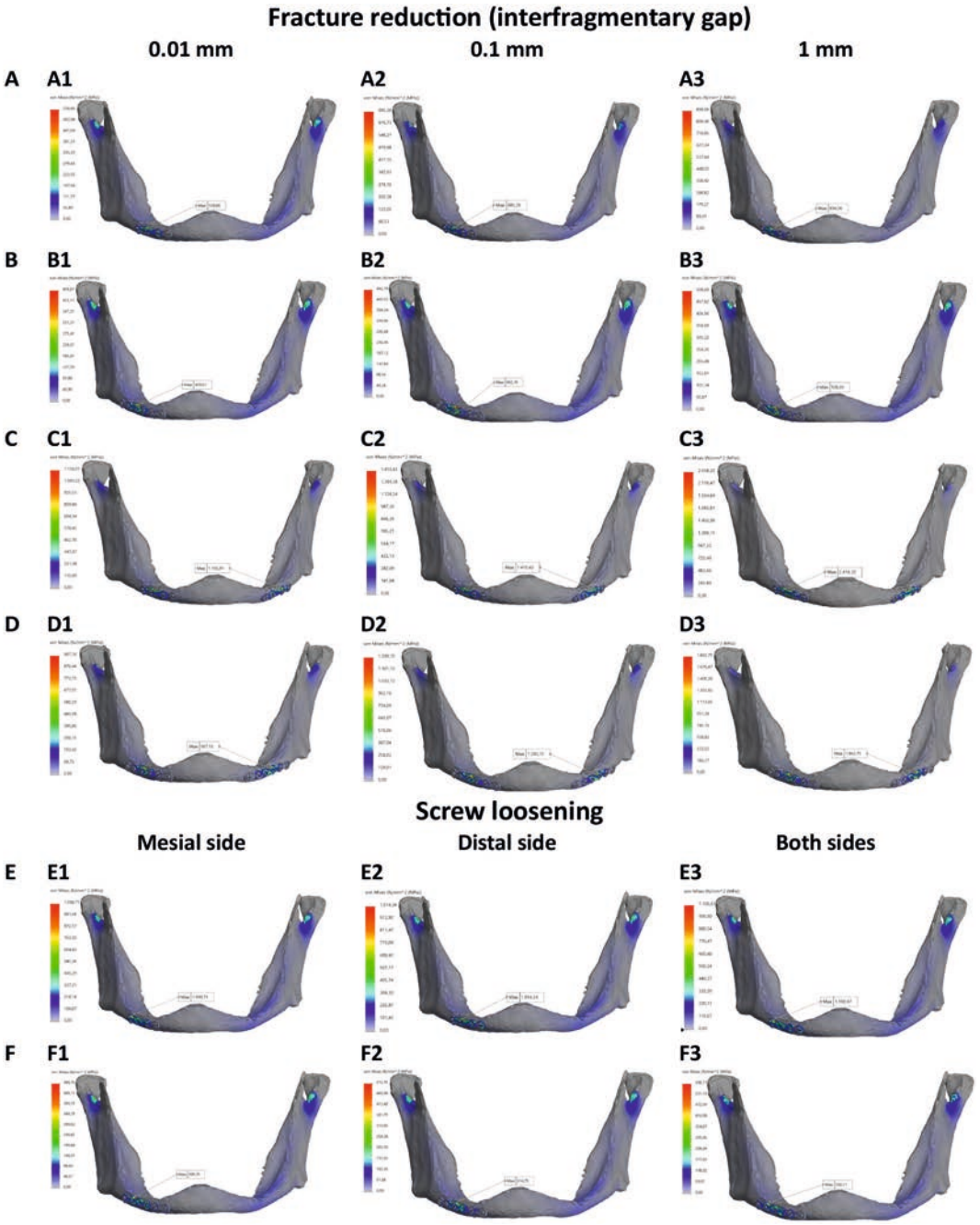

Supplementary Fig. S2. Von-Mises stress of severe atrophic edentulous mandibular body fracture fixation. (**A-D**) Effect of fracture reduction (respectively **1 to 3** for fracture distance of 0.01, 0.1, and 1 mm): (**A-B**) unilateral fracture, (**C-D**) bilateral fracture, (**A,C**) 2.0 mm 4-hole miniplate, and (**B,D**) 2.0 mm 6-hole miniplate fixation. (**E-F**) Effect of loose screws (respectively **1 to 3** illustrating the lose screw on the mesial side, distal side, and both sides of fracture site): (**E**) 2.0 mm 4-hole miniplate, and (**F**) 2.0 mm 6-hole miniplate fixation.

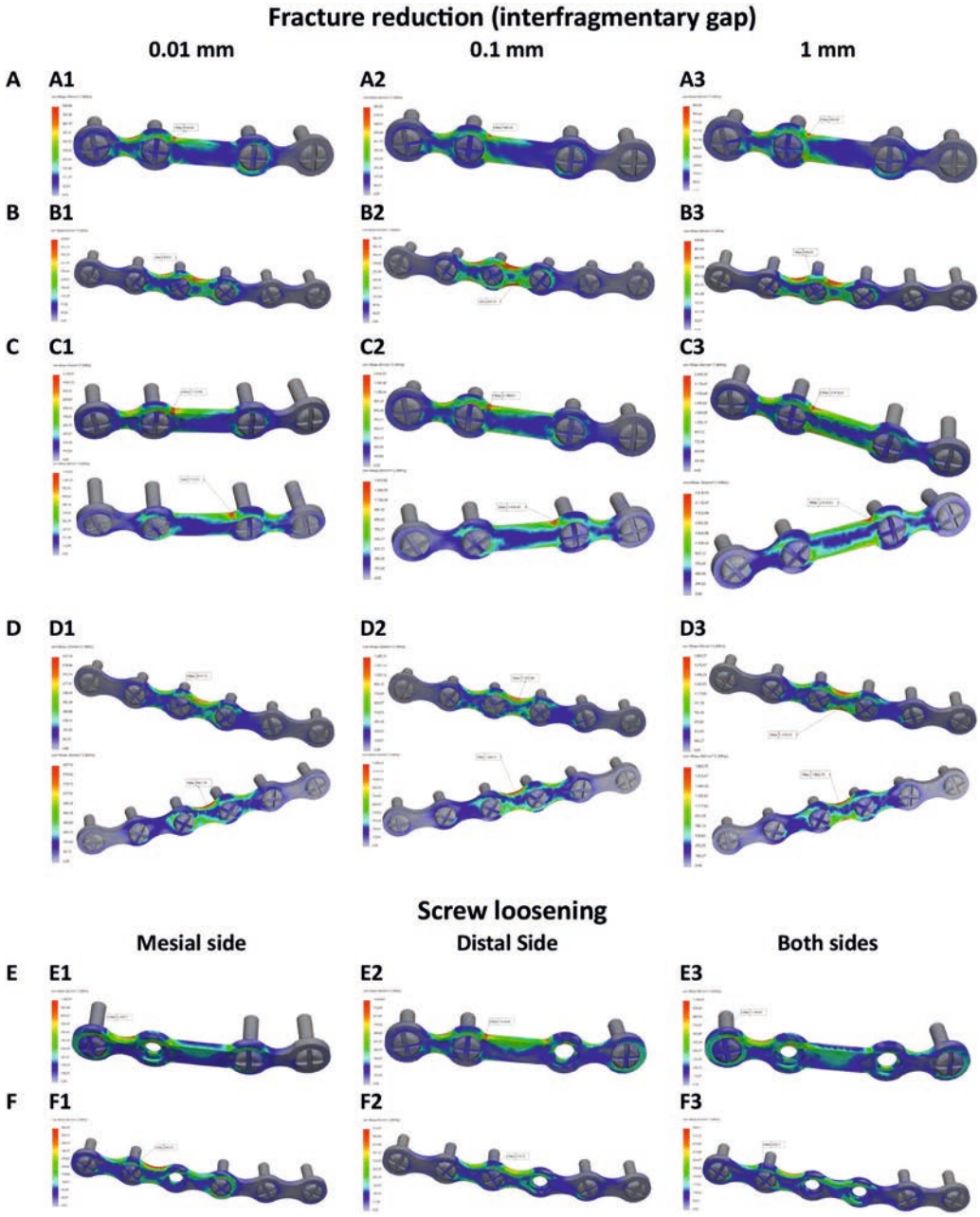

Supplementary Fig. S3. Front view of the stress distribution on the miniplate used for fixation of the severe atrophic edentulous mandibular body fracture. (**A-D**) Effect of fracture reduction (respectively **1 to 3** for fracture distance of 0.01, 0.1, and 1 mm): (**A-B**) unilateral fractures, (**C-D**) bilateral fractures (upper figure: right side fracture miniplate, lower figure: left side fracture miniplate), (**A,C**) 2.0 mm 4-hole miniplate, and (**B,D**) 2.0 mm 6-hole miniplate fixation. (**E-F**) Effect of lose screws (respectively **1 to 3** illustrating the lose screw on the mesial side, distal sides, or both sides of fracture site): (**E**) 2.0 mm 4-hole miniplate, and (**F**) 2.0 mm 6-hole miniplate fixation.

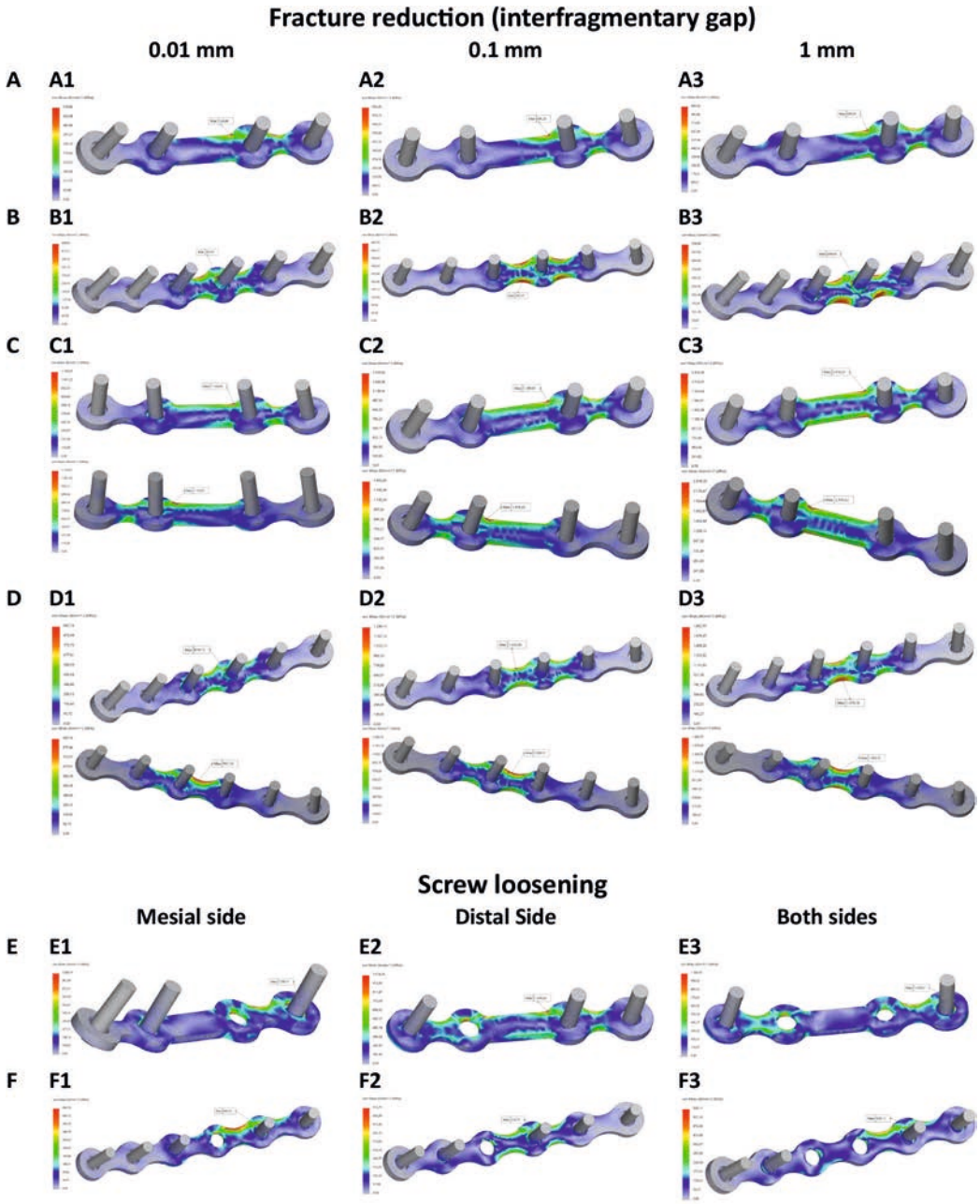

Supplementary Fig. S4. Back view of the stress distribution on the miniplate used for fixation of the severe atrophic edentulous mandibular body fracture. (**A-D**) Effect of fracture reduction (respectively **1 to 3** for fracture distance of 0.01, 0.1, and 1 mm): (**A-B**) unilateral fractures, (**C-D**) bilateral fractures (upper figure: right side fracture miniplate, lower figure: left side fracture miniplate), (**A,C**) 2.0 mm 4-hole miniplate, and (**B,D**) 2.0 mm 6-hole miniplate fixation. (**E-F**) Effect of lose screws (respectively **1 to 3** illustrating the lose screw on the mesial side, distal side, or both sides of fracture site): (**E**) 2.0 mm 4-hole miniplate, and (**F**) 2.0 mm 6-hole miniplate fixation.

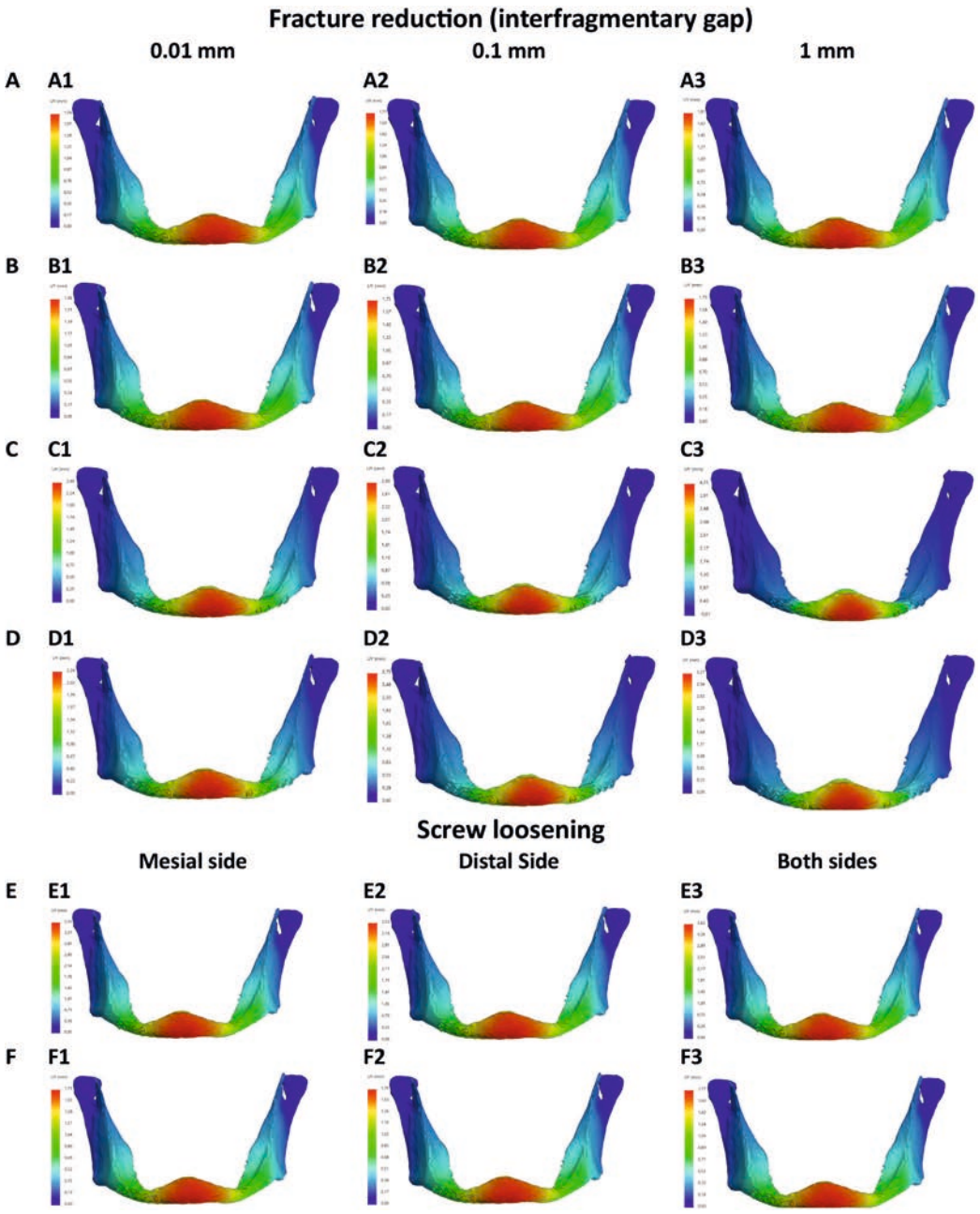

Supplementary Fig. S5. Displacement [mm] of severe atrophic edentulous mandibular body fracture fixation. (**A-D**) Effect of fracture reduction (respectively **1 to 3** for fracture distance of 0.01, 0.1, and 1 mm): (**A-B**) unilateral fracture, (**C-D**) bilateral fracture, (**A,C**) 2.0 mm 4-hole miniplate, and (**B,D**) 2.0 mm 6-hole miniplate fixation. (**E-F**) Effect of loose screws (respectively **1 to 3** illustrating the lose screw on the mesial side, distal side, and both sides of fracture site): (**E**) 2.0 mm 4-hole miniplate, and (**F**) 2.0 mm 6-hole miniplate fixation.

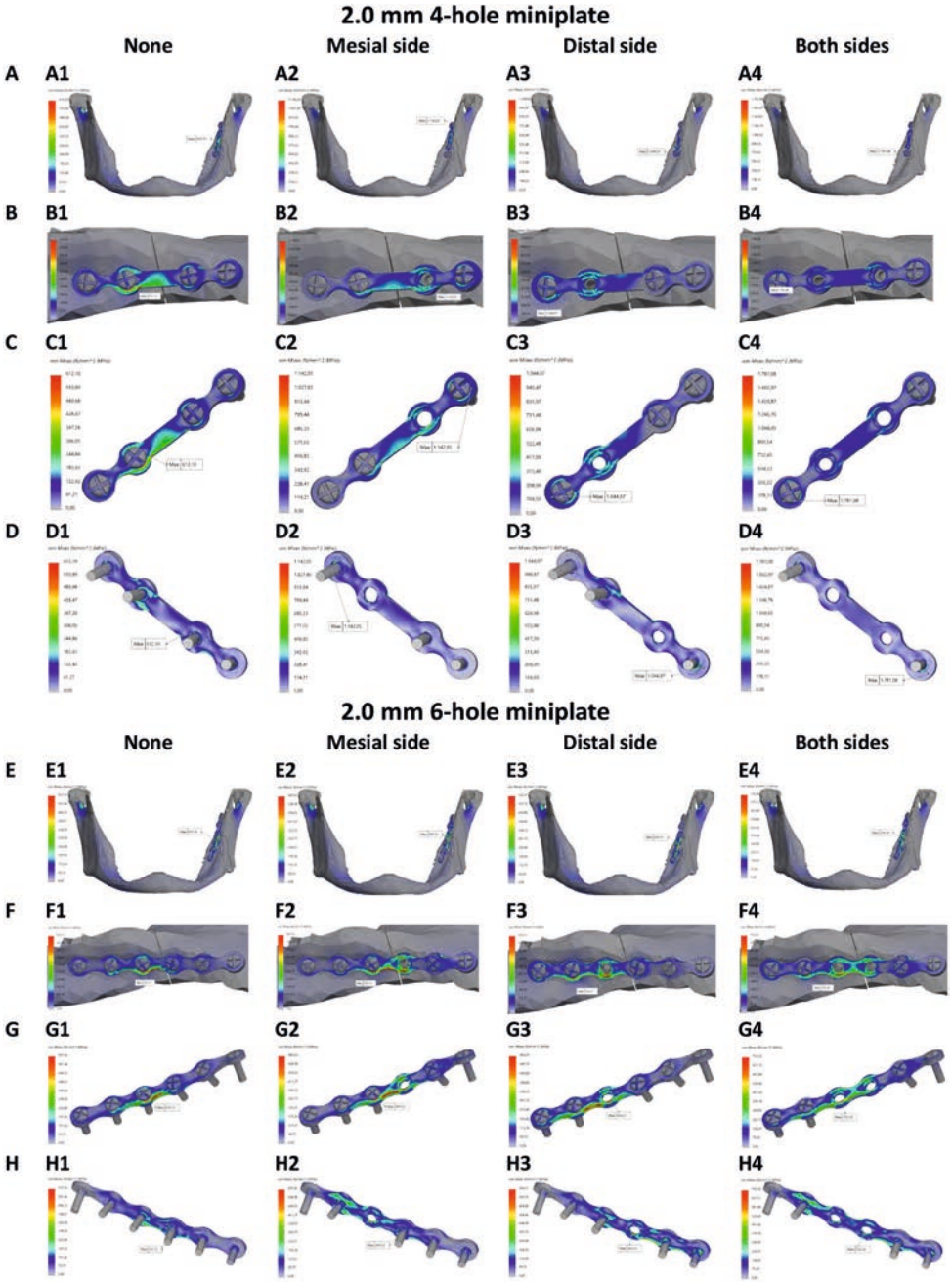

Supplementary Fig. S6. Illustration of fracture stability and stress distribution in the severe atrophic edentulous mandibular angle fracture treated with (**A-D**) 2.0 mm 4-hole versus (**E-H**) 2.0 mm 6-hole miniplate. (**A, E**) General overview of stress distribution. (**B, F**) Illustrating the fracture stability by zooming at the fracture site. (**C, G**) Front view of the stress distribution on the miniplate. (**D, H**) Back view of the stress distribution on the miniplate. (**1-4**) Referring to screw loosening (**1**: none, **2**: mesial side, **3**: distal side, or **4**: both side of the fracture site).

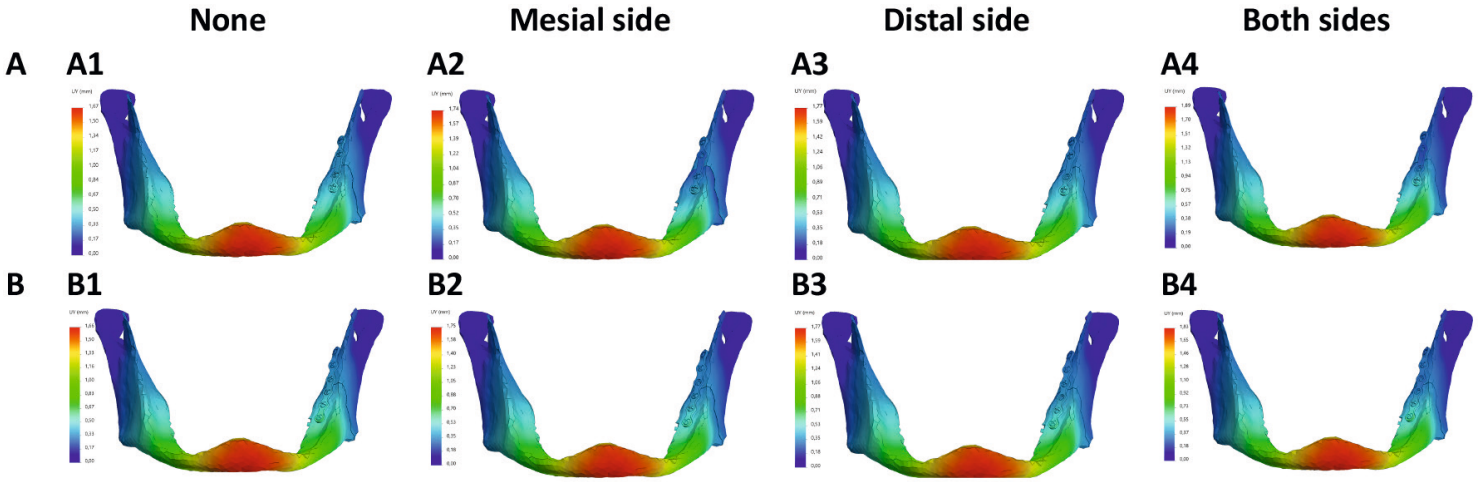

Supplementary Fig. S6. Displacement in a severe atrophic edentulous unilateral mandibular angle fracture fixation with effect of screw loose (**1**: none, **2**: on the mesial side, **3**: distal side, or **4**: both side of the fracture site): (**A**) 2.0 mm 4-hole miniplate, and (**B**) 2.0 mm 6-hole miniplate fixation.

SECTION V

Application of 3D model

CHAPTER 7

Patient satisfaction after conservative treatment of anterior wall frontal sinus fractures

Marlous Marianne Beate Cardinaal, **Omid Daqiq***, Bram Barteld Jan Merema, & Baucke van Minnen

Department of Oral and Maxillofacial Surgery, University Medical Center Groningen, University of Groningen, Hanzeplein 1, 9713 GZ, Groningen, The Netherlands.
Additional information: Marlous Marianne Beate Cardinaal and Omid Daqiq contributed equally to this work and should be considered co-first authors.

Accepted 9 august 2024 and published 10 august 2024
Journal: Journal of Cranio-Maxillofacial Surgery
Cite: Cardinaal MMB, Daqiq O, Merema BBJ, van Minnen B. Patient satisfaction after conservative treatment of anterior wall frontal sinus fractures. J Craniomaxillofac Surg. 2024 Nov;52(11):1228-1234. doi: 10.1016/j.jcms.2024.08.002. PMID: 39181743.

Link: https://www.sciencedirect.com/science/article/pii/S1010518224002300

ABSTRACT

This study aims to determine patient forehead aesthetics satisfaction after conservative treatment of non-dislocated and dislocated anterior wall frontal sinus fractures.

Prospectively, patients older than 15 years of age with a frontal sinus fracture, treated conservatively between the period of 2010-2020, were analysed. The Face-Q questionnaire was used to assess patient satisfaction, and the fracture dimensional properties were measured using computed tomography. The results were compared with a matched non-fractured control group.

The mean total Face-Q questionnaire score was 114.77 (SD=17.38) versus 114.23 (SD=15.23) (research- versus control group, respectively), with a mean difference of 0.55 (SD=4.85), which was not significant (p=0.91). The size of impression area did not appear to have a linear relationship with patient satisfaction within the entire population (p=0.87; r=0.00). Presence of a scar in the fracture site was a significant predictor of patient satisfaction, contributing to 31% of the entire population's overall score (p=0.01) and 57% in the dislocated fracture population (p=0.003).

The conservatively treated patients' satisfaction score was comparable to the control group. A higher satisfaction score after a conservative treatment is associated with the absence of a scar on the fracture site, even with dislocations up to 6 mm at the deepest impression point.

Keywords
Frontal sinus fracture, Conservative treatment, Patient satisfaction, Forehead aesthetics, Fracture dimensional properties.

INTRODUCTION

Frontal sinus fractures comprise approximately 5% to 15% of all facial bone fractures (Banica et al., 2013; Chouake & Miles, 2017; Dedhia et al., 2019; McRae M et al., 2008; Ravindra et al., 2015). They are mainly caused by assaults, motor vehicle accidents, falling objects, and penetrating trauma (Banica et al., 2013; Gómez Roselló et al., 2020). They commonly occur in young males between 20 to 31 years of age (Banica et al., 2013; McRae M et al., 2008). The fracture classification is primarily based on the involvement and degree of dislocation of the anterior wall, posterior wall, nasofrontal duct, cerebrospinal fluid leakage, or a combination of these (Ioannides & Freihofer, 1999; Jing & Luce, 2019; Phang et al., 2016; Strong, 2009; Vincent et al., 2019). The decision to undertake a surgical or a conservative approach is based on the classification. When functional sinus problems are not expected, e.g., in cases of isolated anterior wall fractures without obstruction of the nasofrontal duct, aesthetic aspects have to be taken into account during the decision making (Klassen et al., 2015). According to Kim et al. (2012), a 0-2 mm dislocation of the frontal sinus wall does not cause cosmetic deformation and so a conservative treatment is preferred (Kim et al., 2012). The choice between a surgical and a conservative approach is more debatable for dislocations between 2-5 mm, with the preference being to observe and wait for the swelling to reduce (Dalla Torre et al., 2014; Dedhia et al., 2019; Strong, 2009; Vincent et al., 2019). According to Strong et al. (2009), the risk of aesthetic disturbance increases with an increase in deformation (Strong, 2009). Recent studies have proposed algorithms for frontal sinus fracture management, but they did not take patient aesthetics and satisfaction into consideration (Becelli et al., 2021; Calis M et al., 2022).

Nowadays, patient satisfaction is seen as an important parameter for optimal healthcare (Shirley & Sanders, 2013). It appears that dissatisfaction leads to less compliance with follow-up appointments whereas satisfaction leads to higher treatment adherence (Hall & Dornan, 1990; Shirley & Sanders, 2013).

The purpose of this study was to determine the effect of conservative treatments of anterior wall frontal sinus fractures on patient forehead aesthetics satisfaction. Furthermore, the study aimed to identify the factors that play a role in the patient satisfaction outcomes. In addition, little is known about the relationship between patient satisfaction and the objectifiable properties (e.g., fracture dimensional properties, and the presence or absence of a scar) of frontal sinus fractures.

MATERIALS AND METHODS

Study set-up

In this prospective study, patients with frontal sinus fractures treated at the University Medical Center Groningen (UMCG) in the period 2010 to 2020 were included. In view of the development of the frontal sinus, the included patients had to be older than 15 years of age.

They were all treated conservatively for anterior wall frontal sinus fractures (Fig. 1). Fracture dislocation was not obligatory for the inclusion. Conservative therapy was based on intact sinus drainage and absence of cerebrospinal fluid leakage. Patients with post-traumatic swelling within 3 months after trauma were not included. Patients with systematic diseases such as Acromegaly or Paget's disease which may influence bone formation (Bertoldi et al., 2014; Bidner S & Finnegan M., 1989; Mazziotti et al., 2017; Singer, 2016), patients using prednisone which may disturb bone metabolism (Ton et al., 2005), and patients with a body dysmorphic disorder which could affect the perception of the body (Hundscheid T et al., 2014), were excluded from the study. Furthermore, patients with mental or intellectual disabilities were excluded since they were unable to fill in the questionnaire properly.

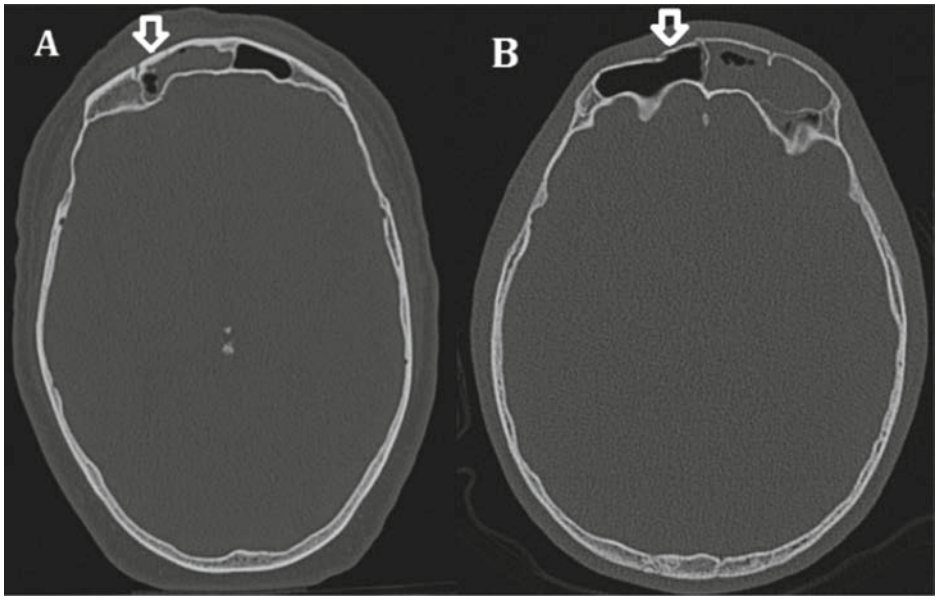

Fig. 1. Examples of non-dislocated and dislocated frontal sinus fractures: (A) a 70 year old male with a non-dislocated fracture, (B) a 22 year old male with a dislocated fracture.

A control group, consisting of subjects without a forehead fracture and with no history of trauma, was included for comparison purposes. The exclusion criteria were identical to that for the research group. The control group subjects were selected from UMCG's Centre of Dentistry and Oral Healthcare database. The VistaDent OC software (Dentsply Sirona Orthodontics, Islandia, New York) was used for the matching process where random blind matching was applied to randomly match the controls with the treated cases according to similar age and gender combinations for the purpose of eliminating the risk of selection bias.

Face-Q questionnaire

Patient satisfaction with the aesthetic appearance of the frontal head was measured by using the validated Face-Q questionnaire. The evaluation was based on questions

regarding the aesthetic appearance of the face in general life and social functioning as well as the subject's psychological well-being (Klassen et al., 2010, 2015; Pusic et al., 2013). The validated questionnaire has been widely used in various settings (e.g., in case of facial reconstruction, surgical fixation, or radiographic fracture analysis) (Chen et al., 2021; Elegbede et al., 2018; Gabrick et al., 2020). The study used a validated Dutch translated Face-Q questionnaire. The questionnaire contains 34 questions, and each can be scored from 1-4 points. The higher the total score, the higher the subject's satisfaction. The subjects received an information letter with a link to the Face-Q questionnaire on the Research Electronic Data Capture (REDCap) secure website. REDCap is used in the UMCG for building and managing online surveys.

Objectifiable fracture properties

The fracture objectifiable properties section consists of five items, namely: (1) fracture dimensions based on the measurements from the computed tomography (CT) images, (2) presence of a scar on the forehead, (3) fracture dislocation, (4) age, and (5) gender.

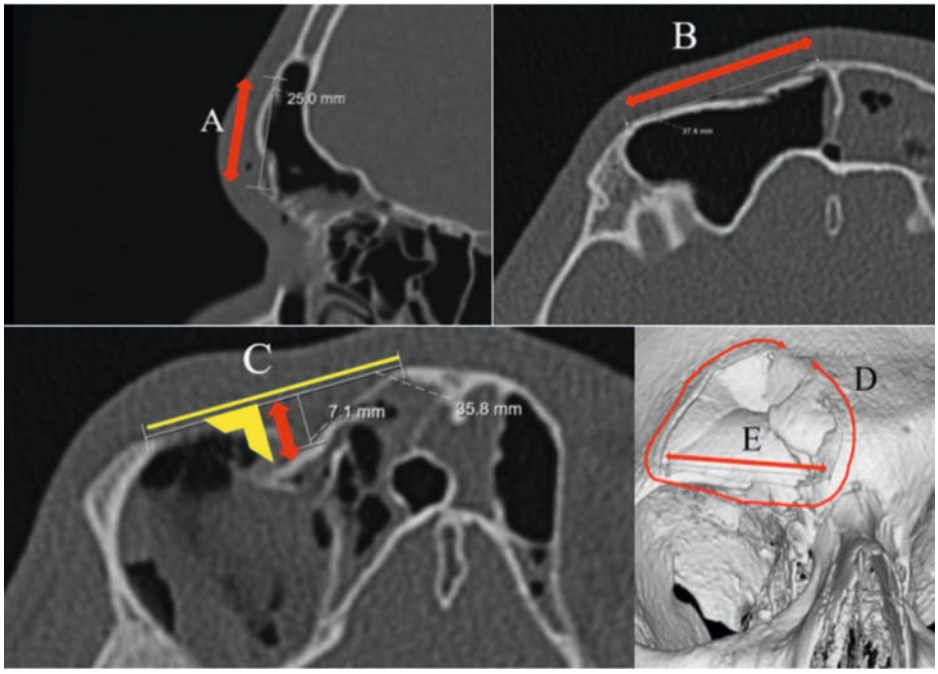

Fig. 2. Dimensional fracture measurement properties of a frontal sinus fracture. (A-E) DICOM-viewer CT measurements: (A) length, (B) width, (C) deepest impression point, (D) area, and (E) largest diagonal length.

Fracture dimensional measurement

Using the computed tomography (CT) images in the Digital Imaging and Communications in Medicine (DICOM) viewer enabled the dimensional measuring of each fracture (Fig. 2). In the study, the fracture dimensions were defined by measuring the length (parallel to the

sagittal plane), the width (parallel to the transverse plane), and impression depth (deepest fracture inward point parallel to transverse plane) in millimetres (mm). Furthermore, the area of the fracture in square-millimetres (mm^2), and the greatest diagonal length in mm were measured from the three-dimensional (3D) reconstruction images in the DICOM-viewer (Calis M et al., 2022).

Presence of scar, fracture dislocation, age, and gender

The presence of a scar, resulting from lacerations sustained in the accident, was an independent variable that was examined in relation to satisfaction. The question "Did a scar form after breaking the bone in your forehead?" was additionally asked in the questionnaire. Possible answers were: absent, present at the site of the fracture, or present at another site than the fracture.

Furthermore, the study investigated whether fracture dislocation influenced patient satisfaction. Fracture dislocation was defined as a displacement at the fracture site in the transverse plane with the impression depth of more than 0 mm (Fig. 1 and Fig. 2C). Finally, the effect of age and gender were examined in relation to satisfaction.

Statistical analysis

The sample size power analysis was done by using G*Power software (version 3.1.9.7, Heinrich-Heine-Universität Düsseldorf, Düsseldorf, Germany). Using power analysis, it was calculated that at least 34 subjects were required to detect the effect size at the significance level (α) of 0.05 and two-tailed power (1-β) of 0.80.

The rest of statistical analysis was conducted in SPSS software (version 26, IBM Cooperation, Armonk, New York). The significance value was set at $p \leq 0.05$ for all the analysis. The total score from the questionnaire was set as the dependent variable. The independent variables were the objectifiable properties: the fracture dimensional measurements from the CT images, the presence of scar tissue caused by the trauma, gender, age, and dislocation.

Two hypotheses were set for the statistical analysis (H0: not significant; H1: significant). The first hypothesis was that the satisfaction outcome is the same for conservatively treated patients with a frontal sinus fracture compared to a control group of subjects without fractures. The mean difference score was computed based on the research group's total scores in the Face-Q questionnaire and those of the matched control group. Depending on the sample size, the Shapiro-Wilk test or Kolmogorov-Smirnov test was used to analyse if the difference score was normally distributed with descriptive statistics used for determining the normality. Based on the normality of the data, either the Paired-T test or the Wilcoxon signed rank test was applied to compare the two groups.

The second hypothesis was that the objectifiable fracture properties are associated with the patient's satisfaction outcome. The independent variables were evaluated using multiple

linear regression analysis. This was conducted by creating dummy variables in the SPSS for the nominal variables of gender, dislocation, and the presence of a scar. The assumptions for performing accurate multiple regressions were that each independent variable had to have a linear relationship with the dependent variable. In addition, the residuals had to be normally distributed. Finally, the homoscedasticity of the variances was tested. When these predefined assumptions were met, the relationship between the dependent and independent variables was modelled by using the forward selection procedure.

RESULTS

The flow diagram of the inclusion process is shown in Fig. 3. Among the 22 included research subjects, 18 (81.1%) were males and 4 (18.2%) were females, with a mean age of 46.9 (SD=17.14) years, shown in Table 1. There were 12 cases with dislocated fractures and 10 with non-dislocated fractures. The control group also consisted of 22 subjects, selected, and matched to the research group according to age and gender.

Table 1. Demographic data of the research and control group.

	Research group	Control group	Total
Population size (n)	22	22	44
Male (%)	18 (81.8%)	18 (81.8%)	36 (81.8%)
Female (%)	4 (18.2%)	4 (18.2%)	8 (18.2%)

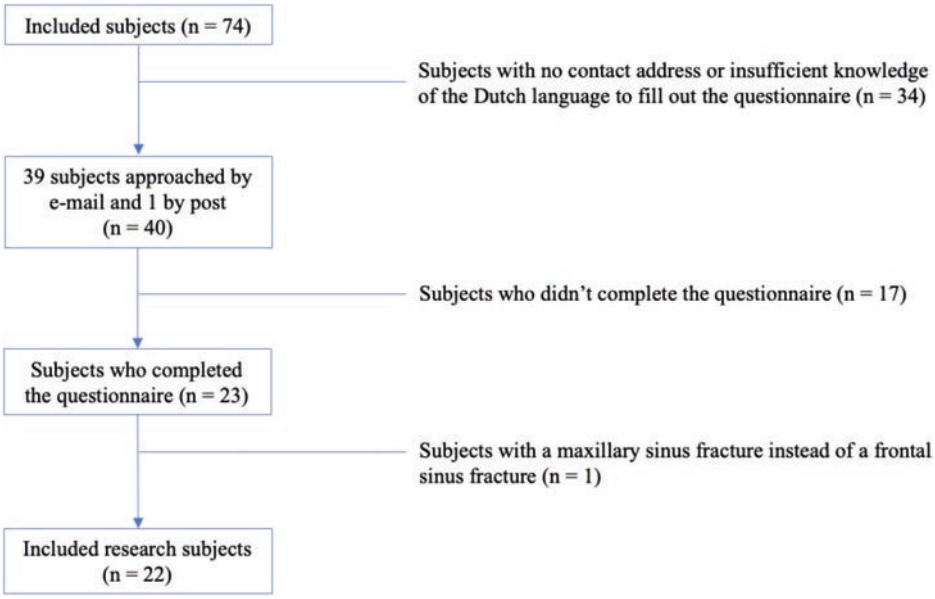

Fig. 3. Flowchart of the inclusion process.

Patient satisfaction

The Face-Q questionnaire satisfaction scores are shown in Table 2. The mean total score difference between the research and control group was 0.55 (SEM=4.85). The Shapiro-Wilk test gave a p-value higher than α for this difference score (p=0.54), meaning a normal distribution.

The Face-Q satisfaction total score difference illustrated a normal distribution (Supplementary Fig. S1). The histogram showed a gauss-curve with a skewness of -0.55 (SD=0.49) and a peak of 0.51 (SD=0.95), indicating a normal distribution (Supplementary Fig. S1A). The box plot demonstrated an outlier in the total score difference of -53 between two 56 years old males within the research- and control group (Supplementary Fig. S1B). Finally, a normal distribution could be observed in the Q-Q plot as the points of the total score difference lay mainly in a straight-line (Supplementary Fig. S1C). The paired t-test showed that the differences in total scores within the two groups were not significant (p=0.91).

Table 2. Face-Q questionnaire patient aesthetics satisfaction scores

Groups	Total score			Total score difference	Paired T-test	Shapiro-Wilk test *
	Mean (SD)	Median	Range	Mean (SEM)	P ≤ 0.05	P < 0.05
Research	114.77 (17.38)	117.50	62	0.55 (4.85)	0.91	0.54
Control	114.23 (15.23)	119	54			

Abbreviation: SD (standard deviation), SEM (standard error mean), p (significance).

Fracture objectifiable properties of the total population

The outcomes of the statistical analysis of the total population are shown in Table 3. The forward multiple regression included the independent variables from the model, with a cut-off of p<0.05. The area of the impression (p=0.87; r=0.00) had no linear relationship with patient satisfaction, so it was not analysed in the forward multiple regression. Only the variable "presence of scar" was found to have a p-value of <0.05 and was included in the initial model. Adding the independent variables regarding length, width, deepest impression point, area, and the largest diagonal length separately did not lead to a significant difference. Furthermore, gender, age, and dislocation in combination with a scar were not found to be significant predictors of a patient's satisfaction with the forehead. As a result, only the "scar" variable was included in the final model. The absence of a scar (β=-21.92; R2=0.31; p>0.001) and the presence of a scar outside the fracture site (β=-1.92, R2=0.31, p>0.001) were significant predictors of patient satisfaction. The regression equation for patient aesthetics satisfaction across the entire population is shown in equation 1.

The histogram of the final model showed normal distribution of the residues. In addition, the normality of the residues was apparent from the straight-line position in the P-P plot. Therefore, the assumption of homoscedasticity was met (Supplementary Fig. S2).

Table 3. Linear relationship between the fracture objectifiable properties and patient aesthetics satisfaction score for the total population with frontal sinus fracture.

Variables	Mean (SD)	p-value (<0.05)	r-value
Length (mm)	21.30 (25.59)	0.75	-0.05
Width (mm)	25.18 (31.43)	0.79	-0.03
Deepest impression point (mm)	3.15 (3.25)	0.67	-0.52
Area (mm^2)	821.06 (1352.17)	0.87	0.00
Largest diagonal length (mm)	28.05 (33.13)	0.73	-0.04
Scar tissue	-	0.01	Yes (scar present but not at the fracture site): -1.92 No (there is no scar resulted by the fracture): -21.92
Crack/Dislocation	-	0.78	2.15
Gender	-	0.80	2.47
Age	-	0.21	-0.28

Abbreviation: SD (standard deviation), p-value (significance), and r-value (regression coefficient).
Note: the variables in the table are the independent variables and the Face-Q patient satisfaction scores are the dependent variable in the regression analysis.

Equation 1. Regression of patient aesthetics satisfaction across the entire population.

*Patient Satisfaction = 122.92 + (-21.92 * Absence of scar tissue) + (-1.92 * Presence of scar tissue outside the fracture site).*

Note: 122.92 (constant), -21.92 (unstandardised coefficient β for absence of scar tissue), and -1.92 (unstandardised coefficient β for presence of scar tissue outside the fracture site).

Objectifiable properties of dislocated fractures

Of the 22 participants, 12 were found to have a dislocated fracture, and 10 had a non-dislocated fracture. The detailed fracture measurement values for each case are shown in supplementary Table S1. The outcome of the statistical analysis of the dislocated fractures is shown in Table 4. Each trait had a linear relationship, so they were all subjected to a multiple regression analysis. None of the patients with a dislocated fracture had a scar outside of the fracture site. When performing the forward multiple regression analysis, the "scar presence" variable was found to have a p-value ‹0.05, so it was included in the initial model. Further in this group, the separate addition of length, width, deepest impression point, area, largest diagonal length, gender, age, length-width ratio, length-depth ratio, length-area ratio, width-depth ratio, width-area ratio, and depth-area ratio as independent variables did not lead to significance. Only the scar tissue variable was included in the final model and was found to be a significant predictor of patient satisfaction (β=-26.63; R2=0.57; p›0.001). The regression equation for patient forehead aesthetics satisfaction among the dislocated fracture group is shown in equation 2.

Table 4. Linear relationship between the objectifiable properties and patient aesthetics satisfaction score for the population with a dislocated fracture.

Variables	Mean (SD)	p-value (<0.05)	r-value
Length (mm)	39.04 (22.22)	0.38	-0.21
Width (mm)	46.16 (28.79)	0.46	-0.14
Deepest impression point (mm)	5.77 (1.91)	0.09	-4.55
Area (mm^2)	1505.28 (1538.48)	0.69	-0.001
Largest diagonal length (mm)	51.43 (28.01)	0.35	-0.18
Scar tissue	-	0.003	Yes (scar present but not at the fracture site): - No, (there is no scar resulted by the fracture): -26.63
Gender	-	0.85	-3.55
Age	-	0.17	-0.41
Ratio (Length/Width)	-	0.63	11,34
Ratio (Length/Depth)	-	0.74	0.43
Ratio (Length/Area)	-	0.18	203.82
Ratio (Width/Depth)	-	0.74	0.31
Ratio (Width/Area)	-	0.16	255.60
Ratio (Depth/Area)	-	0.18	491.53

Abbreviation: SD (standard deviation), p-value (significance), and r-value (regression coefficient).
Note: the variables in the table are the independent variables and the Face-Q patient satisfaction scores are the dependent variable in the regression analysis.

Equation 2. Regression equation for patient aesthetics satisfaction with a dislocated fracture.

*Patient satisfaction = 124.63 + (-26.63 * Absence of scar tissue).*

Note: 124.63 (constant), and -26.63 (unstandardized coefficient β for absence of scar tissue).

The histogram showed a normal distribution of the residues in this group. The normality in the P-P plot was due to the location of the residues on the line. The last assumption of homoscedasticity was met as the scatterplot demonstrated that the variances were homogeneously distributed (Supplementary Fig. S2).

DISCUSSION

To date, no study in the literature has reported the effect of conservative treatment of frontal sinus fractures and fracture objectifiable properties on patient satisfaction with the aesthetics of the forehead. Therefore, this study is the first of its kind. The study investigated two questions. Firstly, "How does the aesthetic satisfaction with the forehead among patients with a conservatively treated fracture of the anterior wall differ from those without a fracture?" Secondly, "How does the degree of satisfaction with a conservative policy relate to the objectifiable properties of the frontal sinus fracture?"

In this study, patients older than 15 years of age with a conservatively treated frontal sinus fracture were included. Since only 5-15% of facial fractures are frontal sinus fractures, and since according to the current protocols and algorithms only 47% are conservatively treated, a small group of patients could be included.(Banica et al., 2013; Chouake & Miles, 2017; Gossman et al., 2006; Ravindra et al., 2015) Therefore, the desired sample size of 34 subjects was not achieved. The small study population size with a small power may have influenced the non-significant difference in the total score (conservatively treated patients compared to the control group). Perhaps, a larger sample size in the future studies may result in a more significant difference between the groups. Moreover, the validity of the study was ensured by matching the research group exactly with the control group based on age and gender. Selection bias was eliminated by applying random blind matching for subjects of the same age and gender within the groups.

Furthermore, the demographics of this study are consistent with the literature (Table 1). Johnson and Roberts (2021) also had a higher proportion of males (84.1%) in their meta-analysis of frontal sinus fracture treatments (Johnson & Roberts, 2021). In contrast to the mean age of 46.91 in this study, their relevant meta-analysis had an average age of 23 to 43 years (Johnson & Roberts, 2021). The outcome of this study is in line with the expectation that there is no difference in patient forehead satisfaction between conservatively treated frontal sinus fracture patients with no or moderate fracture dislocation versus subjects without a fracture, since the treatment strategy is mainly based on aesthetic significance (Kim et al., 2012). In contrast, Weathers et al. (2013) described that the decision to switch to a surgical treatment depends on the size of the aesthetic deformity (Weathers et al., 2013).

An outlier was observed in the study on determining the normality of the difference scores. There was a difference of -53 in the scores of two 56 year old males in the study- and control group (Supplementary Fig. S1B). However, it was decided not to remove this outlier from the data set to protect the validity of the study since it does not concern a measurement or input error. In the analysis, age and gender were excluded as possible confounders when determining the satisfaction difference between patients with a frontal sinus fracture and those without a fracture. However, other factors that may influence patient satisfaction with the facial area cannot be ruled out. For example, ethnicity can play a role in skin type. Caucasians have a thinner epidermis compared to Koreans, which may affect patient satisfaction with the aesthetics of the forehead (Lee et al., 2002).

The study used CT images to measure the dimensional properties of the fractures (Fig. 2) since, according to Calis et al. (2022), CT measurements can be applied to determine the dimensional properties of a frontal sinus fracture (Calis M et al., 2022). Using this method enables the specialist to determine the exact dimensional properties of the fracture and to choose the proper treatment (Becelli et al., 2021; Calis M et al., 2022; Johnson & Roberts, 2021; Kim et al., 2012). Kim et al. (2012) analysed the area and depth of a frontal sinus fracture of the anterior wall using CT scans, but in relation to later contour changes (Kim et al., 2012).

Our study's mean fracture depth of the entire population, 3.15 mm (SD=3.25), is very similar to the 3.9 mm mean depth reported by that study (Table 3) (Kim et al., 2012). Although Kim et al. (2012) found out that the fracture depth is a statistically significant predictor of late contour changes (Kim et al., 2012), this study shows that fracture depth is not automatically a statistically significant predictor of patient (dis)satisfaction. On analysing the dislocated fracture group, we measured an average depth of 5.77 mm (SD=1.91). Although our group with dislocation was relatively small, a depth up to 5-6 mm was not a significant predictor of patient satisfaction and conservative treatment seemed the right choice. A conservative policy might even be followed in certain cases with a dislocation of ›5-6 mm, in contrast to the surgical treatment advice for such dislocated fractures (Dalla Torre et al., 2014). However, this was only substantiated by a few cases in the study group. Furthermore, CT seems to be the most practical tool for the fracture dimensional measurements based on three reasons. First, most of the surgeons only have direct access to the CT images in three directions for fracture assessment. Second, a three-dimensional (3D) software package (e.g., Mimics, 3-Matic) is needed for the extensive fracture dimensional measurements (e.g., depth of depression), which requires the presence of an expert medical engineer. However, there are limited hospitals and surgeons with access to these software and experts. Third, it is not always possible to overlay the anatomical contour of the face by means of mirroring (e.g., in case of midline fractures) even with the use of the 3D software. A solution could be to implement statistical shape modelling for determining the intact bony contours cases of e.g., midline dislocations (Fuessinger et al., 2019; Rodriguez-Florez et al., 2017).

Finally, the study shows that the presence of a scar is a significant predictor of patient satisfaction in both the entire population and the population with dislocated fractures (Table 3 and 4). The presence of a scar prior to the trauma is therefore a possible confounder. Another possible confounder is the cause of the trauma or trauma mechanism. The prospective study by Harris et al. (2009), examining the predictors of patient satisfaction and surgeon satisfaction after orthopaedic trauma from a motor vehicle collision, showed lower patient satisfaction in patients who blamed others for their injuries (Harris et al., 2009). The time gap between the trauma and filling the questionnaire ranged from 27 to 138 months, with an average of 78 months. Therefore, there was at least a gap of more than 2 years from the initial trauma until filling the Face-Q questionnaires. This time gap means, by the time the subjects filled the questionnaire, there was hardly any chance of residual swelling in the forehead region. Therefore, in this study, possible residual swelling is negligible. Furthermore, since the dimensional measurement properties were not a significant predictor of patient satisfaction in the group (Table 3 and 4), the surgeon should exercise caution with operative therapy in the cases of minimally dislocated fractures of the anterior frontal sinus wall. Thus, it seems that optimal wound management to reduce the visible scar is more compelling for patient satisfaction compared to fracture management. However, to be able to draw a reliable and valid conclusion, follow-up research with a larger patient population is necessary.

In conclusion, the aesthetics of the forehead appear to be similar in relation to the degree of satisfaction among conservatively treated frontal sinus fracture patients with a dislocation up to 5-6mm, and subjects without a fracture in the control group. This means that the conscious decision to conservatively treat the patients in the research population instead of operating is supported. Furthermore, the absence of a scar on the fracture site is a significant predictor of patient satisfaction. Finally in the literature, it seems that the dislocation threshold for surgical approach might be overestimated. Especially, considering that in patients with no scar on the forehead, surgery may result in creating a scar, and thereby resulting in dissatisfaction in the aesthetics of the forehead. At the end, we recommend that patient satisfaction should be taken into consideration during the shared decision-making process of frontal sinus fracture management.

DECLARATIONS

Competing interests

None. All authors have viewed and agreed to the submission of the manuscript.

Funding

None.

Ethics approval and consent to participate

Medical Ethics Review Board of the University Medical Centre Groningen (METc UMCG) approved the research in Groningen 5 November 2020.

Participants consent

The participants were consented for participation in accordance with the principles laid down in the Declaration of Helsinki 1964 and its later amendments.

REFERENCES

Banica, B., Ene, P., Dabu, A., Ene, R., & Cirstoiu, C. (2013). Rationale for Management of Frontal Sinus Fractures. *Maedica A Journal of Clinical Medicine*, *8*(4), 398–403. https://www.ncbi.nlm.nih.gov/pmc/articles/PMC3968481/

Becelli, R., Palmieri, M., Facchini, V., Armocida, D., Pesce, A., Kapitonov, A., Zappalà, M., Colangeli, W., Bozza, F., Salvati, M., Santoro, A., & Frati, A. (2021). Management of frontal sinus fractures: A comprehensive review and treatment algorithm from Sapienza university of Rome. *Interdisciplinary Neurosurgery: Advanced Techniques and Case Management*, *26*, 101318. https://doi.org/10.1016/j.inat.2021.101318

Bertoldi, I., Cantarini, L., Filippou, G., & Frediani, B. (2014). Paget's disease. *Reumatismo*, *66*(2), 171–183. https://doi.org/10.4081/reumatismo.2014.789

Bidner S, & Finnegan M. (1989). Femoral fractures in Paget's disease. *Journal of Orthopaedic Trauma*, *3*(4), 317–322. https://doi.org/10.1097/00005131-198912000-00011

Calis M, Kaplan GO, Küçük KY, Altunbulak AY, Akgöz Karaosmanoğlu A, Işıkay Aİ, Mavili ME, & Tunçbilek G. (2022). Algorithms for the management of frontal sinus fractures: A retrospective study. *Journal of Cranio-Maxillofacial Surgery*, *15*(10), 749–755. https://doi.org/10.1016/j.jcms.2022.09.007

Chen, J., Zhang, T., Zhu, X., & Huang, W. (2021). Fat Repositioning With a Combination of Internal Fixation and External Fixation in Transconjunctival Lower Blepharoplasty. *Aesthetic Surgery Journal*, *41*(8), 893–902. https://doi.org/10.1093/asj/sjab059

Chouake, R. J., & Miles, B. A. (2017). Current opinion in otolaryngology and head and neck surgery: Frontal sinus fractures. *Current Opinion in Otolaryngology and Head and Neck Surgery*, *25*(4), 326–331. https://doi.org/10.1097/MOO.0000000000000369

Dalla Torre, D., Burtscher, D., Kloss-Brandstätter, A., Rasse, M., & Kloss, F. (2014). Management of frontal sinus fractures - Treatment decision based on metric dislocation extent. *Journal of Cranio-Maxillofacial Surgery*, *42*(7), 1515–1519. https://doi.org/10.1016/j.jcms.2014.04.023

Dedhia, R. D., Morisada, M. V., Tollefson, T. T., & Strong, E. B. (2019). Contemporary management of frontal sinus fractures. *Current Opinion in Otolaryngology and Head and Neck Surgery*, *27*(4), 253–260. https://doi.org/10.1097/MOO.0000000000000546

Elegbede, A., Mermulla, S., Diaconu, S. C., McNichols, C., Liang, Y., Liang, F., Rasko, Y. M., Grant, M. P., & Nam, A. J. (2018). Patient-reported Outcomes in Facial Reconstruction: Assessment of FACE-Q Scales and Predictors of Satisfaction. *Plastic and Reconstructive Surgery - Global Open*, *6*(12), e2004. https://doi.org/10.1097/GOX.0000000000002004

Fuessinger, M. A., Schwarz, S., Neubauer, J., Cornelius, C.-P., Gass, M., Poxleitner, P., Zimmerer, R., Metzger, M. C., & Schlager, S. (2019). Virtual reconstruction of bilateral midfacial defects by using statistical shape modeling. *Journal of Cranio-Maxillofacial Surgery*, *47*(7), 1054–1059. https://doi.org/10.1016/j.jcms.2019.03.027

Gabrick, K., Smetona, J., Iyengar, R., Dinis, J., Chouiari, F., Peck, C. J., Persing, J., & Alperovich, M. (2020). Radiographic Predictors of FACE-Q Outcomes Following Non-Operative Orbital Floor Fracture Management. *Journal of Craniofacial Surgery*, *31*(4), e388–e391. https://doi.org/10.1097/SCS.0000000000006356

Gómez Roselló, E., Quiles Granado, A. M., Artajona Garcia, M., Juanpere Martí, S., Laguillo Sala, G., Beltrán Mármol, B., & Pedraza Gutiérrez, S. (2020). Facial fractures: classification and highlights for a useful report. *Insights into Imaging*, *11*(1). https://doi.org/10.1186/s13244-020-00847-w

Gossman, D. G., Archer, S. M., & Arosarena, O. (2006). Management of frontal sinus fractures: A review of 96 cases. *Laryngoscope*, *116*(8), 1357–1362. https://doi.org/10.1097/01.mlg.0000226009.00145.85

Hall, J. A., & Dornan, M. C. (1990). Patient sociodemographic characteristics as predictors of satisfaction with medical care: a meta-analysis. *Social Science & Medicine*, *30*(7), 811–818. https://doi.org/10.1016/0277-9536(90)90205-7

Harris, I. A., Dao, A. T. T., Young, J. M., Solomon, M. J., & Jalaludin, B. B. (2009). Predictors of patient and surgeon satisfaction after orthopaedic trauma. *Injury*, *40*(4), 377–384. https://doi.org/10.1016/j.injury.2008.08.039

Hundscheid T, van der Hulst RR, Rutten BP, & Leue C. (2014). Stoornis in de lichaamsbeleving bij patiënten binnen de cosmetische chirurgie [Body dysmorphic disorder in cosmetic surgery - prevalence, psychiatric comorbidity and outcome]. *Tijdschrift Psychiatrie*, *56*(8), 514–522. https://www.tijdschriftvoorpsychiatrie.nl/en/artikelen/article/50-10351_Stoornis-in-de-lichaamsbeleving-bij-patienten-binnen-de-cosmetische-chirurgie

Ioannides, C., & Freihofer, H. P. (1999). Fractures of the Frontal Sinus: Classification and its Implications for Surgical Treatment. *Am J Otolaryngol*, *20*(5), 273–280. https://doi.org/10.1016/s0196-0709(99)90027-3

Jing, X. L., & Luce, E. (2019). Frontal Sinus Fractures: Management and Complications. *Craniomaxillofacial Trauma & Reconstruction*, *12*(3), 241–247. https://doi.org/10.1055/s-0038-1675560

Johnson, N. R., & Roberts, M. J. (2021). Frontal sinus fracture management: a systematic review and meta-analysis. *International Journal of Oral and Maxillofacial Surgery*, *50*(1), 75–82. https://doi.org/10.1016/j.ijom.2020.06.004

Kim, D. W., Yoon, E. S., Lee, B. Il, Dhong, E. S., & Park, S. H. (2012). Fracture depth and delayed contour deformity in frontal sinus anterior wall fracture. *Journal of Craniofacial Surgery*, *23*(4), 991–994. https://doi.org/10.1097/SCS.0b013e31824dfcb1

Klassen, A. F., Cano, S. J., Schwitzer, J. A., Scott, A. M., & Pusic, A. L. (2015). FACE-Q scales for health-related quality of life, early life impact, satisfaction with outcomes, and decision to have treatment: Development and validation. *Plastic and Reconstructive Surgery*, *135*(2), 375–386. https://doi.org/10.1097/PRS.0000000000000895

Klassen, A. F., Cano, S. J., Scott, A., Snell, L., & Pusic, A. L. (2010). Measuring patient-reported outcomes in facial aesthetic patients: development of the FACE-Q. *Facial Plastic Surgery : FPS*, *26*(4), 303–309. https://doi.org/10.1055/s-0030-1262313

Lee, Y., Hwang, A. K., Hwang, K., & Hwang, K. (2002). Skin thickness of Korean adults. *Surg Radiol Anat*, *24*, 183–189. https://doi.org/10.1007/s00276-002-0034-5

Mazziotti, G., Maffezzoni, F., Frara, S., & Giustina, A. (2017). Acromegalic osteopathy. *Pituitary*, *20*(1), 63–69. https://doi.org/10.1007/s11102-016-0758-6

McRae M, Momeni R, & Narayan D. (2008). Frontal sinus fractures: a review of trends, diagnosis, treatment, and outcomes at a level 1 trauma center in Connecticut. *Connecticut Medicine*, *72*(3), 133–138.

Phang, S. Y., Whitehouse, K., Lee, L., Khalil, H., McArdle, P., & Whitfield, P. C. (2016). Management of CSF leak in base of skull fractures in adults. *British Journal of Neurosurgery*, *30*(6), 596–604. https://doi.org/10.1080/02688697.2016.1229746

Pusic, A. L., Klassen, A. F., Scott, A. M., & Cano, S. J. (2013). Development and Psychometric Evaluation of the FACE-Q Satisfaction with Appearance Scale. A New Patient-Reported Outcome Instrument for Facial Aesthetics Patients. *Clinics in Plastic Surgery*, *40*(2), 249–260. https://doi.org/10.1016/j.cps.2012.12.001

Ravindra, V., Neil, J., Shah, L., Schmidt, R., & Bisson, E. (2015). Surgical management of traumatic frontal sinus fractures: Case series from a single institution and literature review. *Surgical Neurology International*, *6*(1), 141. https://doi.org/10.4103/2152-7806.163449

Rodriguez-Florez, N., Bruse, J. L., Borghi, A., Vercruysse, H., Ong, J., James, G., Pennec, X., Dunaway, D. J., Jeelani, N. U. O., & Schievano, S. (2017). Statistical shape modelling to aid surgical planning: associations between surgical parameters and head shapes following spring-assisted cranioplasty. *International Journal of Computer Assisted Radiology and Surgery*, *12*(10), 1739–1749. https://doi.org/10.1007/s11548-017-1614-5

Shirley, E. D., & Sanders, D. O. (2013). Patient satisfaction: Implications and predictors of success. *Journal of Bone and Joint Surgery*, *95*(10), e69. https://doi.org/10.2106/JBJS.L.01048

Singer, F. R. (2016). Bone Quality in Paget's Disease of Bone. *Current Osteoporosis Reports*, *14*(2), 39–42. https://doi.org/10.1007/s11914-016-0303-6

Strong, E. B. (2009). Frontal Sinus Fractures: Current Concepts. *Craniomaxillofacial Trauma & Reconstruction*, *2*(3), 161–175. https://doi.org/10.1055/s-0029-1234020

Ton, F. N., Gunawardene, S. C., Lee, H., & Neer, R. M. (2005). Effects of low-dose prednisone on bone metabolism. *Journal of Bone and Mineral Research*, *20*(3), 464–470. https://doi.org/10.1359/JBMR.041125

Vincent, A., Wang, W., Shokri, T., Gordon, E., Inman, J. C., & Ducic, Y. (2019). Management of Frontal Sinus Fractures. *Facial Plastic Surgery*, *35*(6), 645–650. https://doi.org/10.1055/s-0039-3399521

Weathers, W. M., Wolfswinkel, E. M., Hatef, D. A., Lee, E. I., Brown, R. H., & Hollier, L. H. (2013). Frontal Sinus Fractures: A Conservative Shift. *Craniomaxillofacial Trauma & Reconstruction*, *6*(3), 155–160. https://doi.org/10.1055/s-0033-1349210

SUPPLEMENTARY DATA

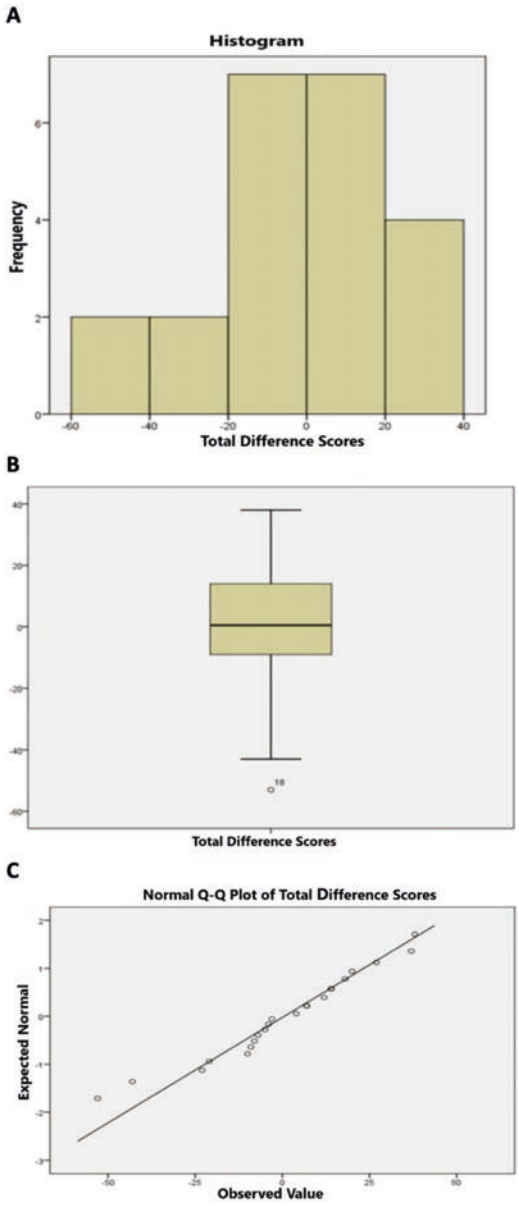

Supplementary Fig. S1. Face-Q patient satisfaction score.
A: Histogram showing the distribution of the total score difference. It shows a gauss-curve with skewness of -0.55 (SD=0.49) and a peak of 0.51 (SD=0.95). This indicates a normal distribution.
B: Box plot showing the distribution of the total score difference. It demonstrates an outlier (number 18) with a total score difference of -53 between two 56 year old males in the research- and control groups.
C: Q-Q plot showing that the points of the total score difference lie mainly in a straight-line, meaning a normal distribution.

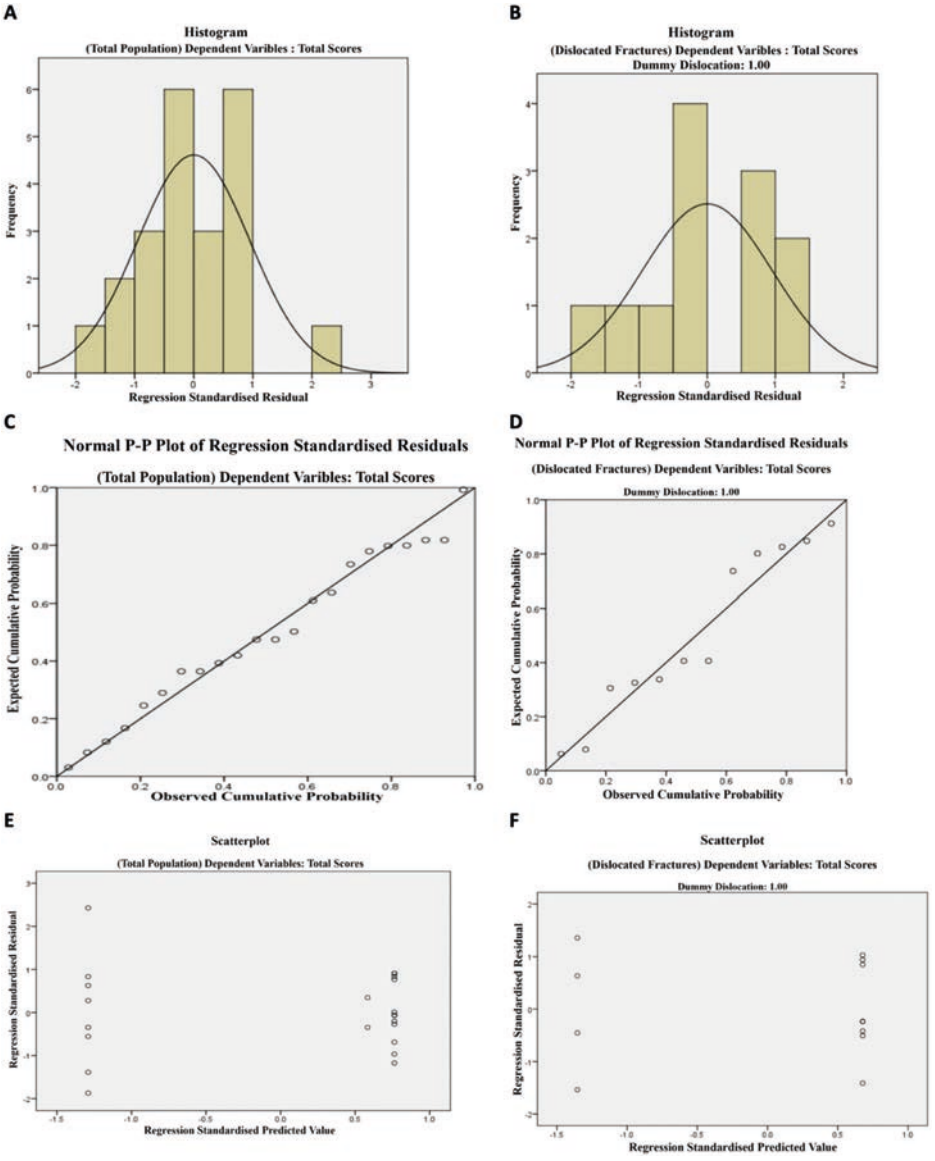

Supplementary Fig. S2. Fracture measurement properties for the total population (**left** side) and dislocated fractures (**right** side).
A-B: The Histograms illustrate a normal residue distribution.
C-D: P-P plots showing that the points lie mainly near the straight-line. This means normality of the residues with homoscedasticity.
E-F: Scatter plot showing homogeneous variance distribution, and therefore normality.

Supplementary Table S1. CT measurements in the DICOM-viewer of the fracture dimensions for cases with a dislocated fracture in the research group (N=12).

Case Nr.	Length (mm)	Largest diagonal length (mm)	Width (mm)	Deepest impression point (mm)	Area (mm^2)
1	36.40	54.40	38.40	5.40	922.25
2	25.00	34.50	37.40	7.10	697.12
3	63.00	80.90	70.10	7.90	2708.48
6	79.90	93.50	91.90	8.90	4121.00
12	74.00	99.20	97.00	3.90	4597.92
14	27.00	36.50	32.90	7.50	703.37
16	33.50	51.80	40.40	4.60	808.39
18	27.60	29.00	18.10	3.70	266.28
19	31.10	39.20	38.10	5.10	854.81
21	44.90	63.80	65.20	7.30	2106.66
22	11.00	13.00	11.40	4.90	91.53
27	15.10	21.30	13.00	2.90	185.57

SECTION VI

Discussion

CHAPTER 8

General discussion and future perspective

GENERAL DISCUSSION AND FUTURE PERSPECTIVE

The applicability of three-dimensional (3D) modelling and finite element analysis (FEA) in craniomaxillofacial (CMF) surgery, particularly for the evaluation and management of facial fractures has been evaluated in this thesis. A systematic and reproducible approach was employed to develop and validate an anatomically accurate FEA model of the mandible. The findings are encouraging for the model's potential implementation in clinical practice, especially for assessing complex mandibular fracture patterns (e.g., in severely atrophic mandibles, or in comminute fractures), and in evaluating osteosynthesis techniques (e.g., miniplate systems, or patient-specific implants). The methodology outlined is also adaptable for the analysis of other bone fractures within the CMF region. Additionally, the impact of 3D model in CMF surgery was further examined through the analysis of frontal sinus fractures, reinforcing the role of 3D model in improving diagnostic and therapeutic strategies. The steps undertaken in this thesis are summarised in Figure 1.

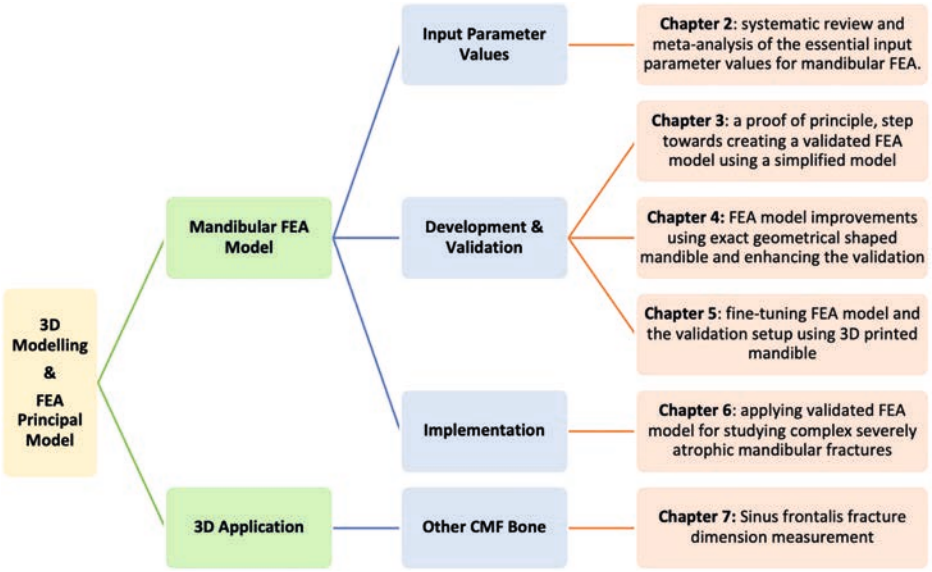

Figure 1. Steps that were taken to develop a validated FEA model and applying 3D in other bones in CMF region.

FEA input parameter values

In the thesis, the first step was to establish the true fundamental input parameters value for the mandibular FEA setup (e.g., force, material properties, fixture, or boundary condition) along with the factors that can influence them (e.g., sex, or age) through an evidence based systemic review with meta-analysis[1] (*Section II: Chapter 2*). This was necessary because the literature shows variations and discrepancies regarding these parameters, along with uncertainties about what the exact true values are[2–17]. Relevant and reliable data on maximum bite force (MBF) (n:60), muscle force (masseter, temporalis, and pterygoid)

(n:5), and mandibular bone properties (incl. cortical and trabecular segment) (n:5) were obtained. These data are considered relevant as they are critical input parameter values for the development of a mandibular FEA model. The quality and reliability of the data were assessed using risk of bias checklists along with evaluating the methodologies used for data collection and the procedures by which the measurements were obtained. Other critical parameters such as boundary conditions or fixture were not obtained. This limits the comprehensiveness of the FEA model. The found values can be readily incorporated into a general mandibular FEA setup; however, aside from bite force, it is questionable whether the rest of the parameters are accurate enough to setup a precise FEA model that can be matched to a specific patient in the clinical setting. This limitation primarily arises from the absence of stratified subgroups (e.g., based on sex or age) and limited data that would allow for more individualized model calibration in a clinical context. The validation of the FEA model by polymer model testing, after fine tuning, suggests that the most critical parameters (including forces, material properties, fixtures, and boundary conditions) were correctly introduced in our FEA model (*Chapter 5*).

Thebtainned MBF values allow for incorporation of patient specific bite forces in the FEA setup, tailored to patients' characteristics such as age, sex, or bite region. On average, males exhibit 1.3 times higher bite force than females, with peak MBF in individuals aged 20–60 years, followed by those under 20, and lowest in those over 60. Highest force is observed at the molar region, decreasing through premolars to the incisors. It is generally expected that the moment remains constant, implying that the MBF should be inversely proportional to the distance from the temporomandibular joint[18,19]. However, the observed force distribution from the molar region to the anterior region does not follow a logical progression with a constant moment. This deviation is partly attributed to both the functional impact of the masticatory muscle forces and the distinctive geometrical shape of the mandible[19–23]. This justifies further investigation into the underlying biomechanical factors that may influence the distribution of forces. The variation in bite forces suggests that, in individual cases, mandibular fractures treated with osteosynthesis could be treated with a weaker plate due to lower bite force exerted on the fractured mandible. The meta-analysis (*Chapter 2*) demonstrates that even three months postoperatively, the increase in MBF does not reach the levels observed in a healthy dentulous population with intact mandible, with a factor difference of 2.5 in the molar region and 2 in the incisal region. This also indicates that for development of new osteosynthesis implants the strength requirement can be reduced due to the lower bite force. This opens the possibility for optimising osteosynthesis design through the application of novel materials, potentially enabling the adaptation of a more diverse, adjustable, and cost-effective osteosynthesis options. Moreover, additional research would be beneficial for a more comprehensive understanding of MBF variability across different populations by using a large sample size, with an equal distribution of male and female participants across standardised age categories (e.g., based on life stage), with MBF measured at various bite locations (e.g., molar, premolar, incisal), and diverse subgroups (e.g., based on occlusion, dental stage, history of dental restoration, or facial morphology).

The found mastication muscle forces and mandibular bone property values are applicable in a general mandibular FEA model. However, their application in patient specific FEA models is limited due to the small number of studies, demographic variabilities, and inconsistencies in the measurement methodology. Regarding muscle force, capturing inter-individual variability necessitates the use of large sample size with stratified differentiation based on sex and age. Individual muscle forces can be possibly quantified using computed tomography (CT)[24], magnetic resonance imaging (MRI)[20,25–27], or electromyography (EMG)[21,28–30]. Ideally, such analyses should be done across different bite regions (e.g., incisal, and molar). Regarding biomechanical mandibular bone properties, it is recommended to have a larger sample of male and female cadavers in future studies, preferably in various age ranges, with the samples collected from different mandibular bone regions (e.g., angle, ramus, and body), as well as differentiation between cortical and trabecular bone segments.

Finally, no studies were identified in the literature addressing the definition of fixture or fixation (temporomandibular joint), nor the boundary condition (e.g., friction). This lack of studies may be attributed to the challenges involved in defining these components through physical in vivo testing. However, should it be feasible, future studies focusing on these areas would provide valuable insights. For instance, in terms of friction, different sensor gauges could be employed to assess the friction between fracture surfaces or between the bone and osteosynthesis materials.

Another subject concerns the assessment of the magnitude of the error in the FEA. Bone properties may change from patient to patient. Moreover, they are likely not homogeneous over the mandible. Furthermore, it might be hard to get accurate values for the friction between the osteosynthesis and the mandible. Therefore, one likes to know how sensitive the outcomes are for the magnitude of the friction. For example, if we know between which bounds Youngs modulus, Poisson's ratio, and friction varies, then by an optimisation-based process one can compute an interval in which the maximum stress will occur. Given the uncertainties and unknown input parameters in the model, incorporating an appropriate safety factor is advisable to enhance the robustness and clinical applicability of the simulation outcomes. However, an appropriate safety margin has not yet been clearly defined and warrants further investigations. One potential strategy involves using the material properties of the bone or the osteosynthesis, particularly using the ratio between the yield strength and the maximum stress, to ensure the fixation integrity under physiological loading conditions. A safety factor of 1.5 is often employed in aerospace industry[31]. However, to our knowledge, this standard has not yet been fully established in medical or surgical application. Therefore, future research should aim to establish clinically relevant safety factors tailored to craniofacial biomechanics.

Mandibular FEA model

In CMF surgery, application of 3D and FEA has been extensively applied in a trauma, reconstructive, or oncologic setting[5–7,9–14,32–35]. In the trauma setting, the complex mandibular

fractures (e.g., in severe atrophic mandible or comminute fractures) fixation remains challenging in terms of achieving optimal fracture fixation without the need for revision surgery as these non-routine fractures cannot always be treated using standard fixation systems or methodologies. One way to plan the surgical treatment of these fractures is the use of computer-aided 3D modelling and FEA simulations. However, a validated FEA that could be used in the clinical setting is lacking. Therefore, in the thesis, the necessary measures were taken to create such a model. This was achieved by a systematic approach to create a valid evidence-based static FEA model principle (*Section III: Chapter 3-5*).

Across the three studies (*Chapter 3-5*), the FEA was validated through using mechanical testing of mandibular replicas (Synbone and 3D printed), mounted onto a calibrated mechanical test bench using a custom-designed fixation device (see section: *FEA validation process*). Additionally, the outcomes were compared to the current understanding of fracture management in CMF surgery by incorporating the expertise of the CMF surgeons, using established guidelines, and relevant literature. The initial proof of principle study (*Chapter 3*) successfully demonstrated that (linear) static FEA is a viable and applicable tool in CMF surgery for mandibular fracture fixation analysis and assessment of osteosynthesis material[4]. However, the FEA contained a simplified 3D mandible model, which did not fully resemble the complex anatomical geometry of the human mandible and not fully matching the mechanical testing. In the subsequent research phases (*Chapter 4-5*), the FEA model was significantly improved by using a precisely geometrical shaped 3D mandible model in the FEA along with fully matched conditions between FEA and mechanical testing validation setup[2,3]. This ensures enhancing the model's fidelity and reliability. Following the completion of these three extensive studies[2–4] (*Chapter 3-5*), the static FEA model has achieved a level of validation that supports its application in the simulation of complex mandibular fractures under static loading conditions (constant-in-time load), without the necessity for routine mechanical validation. This means that the final fine-tuned FEA model can be potentially applied for analysing non-standard complex mandibular fractures and assessing osteosynthesis systems in the clinical setting (see example Figure 2).

The next step was to gain insight in the treatment of other mandibular fractures, with remaining clinical questions regarding optimal treatment, only by our FEA model. In this way biomechanical insights can be generated to inform the management of similar fracture cases, particularly in situations where clinical evidence remains inconclusive or insufficient. This was investigated by simulating mandibular body and angle fracture in a 3D digital twin of a Luhr Class III[36] severely atrophic edentulous mandible using different clinically relevant fixation scenarios (*Section IV: Chapter 6*). For these fractures, literature offers limited evidence to support specific fixation strategies, and optimal management remains uncertain, even among experienced surgeons[37–41]. The FEA findings align with clinical observations[42,43] and provide valuable insight into the biomechanical behaviour of these fractures. Notably, factors such as the number of fractures, fracture reduction accuracy, osteosynthesis type, and screw loosening near the fracture site does influence fracture fixation stability.

Although repetitive forces are not implemented in the model, and other factors, like local bone quality may play a role in the eventual successful healing, the application of the FEA model is helpful for understanding optimal fixation strategies. The next step would be to apply the FEA model to investigate other complex mandibular fractures (e.g., comminuted, or wedge fractures). This can be combined with simulation of current fixation methods and configurations, or development of new fixation systems. For example, one could simulate the effects of conventional osteosynthesis techniques (e.g., miniplates or reconstructive plates), develop advanced patient-specific 3D printed implants, evaluate the performance of monocortical versus bicortical screws, or compare locking versus non-locking plating systems. Ultimately, the FEA model can be used for pre-surgical fracture analysis (see *future perspective*), where the surgeon can assess the fracture stability by evaluating the fracture integrity under different fixation scenarios. Next the surgeon can select the proper fixation system and method. In cases where the commercially available fixation methods are not suitable, the FEA model can be used to design a patient tailored implant. However, its application in the clinical setting remains limited, as addressed in the limitations later in this section and in the future perspectives section.

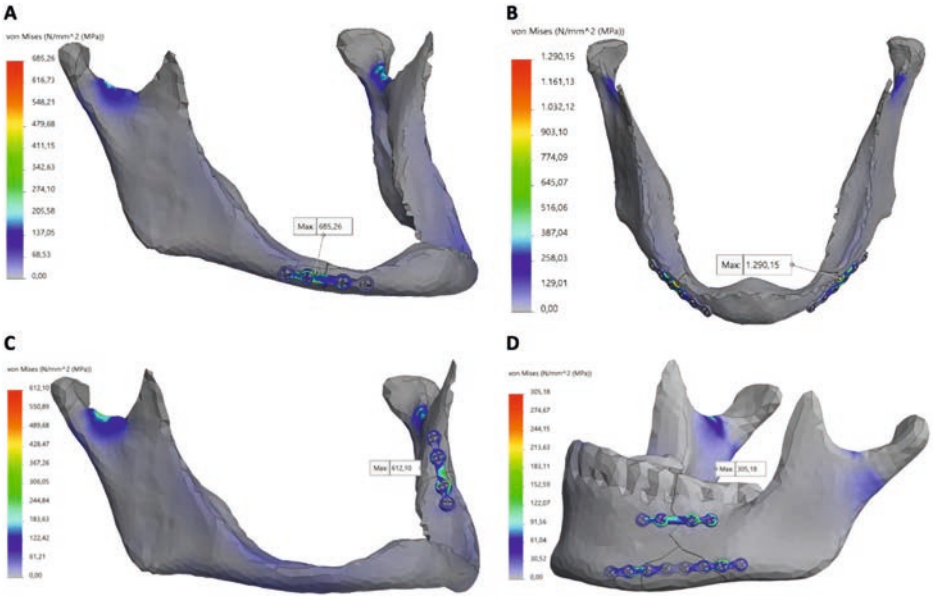

Figure 2. Example of validated FEA model application (e.g., stress distribution and peak stress location in megapascal unit) for fracture fixation assessment in (**A-C**) a severely atrophic edentulous mandible and (**D**) a non-atrophic dentulous mandible. (**A**) Unilateral body fracture fixated with a 2.0 4-hole miniplate. (**B**) Bilateral body fracture fixated using two 2.0 6-hole miniplate. (**C**) Unilateral angle fracture fixated with a 2.0 4-hole miniplate at the upper border. (**D**) Unilateral wedge fracture fixated using a 2.0 mm 4-hole 1mm thick miniplate at the upper border and a 2.0 8-hole miniplate at the lower border. *FEA setup*: The mandible models contain jagged-line fracture(s) with an interfragmentary distance of 0.1 mm, fixated using titanium miniplate(s) with a thickness of 1.0 mm. Further, a 150 N load applied at the anterior incisal region with fixture defined at the condylar regions, and the boundary conditions were according to the non-compression plating system.

The validated FEA model offers several key advantages. First, the FEA offers a highly adjustable and flexible model for investigating various mandibular fracture patterns and fixation systems under static loading conditions (e.g., constant-in-time incisal, or molar loading). The FEA model used (linear) static analysis, where a constant-in-time load was applied to the 3D model, resulting in a linear relationship between load and induced responses. However, the fixation biomechanical behaviour might be different when dynamic cyclic loading conditions are introduced into the FEA model (e.g., increased risk of screw loosening), potentially requiring a larger safety margin (possibly even exceeding the 1.5 factor commonly used in industry)[44–51]. Second, the 3D mandible models can be readily modified to assess specific clinical scenarios, allowing for the creation and analysis of fractures at targeted anatomical locations. Moreover, the base 3D mandible model can be replaced with other geometrically shaped mandibles generated through segmentation of imaging data such as cone-beam computed tomography (CBCT) (as demonstrated in *Chapter 6*). However, introducing new functional 3D mandible model into the FEA remains a challenging task, demanding specific software's and expertise, which could be automated to streamline the process (further discussed in *future perspective*). It is found in our studies to be crucial that the cortical and trabecular bone segments are clearly defined in the new 3D model, and that the FEA setup, including condylar fixture regions and boundary conditions, remains consistent with the validated model (as outlined in *Chapter 5*). Third, the FEA model facilitates the investigation of various osteosynthesis or implant systems, along with assessment of different fixation scenarios (as shown in *Chapter 4-6*). This process requires manual 3D modelling and accurate placement of the implant at the fracture site, a task that would benefit from automation to enhance both efficiency and precision (*see future perspective*). Once the fracture mandible and fixation system are assembled, the validated FEA setup can be easily applied to the model. Fourth, the FEA model allows for flexible adjustment of applied loads (e.g., bite force at molar or incisal region), fixtures, material properties (e.g., bone or osteosynthesis), and boundary conditions according to the specific requirements of the studied scenario (see *Chapter 2* for input values). Such adjustments enable the investigation of varying stress, strain, displacement, and force distributions under different conditions. Fifth, the static simulation FEA model is validated, eliminating the need for additional experimental verification of simulation outcomes. This distinguishes the model as a robust and reliable tool for biomechanical fracture analysis and highlights its potential for clinical application. This means that the FEA model can be applied in clinical settings to investigate complex non-routine mandibular fracture fixations (e.g., comminute fractures or in severely atrophic mandibles) (see *Chapter 6*). However, the validity of the model should be re-evaluated when introducing new conditions, such as dynamic loading, to reassess its accuracy, precision, and reproducibility. Last, observation of previously published mandibular FEA models reveals that their applicability for routine clinical use remains uncertain since the FEA model outcomes were not fully validated[8,11,13,14,34,35]. In contrast, this thesis presents a well-defined and validated static FEA model with clear potential for clinical application, particularly in the analysis of complex mandibular fractures (as shown in *Chapter 6*). The model's input parameters (e.g., bite force, muscle force, and mandibular bone properties)

were meticulously defined through an evidence-based systematic review[1] (*Chapter 2*). Its precision was further confirmed through precisely matched mechanical validation experiments[2–4] (*Chapter 3-5*). Moreover, the FEA setup developed here can be adapted for modelling other CMF bone fractures. Therefore, the validated FEA model is a clinically applicable tool for fracture analysis, offering a promising prospect for the integration of computer-aided surgical treatment planning in CMF surgery. Additionally, this approach can enhance patient care by guiding fracture treatment and supporting the surgeon's presurgical decision-making process. It enables optimal fracture treatment, minimising the need for revision surgery (e.g., due to screw loosening, or mal/non-union). In cases requiring surgical revision, the FEA model can be employed to evaluate the underlying causes of failure, thereby informing and optimising fixation strategies to reduce or potentially eliminate the necessity for subsequent revision procedures.

Several refinements can still be made concerning the limitations of the 3D modelling and the FEA model. First, Solidworks may not be optimal for complex FEA simulations. It was used in this thesis due to being the only FEA capable 3D modelling software available through the university with unrestricted 24/7 access. Future studies could consider more advanced simulation software's suited for complex FEA models (e.g., Abaqus, or Ansys). They offer enhanced simulation precision through advanced mesh controls, diverse element formulations, and support complex material models, thereby providing greater flexibility and accuracy in sophisticated FEA simulations. Second, as previously noted, the FEA model was based on (linear) static analysis (constant-in-time loading). However, in a clinical setting, dynamic analysis may better reflect the cyclic nature of masticatory forces, offering insights into structural behaviour under repetitive loading[44–51]. In case of fracture fixation, it enables more realistic simulation of physiological chewing forces and their impact on fixation stability and fracture integrity[45–47,49,50]. Third, the FEA model applied an incisal load, though molar or premolar loads would affect fracture biomechanics differently. However, the model can easily accommodate these variations by repositioning the force to the desired location, allowing for assessment of fracture fixation stability under different loading conditions. Fourth, the 3D mandible model's material properties were defined as linear elastic isotropic, neglecting nonlinear effects from large displacements. This assumption is valid only when stresses remain below the yield point. Future studies should explore nonlinear models (e.g., nonlinear isotropic) to better understand complex mandibular material behaviour under load. Fifth, in the FEA model, most boundary conditions were defined as contact, including interfaces between fracture surfaces, the miniplate and screws, and the miniplate and mandible. Contact was defined without friction, whereupon a load application, only normal forces would be exchanged between the surfaces of the parts. The screw-mandible boundary conditions were set as bonded, representing tightly secured screws inside the mandible screw holes, keeping the miniplate fixed against the mandible in accordance with the non-locking plating principle[38,52–54]. However, unaccounted biomechanical phenomena (e.g., presence of friction or interface forces on the osteosynthesis) may influence the outcomes. Future studies could incorporate stress-strain gauge sensors during mechanical testing

(e.g., at FEA-predicted peak strain zones) to quantify stress or forces on the fixation site (miniplate and fracture) and to assess the presence of friction between components. Sixth, the FEA model was applied only to the mandibular bone; however, extending the model to other CMF bones (e.g., maxillary fracture fixation) would be a valuable future direction. Additionally, this approach may also be adapted for use in other fields, including trauma or orthopaedic surgery. For instance, assessing the impact of subtrochanteric fracture location on surgical management, comparing intermedullary nail (IMN) with extramedullary plate (EMP) fixation system[55]. If the model is applied to other bones, it is recommended to conduct a systematic review, similar to the one performed at the start of this thesis (*Chapter 2*)[1], to collect necessary input parameters (e.g., studied bone material properties or forces) for accurate simulations. Seventh, a converged mesh was used in the FEA model to ensure accurate and reliable results; however, this approach led to a relatively long computation time of approximately 45 minutes to two hours using a high-performing computer (12th Gen® Intel Core™ i9-12950HX CPU @ 2.30 GHz processor with 32 GB of RAM). Such processing times may limit the model's practicality for routine use in a clinical setting. To address this, future research could explore strategies to reduce computational time, such as modelling certain region of the bone as rigid bodies or simplifying less critical areas using coarser mesh elements. These optimisations may enhance the model's feasibility for real-time routine clinical applications. Eighth, it was assumed that the plates do not have any a priori stress. There might however be some stress due to the amendment of the plate to the generally non-straight mandible. In some cases, the plate may have been pre-bend to fit the anatomical contour of the mandible, potentially inducing localised plastic deformation in part of the plate. It is therefore recommended to quantify and bound the potential error that can be introduced by this in the outcomes (e.g., introducing regional residual forces or stresses on the plate). Finally, currently the stability of the fracture is based on the surgeon's expertise. It is recommended to make this more quantitative by establishing clear acceptable threshold for stress and displacement at the fracture site; thereby, one can immediately tell whether the fracture fixation is stable, unstable, or at risk of instability.

FEA validation process

One of the main challenges of designing an authenticated FEA model is the validation process. This means determining whether the in-silico simulations are accurate and represent the true clinical outcomes. However, there is no clear guideline regarding how to validate the FEA outcomes, nor a clear instruction of how it should be done properly. The literature suggests that one way to do this is by introducing mechanical tests of mandibular replicas in a similar setup as the FEA's[56–59]. This way one can assess whether the FEA outcomes match the physical mandibular tests and whether they are in line with the clinical fracture fixation practice. Therefore, the thesis took the steps in designing a device and methodology for this purpose (*Section III: Chapter 3-5*).

In this thesis, the following crucial steps were taken in the validation process. First, a mechanical test bench was used to evaluate the FEA outcomes by comparing the load-

displacement values. Meaning, comparing the displacement at identical amount of force and same direction in both FEA versus mechanical tests. Second, it was important that the mechanical test setup was identical to the FEA setup to ensure valid outcomes under matched conditions, including identical geometrical shaped models (mandible and osteosynthesis), location or amount of applied load, fixture, or fixation system (temporomandibular joint), mechanical material properties (mandibular bone, and osteosynthesis), and boundary conditions or interactions between the components. Third, for this purpose, a customised device was designed for positioning the mandible replicas onto the mechanical test bench, consisting of a main frame (allowing to fix the device onto the mechanical test bench) and two mandible holders (enabling to fix the mandible replicas in the customised device). The main frame was made from stainless steel to withstand forces without deformation during loading and it could be adjusted based on different mechanical test bench layouts. The mandible holders were significantly readjusted in the performed studies (Figure 3). In the first design[4] (*Chapter 3*), the mandible was fixated in the device by drilling two holes in the mandibular ramus and using two rod bars to mount it to the main frame (Figure 3A). This setup was not optimal due to weakening of the bone caused by drilling and unintentional movements of the rod bar during loading, which resulted a large difference between FEA and mechanical tests (1.64 mm mean displacement difference). In the second design[3] (*Chapter 4*), the mandible holders were improved by redesigning it as a clamp system, 3D printed from Nylon, which was positioned into the main frame using two rod bars (Figure 3B). This led to a consistently closer and smaller displacement difference (1.13 mm mean displacement difference). However, since the mandible holders deformed after multiple loading, one could not say for sure whether there were no sliding movements between the mandible and clamp system during application of load. In the final setup[2] (*Chapter 5*), the mandible holders were redesigned, consisting of 3D printed nylon inserts and aluminium frame blocks which was mounted into the main frame using bolts (Figure 3C). This modification ensured eliminating any movement (e.g., translation or rotation) at the fixture region during loading which led to consistently low displacement difference between two studies (0.59 ± 0.12 mm mean difference and SD). However, the Nylon inserts deformed after multiple loading cycles, necessitating their replacement after approximately 3-4 test experiments. Computing the interclass correlation coefficient (ICC) between the FEA and the mechanical testing displacement illustrated an excellent interclass correlation (0.93, 95% CI: 0.80-0.96). The outcomes were both reproducible and consistent, and demonstrated excellent correlation with expected biomechanical behaviour, indicating that the static FEA model is valid and may be suitable for application in clinical mandibular fracture analysis.

The minor displacement difference between both studies, which seems to be systematic, can be explained by the following factors. First, it may be attributed to the environmental dissimilarities between the studies. In the dynamic mechanical testing, the displacement is measured based on the movement of the mechanical test bench load bar from the pre-set zero position to the final position upon reaching the failure point, whereas in the static FEA software it is derived from numerical calculations. Loading during mechanical

testing may introduce pre-stress in the mandible and fixation components, potentially resulting in mechanical responses that differ from those predicted by the static FEA model, which warrants further investigations in future studies. Second, there might be still some unknown biomechanical phenomenon that can influence the outcomes (e.g., forces on the osteosynthesis, or presence of friction) and unknown marginal effect from the mandible holders on the displacement. This would be worthwhile to investigate in future studies, possibly by using stress-strain sensor gauges during mechanical testing (e.g., at the peak strain zone predicted in the FEA). Such an approach would enable the quantification of the local stresses or forces at the fixation site and on the mandible fixtures, along with defining the presence of friction and provide data to characterise frictional interactions. This can be further translated to the FEA model. These data could then be incorporated into the FEA model. Alternatively, one could also include the holders in the FEA. Finally, it is worth noting that the study developed a custom-made device specifically for the mechanical testing of the mandible, as the FEA model only involved the simulation of the mandible. Moreover, the same methodology can be extended to design a custom-made device for the mechanical testing of the other bones (e.g., maxilla, or femur) to enable verification of their respective FEA simulations.

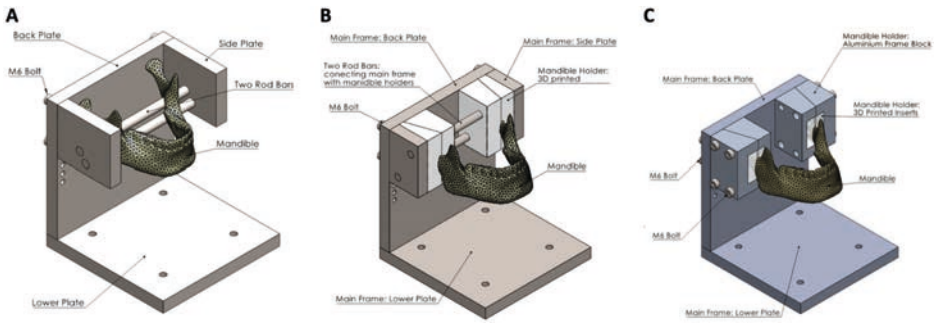

Figure 3. Development of a custom-made device for positioning mandible replicas onto the mechanical test bench. (**a**) Initial design, in which the mandible is placed within the main frame using two rod bars (Study 3)[4]. (**b**) Improves deign, where the mandible is secured using two 3D printed mandible holders, positioned between the side plates of the main frame using two rod bars (Study 4)[3]. (**c**) Refined deign in which the redesigned mandible holders (consisting of frame blocks and 3D printed inserts) are tightened in the back plate of the main frame using bolts (Study 5)[2].

Additional application of 3D computer-aided surgery

In the thesis, the applicability of 3D computer-aided surgery was further explored for other CMF bone fractures (*Section V: Chapter 7*). This was achieved by studying the patient satisfaction in the subjects with conservatively treated anterior wall frontal sinus fractures, using a validated Face-Q questionnaire, alongside measurements of fracture dimensions and the degree of dislocation based on CT data and the 3D reconstruction images in the Digital Imaging and Communication in Medicine (DICOM)[60]. The study showed that patient satisfaction was primarily affected by the aesthetic appearance of the forehead. The main determining factor affecting the satisfaction scores were the presence of a visible scar and

the depth of fracture impression. In the context of computer-aided surgery, it was observed that 3D reconstruction of CT images can be effectively used to measure fracture dimensions. This implies that, based on fracture dimension measurements, the surgeon can estimate whether conservative treatment is feasible, or a surgical approach is required. Additionally, the accuracy of these measurements can be cross verified using 3D imaging files within computer segmentation software (e.g., Mimics). This highlights the need for a precise 3D tool to support clinical decision-making regarding treatment strategy (conservative versus surgical) based on specific fracture characteristics such as fracture location, degree of dislocation, and dimensional parameters.

Future perspective

The future vision is to develop an organic system where the 3D computer-aided surgery together with validated FEA model would be implemented in the clinical trauma setting. The idea is to create a valid computer-based surgical software tool that allows in-silico 3D evaluations and FEA simulations to be easily applied by a surgeon or with a help of medical technician for the treatment of non-routine complex fractures, testing suitable osteosynthesis, or designing patient specific implants. Ideally, it can be also applied in other cases such as an oncological setting where part of the bone is resected due to a tumour and new fixation is needed to restore bone continuity. The system should be user friendly, accessible, and open source, allowing further developments by experts in the field (e.g., adding or updating osteosyntheses database). Ultimately, this dynamic 3D tool will support the surgeon in the decision-making process regarding optimal treatment without the need for revision.

The first step would be to develop an automatic flawless method for converting medical imaging data (e.g., CT, or CBCT) into a 3D workable model. A workable model refers to one in which the 3D bone model can be adjusted (e.g., create screw holes for placing the miniplate screws) and simulations can be performed without mesh errors (e.g., caused by bone geometry or segmentation deformities). In this thesis, it was found one of the biggest challenges, as 3D segmentation and modelling of the imaging data required specific software packages (e.g., Mimics, 3-Matric) and expertise, which led to an extended amount of time to acquire a workable 3D bone model. Such a 3D conversion system might be commercially available; however, an available open-source system will be beneficial in the clinical care.

The second step, in case of fracture, would be to develop an automated fracture reconstruction system. For example, when dealing with comminuted or multifragmentary fractures, the computer could reconstruct the bone fragments into their original anatomical shape using 3D puzzle solving techniques. One approach to do this is applying machine learning artificial intelligence (AI) alongside statistical shape modelling (SSM) (probabilistic distribution-based tools for capturing and displaying patterns of bone shape changes)[61–66]. This can be accomplished by using pre-set mapped bone models as templets together with identifying the anatomical landmarks, which the computer would use to reconstruct the bone fragments into its original shape. It is like solving a jigsaw puzzle in an automatised 3D environment

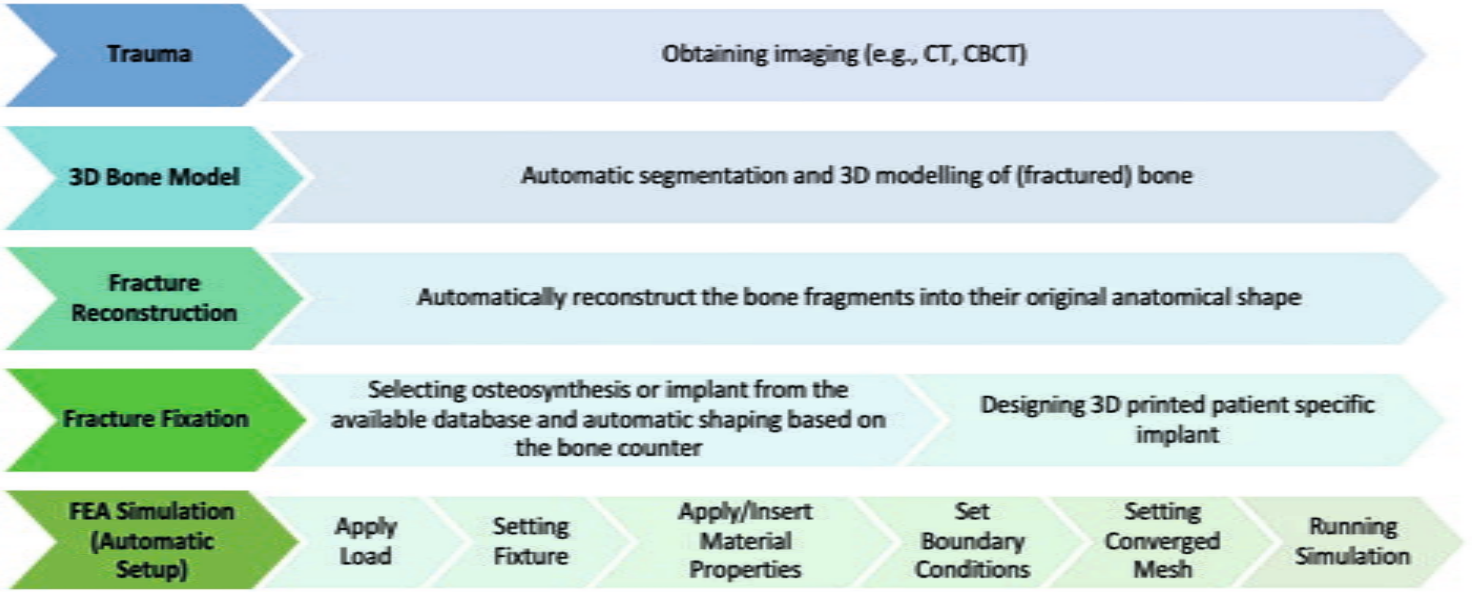

Figure 4. The concept of an automated computer-based surgical software tool that enables in silico simulations for the treatment of non-routine complex fractures, testing suitable osteosyntheses, or designing patient specific implants.

where the bone segments are matched and positioned to their original anatomical place. Additionally, bone digital twins can be applied, where digital models of bones are used for monitoring or analysis of a real-world physical object[67–69]. Furthermore, this setup provides essential inputs for determining fracture severity classification, assist the surgeon with proper fracture reconstruction that could be performed in one attempt, and aids with the fracture treatment planning. Perhaps this can be combined with the automatised 3D bone conversion system as an open-source software package.

The third step would be selection and application of the proper fixation method. There should be an extensive database containing osteosynthesis or implants, allowing the surgeon to easily choose different fixation methods for examination of fracture stability. It is also essential to have a system where the fixation system is automatically shaped or adapted to the selected bone contour. This means that the surgeon selects a fixation method, drags it to the desired position on the fracture region, and the fixation automatically reshapes to fit the selected surface of the bone. Additionally, if the standard osteosynthesis is not sufficient for fracture fixation, it would be valuable to have a setup for designing a custom-made implant tailored to the specific patient. One idea is to draw lines along the fracture fragments where the surgeon believes the fracture should be fixed, after which the software automatically generates a 3D templet of the implant that could be created through 3D printing or milling machine. While such a 3D precision-fit model may already exist in the industry in form of anatomically 3D pre-shaped plates, it remains essential to develop a user friendly open-source system that can be readily implemented in clinical settings.

The final step would be to apply the studied validated FEA model in this research to simulate the fixation stability of fractured bone. It is important to note that the developed a validated static FEA model for 3D simulation of mandibular fracture fixation, and a similar principle could be applied to other bones in the CMF region. The validated simulation setup should ideally be translated to an automatic setting. This can be achieved by using the following setup. First, a load is applied to the bone. In case of the mandible, the mastication force is applied to the selected region (e.g., incisal, molar, or premolar site). The amount of force should then be based on the patient's characteristics (e.g., sex, or age category). Second, the fixture region is defined, which in the case of the mandible would be at the temporomandibular joint regions. Third, the material properties of the parts are applied. One way to do this is by automatically selecting the desired material properties and applying them to the selected parts, such as having a material properties database of implants (e.g., titanium or biodegradable osteosynthesis) and bone (e.g., for cortical and trabecular segments). Additionally, there should be freedom to add extra material properties for custom parts (e.g., 3D printed implant). Fourth, the boundary conditions between the parts are set. Allowing one to easily define the biomechanical interactions between the fracture fragments, osteosynthesis components, and the bone and the fixation system (e.g., as bonded or contact, with or without friction). This way the constraints can be easily defined as well as allowing to assess different interactions (e.g., locking versus non-locking fixations). Fifth,

a converged mesh is created, ensuring that the simulation outcomes become independent of the mesh size. This can be automated, where the software runs multiple mesh sensitivity studies (e.g., stepwise reducing the mesh until the peak stress becomes independent of mesh size). Finally, the FEA outcomes (e.g., stress, strain, and displacement) are generated by running the simulation, and a direct visualisation of what is happening to the fracture stability using the selected fixation is obtained. Additionally, other biomechanical effects, such as creep (time-dependent deformation), could be assessed using the FEA model by incorporating them into a non-linear FEA analysis. This can be achieved by defining creep behaviour within the material properties (e.g., setting a creep constant or specifying time-dependent deformation under constant stress) and by applying a time-dependent loading condition (e.g., a constant force/load applied over predefined time increments).

This computer-aided surgery system would be invaluable in the trauma setting for non-routine complex fractures, where time is of the essence and proper treatment decision-making is crucial. It could streamline the process, starting from obtaining imaging data in the emergency department, though treatment in the operating room, and continuing with monitoring throughout the rehabilitation process (Figure 4).

Conclusion

This thesis presents the integration of 3D modelling within the CMF region and the development of a validated static FEA model for the biomechanical assessment of mandibular fractures. Based on the findings of the studies it can be concluded that the FEA model represents a substantial improvement over previous models, owing to its evidence-based systematic design methodology, rigorous experimental validation, and demonstrated clinical relevance. Validation procedures facilitated robust authentication of the numerical outcomes, with the FEA model exhibiting high accuracy, repeatability, and reliability. The FEA can effectively simulate the biomechanical behaviour of clinically non-routine complex mandibular fractures, assess different fixation strategies, and enable development of patient specific implants. This capability highlights its potential as a predictive tool in clinical practice. It constitutes as an effective computer-assisted surgical planning tool that can aid clinicians in optimising fixation strategies for complex fractures. Through the quantitative assessment of fracture characteristics and the simulation of various treatment modalities, the model facilitates evidence-based patient-specific surgical planning. Additionally, the FEA framework is adaptable and can be extended to simulate other fractured bones within the CMF or orthopaedic regions. Finally, the thesis concludes that the 3D modelling based on imaging data can be effectively applied for the precise quantification of fracture morphology, including fracture dimensional analysis and displacement measurements, which is critical for enhancing diagnostic accuracy and guiding treatment decision-making such as distinguishing between conservative versus operative treatment strategies.

REFERENCES

1. Daqiq, O. *et al.* Finite element analysis of the human mandible: a systematic review with meta-analysis of the essential input parameters. *Sci Rep* **15**, 19582 (2025).
2. Daqiq, O. *et al.* Finite element analysis of mandibular fracture fixation authenticated by 3D printed mandible mechanical testing. *Sci Rep* **15**, 14655 (2025).
3. Daqiq, O., Roossien, C. C., Wubs, F. W. & van Minnen, B. Biomechanical assessment of mandibular fracture fixation using finite element analysis validated by polymeric mandible mechanical testing. *Sci Rep* **14**, 11795 (2024).
4. Daqiq, O., Roossien, C. C., Wubs, F. W., Bos, R. R. M. & van Minnen, B. Optimisation of osteosynthesis positioning in mandibular body fracture management using finite element analysis. *Eur J Transl Clin Med* **6**, 10–25 (2023).
5. Lisiak-Myszke, M. *et al.* Application of Finite Element Analysis in Oral and Maxillofacial Surgery—A Literature Review. *Materials* **13**, 3063 (2020).
6. Merema, B. B. J., Kraeima, J., Glas, H. H., Spijkervet, F. K. L. & Witjes, M. J. H. Patient-specific finite element models of the human mandible: Lack of consensus on current set-ups. *Oral Dis* **27**, 42–51 (2021).
7. Aftabi, H. *et al.* Computational models and their applications in biomechanical analysis of mandibular reconstruction surgery. *Comput Biol Med* **169**, 107887 (2024).
8. Altuncu, F., Kazan, D. & Özden, B. Comperative evaluation of the current and new design miniplate fixation techniques of the advanced sagittal split ramus osteotomy using three-dimensional finite element analysis. *Med Oral Patol Oral Cir Bucal* **28**, 0–0 (2020).
9. Dario, V., Michelangelo-Santo, G., Roberto, B. & Fabio, F. Is All-on-four effective in case of partial mandibular resection? A 3D finite element study. *J Stomatol Oral Maxillofac Surg* **124**, 101463 (2023).
10. Falcinelli, C., Valente, F., Vasta, M. & Traini, T. Finite element analysis in implant dentistry: State of the art and future directions. *Dental Materials* **39**, 539–556 (2023).
11. Gupta, A., Dutta, A., Dutta, K. & Mukherjee, K. Biomechanical influence of plate configurations on mandible subcondylar fracture fixation: a finite element study. *Med Biol Eng Comput* **61**, 2581–2591 (2023).
12. Maintz, M. *et al.* Parameter optimization in a finite element mandibular fracture fixation model using the design of experiments approach. *J Mech Behav Biomed Mater* **144**, 105948 (2023).
13. Xue, R. *et al.* Finite element analysis and clinical application of 3D-printed Ti alloy implant for the reconstruction of mandibular defects. *BMC Oral Health* **24**, 95 (2024).
14. Guerra, R. C. *et al.* Finite element analysis of low-profile reconstruction plates for atrophic mandibles: a comparison of novel 3D grid and conventional plate designs. *Oral Maxillofac Surg* **28**, 595–603 (2024).
15. Garutti, F. C. M. B., Lehmann, R. B., Gialain, I. O. & Lima, F. F. B. de. Analysis of the atrophic mandible rehabilitated with fixed total prosthesis on mono or bicortical implants. *Braz Dent J* **35**, e245621 (2024).
16. Patussi, C. *et al.* Evaluation of different stable internal fixation in unfavorable mandible fractures under finite element analysis. *Oral Maxillofac Surg* **23**, 317–324 (2019).
17. Ammar, H. H., Ngan, P., Crout, R. J., Mucino, V. H. & Mukdadi, O. M. Three-dimensional modeling and finite element analysis in treatment planning for orthodontic tooth movement. *American Journal of Orthodontics and Dentofacial Orthopedics* **139**, e59–e71 (2011).
18. Throckmorton, G. S. Temporomandibular Joint Biomechanics. *Oral Maxillofac Surg Clin North Am* **12**, 27–42 (2000).
19. van Eijden, T. M. Three-dimensional analyses of human bite-force magnitude and moment. *Arch Oral Biol* **36**, 535–9 (1991).
20. Sasaki, K., Hannam, A. G. & Wood, W. W. Relationships between the size, position, and angulation of human jaw muscles and unilateral first molar bite force. *J Dent Res* **68**, 499–503 (1989).
21. Pruim, G. J., de Jongh, H. J. & ten Bosch, J. J. Forces acting on the mandible during bilateral static bite at different bite force levels. *J Biomech* **13**, 755–63 (1980).
22. Kang, Q. S., Updike, D. P. & Salathe, E. P. Theoretical Prediction of Muscle Forces on the Mandible During Bite. *J Biomech Eng* **112**, 432–436 (1990).
23. Abe, M., Medina-Martinez, R. U., Itoh, K. & Kohno, S. Temporomandibular joint loading generated during bilateral static bites at molars and premolars. *Med Biol Eng Comput* **44**, 1017–1030 (2006).
24. Sella-Tunis, T., Pokhojaev, A., Sarig, R., O'Higgins, P. & May, H. Human mandibular shape is associated with masticatory muscle force. *Sci Rep* **8**, 6042 (2018).

25. Takahashi, M., Yamaguchi, S., Fujii, T., Watanabe, M. & Hattori, Y. Contribution of each masticatory muscle to the bite force determined by MRI using a novel metal-free bite force gauge and an index of total muscle activity. *Journal of Magnetic Resonance Imaging* **44**, 804–813 (2016).
26. Ogawa, T. *et al.* Functional properties and regional differences of human masseter motor units related to three-dimensional bite force. *J Oral Rehabil* **33**, 729–40 (2006).
27. Merema, B. B. J., Sieswerda, J. J., Spijkervet, F. K. L., Kraeima, J. & Witjes, M. J. H. A Contemporary Approach to Non-Invasive 3D Determination of Individual Masticatory Muscle Forces: A Proof of Concept. *J Pers Med* **12**, (2022).
28. Bakke, M., Michler, L., Han, K. & Möller, E. Clinical significance of isometric bite force versus electrical activity in temporal and masseter muscles. *Scand J Dent Res* **97**, 539–51 (1989).
29. Tortopidis, D., Lyons, M. F. & Baxendale, R. H. Bite force, endurance and masseter muscle fatigue in healthy edentulous subjects and those with TMD. *J Oral Rehabil* **26**, 321–8 (1999).
30. van der Bilt, A., Tekamp, A., van der Glas, H. & Abbink, J. Bite force and electromyograpy during maximum unilateral and bilateral clenching. *Eur J Oral Sci* **116**, 217–22 (2008).
31. Acar, E., Kale, A., Haftka, R. T. & Stroud, W. J. Structural Safety Measures for Airplanes. *J Aircr* **43**, 30–38 (2006).
32. Aquilina, P., Chamoli, U., Parr, W. C. H., Clausen, P. D. & Wroe, S. Finite element analysis of three patterns of internal fixation of fractures of the mandibular condyle. *British Journal of Oral and Maxillofacial Surgery* **51**, 326–331 (2013).
33. Szucs, A., Bujtár, P., Sándor, G. K. B. & Barabás, J. Finite element analysis of the human mandible to assess the effect of removing an impacted third molar. *J Can Dent Assoc* **76**, a72 (2010).
34. Kahveci, K. & Ayranci, F. Finite element analysis of different internal fixation methods for the treatment of atrophic mandible fractures. *J Stomatol Oral Maxillofac Surg* **124**, 101276 (2023).
35. Vajgel, A. *et al.* Comparative Finite Element Analysis of the Biomechanical Stability of 2.0 Fixation Plates in Atrophic Mandibular Fractures. *Journal of Oral and Maxillofacial Surgery* **71**, 335–342 (2013).
36. Luhr, H.-G., Reidick, T. & Merten, H.-A. Results of treatment of fractures of the atrophic edentulous mandible by compression plating: A retrospective evaluation of 84 consecutive cases. *Journal of Oral and Maxillofacial Surgery* **54**, 250–254 (1996).
37. Bera, R. N. & Tiwari, P. Current Evidence for the Management of Edentulous Atrophic Mandible Fractures: A PRISMA-SWiM Guided Review. *Craniomaxillofac Trauma Reconstr* **16**, 317–332 (2023).
38. Madsen, M. J., McDaniel, C. A. & Haug, R. H. A Biomechanical Evaluation of Plating Techniques Used for Reconstructing Mandibular Symphysis/Parasymphysis Fractures. *Journal of Oral and Maxillofacial Surgery* **66**, 2012–2019 (2008).
39. Mugino, H., Takagi, S., Oya, R., Nakamura, S. & Ikemura, K. Miniplate osteosynthesis of fractures of the edentulous mandible. *Clin Oral Investig* **9**, 266–270 (2005).
40. Ellis, E. & Price, C. Treatment Protocol for Fractures of the Atrophic Mandible. *Journal of Oral and Maxillofacial Surgery* **66**, 421–435 (2008).
41. Emam, H. A., Ferguson, H. W. & Jatana, C. A. Management of atrophic mandible fractures: an updated comprehensive review. *Oral Surg* **11**, 79–87 (2018).
42. Haerle, Franz., Champy, M. & Terry, B. C. *Atlas of Craniomaxillofacial Osteosynthesis*. (Georg Thieme Verlag, Stuttgart, 2009). doi:10.1055/b-002-72255.
43. Ehrnfeld, M., Manson, P. N. & Perin, J. *Principles of Internal Fixation of the Craniomaxillofacial Skeleton*. (Georg Thieme Verlag, Stuttgart, 2012). doi:10.1055/b-002-85491.
44. Djebbar, N., Serier, B. & Bouiadjra, B. B. Finite element analysis in static and dynamic behaviors of dental prosthesis. *Structural Engineering and Mechanics* **55**, 65–78 (2015).
45. Kayabaşı, O., Yüzbasıoğlu, E. & Erzincanlı, F. Static, dynamic and fatigue behaviors of dental implant using finite element method. *Advances in Engineering Software* **37**, 649–658 (2006).
46. Kuntamukkula, S., Sinha, R., Tiwari, P. K. & Paul, D. Dynamic Stability Assessment of the Temporomandibular Joint as a Sequela of Open Reduction and Internal Fixation of Unilateral Condylar Fracture. *Journal of Oral and Maxillofacial Surgery* **76**, 2598–2609 (2018).
47. Dicker, G. J. *et al.* Static and dynamic loading of mandibular condyles and their positional changes after bilateral sagittal split advancement osteotomies. *Int J Oral Maxillofac Surg* **41**, 1131–1136 (2012).
48. Lanyon, L. E. & Rubin, C. T. Static vs dynamic loads as an influence on bone remodelling. *J Biomech* **17**, 897–905 (1984).
49. Tams, J., van Loon, J.-P., Rozema, F. R., Otten, E. & Bos, P. R. M. A three-dimensional study of loads across the fracture for different fracture sites of the mandible. *British Journal of Oral and Maxillofacial Surgery* **34**, 400–405 (1996).

50. Tams, J., van Loon, J.-P., Otten, E., Rozema, F. R. & Bos, R. R. M. A three-dimensional study of bending and torsion moments for different fracture sites in the mandible: an in vitro study. *Int J Oral Maxillofac Surg* **26**, 383–388 (1997).
51. Shetty, V., McBrearty, D., Fourney, M. & Caputo, A. A. Fracture line stability as a function of the internal fixation system. *Journal of Oral and Maxillofacial Surgery* **53**, 791–801 (1995).
52. Bohner, L. *et al.* Treatment of Mandible Fractures Using a Miniplate System: A Retrospective Analysis. *J Clin Med* **9**, 2922 (2020).
53. Braasch, D. C. & Abubaker, A. O. Management of Mandibular Angle Fracture. *Oral Maxillofac Surg Clin North Am* **25**, 591–600 (2013).
54. Raut, R., Keerthi, R., Vaibhav, N., Ghosh, A. & Kamath Kateel, S. Single Miniplate Fixation for Mandibular Symphysis and Parasymphysis Fracture as a Viable Alternative to Conventional Plating Based on Champy's Principles: A Prospective Comparative Clinical Study. *J Maxillofac Oral Surg* **16**, 113–117 (2017).
55. Daqiq, O. Subtrochanteric fracture location effect on surgical management using intermedullary nail (IMN) versus extramedullary plate (EMP): a finite element method analysis. *Eur J Transl Clin Med* **7**, 22–32 (2024).
56. Kelly, B. & Costello, C. FEA modelling of setting and mechanical testing of aluminum blind rivets. *J Mater Process Technol* **153–154**, 74–79 (2004).
57. Kluess, D. *et al.* A convenient approach for finite-element-analyses of orthopaedic implants in bone contact: Modeling and experimental validation. *Comput Methods Programs Biomed* **95**, 23–30 (2009).
58. Manea, A. *et al.* New Dental Implant with 3D Shock Absorbers and Tooth-Like Mobility—Prototype Development, Finite Element Analysis (FEA), and Mechanical Testing. *Materials* **12**, 3444 (2019).
59. Richmond, B. G. *et al.* Finite element analysis in functional morphology. *Anat Rec A Discov Mol Cell Evol Biol* **283A**, 259–274 (2005).
60. Cardinaal, M. M. B., Daqiq, O., Merema, B. B. J. & van Minnen, B. Patient satisfaction after conservative treatment of anterior wall frontal sinus fractures. *Journal of Cranio-Maxillofacial Surgery* **52**, 1228–1234 (2024).
61. van Veldhuizen, W. *et al.* Automatic virtual reconstruction of acetabular fractures using a statistical shape model. *European Journal of Trauma and Emergency Surgery* **50**, 2925–2936 (2024).
62. Niño-Sandoval, T. C., Jaque, R. A., González, F. A. & Vasconcelos, B. C. E. Mandibular shape prediction model using machine learning techniques. *Clin Oral Investig* **26**, 3085–3096 (2022).
63. Heimann, T. & Meinzer, H.-P. Statistical shape models for 3D medical image segmentation: A review. *Med Image Anal* **13**, 543–563 (2009).
64. Lamecker, H., Seebass, M., Hege, H.-C. & Deuflhard, P. A 3D statistical shape model of the pelvic bone for segmentation. in *Medical Imaging 2004: Image Processing* (eds. Fitzpatrick, J. M. & Sonka, M.) vol. 5370 1341 (SPIE, 2004).
65. Lorenz, C. & Krahnstover, N. 3D statistical shape models for medical image segmentation. in *Second International Conference on 3-D Digital Imaging and Modeling (Cat. No.PR00062)* 414–423 (IEEE Comput. Soc). doi:10.1109/IM.1999.805372.
66. Semper-Hogg, W. *et al.* Virtual reconstruction of midface defects using statistical shape models. *Journal of Cranio-Maxillofacial Surgery* **45**, 461–466 (2017).
67. Lee, J.-H. *et al.* Effectiveness of creating digital twins with different digital dentition models and cone-beam computed tomography. *Sci Rep* **13**, 10603 (2023).
68. Demir, O., Uslan, I., Buyuk, M. & Salamci, M. U. Development and validation of a digital twin of the human lower jaw under impact loading by using non-linear finite element analyses. *J Mech Behav Biomed Mater* **148**, 106207 (2023).
69. Ahn, S. *et al.* Toward Digital Twin Development for Implant Placement Planning Using a Parametric Reduced-Order Model. *Bioengineering* **11**, 84 (2024).

SECTION VIII

Summary / Samenvatting

CHAPTER 9

Summary

INTRODUCTION

Facial fracture management in craniomaxillofacial (CMF) surgery using three-dimensional (3D) modelling and finite element analysis (FEA) was studied in this thesis. The research focused on assessing the applicability, development, validation, and implementation of 3D modelling and FEA principle for mandibular fracture fixation. This was achieved through systematic approach to determine the mandibular FEA input parameter values through a systemic review with meta-analysis (**Chapter 2**), design a validated mandibular FEA model (**Chapter 3-5**), and demonstrates its applicability in complex fracture analysis (**Chapter 6**). Additionally, the impact of 3D was further explored in CMF surgery by assessing sinus frontalis fractures (**Chapter 7**).

KEY FINDINGS

Mandibular FEA input parameters

In **section II**, **chapter 2**, the essential true input parameters value needed for a proper mandibular FEA setup are explored, through a systematic review with meta-analysis of the literature containing in vivo physical human mandibular tests. This was necessary due to differences and discrepancies in the literature regarding these parameters. True values are those obtained through empirical physical testing, in contrast to values derived from theoretical calculations or computational simulations. These input parameters are the applied forces (e.g., bite and muscle force), mandibular fixture (temporomandibular joint), mandibular bone material properties (cortical and trabecular), and the boundary conditions (e.g., friction). Additionally, assessing the factors that influence these components (e.g., sex, or age). The study was registered in PROSPERO (CRD42022315303) with the search conducted in PUBMED and EMBASE (last search 6 November 2024). After screening 13023 records, 66 records were included; where only the maximum bite force (MBF) (n=60), muscle force (n=5), and mandible material properties (n=5) were found and assessed. Meta-analysis could be only applied for the MBF studies, showing the major influence of sex, age, and bite location (e.g., molar, premolar, and incisal), along with the presence of mandibular fracture or dentures. In the healthy dentulous population, males have a higher MBF than females. Individuals aged 20 to 60 years exhibit a higher MBF, followed by those under 20 and over 60. In cases of fractured mandibles fixated with miniplate osteosynthesis, MBF gradually increases during the postoperative follow-ups; however, three months postoperatively, it remains notably lower than that of a healthy non-fractured individual (mean factor difference of 2.5 in molar and 2 in incisal region). Further, MBF remains higher in partial versus complete denture wearers. Additionally, across all subgroups, highest MBF was recorded in the molar region, followed by the premolar, and the lowest in the incisal region. Concerning muscle force (n=5), only general values are available for the masseter (superficialis and profunda), temporalis (anterior and posterior), pterygoid (medial and lateral). Regarding mandibular bone material properties (n=5), the elastic modulus varied across studies with each study

also measuring other mandibular bone properties (e.g., compressive strength, Poisson's ratio). As for the muscle force and mandible material properties, it remains unclear whether the values are applicable in FEA to every individual, underscoring the need for additional research. Finally, regarding other FEA input values, no studies were found in the literature addressing the definition of mandibular fixture (temporomandibular joint) or boundary conditions (e.g., friction). This gap in research may be due to the difficulties in defining these components through physical in vivo testing; however, if feasible, future studies in these areas could offer valuable insights. In conclusion, the systematic review gives a comprehensive overview of MBF, muscle force, and mandible material properties that can be applied as guideline for defining mandibular FEA input parameters. Further, future in vivo studies are required to uncover the unknown parameters (e.g., friction) and to better specify the known parameters (e.g., muscle forces and material properties).

Creating validated mandibular FEA

In **section III**, **chapter 3-5**, the necessary steps were taken to develop a validated FEA model. The first step, in **chapter 3**, was to evaluate the applicability of FEA in CMF surgery as a proof of concept by taking the first initiative to develop a functional validated FEA model for mandibular fracture fixation. A geometrically simplified mandible 3D model was created to study the impact of mandibular body height (18, 14, and 10 mm representing moderate to severe atrophic) and plate positioning (placed at the superior mandibular border and lowered towards the inferior border along the fracture line), using a unilateral mandibular body fracture fixed with a 2.3 mm 6-hole titanium miniplate. FEA was conducted in two simulation software's (Solidworks and Comsol Multiphysics) and validated through mechanical tests of Synbone polymeric mandible replicas, positioned in a mechanical test bench using a custom-made device. The device featured an adjustable main plate that facilitated positioning it onto a mechanical test bench, along with two rod bars which acted as mandible holders fixing the mandible inside onto the device. The study made sure that the FEA and testing setup were aligned, where displacement at 200 N load was compared. FEA outcomes showed increased stress and displacement with reduced mandibular height and when the plate was lowered from the superior towards the inferior border. It effectively visualised fracture stability variations, closely matched mechanical test results (1.64 mm mean displacement difference), aligned with clinical insights, and proved useful for fracture fixation analysis. However, several limitations were noted. The simplified 3D mandible model did not fully feature a realistically shaped mandible versus the mechanical tests using the anatomically accurate Synbone mandibles. Additionally, in mechanical tests, rods were inserted into drilled holes in the ramus and angle regions, introducing slight variations between the tests and slight discrepancies from the FEA setup. These issues were addressed in the subsequent study.

Chapter 4 presents the follow-up study, where three anatomically accurate Synbone mandibles with identical straight-line fractures in the symphysis, parasymphysis, and angle regions were selected and modelled in the FEA using Solidworks software as a digital twin. Fractures

were fixated using a 2.0 mm 4-hole 1.0 mm thick miniplate positioned in three configurations, namely superior border, inferior border, and a dual plate combination. A custom made device, consisting of 3D printed mandible holder fixtures fabricated from polyamide 6 (PA6) and an adjustable main plate, was used in the polymeric mandible mechanical testing (PMMT) for positioning the mandible onto the mechanical test bench ensured consistent and realistic matched fixation in both FEA and PMMT. Mechanical tests on Synbone foam strips (comparable to the mandible replicas) were performed to define the properties. As a result, FEA effectively visualised fracture stability across fixation methods, with the two-plate configuration providing the most stability, followed by superior border plating, and least with inferior plating. The PMMT results showed a similar displacement pattern as the FEA (total displacement difference of 1.13 mm) with a smaller gap compared to the previous study, which is supporting FEA validity. The findings were in line with current clinical understanding of fracture management, reinforcing the FEA model as a reliable tool. Despite promising results, there was still room for improvements. First, Synbone mandibles, intended for educational use, showed a wide variability in cortical-trabecular compositions. Therefore, for mechanical tests one should use 3D-printed mandible with exact known material properties. Second, in the PMMT, the 3D-printed mandible holders still allowed slight movement (rotation or translation) and deformed over time during application of load, requiring design optimisation. Third, fracture reduction was not measured in PMMT, while FEA used a fixed 0.1 mm gap, which can potentially contribute to the slight displacement variations between the studies.

In **chapter 5**, a final step was taken to fine tune the FEA model in Solidworks and the validation method so called 3D printed mandible mechanical testing (3D-MMT). The main study setup was like the previous study, but with significant improvements based on the previous findings. First, jagged-line fractures, more clinically realistic than straight-line ones, were modelled in the symphysis, parasymphysis, and angle regions, with similar fixation using a 2.0 mm 4-hole titanium miniplate in three configurations (superior, inferior, and dual plating). Second, FEA fracture reduction was matched to the 0.1 mm gap distance measured in 3D-MMT. Third, mandibles for mechanical testing were 3D printed from polyamide 12 (PA12), chosen for its well-defined properties, cost-effectiveness, and testing suitability, this way ensuring identical geometry and material properties in both studies. Lastly, the mandible holders were further improved through the design of aluminium outer frame blocks incorporating PA6 inserts, which were rigidly fixed to the main plate of the custom-made device to minimise movements at the fixation points. The outcomes aligned with the previous study and were in line with the current clinical understanding of fracture management. First, dual plating offered the best stability, followed by superior and then inferior border plating. Second, stress and displacement were lowest in symphysis fractures, higher in parasymphysis, and highest in angle fractures under incisal load. Third, displacement differences between FEA and 3D-MMT were consistently lower compared to previous study (mean total difference and standard deviation of 0.59 ± 0.12 mm). Additionally, interclass correlation coefficient (ICC) was calculated by estimating variance components in a mixed

effect model for the displacement differences, showing an excellent ICC (0.93, 95% CI: 0.80–0.96), confirming strong consistent agreement between FEA and 3D-MMT. This validates FEA for studying complex fractures without requiring mechanical testing. Finally, 3D printed mandibles proved superior to commercially available replicas (e.g., Synbone or Sawbone) for validation process.

Applying validated FEA model

In **section IV**, **chapter 6**, the validated FEA model was applied for assessing complex mandibular fractures. This was achieved by investigating the biomechanical behaviour of severely atrophic edentulous mandibular fracture fixation under different clinically relevant scenarios. First, the effect of fracture side (unilateral versus bilateral), fracture reduction (fracture surface distance of 0.01, 0.1, and 1 mm), miniplate type (2.0 mm 1.0 mm thick 4-hole versus 6-hole), and screw loosening (mesial, distal, and both side of fracture) were assessed for the mandibular body fracture. Second, the effect of miniplate type and screw loosening were investigated for the unilateral angle fracture. The FEA setup was identical across all studies. The study reported two key outcomes. First, the validated FEA model proved effective for simulating complex fractures, as it accurately assessed fracture fixation in severely atrophic edentulous mandibles and aligning with clinical knowledge. Given the clinical challenges and uncertainties in treating such fractures, this in silico approach offers a valuable alternative to study their fixation. Second, the model provided new insights into critical factors affecting fracture stability in severely atrophic mandibles. Concerning body fracture simulations, the study found that bilateral fractures generate higher stress and displacement than unilateral ones, indicating a need for stronger fixation. Further, the 6-hole miniplate consistently outperformed the 4-hole, though the latter can still be effective for well-reduced unilateral fractures. Furthermore, fracture reduction was critical, where a 0.01 mm gap provided optimal stability, while larger gaps (0.1 and 1 mm) weakened fixation. Additionally, screw loosening increased stress and displacement, with maximum instability when both screws on the fracture side were removed. Finally, the 6-hole plate was less affected by screw loosening, reinforcing its preference for improved stability. Regrading unilateral angle fracture, the superiorly positioned 6-hole miniplate offered better stability than the 4-hole, though the difference in stress and displacement was minimal, indicating that a 4-hole plate may still be sufficient. Further, screw loosening reduced fixation stability, with the greatest impact when both fracture-side screws were loose. In this case, stability was more affected in the 4-hole plate, reinforcing the 6-hole plate as a better option when loosening is a concern. In conclusion, the validated FEA model proved effective for evaluating fixation in severely atrophic mandibles and is suitable for simulating other complex mandibular fractures.

Applicability of 3D in other bones in the CMF region

Section V, **chapter 7**, briefly explored the use of 3D models for evaluating other bone fractures in CMF region, focusing on patient satisfaction in conservatively treated sinus frontalis fractures. **The study aims** to determine patient forehead aesthetics satisfaction after conservative

treatment of non-dislocated and dislocated anterior wall frontal sinus fractures. Prospectively, patients older than 15 years of age with a frontal sinus fracture, treated conservatively between the period of 2010-2020, were analysed. The Face-Q questionnaire was used to assess patient satisfaction, and the fracture dimensional properties were measured using computed tomography. The results were compared with a matched non-fractured control group. In the study, the mean total Face-Q questionnaire score was 114.77 (SD=17.38) versus 114.23 (SD=15.23) (research- versus control group, respectively), with a mean difference of 0.55 (SD=4.85), which was not significant (p=0.91). The size of impression area did not appear to have a linear relationship with patient satisfaction within the entire population (p=0.87; r=0.00). Presence of a scar in the fracture site was a significant predictor of patient satisfaction, contributing to 31% of the entire population's overall score (p=0.01) and 57% in the dislocated fracture population (p=0.003). In conclusion, the conservatively treated patients' satisfaction score was comparable to the control group. A higher satisfaction score after a conservative treatment is associated with the absence of a scar on the fracture site, even with dislocations up to 6 mm at the deepest impression point. In addition, this study as an example shows that 3D model (CT fracture dimensional measurement and degree of dislocation) can have an impact in fracture management decision making process (e.g., conservative versus surgical approach). Therefore, 3D models of medical images (CT reconstruction in DICOM or 3D segmentation in 3D imaging software's) are applicable and essential tools in CMF surgery.

CONCLUSION

This thesis presents the integration of 3D modelling techniques within the CMF region and the development of a rigorously validated FEA model for the biomechanical assessment of mandibular fractures. A validated static FEA model was developed for mandibular fracture analysis which accurately replicated the biomechanical behaviour of non-comminuted fractures fixation. Validation was achieved through comparing FEA outcomes with mechanical testing on mandible replicas using a custom-made device that was matched to the FEA setup. The outcomes were also aligning with the current clinical understanding of fracture management. Furthermore, the validated FEA model proved suitable for analysing complex fractures as it was applied for simulation of severely atrophic edentulous mandibular fracture analysis. This offered new insights into the fixation of severely atrophic mandibular fractures along with proving the promising potential of the validated FEA for studying non-routine complex mandibular fractures. Therefore, the findings presented in this thesis substantiate the conclusion that the proposed FEA model represents a marked advancement over prior models, owing to its evidence-based and systematically structured design methodology, thorough experimental validation, and demonstrated clinical relevance. This FEA capability demonstrates significant potential as a predictive tool in clinical settings. It functions as an effective computer-assisted system for surgical planning and helping clinicians to optimise fixation strategies for complex fractures. By quantitatively analysing fracture features and

simulating different fixation strategies, the model supports evidence-based personalised surgical planning for each patient. Additionally, the FEA approach is inherently adaptable and may be extended to simulate fractures in other CMF bones or broader orthopaedic contexts. However, the static FEA model (constant-in-time loading) might not fully resemble the cyclic biomechanics of the mastication forces in the clinical setting. Therefore, adapting the model to a dynamic FEA framework may more accurately capture the cyclic characteristics of masticatory forces, providing new insights into the structural response under repetitive loading conditions. Additionally, the static FEA enables the assessment, quantification, and visualisation of the biomechanical performance of various fracture fixation types and methods; however, it remains challenging to definitively determine the clinical stability of the fixation configuration or the sufficiency of plate strength under physiological conditions in the clinical setting. Furthermore, converting clinical CT data into a generic workable 3D digital twin model requires specialized and often costly software's, considerable expertise, and significant processing time. Thereby, this renders the process challenging, underscoring the importance of implementing an open-source automation process. Similarly, the assembly of 3D models and the setup of FEA require specialised knowledge and manual input, including 3D modelling of the osteosynthesis material, adaptation of the 3D miniplate to conform to the bone's anatomical contours, configuring of FEA parameters, and interpretation of the simulation outcomes. To address these challenges, it is imperative to develop an open-source user-friendly platform that streamlines and automates these processes, thereby making them more accessible to clinicians and technicians without extensive technical backgrounds. Finally, the research results demonstrates that 3D modelling derived from medical imaging data enables accurate quantification of fracture morphology, including measurements of fracture dimensions and displacements, as exemplified by its application to sinus frontalis fractures. Such capabilities are essential for improving diagnostic accuracy, supporting clinical decision-making, and ultimately enhancing patient care.

CHAPTER 10

Samenvatting

INTRODUCTIE

In dit proefschrift werd de behandeling van aangezichtsfracturen bestudeerd met behulp van driedimensionale (3D) computermodellen en volgens de eindige-elementen analyse (EEA; Eng. Finite Element Analysis of FEA) binnen mondziekten, kaak- en aangezichtschirurgie (MKA-chirurgie). Het onderzoek richtte zich met name op het ontwikkelen en valideren van een 3D-computer model welke gebaseerd is op de EEA van de fixatie van mandibula (onderkaak) fracturen. Als eerste werd een systematisch literatuuronderzoek uitgevoerd, waarmee de benodigde invoerparameters voor de opzet van een EEA-model van de mandibula werden bepaald (hoofdstuk 2)**.** Het op basis hiervan werd een nieuw EEA-model ontworpen wat aan de hand van niet-complexe fracturen werd gevalideerd en door ontwikkelt (hoofdstukken 3 t/m 5). Vervolgens werd het ontwikkelde EEA-model toegepast voor de analyse van complexe fracturen (hoofdstuk 6). Daarnaast werd de impact van 3D analyse van aangezichtsfracturen verder onderzocht door het beoordelen van sinus frontalis (voorhoofdsholte) fracturen (hoofdstuk 7).

BELANGRIJKSTE BEVINDINGEN

EEA-invoerparameters voor mandibula fracturen

In Sectie II, Hoofdstuk 2, zijn de waarden van de essentiële invoerparameters geïdentificeerd die noodzakelijk zijn voor het opstellen van een accurate en betrouwbare eindige-elementen analyse (EEA) van de mandibula. Dit werd gerealiseerd door het opstellen van een systematisch literatuuroverzicht, specifiek gericht op studies waarin in-vivo fysieke testen op menselijke onderkaken zijn uitgevoerd. Deze invoerparameters omvatten de optredende krachten op het kaakbot tijdens functie (bijt- en spierkrachten), het fixatiepunt van de mandibula aan de schedel (kaakgewricht), de materiaaleigenschappen van het kaakbot (corticaal en trabeculair), en frictie of wrijvingskrachten tijdens functie van de onderkaak. Daarnaast werden de factoren die deze componenten beïnvloeden, zoals geslacht en leeftijd, geëvalueerd. Deze benadering was noodzakelijk vanwege de aanzienlijke variabiliteit en inconsistenties in de literatuur met betrekking tot de invoerparameters. In deze studie werd specifiek gezocht naar daadwerkelijk gemeten waarden, die zijn verkregen uit empirische fysieke testen op menselijke onderkaken, in tegenstelling tot waarden die zijn afgeleid uit theoretische aannames of numerieke modellering.

De studie werd geregistreerd in PROSPERO (CRD42022315303), en de systematische zoekopdracht werd uitgevoerd in PubMed en Embase, met de laatste zoekopdracht op 6 november 2024. Na het screenen van 13.023 records werden 66 artikelen geselecteerd. Hierbij werd bruikbare informatie gevonden over de maximale bijtkracht (Eng. mandibular bite force of MBF) (n=60), spierkracht (n=5), en materiaaleigenschappen van de mandibula (n=5). Een meta-analyse kon uitsluitend worden toegepast op de MBF-gegevens, waaruit bleek dat geslacht, leeftijd, en bijtlocatie (o.a. molaar-, premolaar- en incisale regio) een

aanzienlijke invloed hebben op de bijtkracht. Daarnaast bleek ook de aanwezigheid van mandibula fracturen of gebitsprothesen invloed te hebben op de MBF. Binnen de gezonde dentate (betande) populatie vertonen mannen een hogere gemiddelde MBF dan vrouwen. Personen tussen de 20 en 60 jaar laten de hoogste MBF-waarden zien, gevolgd door individuen jonger dan 20 en ouder dan 60 jaar. In gevallen van een mandibulafractuur die is gefixeerd met miniplaatosteosynthese, vertoont de MBF een geleidelijke toename tijdens de postoperatieve follow-up momenten. De MBF blijft echter gedurende de eerste drie postoperatieve maanden aanzienlijk lager dan die van gezonde individuen zonder fractuur, met een gemiddeld verschil van een factor 2.5 in de molaar regio en een factor 2 in de incisale regio. Verder blijft de MBF hoger bij dragers van een gedeeltelijke gebitsprothese in vergelijking met personen met een volledige gebitsprothese. Bovendien werd in alle subgroepen de hoogste MBF gemeten in de molaar regio, gevolgd door de premolaar regio, met de laagste waarde in de incisale regio. Wat betreft spierkracht (n=5), zijn er alleen algemene waarden beschikbaar voor de m. masseter (superficialis en profunda), de m. temporalis (anterieur en posterior), en de m. pterygoideus (mediaal en lateraal). Ten aanzien van de materiaaleigenschappen van het mandibula bot (n=5) varieerde de elasticiteitsmodulus tussen de geïncludeerde studies, waarbij elke studie tevens andere eigenschappen van het mandibula bot heeft gemeten, zoals druksterkte en Poisson's ratio. Wat betreft spierkracht en materiaaleigenschappen van de mandibula blijft onduidelijk in hoeverre de beschikbare waarden toepasbaar zijn in EEA-modellen voor individuele patiënten, hetgeen de noodzaak voor verder onderzoek benadrukt. Ten slotte werden in de literatuur geen studies gevonden die de definitie van mandibulaire fixatie (kaakgewricht) of EEA-randvoorwaarden (Eng: Boundary conditions) bestuderen. Deze kennislacune kan worden verklaard door de complexiteit van het definiëren van deze componenten via fysieke in-vivo testen. Toekomstige studies kunnen mogelijk wel inzicht geven in deze domeinen. Concluderend biedt de systematische review een uitgebreid overzicht van de MBF, spierkracht en materiaaleigenschappen van de mandibula, welke als richtlijn kunnen dienen voor het ontwikkelen van mandibulaire EEA-modellen. Daarnaast zijn toekomstige in-vivo studies essentieel om enerzijds onbekende parameters zoals wrijvingskrachten of frictie te definiëren en daarnaast de al bekende parameters (o.a. spierkrachten en materiaaleigenschappen) beter te specificeren.

Het ontwikkelen van een gevalideerd EEA-model van de mandibula

In **Sectie III, Hoofdstukken 3-5**, worden de verschillende stappen beschreven voor de ontwikkeling van een gevalideerd EEA-model van de mandibula. De eerste stap, beschreven in **Hoofdstuk 3**, betrof het evalueren van de toepasbaarheid van EEA in MKA-chirurgie als 'proof of concept', door te beginnen met de ontwikkeling van een gevalideerd EEA-model voor de fixatie van mandibulafracturen. Er werd een geometrisch vereenvoudigd 3D-model van de mandibula gecreëerd om de invloed van de hoogte van het corpus mandibulae (18, 14 en 10 mm, welke respectievelijk matige tot ernstige atrofie representeren) en de positionering van de osteosyntheseplaat (variërend van de bovengrens tot de onderrand van de mandibula) te bestuderen. Dit werd uitgevoerd met een unilaterale mandibulaire fractuur, gefixeerd met een 2.3 mm 6-gats titanium plaatosteosynthese. De EEA werd uitgevoerd in

twee simulatie softwarepakketten (Solidworks en Comsol Multiphysics). Dit werd gevalideerd aan de hand van mechanische testen van Synbone polymeer mandibula's, gepositioneerd op een mechanische testbank met behulp van een op maat gemaakte testopstelling. De studie toonde overeenkomsten aan tussen de EEA-analyse en de eerdere mechanische experimenten, met een gemiddeld verplaatsing verschil van 1.64 mm. Dit verschil duidt erop dat het EEA-model niet volledig was gevalideerd, waardoor niet met zekerheid kon worden geconcludeerd dat het model al geschikt was voor klinische toepassing zonder aanvullende validatie met mechanische testen. Verdere optimalisatie op basis van de bevindingen uit deze studie werden uitgevoerd in de vervolgstudies zoals beschreven in hoofdstuk 4 en 5. Daarnaast, bleken de EEA-uitkomsten met betrekking tot de positionering van de plaat consistent met de geldende klinische inzichten. Op basis van deze uitkomsten werden wel enkele beperkingen van het model vastgesteld. Ten eerste bleek het vereenvoudigde 3D-model van de mandibula niet voldoende realistisch ten opzichte van de anatomisch accurate Synbone modellen. Daarnaast vertoonden de fixatiepunten van de mandibula in de testopstelling ongewenste variaties, wat leidde tot discrepanties bij de vergelijking met de EEA-resultaten. Ook dit werd nader onderzocht in de vervolgstudies.

Hoofdstuk 4 beschrijft de vervolgstudie van hoofdstuk 3, waarbij drie anatomisch accurate Synbone mandibula's met identieke rechtlijnige fracturen in de symfyse-, parasymfyse- en angulus regio's werden bestudeerd. Op basis hiervan werd een 3D-digitaal tweelingmodel van de mandibula gegenereerd en vervolgens toegepast in de EEA-analyse welke uitgevoerd werd met Solidworks software. De mandibula fracturen werden gefixeerd met een 2.0 mm 4-gats miniplaat van 1.0 mm dikte, gepositioneerd in drie configuraties: de bovenrand, de onderrand, en een combinatie van twee platen. Voor de mechanische testen van de mandibula's werd gebruik gemaakt van een op maat gemaakte testopstelling met 3D-geprinte kaakhouders vervaardigd uit polyamide 6 (PA6). Hierdoor werd een consistente en realistische fixatie gewaarborgd, zowel in het EEA-model als in de controle opstelling met fysieke mechanische testen. Daarnaast werden mechanische testen uitgevoerd op de Synbone schuim strips om de materiaaleigenschappen van de artificiële kaken beter te definiëren. De uitkomsten van de mechanische testen vertoonden een vergelijkbaar verplaatsingspatroon als de EEA. De verschillen tussen de EEA en de mechanische testen waren kleiner dan in de voorgaande studie, met een gemiddeld verplaatsingsverschil van 1.13 mm. De bevindingen waren opnieuw consistent met de huidige klinische inzichten omtrent fractuurfixatie. Ondanks de veelbelovende resultaten bleef er ruimte voor verbetering. Ten eerste vertoonden de Synbone mandibula's, die bedoeld zijn voor educatief gebruik, een grote variabiliteit in de samenstelling van corticaal en trabeculair bot. Daarom zou voor mechanische tests een 3D-geprinte mandibula met exact bekende materiaaleigenschappen moeten worden gebruikt. Ten tweede lieten de 3D-geprinte mandibula houders nog lichte beweging (rotatie of translatie) toe en vervormden zij in de loop van de tijd tijdens herhaalde mechanische belasting. Ten derde werd de gap in de fractuurspleet van de Synbone modellen na anatomische fractuurreductie niet gemeten. In de EEA-analyse werd een gap van 0.1 mm gehanteerd, wat mogelijke lichte variaties in de resultaten kan geven.

Hoofdstuk 5 beschrijft de laatste stap in het verfijnen van het ontwikkelde EEA-model in de Solidworks software en het optimaliseren van de validatiemethode van de 3D-geprinte mandibula modellen voor de mechanische testen. Gekartelde fracturen (zigzagpatroon), die klinisch realistischer zijn dan rechtlijnige fracturen, werden gemodelleerd in de symfyse-, parasymfyse- en angulus regio's. De fixatie werd uitgevoerd met een 2.0 mm 4-gats titanium miniplaat in drie configuraties: superieur, inferieur, en een combinatie van deze. Ten tweede werd in de mechanische testmodellen een nagenoeg volledige fractuurreductie bereikt, waardoor voor de EEA-analyse een gap van 0.1 mm werd gehanteerd. Ten derde werden de mandibula's voor mechanische testen 3D-geprint uit polyamide 12 (PA12) met goed gedefinieerde materiaaleigenschappen, waardoor geometrie en materiaaleigenschappen in beide studies op elkaar werden afgestemd. Ten slotte werden de mandibula houders verder geoptimaliseerd door het ontwerpen van aluminium blokken met PA6 inzetstukken, om beweging ter hoogte van de fixatiepunten te minimaliseren. De verplaatsingsverschillen tussen de EEA en de mechanische tests waren daarmee nog geringer dan in de voorgaande studies, met een gemiddeld totaal verschil en standaarddeviatie van 0.59 ± 0.12 mm. Bovendien werd de interclass correlatiecoëfficiënt (ICC) berekend door de variantiecomponenten te schatten met behulp van een mixed-effect model op basis van de verplaatsingsverschillen, wat resulteerde in een uitstekende ICC van 0.93% (0.93, 95%CI: 0.80–0.96). Hieruit werd geconcludeerd dat het in deze studie ontwikkelde EEA voor de mandibula voldoende gevalideerd is voor het bestuderen van complexe fracturen zonder dat aanvullende mechanische testen noodzakelijk zijn.

Toepassing van het gevalideerde EEA mandibula model

In **Sectie IV, Hoofdstuk 6**, werd het gevalideerde EEA-model zoals beschreven in hoofdstuk 5, ingezet voor de evaluatie van complexe mandibulafracturen. Dit werd gerealiseerd door het biomechanische gedrag van de fixatie van ernstig atrofische edentate mandibula fracturen te analyseren onder verschillende klinisch relevante scenario's. Ten eerste werd voor fracturen van het corpus mandibulae de invloed geëvalueerd van (1) de fractuurlocatie (unilateraal versus bilateraal), (2) de mate van fractuurreductie (fractuuroppervlakte-afstanden van 0.01, 0.1, en 1 mm), (3) het type miniplaat (2.0 mm dikke 1.0 mm 4-gats versus 6-gats), en (4) losgeraakte schroeven (mesiaal, distaal, en aan beide zijden van de fractuur).Ten tweede werd, voor de unilaterale angulus fractuur, de invloed onderzocht van het type miniplaat en van losgeraakte schroeven. Deze studie leverde twee belangrijke bevindingen op. Ten eerste kon het gevalideerde EEA-model effectief worden ingezet voor het simuleren van complexe mandibula fracturen. Gezien de klinische uitdagingen en onzekerheden bij de behandeling van dergelijke fracturen, biedt deze in-silico benadering een waardevolle aanvulling voor het bestuderen van de fixatie mogelijkheden. Ten tweede bood het model nieuwe inzichten in kritieke factoren die de fractuurstabiliteit beïnvloeden bij de ernstig atrofische mandibula. Met betrekking tot de simulaties van corpus mandibula fracturen toonde de analyse aan dat bilaterale fracturen hogere spanningen en verplaatsingen veroorzaken dan unilaterale fracturen, wat wijst op de noodzaak voor sterkere fixatie. Daarnaast presteerde de 6-gats miniplaat consequent beter dan de 4-gats miniplaat. De

laatste kan nog steeds effectief zijn bij goed-gereduceerde unilaterale fracturen, mits er geen schroeven losraken. Bovendien bleek fractuurreductie cruciaal te zijn, waarbij een fractuur gap van 0.01 mm de optimale stabiliteit bood, terwijl grotere gap (0.1 en 1 mm) de fixatie verzwakten. Daarnaast leidden loszittende schroeven tot verhoogde spanningen en verplaatsingen, met de grootste instabiliteit wanneer aan beide zijden van de fractuur schroeven werden verwijderd. In een dergelijke situatie werd de stabiliteit van de 4-gats plaat sterker beïnvloed, wat de 6-gats plaat bevestigt als betere optie wanneer er een verhoogd risico is op losse schroeven. Door de betere stabiliteit van de gereponeerde fractuur met een 6-gats plaat bleek deze minder gevoelig voor het optreden van losse schroeven. Voor de unilaterale angulus fractuur bood de langs de linea obliqua externa geplaatste 6-gats miniplaat een betere stabiliteit dan de 4-gats plaat. Hierbij bleek echter wel dat het verschil in spanning en verplaatsing tussen de situatie met een 4-gats miniplaat ten opzichte van een 6-gats miniplaat minimaal was. Dit ondersteunt de visie dat een 4-gats plaat in de meeste situaties voldoende kan zijn bij de reductie van angulus mandibula fracturen. Uit de studie kan worden geconcludeerd dat het gevalideerde EEA-model effectief is gebleken voor het evalueren van fixatie bij ernstig atrofische mandibula's en daarmee ook geschikt lijkt voor het simuleren van andere complexe mandibulaire fracturen.

Toepasbaarheid van 3D in andere botfracturen in het MKA-gebied

Sectie V, Hoofdstuk 7 verkent het gebruik van 3D-modellen voor de evaluatie van andere botfracturen in het MKA-gebied, met een focus op de patiënttevredenheid bij conservatief behandelde voorwandfracturen van de sinus frontalis. Het doel van de studie was het vaststellen van de patiënttevredenheid over de esthetiek van het voorhoofd na conservatieve behandeling van niet-verplaatste (niet gedisloceerde) en verplaatste (gedisloceerde) fracturen van de voorwand van de sinus frontalis. In een prospectief onderzoek werden patiënten geanalyseerd van 15 jaar en ouder die tussen 2010 en 2020 die conservatief (zonder chirurgische interventie) werden behandeld voor een sinus frontalis fractuur. De Face-Q vragenlijst werd gebruikt om de patiënttevredenheid te meten, terwijl de fractuurafmetingen werden bepaald op basis van de computertomografie (CT) scans. De resultaten werden vergeleken met een vergelijkbare controlegroep zonder fracturen. De gemiddelde totale Face-Q score 114.77 (SD = 17.38) voor de fractuurgroep versus 114.23 (SD = 15.23) voor de controlegroep met een gemiddeld verschil van 0.55 (SD = 4.85) ($p = 0.91$). De diepte van het fractuurgebied vertoonde geen lineaire relatie met de patiënttevredenheid binnen de fractuurgroep ($p = 0.87$; $r = 0.00$). De aanwezigheid van een litteken in het fractuurgebied bleek een significante voorspeller te zijn van de patiënttevredenheid in de fractuurgroep, met een bijdrage van 31% aan de totale score in de groep ($p = 0.01$) en 57% in de verplaatste fractuur populatie ($p = 0.003$). Concluderend was de tevredenheidsscore van de conservatief behandelde patiënten met een sinus frontalis fractuur vergelijkbaar met die van de controlegroep zonder doorgemaakte fractuur. Een hogere tevredenheidsscore na conservatieve behandeling was geassocieerd met de afwezigheid van een litteken in het fractuurgebied, zelfs bij verplaatsingen tot 6 mm op het diepste punt van de fractuur. Daarnaast toont deze studie als voorbeeld aan dat 3D-modellen, zoals CT-gebaseerde

fractuurdimensiemetingen en de mate van verplaatsing, een invloed kunnen uitoefenen op het besluitvormingsproces bij de behandelkeuze van fracturen (bijv. de keuze tussen een conservatieve en chirurgische benadering).

Conclusie

Dit proefschrift presenteert de toepassing van 3D-computer modellen binnen het MKA-gebied en de ontwikkeling van een gevalideerd EEA-model voor de biomechanische beoordeling van mandibulafracturen. In dit proefschrift is een gevalideerd statisch EEA-model ontwikkeld voor de analyse van mandibulafracturen, dat het biomechanische gedrag van de fixatie van niet-commutatieve fracturen nauwkeurig nabootst. De validatie werd uitgevoerd door de resultaten van het EEA te vergelijken met mechanische testen op mandibula replica's, waarbij gebruik werd gemaakt van een op maat gemaakte testopstelling die was afgestemd op de EEA-opzet. De resultaten kwamen overeen met de huidige klinische inzichten van behandelconcepten van mandibula fracturen. Verder bleek het gevalideerde EEA-model geschikt voor de analyse van complexe fracturen, op basis van de gevonden uitkomsten de simulatie van reductie en fixatie van ernstig atrofische edentate mandibulafracturen. Deze bevindingen hebben nieuwe inzichten verschaft in de fixatie van complexe mandibula fracturen en benadrukken de potentie van het gevalideerde EEA-model als instrument voor de analyse van niet-routinematige complexe mandibulaire fracturen. Het ontwikkelde EEA-model is met de uitgevoerde studies substantieel verbeterd ten opzichte van in de literatuur beschreven simulatiemodellen en daarnaast veel potentie heeft voor klinische toepassingen. Dit is vooral door de systematische werkwijze waarop de EEA-model is ontworpen en gevalideerd werd met behulp van de gematchte mechanische testen. Het ontwikkelde EEA-model heeft een goede potentie om toegepast worden als een effectief computerondersteund hulpmiddel bij de voorbereiding van chirurgische behandeling van complexe fracturen, en biedt het ondersteuning aan clinici bij het optimaliseren van fixatiestrategieën. Bovendien is de EEA-opzet aan te passen voor de analyse van andere botfracturen binnen zowel het MKA- als orthopedische domein. Het statische EEA-model, waarin gebruik wordt gemaakt van tijdonafhankelijke, constante belasting, weerspiegelt echter mogelijk niet volledig de cyclische biomechanica van kauwkrachten zoals die zich in de klinische praktijk voordoen. Het omzetten van het model naar een dynamisch EEA-model kan de cyclische aard van kauwkrachten nauwkeuriger weergeven, wat kan bijdragen aan nieuwe inzichten in de biomechanische impact van kauwkrachten op fractuurfixatie. Het statische EEA-model maakt het mogelijk om de biomechanische prestaties van verschillende typen en methode betreft fractuurfixatie te beoordelen en te visualiseren. Toch blijft het in de klinische praktijk uitdagend om met zekerheid de stabiliteit van de fractuurfixatie en de voldoende sterkte van de plaat onder fysiologische omstandigheden vast te stellen. Daarnaast vereist het omzetten van CT-beelden naar een generiek bruikbaar 3D-digitaal tweelingmodel specifieke kostbare software, aanzienlijke expertise, en een uitgebreide verwerkingstijd. Dit maakt het proces complex en benadrukt het belang van het ontwikkelen van een open-source geautomatiseerd proces. Bovendien vereist het samenstellen van 3D-modellen en het opzetten van het EEA-model gespecialiseerde kennis en handmatige

input. Dit omvat onder meer het 3D-modelleren van de osteosynthese, het aanpassen van de 3D-miniplaat aan de anatomische contouren van het bot, het configureren van EEA-parameters, en de interpretatie van de EEA-uitkomsten. Om deze uitdagingen te overwinnen, is het van cruciaal belang een open-source gebruiksvriendelijk platform te ontwikkelen dat deze processen stroomlijnt en automatiseert, waardoor ze toegankelijker worden voor clinici en technici zonder uitgebreide technische achtergrond.

Tot slot toont dit proefschrift aan dat fractuurmorfologie kwantitatief kan worden bepaald door middel van 3D-computer modellen op basis van medische beeldvorming, bijvoorbeeld door het meten van fractuurafmetingen en de mate van dislocatie. Dergelijke mogelijkheden zijn van essentieel belang voor het verbeteren van de diagnostische nauwkeurigheid, het ondersteunen van klinische besluitvorming, en het uiteindelijk optimaliseren van de patiëntenzorg.

APPENDIX

About the author
List of publications
Dankwoord
Sponsors

سلام جان
Елена Лиза
امید، رویا، آرزو
Ромми
والنتینو
Тобиас
زنده باد زندگی

ABOUT THE AUTHOR

Omid Daqiq p/o Goudberg (nickname: *Valentino*) was born on the 23rd of April 1990, in Ryazan, Soviet Union. He never got to know his mother (Elena-Lisa), who passed away during childbirth. He was raised by his father (Salam Jan), in Iran until the age of 12. Following his father's death, he arrived in the Netherlands in 2004 as an unaccompanied asylum seeker, without any family. There, he grew up in various foster homes. Due to the absence of official documents (e.g., a birth certificate or identity card), he remained stateless until 2022. Nevertheless, this did not stop him from pursuing his lifelong dream of becoming a doctor.

He completed his senior general secondary education (HAVO) at the Vincent van Gogh School in Assen (2008). Thereafter, he began studying Engineering at the University of Applied Sciences in Groningen (2008-2012), completing the program in 2016. Subsequently, he obtained a pre-master in Life Science and Technology at the University of Groningen (2013), followed by his master's degree in Biomedical Engineering at the same university (2013–2015). During his master study, he also earned a pre-university education degree (VWO) from the Open University in Groningen and completed the propaedeutic year of Medical Imaging and Radiation Therapy at the University of Applied Sciences in Groningen (2013–2014). These academic achievements enabled him to get accepted to studying medicine at the University of Amsterdam, at the Academic Medical Center (AMC) (2014-2019). Remarkably, he accomplished all of this without a residence permit and while being stateless.

After completing his medical degree, he was unable to begin working as a doctor due to the lack of official documentation. Nevertheless, he remained hopeful and continued contributing through voluntary work, including research activities. In 2022, following the fall of Kabul, he was finally able to obtain proof of identity from the Afghan embassy. This enabled him to apply for and receive a work permit as a researcher, allowing him to officially start his PhD program at the University Medical Center Groningen (UMCG). Obtaining a work permit finally allowed him to start a new life in the Netherlands. In November 2024, he married his long-standing girlfriend, Rommy Anna Goudberg. Subsequently, in February 2025, he became the proud father of a son, Tobias Benjamin Goudberg. In September 2025, he began his specialisation as General Practioner (GP) at the University Medical Center Groningen (UMCG). Additionally, he maintains a strong interest in surgical procedures, including minor and aesthetic procedures. Furthermore, he is passionate about new technologies in computer science, including artificial intelligence and digital innovations in medicine.

In his free time, he enjoys a variety of activities including sports (ranging from cycling and hiking to playing table tennis with friends), music, cooking, nature, and traveling to explore new places around the world. Most of all, he values spending quality time with loved ones, both friends and family.

LIST OF PUBLICATIONS

Finite element analysis of the human mandible: a systematic review with meta-analysis of the essential input parameters.
Daqiq O, Gareb B, Spijkervet FKL, Wubs FW, Roossien CC, van Minnen B.
Sci Rep. 2025 Jun 4;15(1):19582. doi: 10.1038/s41598-025-03959-9. PMID: 40467626.

Optimisation of osteosynthesis positioning in mandibular body fracture management using finite element analysis.
Daqiq O, Roossien CC, Wubs FW, Bos RR, van Minnen B.
Eur J Transl Clin Med 2023;6(2):10-25. doi:10.31373/ejtcm/163427.

Biomechanical assessment of mandibular fracture fixation using finite element analysis validated by polymeric mandible mechanical testing.
Daqiq O, Roossien CC, Wubs FW, van Minnen B. Sci Rep. 2024 May 23;14(1):11795. doi: 10.1038/s41598-024-62011-4. PMID: 38782942.

Finite element analysis of mandibular fracture fixation authenticated by 3D printed mandible mechanical testing.
Daqiq O, van Minnen B, Spijkervet FKL, Wubs FW, Lunter G, Roossien CC.
Sci Rep. 2025 Apr 26;15(1):14655. doi: 10.1038/s41598-025-98732-3. PMID: 40287549.

In silico analysis of severely atrophic edentulous mandibular body and angle fracture fixation using a validated finite element analysis model
Daqiq O, Wubs FW, Spijkervet FKL, Roossien CC, van Minnen B.
Submitted: JOSM

Patient satisfaction after conservative treatment of anterior wall frontal sinus fractures.
Cardinaal MMB, **Daqiq O**, Merema BBJ, van Minnen B.
J Craniomaxillofac Surg. 2024 Nov;52(11):1228-1234. doi: 10.1016/j.jcms.2024.08.002. PMID: 39181743.

Subtrochanteric fracture location effect on surgical management using intermedullary nail (IMN) versus extramedullary plate (EMP): a finite element method analysis.
Daqiq O.
Eur J Transl Clin Med. 2024;7(1):22-32. doi:10.31373/ejtcm/187180.

How Does Mechanism of Injury Relate to Similar Fracture Patterns in Bilateral Displaced Intra-articular Calcaneal Fractures?
Daqiq O, Sanders FRK, Schepers T.
J Foot Ankle Surg. 2020 Nov-Dec;59(6):1162-1166. doi: 10.1053/j.jfas.2020.04.006. PMID: 32828628.

DANKWOORD

Leden van het bestuur van de afdeling MKA-chirurgie, het UMCG, de Boering Stichting, en de afdeling P&O, graag begin ik met een citaat: *"Bijzondere mensen blijven altijd in je gedachten"* en dat zijn jullie. Vanaf de eerste dag hebben jullie in mij geloofd en mij gesteund. Dat heeft mij diep geraakt en geïnspireerd. Toen ik bij de afdeling MKA-chirurgie kwam, bracht ik een flink aantal diploma's mee, maar beschikte ik nog niet over de benodigde werkvergunning. Dankzij jullie kon ik toch aan de slag. Ik mocht starten met onderzoekswerk op basis van een nulurencontract, waardoor ik mijn onderzoek kon oppakken en voortzetten. Niet veel later hebben jullie mij op indrukwekkende wijze geholpen bij het verkrijgen van een werkvergunning voor drie jaar. Hierdoor kon ik mijn leven in dit prachtige land officieel voortzetten. Na achttien jaar in Nederland te hebben verbleven, was ik op 1 maart 2022 voor het eerst in staat om mij in te schrijven in de Basisregistratie Personen (BRP) bij het gemeentehuis. Ook kon ik eindelijk een DigiD aanvragen, een inkomen verwerven, een zorgverzekering afsluiten, rijlessen volgen, en als volwaardige burger, beginnen met het betalen van belasting. Jullie hebben mij een nieuwe toekomst gegeven, en daarvoor ben ik jullie voor altijd dankbaar. Dank voor het vertrouwen dat jullie in mij hebben gesteld.

Prof. dr. F. K. L. Spijkervet, eerste promotor, gepensioneerd kaakchirurg, en (voormalige) afdelingshoofd MKA-chirurgie, beste Fred, graag wil ik jou mijn oprechte dank betuigen voor je inzet en betrokkenheid gedurende mijn promotietraject. In de beginfase van het onderzoek was jouw bijdrage vooral op de achtergrond aanwezig, maar naarmate het project vorderde en het meer structuur kreeg, werd jouw betrokkenheid intensiever en van grote waarde. Ik heb onze gesprekken altijd als bijzonder plezierig en inspirerend ervaren. Jouw vermogen om kritisch én oplossingsgericht mee te denken heeft in belangrijke mate bijgedragen aan de voortgang en kwaliteit van het onderzoek. Je constructieve houding en brede blik zijn van onschatbare waarde geweest gedurende dit traject. Het is voor mij een grote eer geweest om jou als promotor te mogen hebben. Nu je onlangs met pensioen bent gegaan, wil ik je ook van harte feliciteren met deze bijzondere mijlpaal. Ik hoop dat je in goede gezondheid en met voldoening kunt genieten van deze nieuwe levensfase, en dat je de tijd en ruimte vindt om jouw persoonlijke plannen en wensen te verwezenlijken.

Dr. B. van Minnen, co-promotor (eigenlijk de eerste promotor), kaakchirurg, en huidig afdelingshoofd MKA-chirurgie, beste Baucke, dit promotietraject is in belangrijke mate bij jou begonnen samen met prof. dr. R. R. M. Bos. Zonder jouw inzet en betrokkenheid was het onmogelijk geweest om het tot een goed einde te brengen. Hoewel je op papier als tweede promotor vermeld staat, heb je gedurende het hele proces feitelijk ook gefungeerd als eerste promotor. In 2014 werd ik via prof. Bos aan jou voorgesteld, en al snel begonnen we samen aan een onderzoek naar de 3D-benadering van aangezichtsfracturen. Vanaf het eerste moment was je enthousiast, betrokken, en altijd bereid om mee te denken. Jouw open houding en toegankelijkheid maakten voor mij direct een groot verschil, zeker in de beginfase van het project. Na een aantal jaren waarin het contact noodgedwongen stilviel

mede vanwege mijn studie geneeskunde in Amsterdam, keerde ik terug naar het noorden. In die periode was het voor mij, door het ontbreken van een werkvergunning, niet mogelijk om klinisch actief te zijn of als arts te werken. Tijdens de COVID-19-pandemie voelde ik sterk de wens om mijn steentje bij te dragen aan de maatschappij, maar dat bleek juridisch niet haalbaar.

In 2020 nam ik opnieuw contact met je op, evenals met prof. Bos, en samen hebben jullie de mogelijkheid gecreëerd om via een nulurencontract het onderzoek weer op te starten. Dit vormde uiteindelijk de basis voor een formeel promotietraject, waarmee ook de aanvraag voor een werkvergunning kon worden onderbouwd. Daarmee kreeg mijn toekomst opnieuw perspectief. Je was gedurende het hele traject een constante steun: oplossingsgericht, meedenkend, en nooit afwijzend. Naast inhoudelijke begeleiding bood je ook altijd ruimte voor persoonlijke gesprekken. Je was voor mij niet alleen een buitengewoon kundige promotor, maar ook een betrokken mentor. Het was een groot genoegen om met jou samen te mogen werken. Jouw alertheid, punctualiteit, open blik en oplossingsgerichte instelling kenmerken jou als een bijzonder mens. Ik heb veel van je geleerd, zowel professioneel als persoonlijk, en ben je zeer dankbaar voor de waardevolle en leerzame jaren die we hebben gedeeld.

Prof. dr. R. R. M. Bos (gepensioneerd kaakchirurg), beste Ruud, alles begon eigenlijk bij jou. In 2014 stuurde ik je een e-mail met de vraag of ik mijn bachelor thesis voor de opleiding werktuigbouwkunde onder jouw begeleiding mocht uitvoeren. Jouw directe en enthousiaste reactie vormde het begin van een langdurige en inspirerende samenwerking. Na afronding van mijn thesis zijn we door de jaren heen in contact gebleven. Je bent voor mij altijd een bron van inspiratie geweest. Onze gesprekken heb ik als bijzonder waardevol ervaren; je was altijd positief, betrokken en stimulerend in je benadering. Een herinnering die me in het bijzonder is bijgebleven, is het moment waarop ik geneeskunde studeerde aan de Universiteit van Amsterdam. Je stuurde me toen een bericht dat je de volgende dag in Amsterdam zou zijn voor een vergadering, en stelde voor om samen te gaan eten voordat je de trein terug naar het noorden zou nemen. Tijdens dat diner was ik onder de indruk van hoe snel jij een bord vol oesters wist te verorberen, een luchtige, maar blijvende herinnering aan jouw levendige karakter. Zoals eerder benoemd, keerde ik later terug naar het noorden, maar door het ontbreken van een werkvergunning kon ik geen klinisch werk verrichten. In die periode nam ik opnieuw contact op met jou, en ook met Baucke, samen kwamen we tot het idee om het onderzoek weer op te pakken en er een promotietraject van te maken. Dank voor je inzet, vertrouwen en hulp in al die jaren. Ik ben je zeer dankbaar voor alles wat je voor mij hebt betekend.

Dr. ir. C. C. Roossien (Biomedical Engineering, Faculty of Science and Engineering), co-promotor, **beste Charissa,** hartelijk dank voor jouw waardevolle bijdrage gedurende mijn promotietraject. Vanuit de afdeling Biomedical Engineering was je vanaf het prille begin betrokken bij mijn thesis, en later steeds intensiever in je rol als copromotor. Jouw expertise op biomedisch gebied en je brede netwerk zijn van onschatbare waarde geweest voor het

succes van mijn onderzoek. Ik heb het altijd als prettig ervaren dat ik je op een laagdrempelige manier kon benaderen, via e-mail of app en dat je altijd bereid was om mee te denken en te sparren. Een van de mooie ontwikkelingen die mede dankzij jouw betrokkenheid tot stand is gekomen, is mijn rol als begeleider van Biomedical Engineering-studenten vanuit het UMCG tijdens hun thesisperiode. Daarnaast hebben we vele waardevolle gesprekken gevoerd over het onderzoek, de thesis, en ook over het leven zelf. Dat alles heeft deze jaren extra leerzaam en betekenisvol gemaakt. Ik wil je dan ook hartelijk danken voor jouw inzet, begeleiding en betrokkenheid gedurende deze bijzondere periode.

Assoc. Prof. dr. F. W. Wubs (Numerical Mathematics, Faculty of Science & Engineering), beste Fred, jij bent vanaf het allereerste begin betrokken geweest bij mijn onderzoekswerk, vanaf mijn bachelor thesis in werktuigbouwkunde en later bij mijn masterthesis in Biomedical Engineering. Toen ik opnieuw begon met onderzoek aan het UMCG, was jij een van de eersten die ik benaderde. Je was direct bereid om mij opnieuw te ondersteunen. Jouw expertise op het gebied van de eindige-elementenmethode is van grote waarde geweest voor mijn onderzoek. Vanaf dag één was je nauw betrokken als copromotor, en ik heb het bijzonder gewaardeerd dat je altijd tijd vrijmaakte voor mij en voor ons project. Zonder jouw hulp had deze thesis niet tot stand kunnen komen. Zo regelde je in de beginfase onder andere een RUG-account voor mij, waardoor ik toegang kreeg tot de benodigde computerprogramma's binnen jouw faculteit. Je was altijd beschikbaar om mee te denken, vragen te beantwoorden en oplossingen te zoeken bij uitdagingen in het onderzoek. Jij was eigenlijk als co-promotor betrokken geweest tijdens mijn promotietraject. Tijdens jouw pensionering heb ik je ook beter leren kennen als mens, onder andere via gesprekken met je familie over jouw extra curriculaire bezigheden zoals muziek maken in een band, betrokkenheid bij de kerk, intensief sporten en zwemmen, en het oppassen op je kleinkinderen. Ik wil je danken voor je tijd, expertise, inzet, en de inspirerende gesprekken die we in de afgelopen jaren hebben gehad.

Dr. N. B. van Bakelen (Kaakschirurg, Chef de Clinique, en Staf MKA-chirurgie), **beste Nico,** hartelijk dank voor jouw hulp en bijdrage. Jij hebt mij enorm geholpen tijdens de periode dat Baucke afwezig was vanwege zijn indrukwekkende fietstocht van enkele maanden. Ik kon je altijd benaderen via e-mail of even bij je langslopen met vragen, voor overleg of om te sparren. Je was altijd bereikbaar en toegankelijk. Een goed voorbeeld hiervan is toen ik voor de mechanisme-testen gebruik moest maken van een van de poliklinische kamers, dat werd direct en zonder moeite voor mij geregeld. Ik heb onze samenwerking als zeer prettig ervaren, en jouw input was van grote waarde voor het succes van het onderzoek.

Dr. B. Gareb (AIOS MKA-chirurgie), beste Barzi, dank voor jouw inzet bij het uitvoeren van de systematische review en de meta-analyses. Via Baucke heb ik jou leren kennen, en sindsdien heb je mij op waardevolle wijze ondersteund bij dit deel van het onderzoek. Ik kon je altijd benaderen om te overleggen of te sparren, wat ik als prettig en leerzaam heb ervaren. Jouw hulp heeft een belangrijke bijdrage geleverd aan dit promotietraject.

Prof. dr. A. Vissink (Kaakchirurg en staf MKA-chirurgie), **beste Arjan,** jij was niet direct betrokken bij mijn onderzoek, maar wel als lid van de onderzoekscommissie. We hebben fijne gesprekken gehad, die ik zeer heb gewaardeerd. Ik herinner me nog goed dat je aan het begin van het derde jaar van mijn promotietraject vroeg hoe het met de voortgang ging. Ik gaf toen aan dat ik me zorgen maakte over de planning, omdat ik flink achterliep ten opzichte van mijn oorspronkelijke tijdlijn. Wat ik destijds had onderschat, was hoe afhankelijk je als promovendus soms bent van anderen, en hoeveel tijd er verloren gaat met wachten op feedback of input. Jouw reactie was geruststellend: je gaf aan dat dit heel normaal is, en dat vrijwel iedereen hiermee te maken krijgt. Die opmerking bracht me rust, omdat ik me realiseerde dat ik niet de enige was die tegen dergelijke uitdagingen aanliep. Daarnaast stelde je dat, zolang de commissie tevreden is, het traject prima op tijd afgerond zou kunnen worden, en dat er in het uiterste geval altijd ruimte is voor verlenging van de aanstelling. Die woorden gaven me niet alleen perspectief, maar ook vertrouwen. Dank voor jouw geruststellende houding en de menselijke benadering tijdens deze intensieve periode.

J. de Vries en de BBT-afdeling (Biomaterials and Biomedical Technology), **beste Joop,** dank voor jouw hulp bij het beschikbaar stellen van de mechanische trekbank van de afdeling, en voor je uitgebreide ondersteuning bij het instellen van de juiste parameters voor de mechanische testen. Jouw praktische kennis en bereidheid om mee te denken hebben een belangrijke bijdrage geleverd aan dit deel van het onderzoek.

Prof. G. A. Lunter (Medical Statistics, Faculty of Medical Sciences), **beste Gerton,** dank voor de constructieve overleggen over de statistiek en jouw nauwkeurige berekening van de intraclass correlatiecoëfficiënt in het hoofdstuk 5. Jouw inzet en deskundigheid worden zeer gewaardeerd en hebben bijgedragen aan de kwaliteit van dit onderzoek.

Dr. W. P. Krijnen (Statistics and Probability, Faculty of Science and Engineering), **beste Wim,** dank voor jouw hulp bij het uitvoeren van de variantieanalyse van de Synbone-materiaaleigenschappen in het hoofdstuk 4, gebaseerd op de uitkomsten van de mechanische testen. Jouw statistische expertise was van grote waarde voor de onderbouwing van dit onderdeel van het onderzoek.

Dr. K. Delli (MKA-chirurgie), **beste Kostantina,** ik heb je meerdere keren benaderd met statistische vragen tijdens mijn promotietraject, en jij maakte altijd tijd vrij om mij te helpen. Hartelijk dank voor je waardevolle ondersteuning en bereidheid om mee te denken.

Het dagelijks bestuur van de afdeling MKA-chirurgie, dank voor de kans die jullie mij hebben gegeven om mijn thesis binnen de afdeling MKA-chirurgie uit te voeren. Deze mogelijkheid heeft voor mij een belangrijke basis gevormd voor het hele promotietraject.

Stafleden van de afdeling MKA-chirurgie, dank voor jullie hulp en inzet gedurende mijn promotietraject. Ik kon altijd laagdrempelig contact met jullie opnemen, en jullie stonden steeds meedenkend en ondersteunend voor mij klaar. Dat heb ik als zeer waardevol ervaren.

Röntgenafdeling CBCT MKA-chirurgie (Radiologische Laboranten), in het bijzonder wil ik **Mariëlle J. Feddema** (voormalige laborant), **Sigrid Brink-Dob**, **Lisanne J. Woldering**, **Anne Poppinga**, **Suzanne M. Wolters-Barsingerhorn**, en **Liliane M.E. Kamstra-Dooper** hartelijk danken voor jullie hulp bij het maken van de CBCT-scans van de kunstkaken en de kadavers. Ik kon jullie gemakkelijk benaderen, en de scans werden altijd snel en zorgvuldig geregeld. Dank voor jullie inzet en praktische ondersteuning.

Afdeling Radiologie, in het bijzonder dank aan **Jan Braaksma (Radiologie Systeem Specialist)**, voor jouw hulp bij het aanmaken van de CT-scans van de kadaveronderkaken. Jouw bereidheid om mee te werken en praktische ondersteuning waren van grote waarde voor dit onderdeel van het onderzoek.

Sectie Anatomie, Snijzaal, in het bijzonder dank aan **Steve Oosterhoff** voor het lenen van de kadaveronderkaken voor de (CB)CT-scans. Jouw bereidwilligheid heeft een belangrijke bijdrage geleverd aan het onderzoek.

S. van der Werff (Medical Information Specialist, RUG), **beste Sjoukje,** dank voor jouw hulp bij het opstarten van de systematische review en het opstellen van de juiste zoekstrategie. Jouw expertise was van grote waarde voor dit onderdeel van mijn thesis.

3D-Lab UMCG, in het bijzonder dank aan **Dr. Joep Kraeima (Technical Physician & Coordinator 3D lab)** en **Dr. Bram J. Merema (Mechanical Engineer)**. **Beste Joep en Bram,** dank voor jullie inzet bij het 3D-gedeelte van mijn thesis, waaronder onder andere de segmentatie van de CT-scans en het meedenken bij het creëren van het juiste 3D-model. Jullie hebben mij met open armen ontvangen in het 3D-lab en stonden altijd klaar om mij te assisteren. Jullie expertise en hulp heb ik zeer gewaardeerd.

Instrumentenmakerij UMCG, in het bijzonder dank aan **W. de Goede (Hoofd Research Instrumentenmakerij)**. **Beste Wolter,** dank voor jouw inzet en bijdrage bij het ontwerpen en vervaardigen van het custom-made device voor de mechanische testen van de kaken, het maken van de Synbone-samples voor deze testen, en het produceren van de 3D-prints van de mandibula. Ik kon altijd tussendoor bij jou langskomen met vragen en ideeën, en jij zorgde voor een mooi eindproduct. Jouw deskundigheid en flexibiliteit zijn voor mij van grote waarde geweest.

D.M. Post (P&O UMCG), **beste Danielle,** hoewel je niet direct betrokken was bij mijn onderzoek, heb je mij enorm geholpen bij het proces van het aanvragen van een werkvergunning. Dank voor jouw inzet, zonder jouw hulp was dit traject niet mogelijk geweest.

Bestuur van de Boering Stichting, hartelijk dank voor jullie financiële steun, waardoor ik mijn thesis heb kunnen uitvoeren en het wetenschappelijk onderzoek heb kunnen voortzetten.

Strasburg Osteosynthesis Research Group (S.O.R.G.), thank you for your financial support to conduct the 3D printed mandible mechanical testing. Further, thank you for your assistance with the 3D segmentation and 3D modelling of the cadaveric bones used in this thesis.

Verder wil ik iedereen bedanken die op welke wijze dan ook heeft bijgedragen aan dit traject.

Daarnaast wil ik persoonlijk mijn dank uitspreken aan de volgende personen:

Rommy Anna Goudberg, lieve Rommy, in 2016 heb ik jou leren kennen, en vanaf dag één heb jij in mij geloofd. Op 4 november 2024 zijn wij getrouwd en op 11 februari 2025 mochten wij ons prachtige kind Tobias verwelkomen. Dank voor jouw geduld, onvoorwaardelijke steun, en liefde gedurende al die jaren. Zonder jou was het niet mogelijk geweest om zo ver te komen.

Tobias Benjamin Goudberg, jij bent mijn zonnestraal en een groot wonder. Dankjewel voor jouw komst in mijn leven. Jij maakt mijn leven compleet en papa houdt ontzettend veel van jou.

Frits van Dijk, lieve Frits, sinds 2004 ben jij als advocaat betrokken geweest bij mijn leven en heb je mij geholpen bij het verkrijgen van mijn vergunning. We hebben veel gesprekken gevoerd en jij hebt altijd in mij geloofd. Dank je wel voor alles.

Frank Steenhuisen, lieve Frank, jij bent een van de meest bijzondere mensen die ik in mijn leven heb ontmoet. Jarenlang ben jij een grote steun voor mij geweest bij juridische zaken, begeleidde je mij vaak naar de IND en ambassades, en was je er altijd als een vaderfiguur. Helaas ben je sinds 2023 niet meer bij ons, maar ik wil je bedanken voor alles wat je voor mij hebt betekend.

Lieve familie, vrienden en reddende engelen, onder wie Familie Goudberg, Familie Rietdijk (Harald, Fabienne, Femke, Anna & Thomas), Familie Detweiller (Jonathan, Denise, Dominika & Annelies), Familie Havens (Elizabeth & Ashley), Familie Muller (Kees & Rommy), Familie Steenhuisen (Frank & Christien), Familie Kremers (Rob & Joyce), Familie Bodamer (Ernst & Anke), Esmeralda van Boon, Jeffrey van Dodewaard, Martin van Dodewaard, Monique Butter, Prof. Marcel Levi, Prof. Paul van Trotsenburg, Prof. Bart van Verkerke, Pieter van Veen, Peter den Oudsten, Igor Monzon, Christa de Leeuw, Hans Hendrickx, Anna van der Meulen, Stichting voor vluchteling-studenten (UAF), International Kerk (Assen & Vineyard Groningen) en nog veel meer anderen: dank voor jullie geloof in mij en alle hulp die jullie mij hebben geboden om zo ver te komen. Zonder jullie was dit niet mogelijk geweest.

Tot slot, aan mijn vader, Salam Jan Daqiq: dank voor jouw liefde en jouw leven voor mij. Ook al ben je al jaren niet meer hier, je blijft altijd in mijn hart. Ik hou van jou, papa. Ik weet dat je me steunt vanuit de hemel.

SPONSORS

Thank you to the following companies and organizations for their contribution to the printing costs:

- ABN AMRO
- Boering stichting
- Dam Medical
- KLS Martin Group
- Koninklijke Nederlandse Maatschappij tot bevordering der Tandheelkunde (KNMT)
- Materialise NV
- Montagna d'Oro
- Nederlandse Vereniging voor Traumachirurgie (NVT)
- Nederlandse Wetenschappelijke Verenging van Tandartsen (NWVT)
- Noord Negentig
- Straussman Group
- University Medical Center Groningen (UMCG)